Optimised Dynamic Motion Control of Near Spherical Objects

A thesis presented in the partial fulfilment of the requirements for the degree of

PhD
in
Engineering

At
Massey University
Palmerston North
New Zealand

Michael Charles Edmondson

2013

Abstract

This research investigates the development of an automated packing machine for a New Zealand Industrial Company (NZIC). NZIC is a leading international manufacturer that produces automated equipment for a labour intensive industry. The proposed system aims to solve the complex packing of near spherical objects (OBJ) which is currently the most labour intensive task.

A review of the existing full or partially autonomous systems has identified multiple units that have attempted to remove human labour from relevant or simplified versions of the task. Three areas are identified as requiring in-depth investigation and this research sets out to investigate these issues and propose possible solutions.

One failing aspect of the existing systems is the apparent lack of prior analysis on how such a machine would deliver on commercial requirements. This research made an in-depth motion analysis on possible automated solutions and laid the foundation for engineering development. The overall system topology was considered with various abstract layouts and this identified a sequential modular layout was best suited to the commercial interests. Physical consideration began with identifying the fundamental kinematic analysis of various end effector arrangements. The kinematics demonstrated the need to make the system tolerant to extended dwell periods and this means the system must pack a multiple of OBJs per cycle. Three robotic concepts where evaluated by simulations to investigate various means of practical implementation. A robotic gantry layout was chosen as the design that would best meet the requirements of the application. The gantry design is then further developed to make more efficient use of actuators and other beneficial attributes for development. The proposed design has been presented and the businesses case could be viable once the market for NZIC's industry recovers.

A second problem that all the existing systems have suffered from is the lack of fault correction or avoidance. A central component to the proposed design is the

introduction of grasp feedback for the control system. A low cost piezoelectric pressure sensor and means of measuring vertical load have been developed for a simple vacuum grasping unit. This grasp feedback unit has been integrated into a modular end effector (EE) unit that is intended to solve the specific OBJ handling requirements of the application. The EE unit development covers more than just the OBJ grasp by also considering OBJ manipulation and solutions for handling the industries uncontrolled environments. Low cost means of servo actuation are integrated into the EE as means of rotating the OBJ and translating its location along the robot's knuckle. A novel pneumatic system provides a solution capable of handling the working environment in addition to the main focus of intelligent grasp control. Where possible, without a full OBJ packing system being built, the grasp feedback has been simulated and subjected to limited testing. Various control system layouts have been developed for throughout the product life-cycle of the EE. The proposed EE unit demonstrates promise of solving all the OBJ handling issues identified during the review of existing commercial packing systems. The EE now needs to be prototyped to a standard capable of field trialling for the commercial application.

The third requirement is a means to manipulate all three rotational axis of the OBJs. No existing system can successfully complete this function with an acceptable production rate. Several concepts of such devices were prototyped, with one variant demonstrating a potential means of inducing variable and predictable rotation. This design was a mechatronic system that intends to manipulate the OBJ's three rotational degrees of freedom using an ultra low cost layout. The orientation system has been developed across all the mechatronic components including software, and takes into consideration several different designs for throughout the system's life cycle. A position based visual servo control system has been developed to provide a control feedback loop that traces the six degrees of freedom of OBJs. Explained is both the hardware layout for the inspection, plus the algorithms developed for motion tracking. The algorithms developed for motion tracking produce a series of inter-frame references 3D reconstructed from the captured images. A blob tracking search algorithm then matches the references across multiple images. Lastly an intersection of planes algorithm

estimates the OBJ motion. The completion of all elements for the manipulation unit has allowed motion studies of the proposed device. The motion study of the orientation device demonstrated predictable behaviour for steady motion, however the behaviour during transient motion proved too unstable to allow position control of the OBJs. It is concluded that the orientation unit was too low cost for the purpose and a direct acting servo unit should be further investigated.

The outcome of this research is an overall system proposal that should allow the successful commercial application of an automated organised packing of near spherical objects. The proposed end effector arrangement demonstrates promise of reliable OBJ grasping and should be field trialled in order to verify commercial use. The low cost orientation unit should not be progressed further as it seems unlikely to offer reliable positional control. Instead a means of direct rotational manipulation should be investigated.

Acknowledgements

It has been about five years since I set out on the path to complete this project. There are many people who have given me assistance, suggestions and some guidance along the way.

Firstly I would like to thank my supervisor Dr Liqiong Tang who has provided great guidance to myself and especially making sure I kept an academic aspect to my work. It must have been very challenging in her role when I'm based at location remote from the university campus and pushed towards commercial considerations.

This project was jointly funded by a New Zealand Industrial company (NZIC) and the government agency the Foundation for Science Research and Technology (FRST). I will not name the company since this will become a public document and could harm their commercial interests. I would however like to extend my gratitudes to those involved for deciding to proceed with such a project and the opportunity given to myself. Due to the heavy commercial interest I have had to face many challenges and pressures that one would not expect for an academic project. While it certainly is not a direction I would recommend the lessons learnt far exceed what I could expect outside a commercial project. I certainly feel the work contained in the following document only covers a small fraction of my personal and engineering development.

I would like to especially thank the following people at NZIC. Nigel who was my NZIC supervisor and pushed through for this project. Isaac who has been of great help with getting parts ordered or made with NZIC complicated internal systems. Sheldon, Greg and the others within NZIC's test centre that have been accommodating to my work and had to deal with disappearance of tools.

I need to thank those closest to me and I've neglected over this period. My parents Carolyn and Larry who have sacrificed so much for me and given me the best possible upbringing. I often hear my father say to the effect "I'm not sure where he got it from."

In reality it has been my upbringing around workshops, the farm and motor-sport has provided me with curiosity and understanding of machinery. Finally my beautiful Emma who locked me in my room until I finished this thing and who has been such a help in the final editing. Hopefully I'll now have more spare time to spend with you all.

Table of Contents

Abstract....i
Acknowledgements....iv
Index of Figures....x
Index of Tables....xvi
Glossary....xvii
1 Introduction....1
1.1 Background of NZIC and the Industry....1
1.1.1 Processing within NZIC's Industry....2
1.2 Research Goal....4
1.3 Features of the Products....4
1.4 Difficulties and Problems....5
1.5 Research Methodologies....6
1.6 Objectives....7
1.7 Overview and Structure of the Thesis....8
2 Background of Robotic Object Packing within Industry....15
2.1 Brief History and Timelines of Automation and Industrial Robotics....17
2.2 Overview of Industrial Robotic Systems....18
2.3 Existing Automatic Packing Systems....22
2.3.1 Existing System 1....22
2.3.2 Existing System 2....25
2.3.3 Existing System 3....26
2.3.4 Existing System 4....27
2.3.5 Existing System 5....28
2.3.6 Existing System 6....29
2.3.7 Other Systems....31
2.3.8 NZIC Robotic Tray Picker....32
2.4 Review of Existing Systems....35
3 System Design and Investigation....38
3.1 System Layout Overview....38
3.1.1 Rejection of Single Stage Packing....39
3.1.2 Reasoning for Sequential Packing System....40
3.2 System Layout....42

3.3 End Effector Packing Arrangement and Layout....43
3.3.1 Packing Unit Layouts....43
3.3.2 Background of the Analysis of Packing Layouts....44
3.3.3 Analysis of Packing Layouts....49
3.3.4 Conclusions of Packing Layouts....52
3.4 Investigation in the Practical Robotic System....52
3.4.1 Articulated Arm Based Robot....53
3.4.2 Parallel Based Packing Robot....55
3.4.3 Gantry Based Packing Robot....56
3.4.4 Simulation Environment....57
3.4.5 Actuator Torques and Forces....59
3.4.6 Susceptibility to Backlash....66
3.4.7 Review of Robotic Structure Simulation....71
3.5 Gantry Development....72
3.6 Proposed Control Overview....77
3.7 Summary of Robotic System Design....79
4 Investigation, Design and Engineering of Grasp and Orientation Technology....84
4.1 Investigation on End Effectors....84
4.1.1 Existing End Effector Technologies....85
4.1.2 Conceptual End Effector Designs....88
4.1.3 Discussion of End Effector Designs....92
4.1.4 Conclusion and Direction for End Effector Design....93
4.2 System Design of OBJ Grasping End Effector....94
4.2.1 Pneumatic System....96
4.2.2 Vertical Motion....103
4.2.3 Servo Driven Actuation....106
4.2.4 End Effector System Integration....108
4.3 Investigation of OBJ Orientation Unit....111
4.3.1 Discussion of Presented Orientation Solutions....111
4.3.2 Belt Drive Development....113
4.3.3 Conclusions and Recommendation for Orientation Design....114
4.4 Design of OBJ Orientation Unit....115
4.4.1 Base Mechanical Models....115
4.4.2 Electronic/Software Actuation and Sensing....120

5 Visual Servo Control System....126
5.1 System Overview....127
5.2 Hardware Elements....128
5.2.1 Description of OBJs....128
5.2.2 Illumination Environment....129
5.2.3 Image Capture....131
5.3 Feature Extraction....134
5.3.1 Mask Generation....135
5.3.2 Blob Detection....135
5.3.3 Intra-Frame Blob Tracking....142
5.4 Inter-Frame Feature Tracking....145
5.5 Matching Intra-Frame Dot References....149
5.5.1 Intelligent Pass....150
5.6 Determining the Unit Axis of Orientation....151
5.6.1 Finding an Axis with the Intersection of Planes Methodology....151
6 Behaviour Investigation....161
6.1 Base Study of Pneumatic Grasping of OBJs....161
6.1.1 Equipment, Variables and Procedure....162
6.1.2 Conclusion....168
6.2 Intelligent Grasp Sensing....169
6.2.1 Simulation of Pneumatic Grasp....170
6.2.2 Grasp Variable Study....176
6.2.3 Grasp Pressure Response of the NZIC RTP....177
6.3 Verification of Visual Servo Feedback Processing....180
6.3.1 Intra-Frame Blob Matching....181
6.3.2 Determination of Rotation Axis....183
6.3.3 Applied Testing....184
6.4 Principle Behaviour of Rotation System With Spherical OBJs....185
6.4.1 Motion Behaviour Study Procedure....187
6.4.2 Belt Design and Rotation Behaviour....190
6.4.3 Belt Tension and Rotation Behaviour....194
6.4.4 Pocket Design and Rotation Behaviour....195
6.4.5 Conclusions On OBJ Orientator Physical Design....196
7 Conclusions and Recommendations....197

7.1 Conclusion....197
7.2 Future Directions....198
8 References....201
9 List of Relevant Publications by Author....206
A Calculation Details for Robotic Motion Analysis....207
A.1 Matlab Code for Generating Jounce Controlled Motion Curves....207
A.2 Variables Setup for the Comparison between Pack Layouts....209
A.3 Robot Simulation Grasp and Release Coordinates....210
B Conceptual Orientation Solutions....211
B.1 Solenoid Nudging....211
B.2 Perpendicular Driven Rollers....211
B.3 Cross Pattern Driven Rollers....212
B.4 Independently Collinear Driven Rollers....212
C Grasp Effects....214
C.1 Effect of Mass....214
C.2 Effect of Vacuum Depth....215
C.3 Effect of Flow Rate....216
C.4 Effect of Vacuum Cup Spring Rate....217
C.5 Effect of Vacuum Cup Diameter....218
C.6 Effect of LVDT Spring Rate....219
D Orientation Motion Models....220
D.1 Behaviour of the Single Cord Design....221
D.2 Behaviour of the Dual Cord Design....226
D.3 Behaviour of the Flat Belt Design....231
D.4 Effect of Drive Types....236
D.5 Effect of Belt Tension....238
D.6 Effect of Pocket Design....241

Index of Figures

Figure 2.1: An articulated robot moving a work piece between stations (Photo courtesy of Berthold Hermle AG).....21
Figure 2.2: An articulated robot handling a glass panel (Image courtesy of Kuka[80]).....21
Figure 2.3: An articulated or Z type robot for palletising within a bakery. (Image curtsey of Kuka[80]).....21
Figure 2.4: Existing System 1, plane view at the top, side view at the bottom.....22
Figure 2.5: Existing System 2, plan view on the left, front view on the right.....25
Figure 2.6: Existing system 3, plan view on the left, front view on the right.....27
Figure 2.7: Existing system 5, plan view on the top, side view at the bottom.....28
Figure 2.8: Existing system 6, demonstrating the staged layout of packing OBJs with organised layout.....30
Figure 2.9: NZIC's Rapid Tray Picker.....32
Figure 2.10: Control cabinet to guide the Flex-picker's motion.....34
Figure 3.1: Single independent packing unit.....43
Figure 3.2: Optimised single independent packing unit.....43
Figure 3.3: Twin independent packing units.....43
Figure 3.4: Row packing unit.....43
Figure 3.5: Pattern packing unit.....43
Figure 3.6 Motion curves generated for a 1m displacement over 1 second duration. 44
Figure 3.7: The effect of different packing periods on the peak motions experienced by the system. 46
Figure 3.8: The effect of different packing displacements on the peak motions experienced by the system.....47
Figure 3.9: System dwell period from the behaviour of grasp formation. 48
Figure 3.10: Peak acceleration of packing layouts.....50
Figure 3.11: Articulated arm robot concept.....53
Figure 3.12: Articulated arm robotic system.....53
Figure 3.13: Parallel based robotic concept.....54
Figure 3.14: Parallel based robotic system.....55
Figure 3.15: Gantry based robotic system.....56
Figure 3.16: SimMechanics processes.....57
Figure 3.17: Power requirements of the articulated arm structure for axis one.....59

Figure 3.18: Torque requirements of the articulated arm structure for axis one.....60
Figure 3.19: Torque requirements of the articulated arm structure during the final cycle of a tray.....61
Figure 3.20: Power requirements of the parallel structure for axis one.....62
Figure 3.21: Torque requirements of the parallel structure for axis one.....63
Figure 3.22: Torque requirements of the parallel structure during the final cycle of a tray.....63
Figure 3.23: Power requirements of the gantry structure for axis one.....64
Figure 3.24: Torque requirements of the gantry structure for axis one.....65
Figure 3.25: Torque requirements of the gantry structure during the final cycle of a tray.....65
Figure 3.26: Backlash at OBJ pickup location for an arm stucture robot.....67
Figure 3.27: Backlash at OBJ placement locations for an articulated arm structure robot.....68
Figure 3.28: Backlash at OBJ pickup location for a parallel structure robot.....69
Figure 3.29: Backlash at OBJ placement locations for a parallel structure robot.....70
Figure 3.30: Backlash at OBJ pickup location for a gantry structure robot.....71
Figure 3.31: Backlash at OBJ placement locations for a gantry structure robot.....71
Figure 3.32: Layout of the differential drive.....73
Figure 3.33: Power requirements for the proposed robotic system for axis one.....76
Figure 3.34: Torque requirements for the proposed robotic system for axis one.....76
Figure 3.35: Torque requirements for the final packing cycle of the robotic proposed system...77
Figure 3.36: Power requirements for the final packing cycle of the proposed robotic system.....78
Figure 3.37: Backlash at OBJ pickup location for the proposed robotic structure.....79
Figure 3.38: Backlash at OBJ placement locations for the proposed robotic structure.....79
Figure 3.39: Conceptual mock up of the proposed robotic packing system.....81
Figure 3.40: Conceptual mock up of EE and orientation units.....81
Figure 3.41: Estimated profitability of the prototype design.....84
Figure 3.42: Estimated profitability of the production design.....85
Figure 4.1: Intelligent vacuum cup end effector.....93
Figure 4.2: Individual actuated fingers with embedded pressure tactile arrays.....94
Figure 4.3: Flexible fingers with embedded strain gauge wire.....97
Figure 4.4: Pneumatic expandable enclosure.....98
Figure 4.5: System layout of the independent end effectors.....101
Figure 4.6: End effector layout.....102
Figure 4.7: Pneumatic diagram representing the vacuum grasping system utilised by NZIC's RTP.....103

Figure 4.8: The assumed pneumatic system as utilised by competitors in pattern packer systems. 104
Figure 4.9: Individual vacuum cup control.....107
Figure 4.10: Proposed pneumatic grasping system.....108
Figure 4.11: LVDT based end effector system.....113
Figure 4.12: Load cell based end effector grasp sensing.....115
Figure 4.13: Mechanical layout of end effector design.....117
Figure 4.14: Prototype robot end effector control.....118
Figure 4.15: Proposed electrical/electronic layout of production EE. E-Stop and PS routing not shown for clarity.....120
Figure 4.16: Original proof of concept orientation unit.....123
Figure 4.17: Prototype orientation unit.....126
Figure 4.18: Spring rate of the belt tension.....128
Figure 4.19: Narrow belt arrangement.....129
Figure 4.20: Wide belt arrangement.....129
Figure 4.21: Vacuum formed pockets.....130
Figure 4.22: Control system loop.....131
Figure 4.23: Proposed prototype variant of orientation control equipment.....133
Figure 4.24: Proposed production variant of orientation control hardware.....134
Figure 4.25: Control system for proof of concept testing.....135
Figure 5.1: Test OBJs showing various tracking blobs.....139
Figure 5.2: Illumination setup.....140
Figure 5.3: Unpolarised scene.....141
Figure 5.4: Cross polarised scene.....141
Figure 5.5: Effects of imaging a spherical object.....148
Figure 5.6: Raw image captured with cross polarisation.....149
Figure 5.7: Intensity image produced from the raw image.....149
Figure 5.8: Red component of the image.....149
Figure 5.9: Blue component of the image.....149
Figure 5.10: Mask produced using intensity image.....150
Figure 5.11: Colour space of image.....150
Figure 5.12: Blue dots after filtering.....150
Figure 5.13: Green dot after filtering.....150
Figure 5.14: Yellow dot after filtering.....151

Figure 5.15: Diagram of non-infinite length lens and their scene limiting effect on inspecting spherical objects.....153
Figure 5.16: The location of dots Pn prior to alignment procedures.....158
Figure 5.17: The location of dots Pn when P1 is aligned to the Z axis.....158
Figure 5.18: The location of dots Pn when P2 is aligned to the X axis.....158
Figure 5.19: The effect of increasing search sets and the resulting exponential increase in processing loops required. Note that the processing loops are displayed as Log10.....159
Figure 5.20: Extraction of the 6 vectors to define the location of the four closest points.....160
Figure 5.21: Generating a plane of possible rotational axis from a pair of blobs.....166
Figure 5.22: Example of a created axis of rotation from the intersection of different blob planes.....166
Figure 5.23: Axis found by intersection of two different blob planes.....168
Figure 5.24: Measurement of rotation axis found by the intersection of planes.....169
Figure 5.25: Up-close view demonstrating the offset from {0,0,0} as utilised for means of error measurement.....169
Figure 5.26: Dynamic weighting function.....171
Figure 6.1: Porosity testing of real OBJS with test equipment.....176
Figure 6.2: Grasp testing regions on the OBJ's surface.....177
Figure 6.3: Grid for testing the position tolerance of OBJ grasping.....177
Figure 6.4: OBJ Type A vertical lift.....179
Figure 6.5: OBJ type A normal lift.....179
Figure 6.6: OBJ Type B vertical lift.....180
Figure 6.7: Object Type B normal lift.....181
Figure 6.8: Real behaviour of vacuum generator.....184
Figure 6.9: Vacuum system response of the RTP with closed vacuum lines.....184
Figure 6.10: The modelled sensor feedback from proposed grasp unit.....186
Figure 6.11: Example simulation outputs of grasp behaviour 187
Figure 6.12: Prototype LVDT end effector including the PCB.....190
Figure 6.13: Testing grasp pressure response.....191
Figure 6.14: Grasp testing using NZIC's RTP.....191
Figure 6.15: Dot matching consistency of C36 blob matching.....195
Figure 6.16: Dot matching consistency of C45 blob matching.....195
Figure 6.17: Dot matching consistency of C46 blob matching.....195
Figure 6.18: Horn's method.....196

Figure 6.19: Twist method....196
Figure 6.20: IOP Method....196
Figure 6.21: Comparison between IOP and Horns' methods....196
Figure 6.22: Direction of rotation....197
Figure 6.23: Rates of rotation....197
Figure 6.24: Mapped rotational velocity magnitude against modelled and real behaviour....201
Figure 6.25: Mapped rotational velocity direction against models and real behaviour....202
Figure B.1: Solenoid oreintation concept....222
Figure B.2: Perpendicular orientation concept....223
Figure B.3: Perpendicular concept....223
Figure B.4: Co-linear rollers orientation concept....229
Figure C.1: Effect of Mass....230
Figure C.2: Effect of Vacuum Depth on Grasp....231
Figure C.3: Effect of FlowRate on Grasp....232
Figure C.4: Effect of Vacuum Cup Rate....233
Figure C.5: Vacuum Cup Diameter Effects....234
Figure C.6: Effect of LVDT Spring Rates....235
Figure D.1: Motion magnitude behaviour of single cord belts of 30mm separation....237
Figure D.2: Motion direction behaviour of single cord belts of 30mm separation....237
Figure D.3: Motion magnitude behaviour of single cord belts of 40mm separation....238
Figure D.4: Motion direction behaviour of single cord belts of 40mm separation....238
Figure D.5: Motion magnitude behaviour of single cord belts of 50mm separation....239
Figure D.6: Motion direction behaviour of single cord belts of 50mm separation....239
Figure D.7: Warped illustration of the magnitude error of Single Cord of varying belt separation....240
Figure D.8: Warped illustration showing the mean magnitude for single cord belt design of varying separation....240
Figure D.9: Warped illustration showing the mean direction for single cord belt design of varying separation....241
Figure D.10: Warped illustration showing the direction standard deviation for single cord belt design of varying separation....241
Figure D.11: Motion magnitude behaviour of dual cord belts of 30mm separation....242
Figure D.12: Motion direction behaviour of dual cord belts of 30mm separation....242
Figure D.13: Motion magnitude behaviour of dual cord belts of 40mm separation....243

Figure D.14: Motion direction behaviour of dual cord belts of 40mm separation.....243
Figure D.15: Motion magnitude behaviour of dual cord belts of 50mm separation.....244
Figure D.16: Motion direction behaviour of dual cord belts of 50mm separation.....244
Figure D.17: Warped illustration of the magnitude error of dual cord of varying belt separation..
.....245
Figure D.18: Warped illustration of the magnitude error standard deviation of dual cord of varying belt separation.....245
Figure D.19: Warped illustration of the direction error of dual cord of varying belt separation..
.....246
Figure D.20: Warped illustration of the direction error standard deviation of dual cord of varying belt separation.....246
Figure D.21: Motion magnitude behaviour of flat belt of 30mm separation.....247
Figure D.22: Motion direction behaviour of flat belt of 30mm separation.....247
Figure D.23: Motion magnitude behaviour of flat belt of 40mm separation.....248
Figure D.24: Motion direction behaviour of flat belt of 40mm separation.....248
Figure D.25: Motion magnitude behaviour of flat belt of 50mm separation.....249
Figure D.26: Motion direction behaviour of flat belt of 50mm separation.....249
Figure D.27: Warped illustration of the direction error of flat belt of varying belt separation. 250
Figure D.28: Warped illustration of the magnirude error standard deviation of flat belt of varying belt separation.....250
Figure D.29: Warped illustration of the direction error of flat belt of varying belt separation. 251
Figure D.30: Warped illustration of the direction error standard deviation of flat belt of varying belt separation.....251
Figure D.31: Warped illustration of the magnitude error of drive types.....252
Figure D.32: Warped illustration of the magnitude error standard deviation of drive types.....252
Figure D.33: Warped illustration of the direction error of drive types.....253
Figure D.34: Warped illustration of the direction error standard deviation of drive types.....253
Figure D.35: Motion direction behaviour of high belt tension.....254
Figure D.36: Motion direction behaviour of high belt tension.....254
Figure D.37: Warped illustration of the magnitude error of belt tensions.....255
Figure D.38: Warped illustration of the magnitude error standard deviation of belt tensions...255
Figure D.39: Warped illustration of the direction error of belt tensions.....256
Figure D.40: Warped illustration of the direction error standard deviation of belt tension.....256
Figure D.41: Motion Magnitude behaviour of Deep Pocket Design.....257

Figure D.42: Motion Direction behaviour of Deep Pocket Design.....257
Figure D.43: Warped illustration of the magnitude error of pocket designs.....258
Figure D.44: Warped illustration of the magnitude error standard deviation of pocket designs 258
Figure D.45: Warped illustration of the direction error of pocket designs.....259
Figure D.46: Warped illustration of the direction error standard deviation of pocket designs..259

Index of Tables

Table 1.1: Typical features of selected OBJs.....5
Table 2.1:Some major advancements with automation and robotics.....18
Table 3.1: Packing variables and arrangements.....44
Table 3.2: Prefix and suffix codes for Figure 3.10.....49
Table 5.1: Software configuration of different development environments.....144
Table 6.1: Vacuum cup at supplier.....175
Table 6.2: Physical variable range for grasp tolerance testing.....177
Table 6.3: Variable layout within Appendix.....187
Table 6.4: Blob matching simulation.....194
Table 6.5: Variables for orientator motion model.....198
Table 6.6: Test matrix of belt design.....202
Table 6.7: Index of single cord designs.....203
Table 6.8: Comparison between single cord belt separations.....203
Table 6.9: List of figures fro the direct comparison of belt designs.....205
Table 6.10: Failure rate of single cord designs.....206
Table 6.11: Test matrix of belt tension.....206
Table 6.12: Test matrix of pocket design.....207

Glossary

BDC	Brushed DC motor
BLDC	Brushless DC motor
COG	Centre of gravity
EE	End Effector
FRST	Foundation for research, science and technology
GRDP	Grasp or release dwell period
LVDT	Linear variable differential transformer
NZIC	The name given to the New Zealand industrial company
OBJ	The objects handled by NZIC systems
OPM	OBJs per minute
PCB	Printed circuit board
SCADA	Selective compliance articulated robot arm
SCARA	Supervisory control and data acquisition
RTP	Rapid tray packer
ROI	Return on investment
SMA	Second moment of area
SROI	Special region of interest
VTR	Vacuum test rig

1 Introduction

The research undertaken is a confidential project between a New Zealand Industrial Company (NZIC) and Massey University. The project is financially supported by NZIC and the Foundation for Research Science and Technology (FRST). As this research project is confidential and commercially sensitive, in this report the industrial company will be referred to as NZIC and the products and the application of the systems will not be explicitly discussed. NZIC manufactures automatic systems for a very specialised area in the world market. The systems made by NZIC incorporate modern technologies and intelligent features and are sold worldwide.

1.1 Background of NZIC and the Industry

NZIC manufactures equipment for a highly competitive worldwide industry. The industry is similar to many large industries with companies forming a chain of a procedures through which the products reach the market.

The industry chain of procedures consists of four sections:

Primary producers → Processing → Wholesaling/Marketing → Retailers

NZIC's core business is the manufacturing of equipment for companies that process the OBJs. As an example, if NZIC was involved in the petrochemical industry their core business would be designing and manufacturing the speciality equipment associated with production plants for oil refineries.

1.1.1 Processing within NZIC's Industry

The manufacturing of the processing equipment is a highly specialised, advanced and competitive field. Worldwide only a few major companies whose core is solely producing this type of processing equipment exist. In summary the processing task consists of sorting OBJs based on quality and geometry features and then packing the OBJs for the wholesale companies to distribute. NZIC's customers operate these processing facilities. Their goal is to maximise their returns for each OBJ while maintaining the quality expected by the wholesalers and retailers. Traditionally, the processing of the OBJs was manual. In addition to being cost intensive, maintaining a constant quality is difficult. With advanced technology more processes could be partially or totally automated.

The processing of the OBJs can be split into the following seven stages:

Loading → Pre handling → Grading → Sorting → Packing → Output

1. Loading
    - OBJs are delivered from the primary producers in bulk transporting containers. The OBJs are loaded onto the process with the lifting devices.
2. Pre Handling
    - OBJs are subjected to a process to eliminate foreign particles.
3. Grading
    - The main grading procedure is the central element of the entire process. In brief, the OBJs are weighed, inspected with a highly complex machine vision system, and in certain cases, more advanced sensory technology that examine the internal properties.
4. Sorting
    - Each individual OBJ is located individually by a special conveyor. The machine software, with the information from the grading process, directs the OBJs to the defined outlets for each grade.

5. Packing
    - Each outlet has one of many different packing types depending upon the OBJ's value and the wholesale requirements. The lowest grade OBJs are packed into large bulk fill containers. Higher grade OBJs are packed into trays with individual pockets to avoid damage.
6. Output Logistics
    - The trays containing OBJs are palletised to the distribution points.

The most labour intensive task is the grading and sorting of the OBJs. Using state of the art technology a large portion of the grading process can now be automated. With the sorting being automated, the most labour intensive process is the packing of OBJs. NZIC intends to develop potential packing solutions that should reduce the labour requirement and enhance productivity. Automated or semi-automated packing solutions are becoming prevalent within the industry; however, these systems are intended for another type of lower value OBJs. The packing requirement for the high value OBJs is a complicated and delicate process and still the domain of manual labour.

High value OBJs are packed to an organised format. A number of OBJs are placed on a tray with each sitting in an individual pocket. Each OBJ has to be placed in an organised manner so that it is positioned at a certain orientation. The process could be compared to a system packing sports balls. The ball is placed within the packaging and at an orientation so the company name and logos are aligned with all the other balls.

There is a significant difference between packing the unstructured low value OBJs and the organised high value OBJs. NZIC intends to produce an automated system for packing high value OBJs with an organised structure and therefore needs to develop an appropriate new system.

1.2 Research Goal

This research project aims to investigate possible solutions and solve the challenges for the automated organised packing of OBJs. The research first carried out a literature review to investigate the status of existing labour assisted and automated packing systems. Further investigation focuses on potential solutions to issues identified in existing systems. A proposed system structure is based on the evaluation and further considered from these existing systems. The prototype system will require new motion control technologies to manipulate the OBJs. The new motion control of the OBJs will focus on improving the reliability of handling these OBJs during their movement and orientation. The system to be developed is expected to be more accurate and reliable, with a higher speed and productivity than currently available. Ultimately, being a commercial project, the outcome should produce a commercially viable system that can reduce the end user's operational cost and generate a profit for NZIC. Although the final goal of the company is to produce a fully automated system that can pack the OBJs in an organised pattern with high speed, this research is the first step towards a feasibility study and prototype design.

1.3 Features of the Products

The products handled by NZIC's industry have been proven to be difficult for automatic systems to manipulate. The OBJs have different attributes that are not commonly handled successfully because of the variability of the OBJs and their susceptibility to damage.

All the products have the following attributes:

- Fragility
- Different material properties

- A variable size and shape with free-form geometry
- Uneven surface
- A concave or convex top and bottom area

The company has selected two types of OBJs to study, each with minor versions. For convenience, these will be individually known as OBJ_{Ax} and OBJ_{Bx}; the x representing a minor version. Table 1.1 shows the typical features of each OBJ group.

Table 1.1: Typical features of selected OBJs.

	Typical features of OBJ_{Ax}	**Typical features of OBJ_{Bx}**
Shape	Approximately spherical in shape	Elliptical shape
Major diameter	60-140mm	60-80mm
Mass	60-140 g	30-80g
Surface texture	Smooth	Rough
NP and SP geometry	Concave	Convex
Additional features	Has a special region of interest (SROI)	

1.4 Difficulties and Problems

The major difficulty in conducting the research is that almost no literature or systems directly relevant to the research exist. The application is so specific that almost no detailed information is available about the characteristic and behaviour of the OBJs. To meet the required return on investment for customers, the system price is limited to what can only be described as very low for such a robotic and automated solution.

Investigations searching for organised packaging systems found only one such system

that provided the full necessary capability. This system operates at very low rate, therefore has a very questionable commercial viability and there is no record of any system in operation. Surprisingly, not even a simpler non organising automated packing machine was found to adequately perform in a commercial environment. A number of "dumb" pattern picking systems were found. However, these still require human involvement and do not appear to provide a gain over NZIC's existing and presumably economic systems. Chapter 2 which discusses the Background of Robotic Object Packing within Industry gives the readers a detailed review of the existing systems within the industry.

Review of scientific literature has yielded a very small amount of material that is relevant. Many researchers look at using robotic systems with the design of the EEs for the manipulation of a product. These works however tended to focus soley on the design with little consideration on the cost or the packing rate. The literature study revealed that this is a very specific research topic that has not been studied in detail. The challenging aspect is that fundamental information and knowledge for producing the required handling and packing system is lacking. This may also be the reason why all the existing systems can not handle and pack the products in the desired way.

1.5 Research Methodologies

The outcome of the research is a feasibility investigation and a system design proposal for a fully automated reliable prototype system that is capable of handling and packing the OBJs into trays in an organised arrangement. As fundamental knowledge to achieve the operations does not exist in literature, this project intends to adopt a multi-level research structure and modular approach to carry out the research.

- Conduct a fundamental study on the characteristics and behaviour of the OBJs identified by NZIC, by performing a detailed investigation on the interaction

between the different products and different automated systems. This is to search for the methodologies that are capable of manipulating the product in translational and rotational movement.

- Model the promising product manipulating methodologies. Through simulation and testing, establish the analytical models to study the OBJ and system behaviour. Such models are important in the design of mechanics in a practical system and particularly useful for the development of the control systems.
- Design the whole system using modular blocks as any OBJ handling and packing system consists of translational and rotational movement, and a packing operation. Such methodology will make the development work easy to identify faults and then allow easier modifications and control improvements.

1.6 Objectives

To develop the automated system that meets NZIC's requirements, the following objectives are to be fulfilled.

- Conduct a literature study on existing systems such as product handling and packing systems. Such study aims to collect the information related to product behaviour under different operations. Another aim is to identify system advantages and their current failings.
- Form the conceptual solutions for handling system design, then analyse and study each solution and investigate the feasibility against NZIC's requirements. Investigate gentle and reliable object handling manipulators to search for a soultion that can reliably handle NZIC's OBJs.
- Model the promising product handling and packing methodologies and develop the matching control system for further investigation.
- Establish the testing modules. Carry out the simulations and experiment to gain the testing data for analysis and a solid understanding of the models and the

control systems. Compare and study the data with the desired OBJ and the system behaviour and make modifications and improvement.

- Propose a prototype automated system that is capable of meeting NZIC's requirements and performing the operations.

Achieving the objectives will lead to the development of the automatic product handling and packing system that is able to meet NZIC's requirements and fit the constraints for commercial use such as:

- Gentle handling of the OBJs
- Reliable handling operations
- Operating at a commercially viable rate
- The cost of the system must be commercially viable

1.7 Overview and Structure of the Thesis

Chapter 2 Background of Robotic Object Packing within Industry reviews seven existing automated OBJ packing systems with varying degrees of packing rate and performance. The machine types are broadly split into two groups, pattern packers and single OBJ packing machines.

The pattern packer machines are in general, the most successful commercial application due to their low capital cost to OBJ packing rate ratio. However, these machines are limited in operational flexibility and the ability to operate without human supervision. Arguably, three of four pattern packer machines presented could be controlled by hard-wired relay based control logic. It is this lack of system intelligence and fixed hardware design that is the limiting factor with such machines. The information available does not give any reason to believe that the systems have real-time correcting capability to deal with mis-handled OBJs. This non-correcting behaviour which, therefore, requires heavy use of human intervention would appear no more labour efficient than the NZIC

mechanised solution. Further, with such designs there appears no means of adding correcting behaviour even if the control system's intelligence could be improved. The pattern packer machines in all cases would struggle to met the ISO definition of an industrial robot. Ultimately, while these systems are marketed as an automated or robotic solution, the term mechanised is better suited.

The second group of reviewed systems are the single OBJ packing units. The single OBJ machines are a more flexible approach with increased system intelligence compared to pattern packer systems. All these machines have an inherit flexibility built to the structural layouts that allowed various pack types and OBJ formats. The main drawback to these systems and their lack of market success, is the poor capital to production efficiency ratio. Another disappointing aspect found was their inability to take self correcting action or any basic form of disturbance rejection. In all cases, almost the entire structure is capable of the physical corrective action; however it is stopped by the lack of EE feedback and adequately intelligent control system.

In conclusion of the existing systems, no specifically developed automation system has been applied to the NZIC's industry. The pattern packer machines are arguably a mechanised system utilising modern electronics for cost reduction. Modern electronics have not been applied to improve functional operations. The single packer units seem to be developed with the mentality of simply taking a generic robot and sticking it on a production line. These systems would seem to have been developed with no or minimal analysis for the specific application of NZIC.

In Chapter 3 System Design and Investigation, the investigation analyses the overall system requirements and then develops a proposed solution to meet these. The first section of the chapter considers how the OBJ's various degrees of freedom could be manipulated. The humiod concept and simplified hybrid variants are determined as non-viable and this has left a process of sequential modules as the default.

The investigation throughout the remainder of the Chapter 3 is concerned with the overall robot structure to achieve the translational movement. Five EE arrangements are

evaluated using fundamental kinematics. This fundamental analysis considers three single-unit designs, a row packer and a pattern packer. A structure is modelled for each EE arrangement which is then used for the analysis. The various layouts are modelled with different production rates, dwell time[1], and the required displacements. The modelling will demonstrate that the critical feature for a viable system is the capability to withstand extended dwell times. It is concluded that only the multi-OBJ layouts of the row and pattern packer can be realistically expected to maintain the production rate of 250 OPM. A row packer is chosen for the development path since it reduces complexity and yet still meets the required production capacity.

The focus then turns to the engineering of such a row packing robot. A complex simulation environment is developed to consider the size and cost of actuators required for various robot structures. Three types of robots are considered to translate the row of EEs from the orientation units to trays; these are based from articulated, parallel and gantry style structures. The structures are simulated to estimate their required actuator torques/forces across various operating conditions. Evaluation of the simulations will demonstrates the gantry robot as the viable system.

The final section of Chapter 3 looks at developing the robotic structure further and to consider the integration with control system. The initial specification and reasoning for the control system is discussed with some observations from utilising NZIC's tray packer. Finally, a brief production cost to customer value is demonstrated. This evaluation of margin demonstrates the automated packing system could be financially viable across a range of configurations.

Chapter 4 Investigation, Design and Engineering of Grasp and Orientation Technology, investigates the development of new technologies for a viable packing system. The chapter is split into two parts, the first concerns the development of an intelligent grasp system and the second, an OBJ orientation unit. A brief review of robotic EEs is initially given. Discussed is the difference between the common "power grip" approach often applied in automation applications and the challenge of requiring "precision grip"

1 The period require to grasp and release the OBJs.

of the OBJs. Several conceptual precision grip solutions are presented and evaluated. The conclusion evaluating numerous factors such as reliability, prototype or production costing and time to market indicates the best option would be to stay with a pneumatic grasp system. In developing a proposed solution for OBJ grasping the EE study expands from a mechanism to engineering an OBJ handling module to suit the robot structure. Each module becomes an internally controlled device with connections for power source, pneumatic, and communication. This module in addition to grasping the OBJ is intended to rotate it around the vertical axis and the entire unit translates along the robot knuckle.

In the second half of Chapter 4, a low cost fully flexible orientation unit is proposed and built. This system includs all components necessary to achieve the open loop flexible rotational manipulation of the OBJs. This included:

1. Mechanical structure and drive-line
2. Electromechanical actuators
3. Electronics/electrical systems

A base review of existing relevant OBJ rotation systems is presented in section 4.3 with limited applied OBJ orientation units identified in Existing System 5 and 6. No existing orientation system is shown to provide the functionality required for NZIC's system. Therefore in section 4.3 , several conceptual solutions are prototyped. None of the conceptual solutions initially demonstrate an ability to manipulate the OBJ's rotational degrees of freedom. Next, the bi-roller solution is reworked, utilising a belt drive arrangement and this solution demonstrates promise of manipulating the OBJs with a variable rotational axis.

In Section 4.4 , the electromechanical elements for the orientation unit are developed to a prototype design intended for industrial application. A mechanical and BLDC motor drive-line is proposed with the use of a pulley and cord drive. This provides a drive-line that would be ultra low cost in volumes with the use of plastic pulleys/cord and cheap BLDC motors.

The remainder of Chapter 4 describes the remaining mechatronic components required to provide the open loop control of the orientation unit. Several control approaches for the mechanical unit are presented across the different life cycle stages of product. Similar to the EE modules, the prototypes and earlier production variations would initially make use of generic remote IO devices. The latter production systems are proposed with internal embedded control systems operating the functional behaviour and apply abstract instructions to the system controller via industrial Ethernet. The embedded control systems will offer a significant cost reduction, however until the system is proved, the development investment is not warranted.

Chapter 5 describes the vision feedback for the orientation unit's control system. The hardware element of the vision capture sets out the illumination, optical and image capturing process. The hardware elements are explained in detail with practical limitations on the viewing angle and illumination requirements. Discussed is the need for good OBJ edge contrast, even surface illumination, the advantages and constraints of cross polarisation, and the differences between development environments. The software is explained to utilise a blob tracking methodology that estimates rotation vectors based on the movement of reference points. To map the motion between image frames, a blob tracking methodology is been presented. This algorithm begins with a routine that develops a fixed reference per image, and is matches these across image frames. A developed intersection of planes (IOP) algorithm estimates the true 3D rotation vector of the OBJ based on the movement of the traced blobs. Finally estimated rotation vector is subjected to a sanity check and reevaluated if necessarily. The output form the visual servo feedback loop is six degree vector representation the six degrees of motion that OBJ may have moved.

Chapter 6 Behaviour Investigation, looks at the operating of each of the new proposed sub systems from Chapter 4 and 5. A base investigation with grasping both OBJs types is conducted. This initial study verifies vacuum grasping OBJs of type A is valid, and as expect type B OBJs probably require another solution or at least further testing. Two types of surface interaction were investigated by comparing simply grasping the OBJ with a vertical pose against a more complicated mechanism that keeps grasp

perpendicular to the OBJ's surface. This demonstrated that the more complicated grasp unit has a greater consistency of grasping, however, the cheaper implementation of a fixed vertical pose was sufficient if operated with increased Cartesian precision. Next the grasping responses are tested and simulated to prove the working of the low cost new touch sensing end effector. In the absence of a real system, the grasp response is modelled and simulated against changes in several physical variables. This variable study demonstrates the transient grasp response against various states and events. These simulations demonstrate that the proposed low cost sensor EE system has the potential to solve the problems with the reviewed systems. Further the transient response monitoring demonstrates evidence it should provide a fast, real time feedback relating to grasp quality, this is an ability that conventional pressure sensing systems can not provide. As final point the proof of concept EE is carefully implemented on the RTP.

The visual servo feedback algorithms from chapter 5 are tested in a simulation environment. Each critical stage of the algorithm is independently tested against various setup configurations and various signal to noise ratios. The intra-frame blob tracking algorithm is shown by simulation to reliably matching blobs between images captures. The intersection of planes (IOP) and Horn's method of estimating a rotation vector is simulated with each algorithm provides benefits depending upon the hardware configuration and amounts of signal noise. Lastly an applied test is conducted demonstrating the visual servo system successfully tracking the rotational movement of a test OBJ.

The last section of Chapter 6 models and tests the OBJ behaviour while subjected to manipulation from the orientation unit presented in Chapter 4. The hardware variables of belt type, belt tension, pocket shape are tested for model fit and stability. These are measured in terms of rotation axis direction and the magnitude. The single cord belt layout demonstrates the best and most consistent OBJ behaviour, however the flat belt option is presents reasonable model fits. The flat belt was ultimately chosen because of reliability issues using the single cord option. Testing of the remaining variables concluded that a medium belt tension and shallow cup design offered the best motion stability and reduced OBJ damage.

Chapter 7 summaries the outcomes of this research, recommended further improvements and the future directions.

2 Background of Robotic Object Packing within Industry

The automated packaging of OBJs is intertwined with the application of mechatronics and automation control. In many complicated processes, this specifically requires intelligent robotic systems. Narrowing the topic down to a closely defined area is a difficult task as from the definition point of view, automation is deeply involved in robotics, mechatronics and industrial automation.

The ISO standard 8373:2012 defines an industrial robot as:

> *"An automatically controlled, reprogrammable, multipurpose manipulator programmable in three or more axes, which may be either fixed in place or mobile for use in industrial automation applications"[1]*

The Oxford dictionary states the meaning of Automation as:

> *"The use or introduction of automatic equipment in a manufacturing or other process or facility"[2]*

The US Dictionary Merriam Webster defines automation as:

> *"Automatically controlled operation of an apparatus, process, or system by mechanical or electronic devices that take the place of human labor"[3]*

The problem with these dictionary definitions is the scope becomes so large that one could argue many Roman era devices were in fact automated. A wheat mill powered by watermill and passing river could fit the descriptions as it replaces the need for manual grinding and requires little human involvement.

A less formal description of automation can also be found in the Encyclopedia

Britannica.

> *"Automation, the application of machines to tasks once performed by human beings or, increasingly, to tasks that would otherwise be impossible. Although the term mechanization is often used to refer to the simple replacement of human labour by machines, automation generally implies the integration of machines into a self-governing system."[4]*

The Institute of Mechanical Engineers defines:

> *"Mechatronics is a natural choice for explaining a process that seeks, from the outset, to generate definitive engineering system solutions, which are inextricably bound by those integrating technologies associated with the inveterate mechanical, electronic and computer based disciplines"[5]*

From the definitions, it clearly shows that automated packaging of OBJs requires a research in a wide range that covers mechanics, electronics, robotics, system design, control methodologies etc. For the purpose of this research, the work will focus on the following two aspects.

- Study the feasibility of using a dexterous device with less degree of freedom or even only one degree of freedom to handle the OBJs and minimise the cost.
- Investigate and propose an intelligent robotic system that, based on less operational measurement feedback or even just one feedback, has potential to manipulate OBJs in groups, with changing pattern, in different orientation, in high speed, and with a cost as low as possible.

2.1 Brief History and Timelines of Automation and Industrial Robotics

The term automation as governed by the self regulating definition, originates from the period immediately following WWII in the North American motor industry[1]. A variety of sources mention engineers from both Ford and General Motors as the first to coin the word. Prior to this time industrial processes are better described as mechanised machines with only simple forms of action. Technology at this point had provided industry with mechanical systems, electromechanical and fluid based actuators, and the means to measure physical behaviour or states. Automation then arrived with correcting action of logic computing from feedback loop(s) of sensors.

In the same period another device was coming into existence which would change the world forever, the transistor. Now industry not only has the physical means from earlier mechanised machines but more importantly the seeds had been sewn for allowing electronic logic processors to control complex tasks.

In 1956 a company called Unimation was founded by George Devol and Joseph Engelberger[1]. Devol had filed a patent in 1954 for what would eventually become known as an industrial robot. Engelberger was a physicist with a background in complex control systems for nuclear power plants and aerospace. By 1959, the worlds first industrial robot was developed, and 1961 its first application was at General Motors. Unimation's robot at this point was very different from current technology, using of a magnetic drum computer and hydraulic actuators. Unimation would later licence their developments around the world.

Industry continued along with the old and complicated fixed logic via electromechanical relays and pneumatics. There were continuing small improvements along the way, but it was not until after the introduction of the new integrated circuits in the mid 1960s that the fields of automation and particularly robotics prosper. During the late 1960s was the introduction of programmable devices that would now be recognised as a PLC. In

1969, General Motors built a new plant featuring spot-welding robots. These robots could automate around 90% of welding compared with traditional manual labour plants. During this period, new Japanese manufactures began developing their own robot technologies and later became suppliers. As was with the many integrated technologies, the start of massive growth period was in the 1970s. Kuka Robotic had two firsts with its Famulus robot in 1973. This was not only the first 6 axis articulated robot but also the first with all electromechanical actuators. Table 2.1 lists some major advancements in automation and robotics.

Table 2.1:Some major advancements with automation and robotics.

1969	PLCs became available.
1974	ABB released the first fully microprocessor controlled robot, the IRB 6 principally designed by Björn Weichbrodt.
1978	General Motors began the process of developing generic automation/robot control language.
1978	The SCARA robot was developed at University of Yamanashi, Japan by Hiroshi Makino.
1981	The first direct drive robot was developed at Carnegie Mellon University by Takeo Kanade.
1992	Delta robot was released by Demaurex.

2.2 Overview of Industrial Robotic Systems

Industrial robotic systems are intelligent and flexible mechatronic systems for the purpose of automating a process. Common applications of robotic systems typically fall into three categories which are of direct benefit to industry.

1. Reduction of human labour
2. Improved quality control
3. The replacement of human labour from hazardous or uncomfortable tasks

All factors in each application are interrelated, however, at least one of these will be the driving factor for an investment. Each application places a different requirement on the capital investment.

Automation is the only option available in an environment too dangerous for human involvement. The capital investment of such a system is therefore only limited by its overall commercial venture. In the case of manufacturing high value goods, the return on the automation system is weighted against improved quality control and consistency. Either of these direct benefit cases can make a business case allowing a high cost automation system. The benefit to NZIC's customers is through the reduction of the human labour cost per unit of production. Making an investment case for this benefit can be more difficult as the system is competing with people on a solely cost basis. In this case, the automated system is aimed at cost reduction rather adding value to the product. The direct competition with human labour makes the design of such an automated system difficult since there is a much tougher return on investment: A person is a very flexible unit of work and human labour can be relatively cheap.

An industrial robotic system can be broken into various functional components. The following paragraphs present a brief overview of each component. They will not be explained in detail since each component alone is also a vast area to study. Instead several images are shown at the conclusion of this section, which are relevant to the later document materials.

- Mechanical Structure

  This is the mechanical system of the robot that includes the overall base, joints, linkages, actuators etc.

- End Effector (EE)

  An EE is the device attached to the end of the robotic structure that is commonly designed for a specific purpose. Common EEs are devices such as grippers, pneumatic vacuum cups, various welding tools, spray guns, automated measurement tools, etc.

- Power Unit

The power unit is not an entirely separate device but is often separated as a form of the robot actuation system. The common forms of power sources are electric servo motors of various supply, and drive-line configurations. These offer high torque to size ratio and good control behaviour. Cheap systems may utilise simple brush DC or stepper motor forms of actuation. Hydraulic or pneumatic actuators are also common with high load applications.

- Control System

  A means of sensing system inputs and controlling the actuators is achieved with a control system. Today, various forms of control systems are available and suited to different applications. Control systems can be based on embedded electronics, programmable logic controllers or industrial PCs. More recently, controllers are offered in increasingly integrated purposes or suited for centralised controls. Examples of this pattern are intelligent servo drivers that run internal control routines and other distributed IO instrumentation. The non-electronic control systems described earlier are virtually confined to history.

There are many different types of robot structures, actuators, EEs, and control systems used in industrial robots. Figure 2.1 shows an articulated robot moving a work piece between stations. The different elements that make up a robotic system are visible. The mechanical unit is primarily the orange structure attached to a fixed base. Electric servo motors are visible at the base, and joints plus pneumatic grippers form the actuation system. Cabling and pneumatic solenoids can be seen to interface with a hidden electronic control system. Finally, a pinch type EE is just visible above the work station. Figure 2.2 is an articulated robot for handling glass panels with a large pneumatic vacuum cup EE. This robot is designed by Kuka. The robot shown in Figure 2.3 is also an articulated or Z type robot from Kuka that is for palletising within a bakery.

Figure 2.1: An articulated robot moving a work piece between stations (Photo courtesy of Berthold Hermle AG)

Figure 2.2: An articulated robot handling a glass panel (Image courtesy of Kuka[80])

Figure 2.3: An articulated or Z type robot for palletising within a bakery. (Image curtsey of Kuka[80])

2.3 Existing Automatic Packing Systems

Existing competitors to the NZIC and the occasional start ups have tried or attempted the automating the packing of OBJs. The existing prototype or limited commercial systems can be described generally as either pattern packing or single pick and place units. Pattern packing units are the most common and vary from very basic fixed operations to slightly more intelligent and flexible systems. Generally, these pattern packing units are a customised design with basic control and actuation technology for motion.

2.3.1 Existing System 1

The first system illustrated in Figure 2.4 shows the working principle of a unit produced by NZIC's largest competitor and is produced in both twin and single in-feed lateral loading versions. Information about this system is limited by the competitor's marketing material and recounts with production managers or NZIC's technicians.

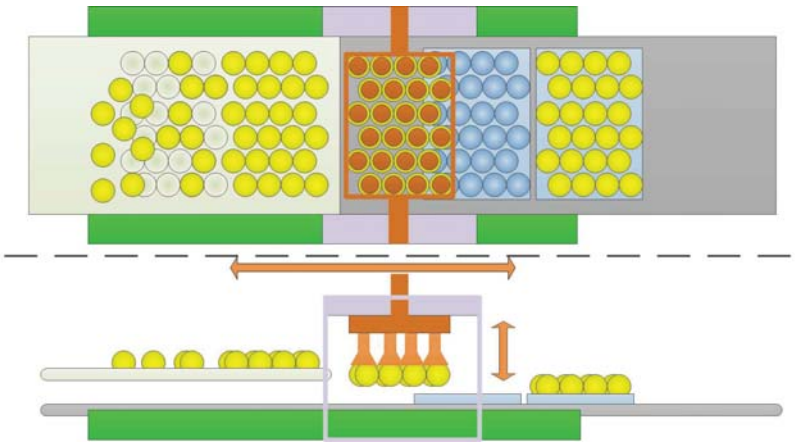

Figure 2.4: Existing System 1, plane view at the top, side view at the bottom

2.3.1.1 System Operation

The system does not appear to utilise feedback via sensor equipment such as machine vision or radar. Fixed teach points are the most likely method of directing the vacuum cup head. The system assumes that the OBJs are in the correct position and moves the head between two points. The design of the in-feed conveyor belt provides a pattern of recessed cups matching the tray format. No information is available that explains how the OBJs are delivered into the conveyor's cups. The OBJs are likely to be transferred to the conveyor with an approach similar to that later presented in Existing System 3.

Following are the unique features of this system:

- Packing guides
- Vacuum cup design
- Extended vacuum buffers
- Vacuum flow
- Lack of feed-back intelligence
- Quick release patterns

Guides are spotted around the edges of the tray as the vacuum cup head is lowered. The marketing material does not specify the operation of the guides and the images simply show them in the assumed final position. The assumed purpose of the guides is to guarantee that the OBJs will fit into the waiting tray as intended. The imagined operational procedure with respect to the guides is as follows:

1. The vacuum head moves to the correct position in the lateral plane.
2. The vacuum head lowers down level to the height of the guides.
3. The guides move inwards to the predetermined dimensions.
4. The vacuum head continues down to the tray and releases the OBJs.
5. The guides return to the original outer location as the vacuum head rises for the next pick operation.

The cup design is either customised design or supplied by a small unknown manufacturer. The vacuum cup has 3.5 bellows and a wide surface cup at the bottom. The addition of a "separate" cup at the base is a rare feature. Multiple bellows are common when handling spherical objects; however, the additional cup at the base is of interest and probably a customised feature. The increased cup surface at the contact point could improve the seal and may be helpful with non uniform surfaces. The downside to the increased surface of the vacuum cup is the decreased flexibility to deform and match the OBJ's geometry.

The buffers for the vacuum cups are of an extreme length and would have to be for a specific reason. The extended buffers may provide two benefits; firstly to improve the vacuum flow at the cup and secondly, to introduce an element of tolerance to the grasping of the OBJs.

The images of the vacuum head show that the tubing is of a wide area and restricted to low vacuum depths. This pipe gives a clue that the system uses a low pressure but high flow vacuum.

A simple mechanical or fluid type gauge is located on the top of the vacuum head. There is unlikely to be any feedback since there is no visible electrical conjugate and most important reading of vacuum pressure is via simple gauge.

Visible in photos are quick release latches around the vacuum cup head. To solve the problem of different tray layouts the system's solution is to change the vacuum head pattern. Changing the vacuum head is a cumbersome solution to producing a flexible grasping unit. However, it is a low cost option of simply changing the head which is likely to include only a sheet of aluminium, seals, vacuum buffers and cups. The quick release on the vacuum head however does not solve the problem of different required patterns on the in-feed conveyor.

2.3.1.2 Evaluation

Producing an accurate evaluation of the system's performance is difficult with no available statistics, images, or video of the system in operation. It is difficult to believe that the system provides reliable handling due to lack of control intelligence at the vacuum head. Even the marketing material shows OBJs incorrectly aligned. A point of note with the system, is that there appears to be no reliable singulation system that directs the OBJs to the in-feed pockets.

A brief discussion with people who have seen the system in operation did do not give a good picture of the system. People are highly involved within the operation, dealing with the unreliable nature of the handling, however, it does greatly increase the packing rate per person. The system is perhaps the most mature and many of the unique features appear in later design iterations. The most important point to learn from this system is that of the extended vacuum cup and buffer design.

2.3.2 Existing System 2

The system shown in Figure 2.5 is a twin in-feed rotating loading unit for the packing of products similar to OBJs into boxes. The system is probably the oldest of the systems examined and may no longer be in production. The OBJs packed by the system are of similar shape and mass to those intended by NZIC but are much tougher. It is unlikely that the same buffered approach can be used with NZIC's intended OBJs due to the potential for damage. The only literature found on the system is a single piece of marketing material. The material focuses on the angled design which improves OBJ alignment and reduces the movement for packing. The horizontal translation of this system is accomplished by rotating both heads around a common axis. The OBJs are supplied to each side of the machine with the tray or box located in the centre. Vacuum heads are positioned ninety degrees apart, resulting in one packing the OBJs while the other is picking up. Vertical travel is achieved with what appears to be an electromechanical linear actuator. The rotation actuator is not visible from the material. The vacuum head appears to be of the same design as System 1, but without the

refinements. Looking at the marketing material and clues from the images suggest that the control is via a simple PLC using teach points for guidance.

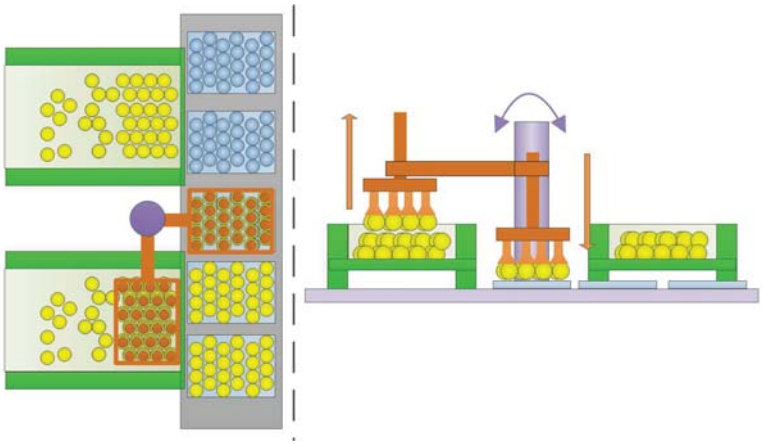

Figure 2.5: Existing System 2, plan view on the left, front view on the right.

2.3.3 Existing System 3

The third presented system shown in Figure 2.6 is another twin in-feed lateral loading unit similar to existing System 1. OBJs are supplied to this system from a shoot onto a pocketed conveyor belt. A vacuum head picks up the OBJs from a formatted arrangement on the in-feed conveyor and transfers them to a tray. The most notable difference between System 1 and System 3 is the design of the vacuum head. The vacuum cups are a very wide and deep with 5.5 bellows. An intersting point of the design, is the flexibility of the system's vacuum cups and conveying systems. The deflection of the system is so large that it must be a conscious feature built into the design. A video shows a surprising amount of vertical give in the packing process. The vacuum cups are seen compressing from their unloaded height of approximately 70mm to 20mm and the conveyor belt is deflected down by 30mm to 40mm. The downside of using multiple bellow vacuum cups and flexible conveyors is the lack of precision in the control and movement. This lack of precision can be seen in the video with the OBJs held at different heights, and offset, from the vacuum cups.

Literature about this system is scarce, although the marketing material mentions a PLC

for control and some information about "advanced" sensors. The control system implies the use of load cells and pressure sensors to limit the force applied to the OBJs. The material also mentions the use of load cells to measure the downward force and vacuum depth on the OBJs. It is not clear if each OBJ is sensed individually or the entire vacuum head. However, from the images and video, it appears the latter.

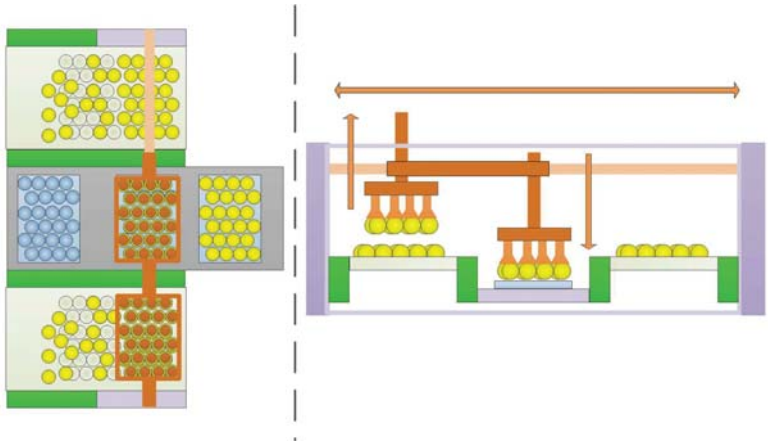

Figure 2.6: Existing system 3, plan view on the left, front view on the right.

The control system must measure the force or pressure applied and assume a reliable seal has been formed between the vacuum cup and the OBJs. An interesting point in the video is the presence of a person who corrects the OBJs' locations on the in-feed conveyor prior to the grasping by the vacuum head.

2.3.4 Existing System 4

The final of the pattern packing systems is a prototype that NZIC is aware of in existence. This system is still a pattern packer similar to the prior three systems, however it is more flexible during operation. The major advantage of the system is its patented mechanical structure that allows the vacuum cups to translate relative to each other. The vacuum head contains at least 8 stepper motors that drive the location of the vacuum cups. The patented system uses threaded collars to expand the distance between components from a common motor driven shaft. This threaded collar approach allows the adjustment between individual vacuum cups on each row and the distance between

rows. The layout of the system is different to those previous, with a single in-feed roller conveyor singulating and supplying the OBJs. The combination of the flexible vacuum head and different conveying assists with OBJ singulation prior to grasping the OBJs and also provides the flexibility to handle different tray layouts. Roller conveyors on the in-feed singulate the OBJs to an organised position prior to being grasped. This singulation is not entirely automated, with manual labour filling empty locations, however, the approach is more labour efficient than the prior three systems. The flexible vacuum head allows the OBJs to be grasped with the same format for any tray layout. Prior to grasping the OBJs, the controller directs the vacuum head to fit the format of the in-feed conveyor. While moving the OBJs the PLC directs the vacuum head to match the tray format. Control of the vacuum flow to each cup does not appear to be an advanced system. To pack trays of different OBJs counts, the cups are simply blocked off, and if one OBJ loses grasp during motion, other OBJs also drop. This points to the system not having individual control or pressure sensing at the individual vacuum cups.

2.3.5 Existing System 5

Another prototype system known to NZIC was intended to pack the OBJs with neither pole visible above the tray. The point of difference between this and the prior systems is the ability to manipulate the OBJs with one rotational axis. The OBJs are delivered to the system with a simple flat conveyor. The OBJs are then aligned into rows with lane dividers and delivered one at a time into a manipulation unit.

The manipulation unit consists of two parallel rollers with the OBJs in the centre. A laser line scanner and camera are utilised to identify the location of the north and south poles. The control system via a PC rotates the OBJs with the rollers until neither pole is visible. OBJs are moved from the manipulation unit to the tray with two small SCARA units that operate in tandem. The end effector of each SCARA unit is a 2-3 bellow vacuum cup. The system was originally planned to operate at over 100 OBJs per minute and is capable of doing this in a lab environment. Details about the real operation

indicates that performance around 50-60 OPM is possible but with a high OBJ loss rate. The system commonly causes crush or penetration damage to the OBJs while packing. To NZIC's knowledge, one system was produced for an investor but is no longer in use.

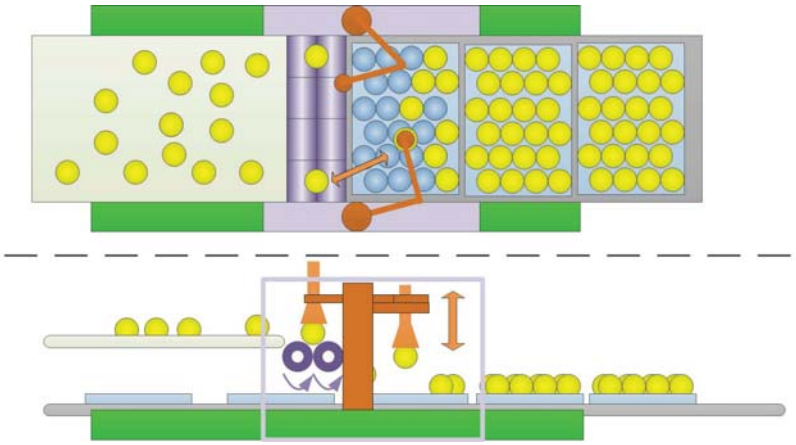

Figure 2.7: Existing system 5, plan view on the top, side view at the bottom.

2.3.6 Existing System 6

The remaining competing unit is the one system that is capable of organising the OBJ within the tray to NZIC requirements, it is illustrated in Figure 2.8. The machine has a multi-stage operation that picks up the OBJ, inspects for the pole and SROI positions, rotates the OBJ based on the inspection and finally places the OBJs in the tray. The operation of the system is broken down into five distinct steps with a cartesian robot moving the OBJs between each stage.

1. Pick-up:

   A cartesian robot with a pneumatic vacuum cup grasps the OBJs from the in-feed conveyor.

2. Pole alignment:

   The OBJ is placed on cup with what appears to be directed airflow to align the pole axis.

3. SROI alignment:

   A cup rotates the OBJ 360^0 on the pole axis in front of a vision system to identify the SROI. The OBJ is then rotated to the correct position.

4. Reposition:

   A vacuum cup rotates the OBJ 90^0 perpendicular to the pole axis so that the SROI is pointing up.

5. Pack:

   The robot transfers the OBJ to a tray.

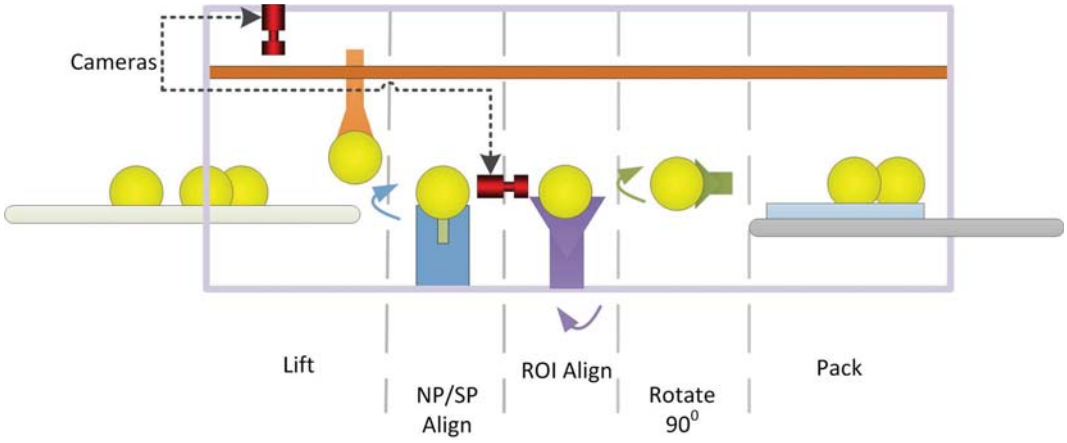

Figure 2.8: Existing system 6, demonstrating the staged layout of packing OBJs with organised layout.

2.3.6.1 Mechanical Structure

The Cartesian robotic structure uses linear drives consisting of ball screws and motors. The grasping is different to the systems mentioned previously by the use of a deep vacuum cup and pressure sensors. The grasp utilises a deep cup design instead of the normal multi bellow designs. In the images, the width of the vacuum cups appears wider than the OBJs. This wide cup approach is a different compared to the other systems mentioned earlier. They attempt to fit a vacuum cup to the OBJs surface, whereas this system effectively attempts to "plug the hole" in the cup with the OBJ. The pneumatic line connects to a small plastic device with a cable attached to the rear. The plastic device is almost certain to be a pressure transducer and likely utilised to determine if a seal has been formed with the OBJ.

Evaluation

This system is the only one capable of carrying out the task of organised OBJ packing. The commercial success of the system is unknown as no records have been found with the exception of the original articles. The company mentioned does not seem to exist anymore and no source could be found for commercial sales. The sources give a high expected system cost and a packing rate of approximately 25-30 OBJs per minute. Neither the cost nor the packing rate are close to commercial viability. The sourced articles make points of a payback in months with 75 units to be sold over two years. These statements seem very optimistic[2] from the figures given and most likely come from the intended manufacturer. Using NZIC's methodology for determining the payback, the realistic period would be at least 8 years for most customers. The system is unlikely to have become a commercial success as the rates and payback do not get close to reaching NZIC's requirements. While the developed system is unlikely to be of much use in its entirety, there are some aspects that could be useful and are not seen in the other systems.

- The pressure sensor on each of the vacuum cups should provide feedback of the vacuum grasping; other systems are severely limited by this lack of control input.
- Discussions explaining the operation of the image processing are of the most interest, in particular the use of artificial neural networks to determine the OBJ's poles and SROI.

2.3.7 Other Systems

Numerous other examples of packing the OBJs have been found using OEM robotics.

2 This calculation for the statement seems to be based on the unrealistic operation of a perfect supply of OBJs operating 24 hours a day, 365 days a year. Further, it does not take into account running costs including one technician per four machines. Labour pricing is likewise based on expensive UK pay-rates. Finally the system is compared to straight manual human packing rather than low cost semi automated approaches which are now common.

Many of these systems use standard OEM equipment and software from manufactures such ABB, Kuka, Mitsubishi etc. They are commonly used as a teaching tool or demonstrations from robotic manufactures.

2.3.8 NZIC Robotic Tray Picker

The robotic tray picker (RTP) as shown in Figure 2.9 is a fully automated machine that has been developed to pack OBJs of type B into trays. The machine uses two conveyor belts, an OEM PC vision system and an OEM multi axis pick and place robot. The central component of the system is a delta robot produced by the company ABB.

Figure 2.9: NZIC's Rapid Tray Picker.

Individual OBJs are delivered to the packing system by the in-feed conveyor. The OBJs are held singulated within a pocket on the roller belt. The belt passes under a camera that inspects the OBJ's position and orientation. The OBJ's position is passed to a robot controller that determines the pick and place motion. The tray position is already known with programming for each tray type. The controller then determines the motion curves for the cartesian and rotational axis, and feeds these to the robot's hardware. The presence of trays is determined by magnetic proxy sensors underneath the conveyor belt. These proxy sensors combined with encoders provide an assumed position to the robot controller. Prior to production, the final OBJ position in a tray is preprogrammed

in a fixed arrangement. During production, the controller simply cycles through the programmed positions until the tray is full. After filling the tray, the robot controller instructs the conveyor belts to move the existing tray out of the packing envelope and supplies the next empty tray.

2.3.8.1 ABB Robot

The NZIC flexpicker is built predominantly around OEM equipment sourced from the Swedish company ABB. ABB supplies the hardware for the actual robot and it's control hardware plus the control planning and machine vision software. NZIC integrates the sourced technologies into a structure for the industry.

2.3.8.2 ABB Flex Picker

The physical operation of moving the OBJ is achieved with an ABB IRB 360 Flex picker[7]. ABB flex picker is a robot commonly known as the parallel robot. The robot model has four degrees of freedom, namely three Cartesian and one rotational. The three Cartesian degrees of freedom are manipulated with three articulated joints that translate the end effector. The articulated joints are actuated with 500 watt servo drives. The fourth rotational degree of freedom is manipulated by a telescoping shaft between the EE and the robot's housing. The shaft is actuated by a smaller servo motor and gearbox combo.

2.3.8.3 ABB Flex-picker Control

The motion control of the ABB flex-picker is achieved with the corresponding control unit shown in Figure 2.10. The control unit receives the desired displacements from a higher level controller. The unit is responsible for the hardware control and internally generates motion profiles with configured constraints such as limiting velocity, acceleration, jerk and obstacle avoidance. The controller has several layers of hardware

that transform the abstract motion profiles to physical motion. A conventional microprocessor computes the path planning, parallel digital electronics generate motion profiles and then these feed to servo drives. The motion controller can be instructed via PLC for most applications; however, NZIC has configured the system to work with ABB's Pickmaster software.

Figure 2.10: Control cabinet to guide the Flex-picker's motion.

2.3.8.4 ABB Pickmaster

The system control of the NZIC flex picker unit works with a software product from ABB. The software has an abstract model of the real system that describes the system layout such as conveyor belts, sensor inputs (include camera), packing arrangements and grasp locations. Additionally, the software includes a basic machine vision functionality which locates the OBJ on the in-feed conveyor.

2.3.8.5 System Critique

NZIC's electronic media demonstrates the RTP operating and accomplishing the desired requirements of the system to a limited point. The system allows placement of OBJs in a tray with one degree of rotation available; this allows the OBJs to be orientated to fit into the tray pockets[3]. However, the ability of the machine to orientate OBJ_b is limited. The system partially relies upon OBJ shape for orientation, and is only able to it rotate to fit the tray. These two limitations produce a problem and reduce the ability of the packing company to maximise profits. Relying on the shape for partial orientation means the system can only rotate OBJs that are elliptical. Due to shape reliance, the system is unable to pack the primary OBJ_a and has difficulties with OBJ_b. Incorrectly orientated OBJs have to be rejected by the system; this results in the OBJ repeating the process. Each time an OBJ goes through the system it requires capacity of the machinery, and is vulnerable to additional damage. Secondly the rotation is limited to a vertical axis which limits the value that the system can add to the packaging process.

The NZIC RTP appears to handle the intended task very well and can pack at a rate of about of 90-120 OPM, which is equivalent to the performance of 2-3 people. The drawback of this system is the cost. Companies often call for a return on investment in less than three years. Analysis of its performance shows that it will require 8-10 years to provide a return on investment, which is too long for the market.

2.4 Review of Existing Systems

The systems reviewed provided the breakdown of known automated OBJ packing systems. No literature or material discovered has provided proof that any of these systems operate at a level of performance which is desired by the NZIC. Existing System 6 was the only unit that achieved the operational capability of fully orientating

3 One degree of orientation is necessary to pack non-spherical OBJ.

OBJs and pack a tray. This system, however, has not been proved commercially successful due to its low packing rate and high cost. Further the layout and working of Existing System 6 does not allow these factors to be greatly improved. The pattern packer type systems from Existing System 1 to 4 appear to operate to a moderate level of success. The commercial utilisation of Existing System 1 and Existing System 3 is known to NZIC, with Existing System 1 being at revision 6 in 2008. It is reasonable to assume both of these systems are still in commercial use; however, feedback from factory managers indicates these systems do not work anywhere near as well as marketing material suggests. The pattern packers work to a reasonable level with specific conditions and human involvement, although their reliability and lack of flexibility is a problem. All four utilise only PLC control and appear to operate in a simple pick and place operation, and rely on vague assumptions. The literature from manufacturers, and image inspection of these systems provides evidence of insufficient feedback. The systems seem to have no feedback to answer vital questions for the control system during operation. Fundamentally the control system should be able to answer the following questions:

- Are the OBJs in the correct position at the point of pick up?
- Are the OBJs held sufficiently by the vacuum cups?
- Is the waiting tray in the correct place?
- Were the OBJs correctly placed in the tray?

Without such knowledge, the systems can not operate unsupervised. Discussion with industry sources also identified the problems with steady reliability.

The marketing material from the companies is deceiving as none of the systems are completely automated. These systems move the OBJs to a tray or box with an automated movement but a person is still required to initially position the OBJs in the pocket conveyor before the pick stage. The necessity of including manual labour in the process does not significantly reduce the operating cost in comparison to the NZIC's or other existing labour assisted systems and appears to require a larger capital investment. An image of Existing System 1 during operation shows a number of vacuum cups

incorrectly lined up above the OBJs' centre. This is an example of where feedback could increase the reliability of the system. Information about NZIC's RTP is easier to obtain within the company. One operating problem for the RTP is the assumed position of the waiting tray. The position of the tray and its pockets is estimated with proxy sensors and teach points. The other existing systems appear to utilise a similar assumption

3 System Design and Investigation

NZIC's objective is to produce a new system that is capable of packing the targeted OBJs in a defined six degree of freedom format. The review of the existing systems has shown that no such system exists. Numerous small advantageous points have been identified for such a system; however, no major break through has been made. The first task to produce a viable solution, is to consider different conceptual options. In this chapter, the overall system layout and configuration will be investigated, developed and explained. Different conceptual solutions will be considered comparing technological constraints and the cost. This chapter begins with an abstract view of the system requirements, detailed costing and engineering design.

3.1 System Layout Overview

Looking at the highest level, the packing system approaches could be split into two different packing methods.

- Single packing movement

  A robotic hand could pick the OBJs off a simple flat belt and place them in a tray with the required orientation.

- Sequential manipulation of OBJ during packing

  The OBJs are subjected to different handling stages to be finally placed in the tray with the correct location and orientation. OBJs are manipulated by three main stages. The first singulates the OBJs, the second orientates the OBJs and the last places the OBJs in the tray.

The single packing solutions that immediately comes into people's minds are shaped by science-fiction or futurist media. Even technically skilled or aware people have difficulty differentiating between what is displaced in media and the current state of robotic

systems. The following section will outline why such a single packing movement is not considered in great depth.

3.1.1 Rejection of Single Stage Packing

The review of robot manipulators demonstrated many works attempting to mimic the functionality of a human hand and it's ability to handle OBJs. While many of these cases show the technological ability or potential to achieve these functions, the major difficulty has been their application to industry and producing a return on investment. An important aspect of this research work is the actual use of the system for commercial gain. The following sections demonstrate the commercial difficulty of using a single motion approach.

3.1.1.1 Humanoid Finger Type Approach

A person can, with some difficulty, rotate an OBJ to any orientation with one hand. The book, Humankind emerging from Campbell, Loy and Cruz-Uribe, has this statement, "The human hand is one of the most advanced mechanisms produced by nature."[8] To produce an artificial device mimicking a human hand is of great cost. The authors above give a total of 25 joints and 58 distinct possible motions[8]. A simple estimate for each servo controlled axis is at least $ 1500 when considering system components[4]. The total for producing a hand with the same controlled degrees of freedom would require $40 000 solely in servo control equipment.

In addition, the human hand is covered with nerves that allow an array of touch sensing across the entire skin surface. Investing a tactical matrix sensor, as used for touch sensing, returns a cost of approximately $1000 for each pad[5]. The coverage of a robotic hand similar to that of a human would require at least 15 pads and further $15 000. Each robotic hand would contain $55 000 worth of electromechanical

4 Including certified electrical equipment, cabling, mechanical fabrication of structure, assembling etc

5 Approximate price from manufacturer of 2D tactile sensors.

components prior to any fabrication and software.

As commercial analysis will later demonstrate, the system would require at least 6 units to pack at a functional rate. This would amount to a total minimum cost of $330 000 for all units.

One could argue that a much simpler design could be implemented using less fingers and avoiding touch sensing. The author has made a study and attempted simulating a 3-finger robot without touch sensing (via taping over their fingers). The task was very difficult and almost impossible, even with human reasoning and vision. The cost of such a unit is still prohibitive at around $18000 per unit and a total of at least $108 000.

3.1.1.2 Hybrid Approaches

Another option could be to grasp each OBJ once and perform a series of rotational manipulations in sequence. This would be a similar idea to the above using the finger type approach of picking up, rotating and then placing the OBJ in a tray. The approach could use belts or rollers and provides the benefits of fewer axes of movement therefore providing a reduced production cost. Because all the parts will be mounted on a robotic unit, it is necessary to use light weight and small components; which would significantly increase the cost. Additionally, since some components will need to be moved during the process, the mechanical packaging is complicated and additional actuators are necessary.

3.1.2 Reasoning for Sequential Packing System

The option of building a single stage packing system was rejected early due to the prohibitive manufacturing cost and its technological risk. The prohibitive cost is because the system depends on high end components for a flexible humanoid concept. Further examples of suitable intelligence based grasping have not been widely adapted

for this industry. Due to the short and medium term objectives, it is in NZIC's commercial interests to maintain the research scope to the integration of known technology. Considerable resources worldwide have been applied to these humanoid grasping devices. Realistically these are still at a base level of research and only a long term option for NZIC. Many industrial or applied projects have fallen into the trap of relying on developing base technologies and eventually running multiplies of time and budget over the initial plan. One famous example of this mistake is the F22 fighter that is 15 years late and a 20-billion over budget. This reasoning does not mean a single stage unit shall forever be excluded. It may be technically possible at some time in the future.

The decision to proceed with the sequential layout of the system is chosen by default since a single stage unit is not viable for near or medium term. A sequential system reduces cost and risk aspects through it simplified and technology tolerant design. This is, however, at the expense of limiting the best outcomes of performance.

The sequential layout has the following advantages over the single movement options.

- Reduces the complexity of the component arrangement

  Integrating different components becomes much simpler as interferences cause fewer problems.

- Fixed location for many components

  Many of the complicated components such as servo systems or sensors can then be located with a fixed position or utilised in a manner such that lower cost models are sufficient. Factors such as size, weight, accuracy, and speed all have a large effect on the cost.

- Reduced system development risk

  It keeps the system modularised, providing a large degree of independence for every module.

3.2 System Layout

The system consists of five sections to pack the OBJs with a defined format. Each section carries out the manipulation of one aspect for the final position and orientation of the OBJs.

1. In-feed

   The OBJs are delivered upon a simple flat belt. The nature of this system results in the OBJs free to move in any direction along the belt. The OBJs could be delivered anywhere across the horizontal location. However, they tend to form groups due to inter-OBJs interferences.

2. Singulation

   The first active component is the singulation stage that separates the OBJs from each other so that they can be manipulated individually. The singulation section collects the OBJs from the in-feed conveyor and delivers them one at a time to the orientation units.

3. Orientation

   The OBJs are delivered to the unit in a random orientation. The orientation unit rotates the OBJs to the correct presentation orientation prior to the pick and place movement.

4. Pick and Place

   The last active module picks up the the OBJs from the orientation unit and places them in the tray.

5. Out-feed

   The Out-feed is a flat conveyor belt that moves the filled trays out of the packing system and to another location in the factory.

The three active stages of the system are 2 to 4 which will be the new sections of this system. The in-feed and out-feed conveyors are in essence a conveyor belt driven by an induction motor and controlled by PLCs. The singulation system is not further investigated in detail. NZIC has their own considerable experience with such systems and this task is more about tuning to a specific application.

The remainder of this chapter will investigate the robotics involved in the pick and place portion of the system. The purpose of the following material is to investigate the overall robotic system design in terms of commercial viability.

3.3 End Effector Packing Arrangement and Layout

The optimal methodology to pack the OBJs is a balancing act between the unit cost, the packing rate and the flexibility of the system. Developing a system that packs each OBJ individually offers the most flexible system as it can pack any arrangement and offers, in theory, the cheapest building cost due to lighter loads. The downside to individual packing of OBJs, is that many overheads for the single unit still exist with a multi-OBJ system. The power output of a normal servo system in general, is not proportional to the cost. In terms relating to this discussion, it will not cost twice the price because it has twice the power. In an ideal case the grasp or release dwell period (GRDP) for 6 to 8 OBJs simultaneously is approximately the same time as grasping a single OBJ[6]. The goal is to pack at 200-300 OPM across as many possible packing formats. Commercially, the system seeks to maximise the OPM per dollar of capital investment while minimising the risk to NZIC.

3.3.1 Packing Unit Layouts

In this section, five generic packing formats are considered and will be evaluated for the their performance. Figures 3.1 - 3.5 show the conceptual idea of the given packing units. Three of these layouts are similar to some of the reviewed commercial systems, such as a single independent unit, twin independent units and a pattern packer. An optimised independent unit will be considered to verify the performance limit of its best possible case. The remaining proposal is that of row packing format.

6 The extra time is due to the grasp period being limited to the slowest of the 6-8 OBJs

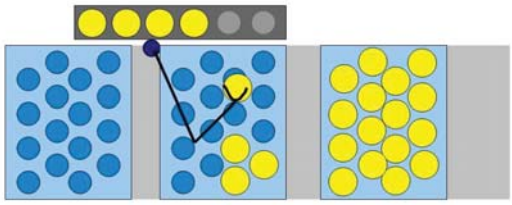

Figure 3.1: Single independent packing unit.

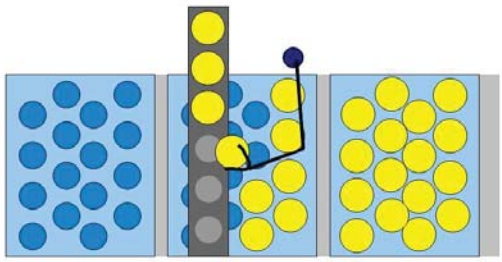

Figure 3.2: Optimised single independent packing unit.

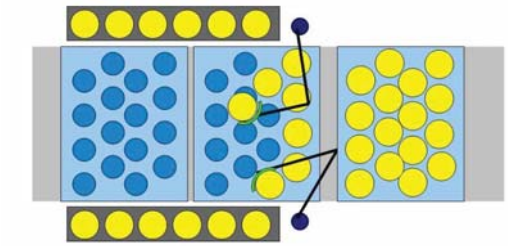

Figure 3.3: Twin independent packing units.

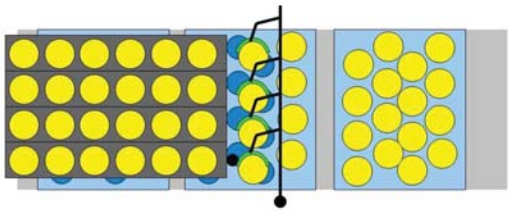

Figure 3.4: Row packing unit.

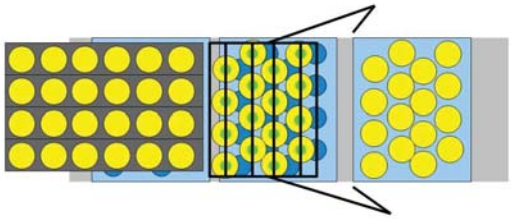

Figure 3.5: Pattern packing unit.

3.3.2 Background of the Analysis of Packing Layouts

To determine those packing arrangements that have commercial potential, basic kinematic calculations are undertaken as means of filtering. The purpose is to identify the performance robustness of each layout when subjected to a range of different operational constraints. Table 3.1 presents the commonly used packing variables and packing arrangements.

Table 3.1: Packing variables and arrangements.

Common packing variables	**Packing arrangement specific based variables**

• Packing rate
• GRDP
• Packing displacement
	• Single unit packing arrangement
	  ○ Variation of robot displacement
	• Multi unit packaging arrangements
	  ○ GRDP is based on Weibull distribution
	  ○ Tray Layout 6.5[7] x 6, 6 x 6, 6x5, 5.5x 4 OBJs

Following is the evaluation of the motion involved with the different packing layouts. As a first screen investigation, the motion calculations are based on the direct path from the initial to final positions. More detailed path simulations with way points will be presented later in this chapter.

To calculate the motion peaks for each of the packing formats, motion profiles are generated. Motion curves are generated using the fifth derivative of displacement (Jounce) to ensure a smooth motion. Figure 3.6 shows the motion curves generated for a unit movement (1m displacement in 1 second). Appendix *A.1 Matlab Code for Generating Jounce Controlled Motion Curves.* outlines the motion profiling code utilised throughout this research.

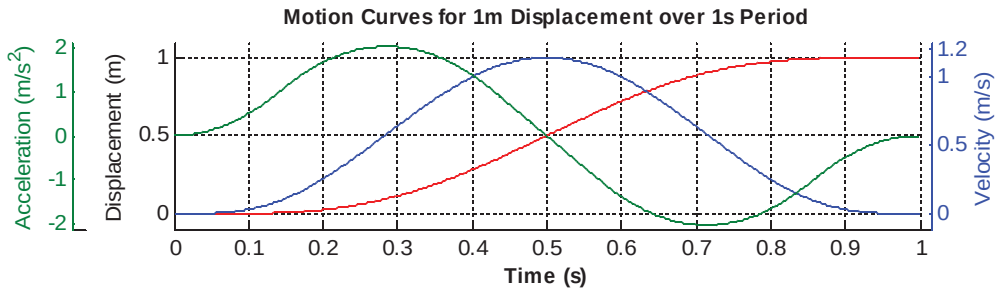

Figure 3.6 Motion curves generated for a 1m displacement over 1 second duration.

Many works in literature or suppliers of OEM equipment form the servo motion curves with either the common triangle (the 3rd derivative) or S curves (the 4rd derivative) polynomial approaches. In these cases either the acceleration or jerk is set at maximum

7 Half values correspond to asymmetrical layouts. The half value is the average OBJ count per row.

value when generating the curve. NZIC's and the author's experience with the RTP has demonstrated that the delicate surface of the OBJs requires very careful application of jerk and acceleration. This can be attributed to the main difference between this research project and the common application of automation. In many industrial applications, the difference between manipulating and damaging a object is relatively large which gives the system a large margin of safety. In the case of NZIC's industry, the difference between manipulating and damaging an OBJ is comparatively small. For this reason, a more delicate motion curve is required.

3.3.2.1 Description and Effect of Generic Variables

The packing rate is the number of OBJs that can be packed in a tray over one minute. The lower limit of 120 OPM, is the limit where the system would have to pack regardless of the economic values. For a limit less than 120 OPM, the factory manager can not justify the factory space. A production packing rate of 200-300 OPM is the goal. In order to balance the return on investment, the system should pack as fast as possible to allow a high market return. However, if the packing rate exceeds the OBJs supply rate then capital costs will be higher than required.

Grasp or release dwell period is the time required for the system to securely grasp or release the OBJs. This period is a critical performance aspect as during this time the OBJs are not moving towards their final positions. Depending upon the packing format and rate, a certain period is acceptable for the movement. The longer the GRDP the less time for the motion between the two points. To maintain a fixed cycle period, a reduction in the allowed motion period has the consequence of an increase in velocity. Figure 3.7 demonstrates the effect on a generic movement using different available values in packing period. The graph shows the peak velocity, acceleration and jerk for the different packing periods. These motions curves are shown with three different displacements.

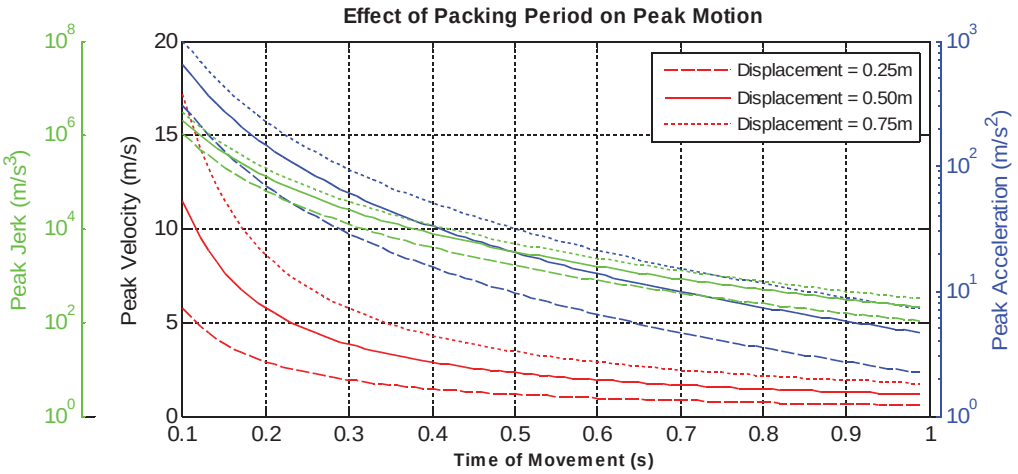

Figure 3.7: The effect of different packing periods on the peak motions experienced by the system.

One of the three generic packing variables is displacement. Similar to the motion period, a change in motion displacement requires a change in the motion dynamics to meet the given cycle rate. Figures 3.7 and 3.8 show the importance of each variable to the system packing capability. The effect of motion period in Figure 3.7 demonstrates the inverse exponential relationship between the period and the resulting motion derivatives. The exponential power is so great that the acceleration and jerk need to be displayed on logarithmic scales. The effect of displacement from Figure 3.8 shows a linear relationship between increased displacement and the resulting velocity, acceleration and jerk. The displacement changes do have an effect on the engineering of the final system however the linear relationship means that minimising displacement is not a critical aspect[8]. The conclusion upon inspecting the variables is such that minimising the displacement is of interest but the critical aspect is maximising the acceptable cycle time.

8 Typically the cost of equipment is not linearly relative to performance figures.

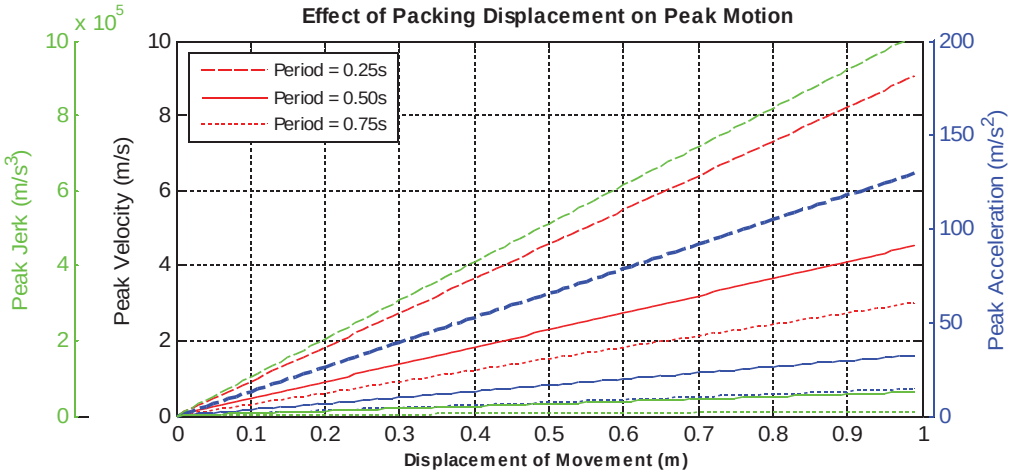

Figure 3.8: The effect of different packing displacements on the peak motions experienced by the system.

3.3.2.2 Description and Effect of Special Cases

The single EE unit layouts have a further variable due to the different displacements of OBJs within the tray. This means that either the whole packing tray must be calculated prior and use different displacements to balance or the motion peak must be changed for each cycle. The effect of the displacement changes has been explained in Section 3.3.2.1 .

The dwell time for grasping and releasing of the multiple OBJ formats is more complex than that of a single OBJ unit. Whereas with the single OBJ system, the dwell time can be estimated by the mean grasp periods; multiple units are dependent upon the mean time and the probability density of grasp periods. The distribution technique is necessary as the system dwell time is limited by the longest grasp and release period. The greater the number of OBJs to grasp, the increased likelihood of a fault occurring. To model the effect, a Weibull distribution is utilised to determine the different dwell time for multiple packing units across different grasping behaviours. Figure 3.9 demonstrates the effect of different grasp period distributions on the dwell time of packing formats. Where t is the mean grasp period and k is Weibull shape factor.

The mean dwell time of a single end effector format is the peak on each curve. The mean dwell time of the 6 wide row packer is given by squares which represent lower 86th percentile, the mean dwell times of a 36 OBJ pattern packer are shown by the diamonds which represents the lower 97th percentile. The percentile for each packing format is found in Equation 3.1, with N being the number of OBJs per cycle.

$$Percentile_{OBJ\ Format} = \frac{N_{OBJs}}{N_{OBJs}+1} \tag{3.1}$$

The percentile biasing for the multi-OBJ format accounts for the packing cycle rate constrained by the longest grasp period of all OBJs, not the mean. Figure 3.9 shows the susceptibility of the multi-OBJs system to the probability density of the grasp period.

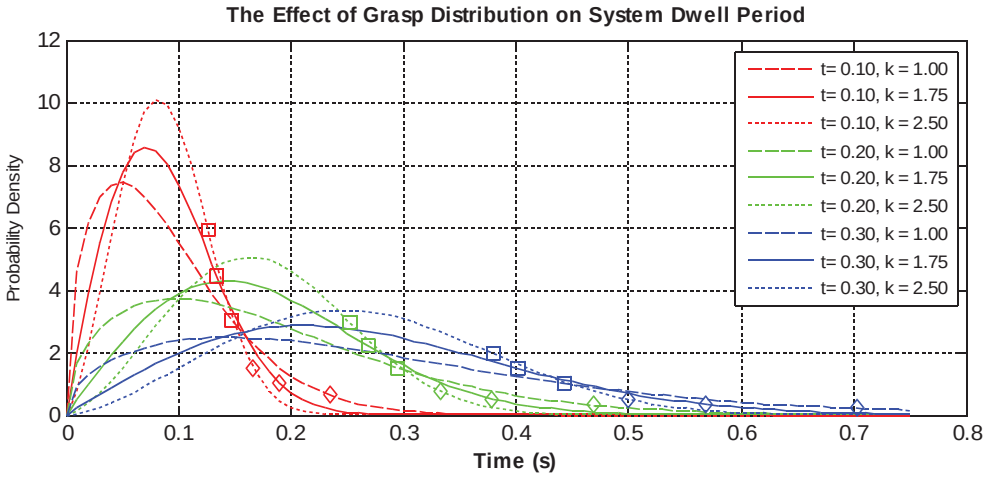

Figure 3.9: System dwell period from the behaviour of grasp formation.

3.3.3 Analysis of Packing Layouts

The filtering of the different layouts investigates the ability of each layout to achieve the necessary performance. For simplification, the ability of the unit to perform will be determined by the peak acceleration for the best, average, and worst case scenario. Appendix A.2 *Variables Setup for the Comparison between Pack Layouts* lists the variables set-up for the comparison between pack layouts.

Figure 3.10 shows the peak acceleration required to pack at the required rates for each of the explained layouts. The code for the legend is as follows: The prefix represents the packing layout, the suffix represents the system operation.

A number of lines can been seen to halt partway through the plot or in the case of SU-W and SOU-W they do not exist completely. A non existing graph denotes an arrangement and operating conditions that is impossible for the given rate. This is due to the GRDP exceeding the total available cycle period. Inspecting the plot, the single unit layouts are incapable of achieving the desired packing rates without the high performance, ultra light equipment and the grasp/release operating at the most optimistic performance.

The twin single EE layout performs better than the single version. Theoretically the twin packing unit could pack at almost the full range of packing rates. It should, however, be achieving 290 OPM with a normal operating case would require the ridiculous peak acceleration of 20 000 $m/s^{2,}$ ABB's 340 flex picker is known as high speed robot and has a peak acceleration of only 100 m/s^2.

The remaining multi-OBJs units both demonstrate the ability to pack OBJs at any of the given rates across the range of perceived operating conditions. A row format above 280 OPM and operating at the worst operating condition could however be pushing the limits of standard equipment.

Table 3.2: Prefix and suffix codes for Figure 3.10.

Prefix	System Layout	Suffix	System Operation
SU	Single unit	B	Best case
SOU	Single optimised unit	N	Normal case
TU	Twin unit	W	Worst case
Row	Row packing unit		
Pat	Pattern packing unit		

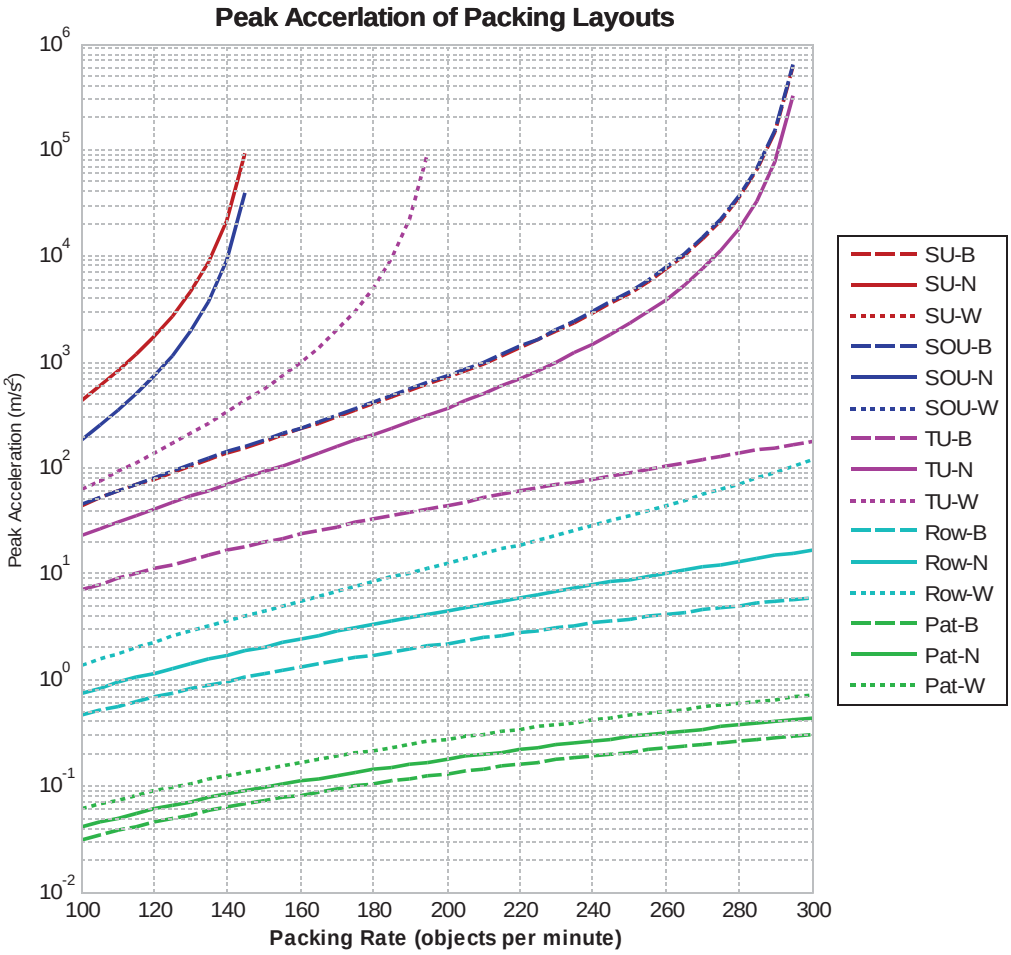

Figure 3.10: Peak acceleration of packing layouts.

3.3.4 Conclusions of Packing Layouts

The analysis of packing layouts demonstrates the theoretical peak jerk, acceleration and velocity for the five given systems. There are varying benefits for each of the outlined systems as already stated. The purpose of this analysis, however, is to filter out nonviable packing layouts. The layout with the greatest achievable packing rate and the least susceptible to the GRDP is that of the pattern packer arrangement. The pattern packer demonstrated the capability to maintain a solid performance for all, even for the worst of conditions. The single unit packer system is at the other end of the spectrum. Only layouts that pack multiple OBJ in one motion give evidence of a viable system performance. The conclusion from the theoretical analysis is that both the row packing and pattern packing layouts are capable of achieving the goals. The pattern packer does show a clear performance advantage over the row packer. In the worse perceived case, the pattern packer is still capable of packing at over 1000 OPM, compared to that of the row packer of around 280 OPM. The row packer, however, has an advantage for all aspects other than the maximum packing rate. The performance of the row packer while not to the level of pattern packer is still sufficient and does so with a reduced complexity. From a commercial view point, the row packer should be chosen due to the following reasons:

- Reduced capital research investment
- Reduced resources for research and development
- Reduced time to market
- Lower production cost

3.4 Investigation in the Practical Robotic System

The previous section determined the conceptual packing layout to achieve the project's

goal. This section will present the investigation into developing a real solution for the packing system. Three generic forms of a robotic manipulator are presented and analysed; an articulated arm, parallel, and a Cartesian style gantry robot. Each of the three robot structures will be explained and then simulated with the use of Matlab's Sim-Mechanics toolbox. The simulations of these robots are then utilised as a basis for selecting the most viable conceptual solution.

3.4.1 Articulated Arm Based Robot

Articulated robots can provide good flexibility to not only reach the intended positions but moving around obstacles throughout the motion path. The arm approach has further the advantage of using articulated joints which simplifies the process of protecting the unit from harsh environments.

A concept in figures 3.11 and 3.12 shows the layout of one such proposed robotic OBJs packing system along with a basic control system. The structure contains two main beams each controlled along their local Y axis. The two main beams control the XZ coordinate governing the centre of the EE knuckle. A wrist unit is made up of two moveable components that allow the knuckle unit to tilt and rotate. Individual EEs translate along the knuckle to grasp the OBJs.

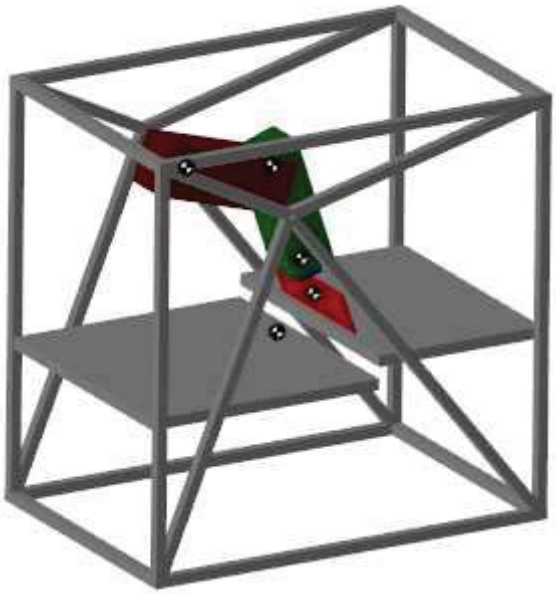

Figure 3.11: Articulated arm robot concept.

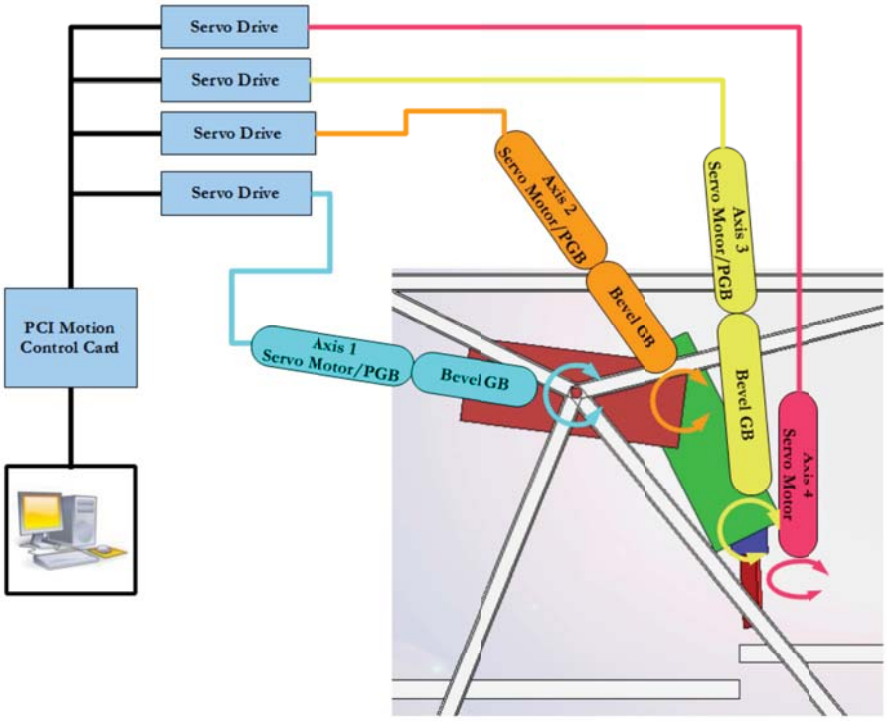

Figure 3.12: Articulated arm robotic system.

3.4.2 Parallel Based Packing Robot

The parallel structure uses a combination of actuator movements for each axis of motion. An example of a parallel robot is the ABB 340 that can move the end effector in three degrees of translation freedom plus a rotation degree. Parallel robots are not that common in industry for a number of reasons. However, due to the parallel inputs from actuators and the remote location of these actuators, the structure has the capability to operate at very high rates. The downside of the parallel or delta structures is the complexity of motion planning and the tolerance requirements for manufacture. The proposed structure shown in Figures 3.13 and 3.14 is a simplification of the three and four jointed parallel type robots. The XZ location is controlled with two main actuated arms (axis 1 and 2). A third axis produces the tilt of the EE and the means of fixing the XZ motion. A fourth axis of control twists the EE assembly.

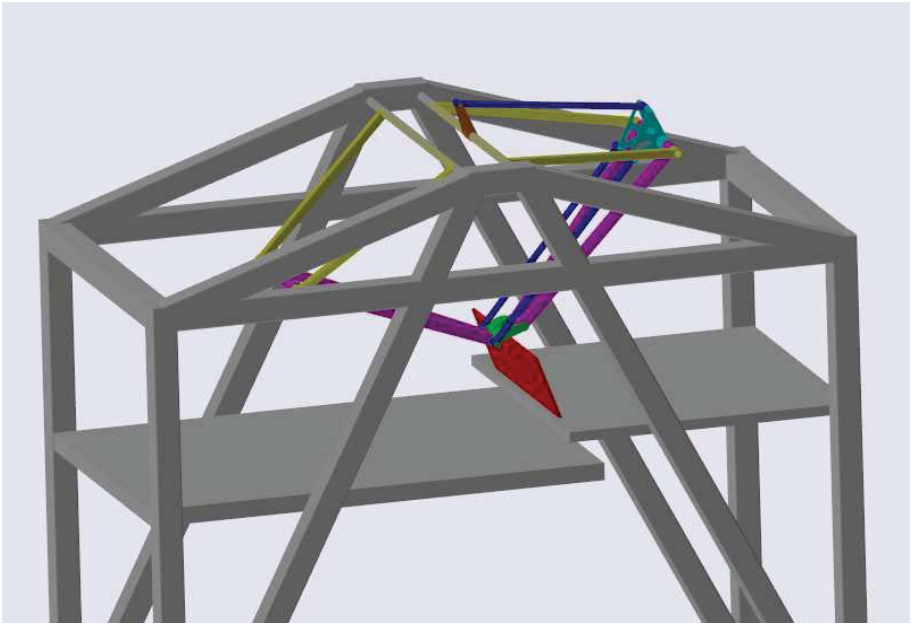

Figure 3.13: Parallel based robotic concept.

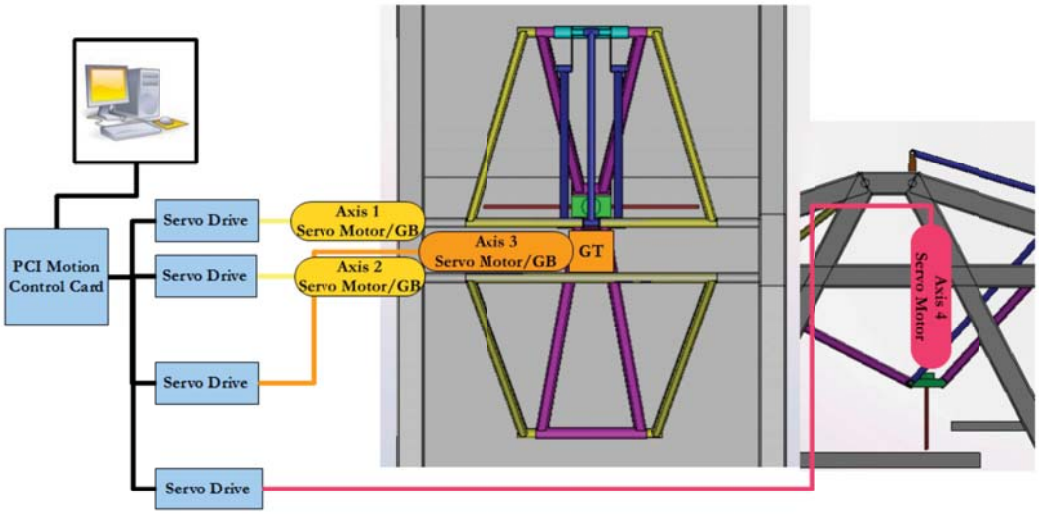

Figure 3.14: Parallel based robotic system.

3.4.3 Gantry Based Packing Robot

The final concept of the three robotic structures is that of a gantry. Common applications for gantry robots are in the motion of large/heavy systems or for precise movement. The structure proposed in Figure 3.15 demonstrates the layout with a simple gantry approach where each of the four degrees of freedom is controlled by a single axis of control. Linear servo manipulators control the XZ displacements. The rotation degrees of freedom are actuated via rotational servo units. The gantry system has the benefit of having a simple structure in terms of both control and construction. This simplest option for OEM manufacturers such as NZIC means a reduced production cost and ultimately, an easier ROI for their customers. The problem with gantry systems is the maintenance requirements due to contaminants on sliding surfaces and the nature of the structural loading. The articulated type (rotational joints) of the preceding structures minimised these effects by design. However, financially a gantry approach could work out cheaper by using a brute force approach to the problem.

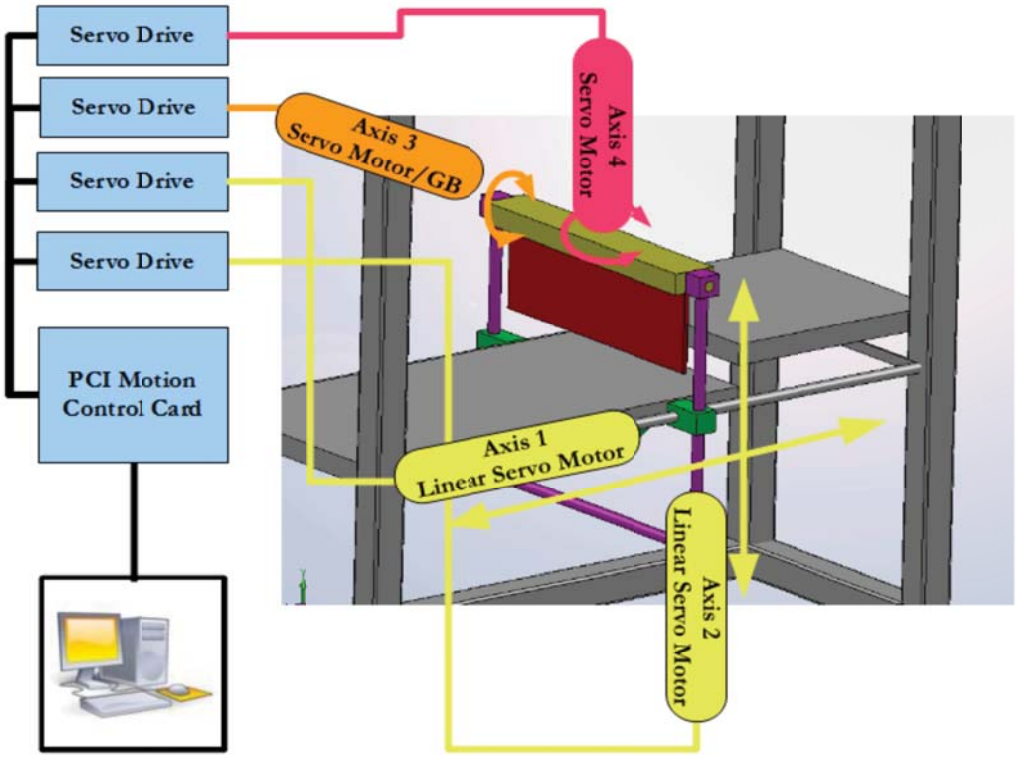

Figure 3.15: Gantry based robotic system.

3.4.4 Simulation Environment

Simulation of the three robotic concepts investigate the probable action and accuracy of various actuation constraints. Each system is modelled to an intended form using the CAD system Solidworks creating a conceptual model for each robot structure. The 3D CAD model is then exported to a skeleton Sim-Mechanics representation within the Simulink environment. The exported models from Solidworks are the theoretical mechanical representation of the core robotic system. The Solidworks adapter splits each assembly into separate physical representations of objects and joints. An object is a rigid body within the assembly; the adapter exports this as a mathematical description of its mass, centre of gravity, inertia tensors and a surface for visualisation. Figure 3.16 graphically presents the whole procedure of the simulation using CAD, Sim-Mechanics and the outcome.

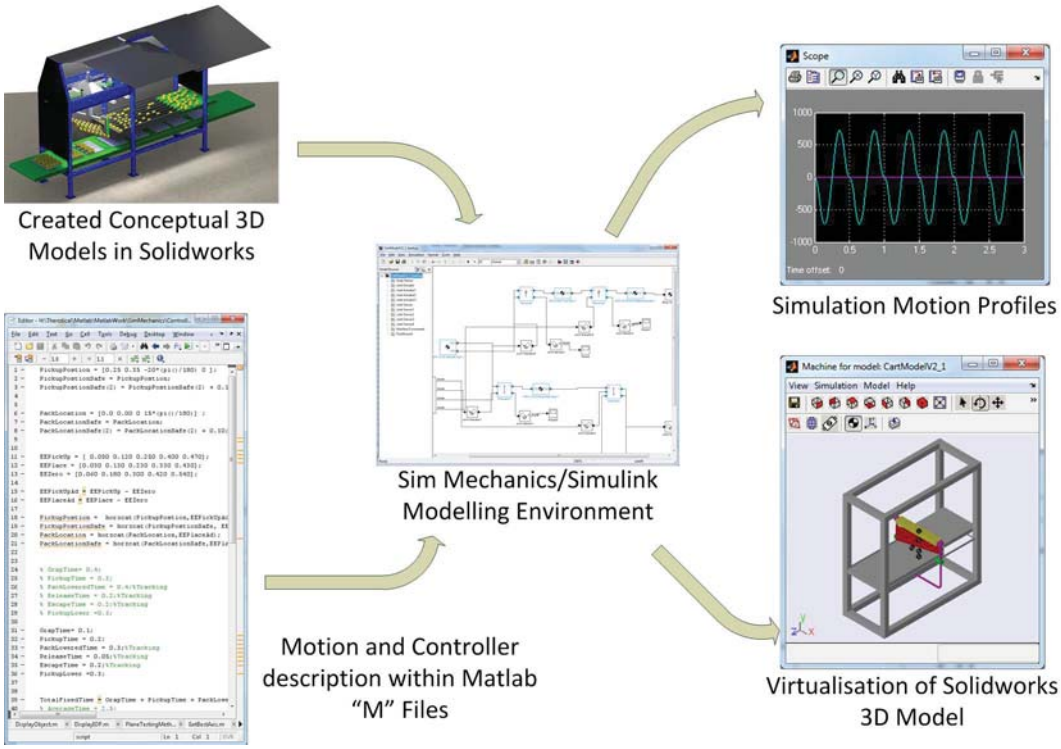

Figure 3.16: SimMechanics processes.

The joints are represented in the models as constraints or relationships between the separate bodies. The adapter takes these constraints and produces massless joints within the SimMechanics model.

The SimMechanic's physical robot model at this point is a representation of the mechanical CAD model with only the effects of gravity. To simulate the actuation on the system, the intelligent control components are added to the model.

- Actuator/Sensors
    - Actuators and sensors are added to the joints or bodies. These actuators can provide manipulation by either force or motion directly. The sensors provide the user with induced motion or the resulting torque/force.
- Controller
    - A hierarchical open loop controller is utilised to produce the motion profiles

for simulation. The top level is an abstract overview of the motion to move OBJ(s) between their initial and final locations. The bottom layer is programmed specifically for the robotic layout. The robot specific layer generates the applied motion profiles for each axis of control.

3.4.4.1 Experimental Factors

The modelled systems are simulated to determine the technical limits of each design and to investigate the "grade" of supplier equipment. For practical machine design, the simulation investigates two aspects of component requirements: induced actions and the susceptibility to actuator repeatability. The induced torques or forces investigate the degree of input required by each actuator. This serves two stages of design evaluation in one process. The designer can see if the required action is possible with any equipment and if possible gives an indication of the required grade of equipment. The susceptibility of design to actuator backlash or repeatability is an important consideration as this has a large effect on manufacturing cost. High accuracy actuator drives have considerable cost. Therefore, a design that allows a high tolerance to actuator position offers a significant price reduction.

3.4.5 Actuator Torques and Forces

Figures 3.17 through 3.25 demonstrate the degree of actuator inputs required by the different robotic structures. The three robotic structures are each illustrated with three actuator plots.

The first plot in each group is a force or torque waveform of the number 1 driven axis with a normalised cycle period to suit the different packing rates. The four different packing rates are identified with different line colours as shown in the legends. The second plot is the mechanical power waveform corresponding to the same actuator.

The final plot for each group is the waveform showing the torque or force for each of the four axes during the largest motion loading. Under the worse case condition of packing, this action is the most distant row of the tray at the highest packing rate of 300 OPM. Appendix A.3 *Robot Simulation Grasp and Release Coordinates* lists the coordinate location utilised for the motion and backlash simulations.

3.4.5.1 Articulated Robot Simulation

Figure 3.17 demonstrates the instantaneous mechanical power waveform through the packing cycle. Inspecting the articulated robotic system's power waveform, many manufacturers produce equipment capable of supplying the necessary peak power for packing rates 150-250 OBJs. The packing rate of 300 OPM requires a significant increase in peak power from the main axis; however, several manufacturers do produce capable drives. The significant increase of peak power and torque values is due to nearing the limits of a row packing solution. Figure 3.17 shows the theoretical peak acceleration rising from 8ms^{-2} at 250 OPM to 18ms^{-2} at 300 OPM.

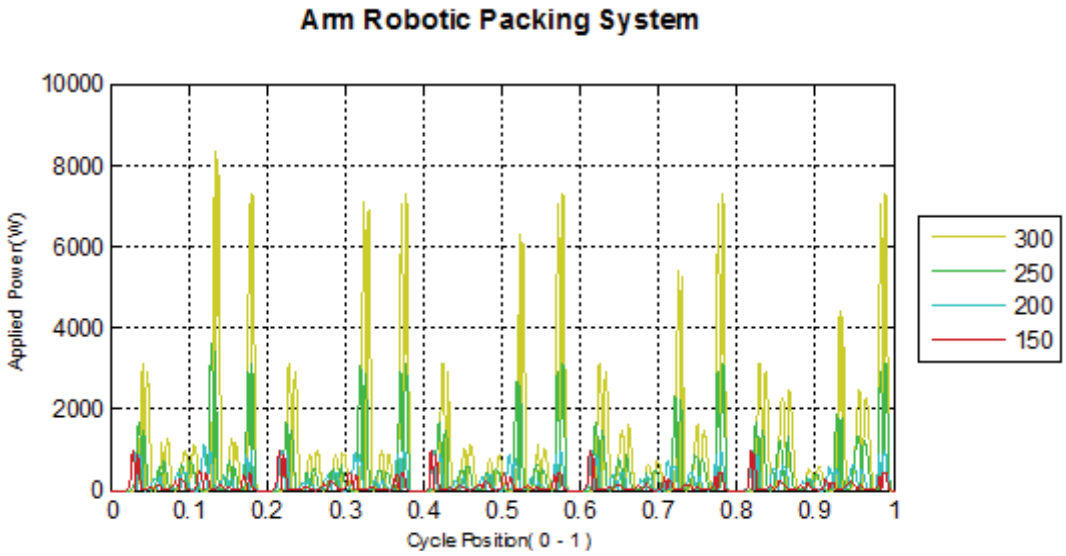

Figure 3.17: Power requirements of the articulated arm structure for axis one.

Figure 3.18 demonstrates the main actuator torque requirements for the articulated robot. The torque waveform shows high peak torques upon the full range of packing rates. The low packing rate of 150 OPM, requires a peak torque action of approximately 400 Nm; no suitable servo gear trains were found capable of such a high torque output shaft. Several industrial drive gearboxes were found capable of such a torque. However, none could be considered for precision motion. No suitable gearboxes manufactured in volume were found capable of producing the 1500 Nm of torque required for 300 OPM.

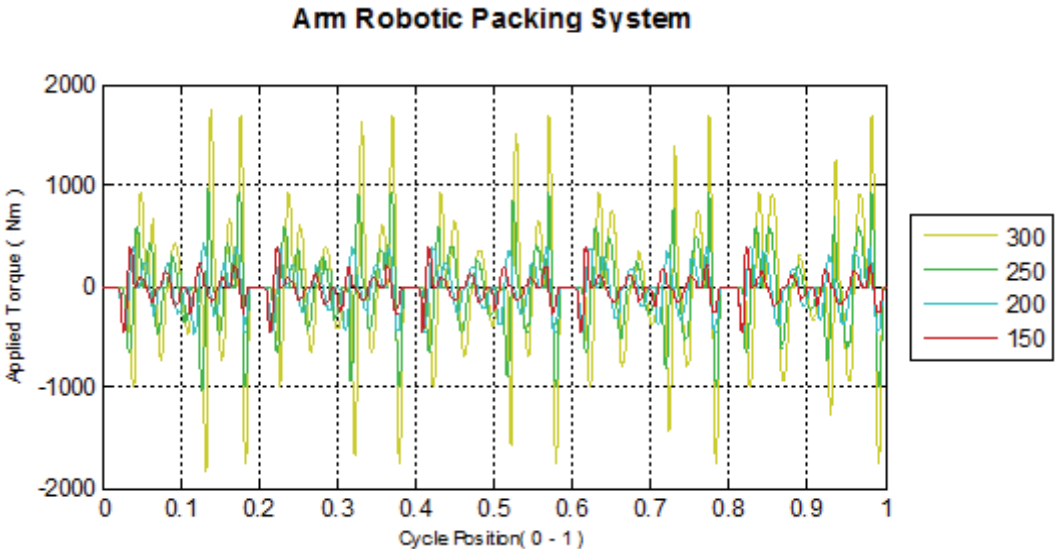

Figure 3.18: Torque requirements of the articulated arm structure for axis one.

Figure 3.19 shows that the unrealistic torque requirement is not limited to one axis. Axis two is seen to require a peak torque of approximately 400 Nm when subjected to peak packing cycle. The minor axes for controlling the tilt and rotation of the EE knuckle are both reasonable.

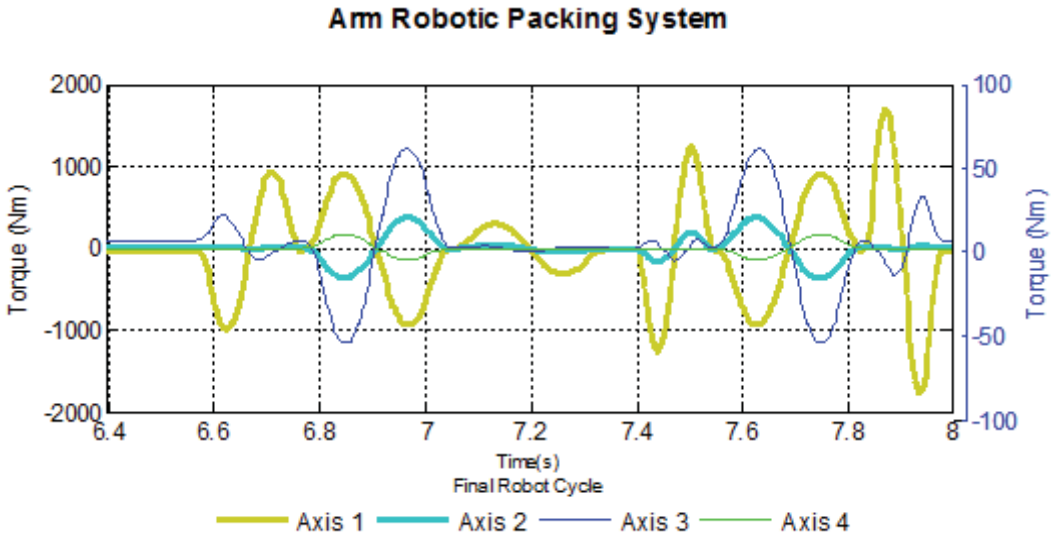

Figure 3.19: Torque requirements of the articulated arm structure during the final cycle of a tray.

3.4.5.2 Parallel Robot Simulation

Figures 3.20 to 3.22 demonstrate the simulated axis actions with the parallel robotic system. Figure 3.20 demonstrates the instantaneous power exhibited by one of the main axes. The peak power can be seen to remain below 1 kW across the whole range of packing rates. Remaining below 1 kW power limit provides the advantage of allowing single phase servo drives. There is no problem sourcing acceptable servo systems as all industrial manufacturers produce adequate equipment. Figure 3.21 demonstrates the torque profile for one of the two primary actuated axes. The peak torques involved are possible with standard manufactured servo drive-lines. However, drive lines that allow high peak torques seldom also provide low backlash.

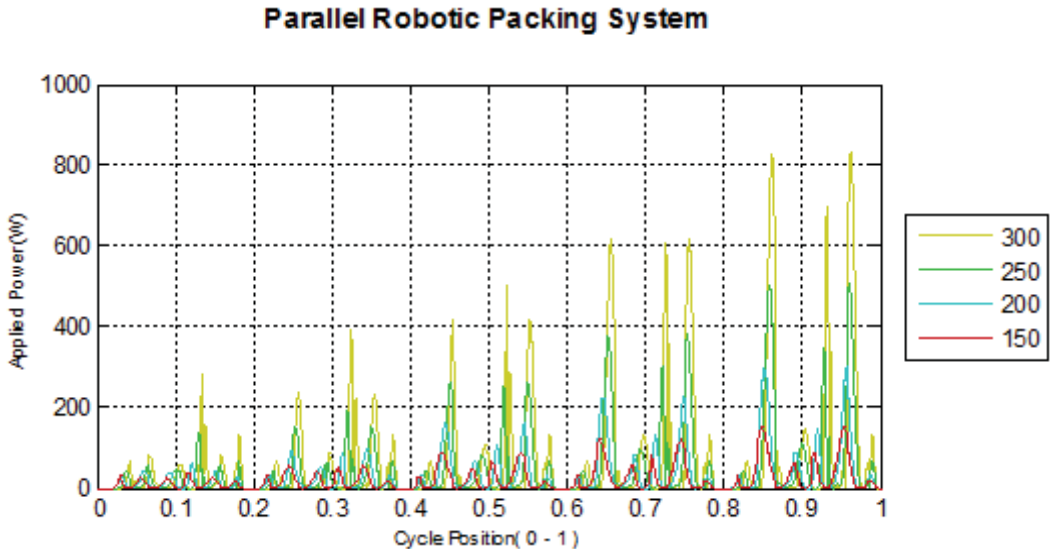

Figure 3.20: Power requirements of the parallel structure for axis one.

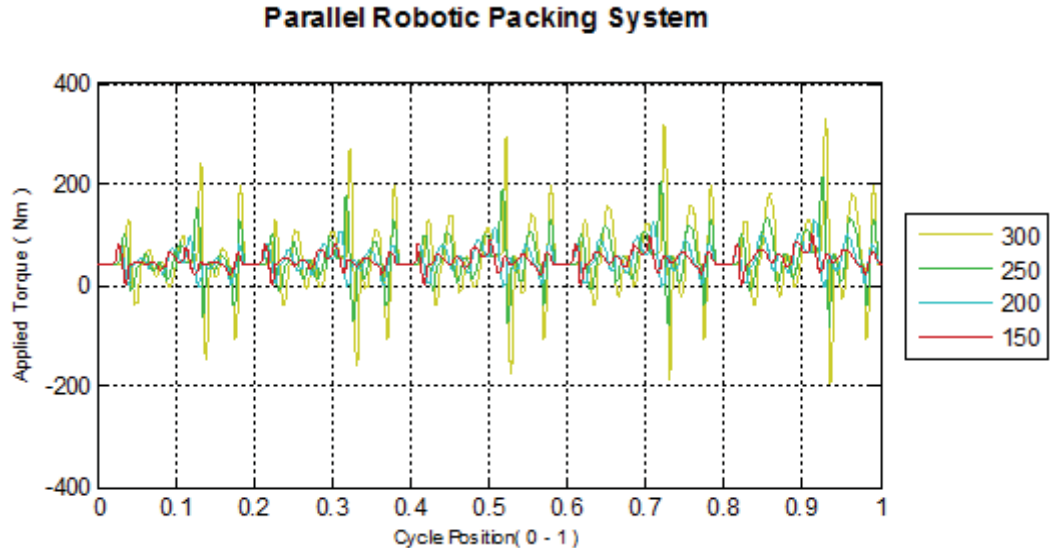

Figure 3.21: Torque requirements of the parallel structure for axis one.

Figure 3.22 demonstrates the torque pulses from all driven axes of the parallel system. The waveforms demonstrate that both primary driven axes have a high torque drive-line requirement. The knuckle tilting and rotating actuators have an approximate peak torque of 40 Nm which is a reasonable value.

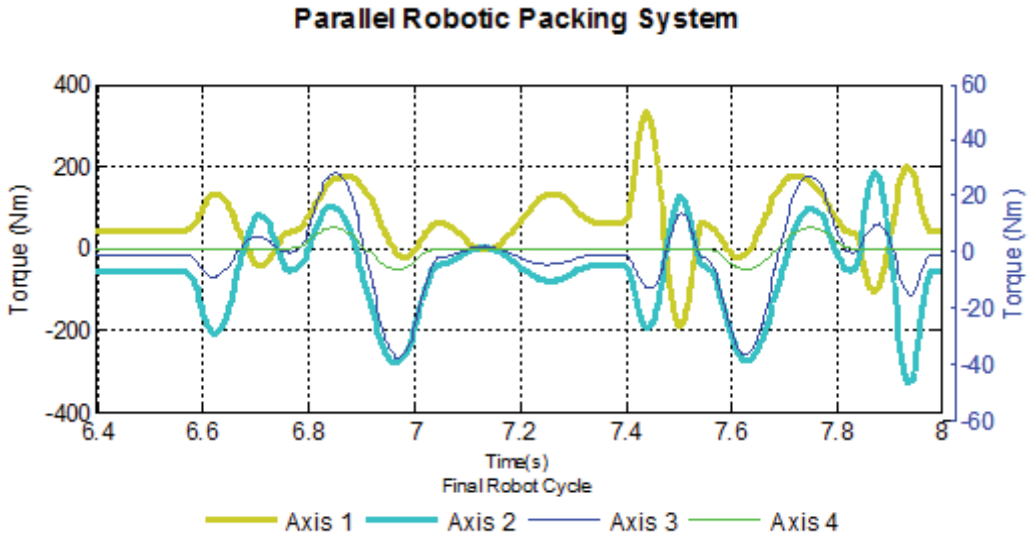

Figure 3.22: Torque requirements of the parallel structure during the final cycle of a tray.

3.4.5.3 Gantry Robot Simulation

Figures 3.23 to 3.25 present the robotic gantry motion response with the same operation constraints mentioned earlier. Figure 3.23 shows instantaneous power similar to the preceding robotic structures. A peak power of approximately 2.75kw is a high value for standard equipment; however, it is not excessive when considered that this a peak for a short period. Figure 3.24 demonstrates the peak force required by the main drive axis. Figure 3.25 further shows that this peak force is exhibited by both main axis drives. While the peak values are not excessive, this design will require two moderately expensive actuators.

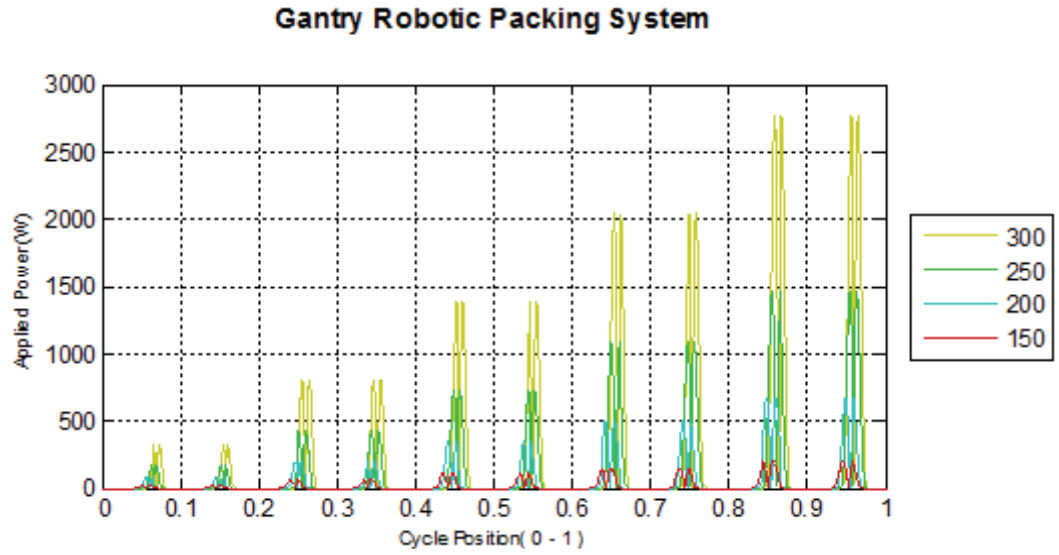

Figure 3.23: Power requirements of the gantry structure for axis one.

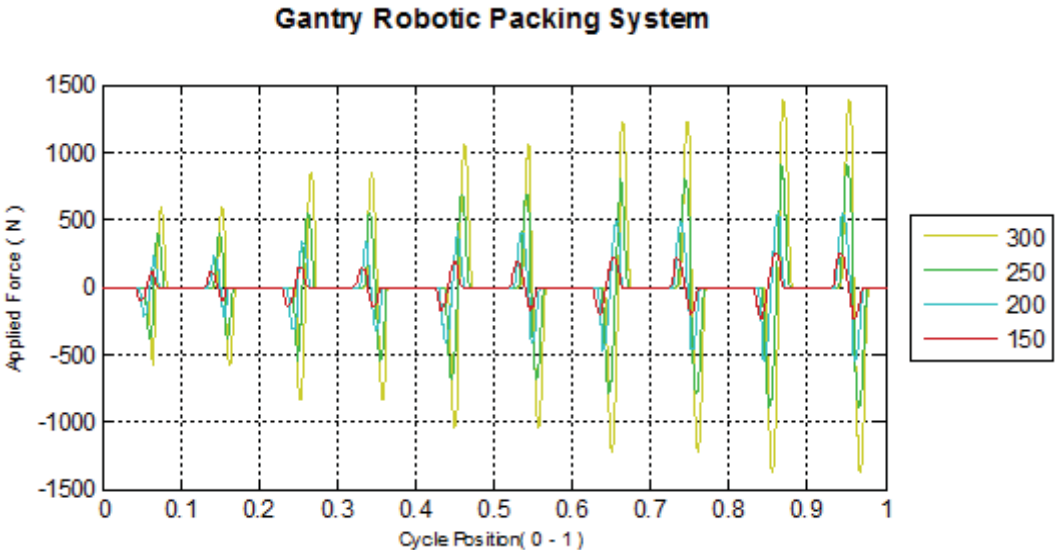

Figure 3.24: Torque requirements of the gantry structure for axis one.

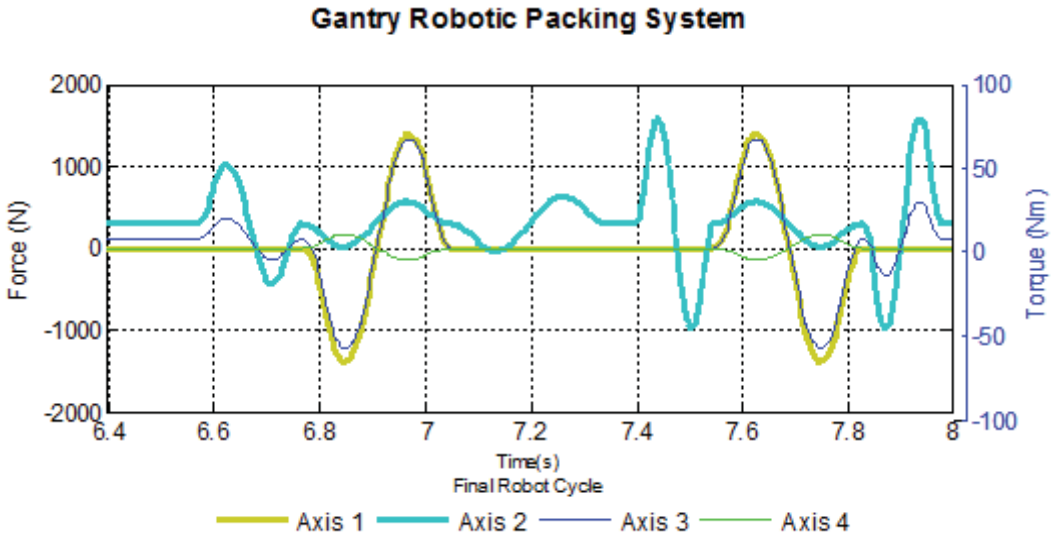

Figure 3.25: Torque requirements of the gantry structure during the final cycle of a tray.

3.4.6 Susceptibility to Backlash

Backlash is an important aspect because of the tolerance and cost effect. Systems that utilise rotational actuation are susceptible to such an effect due to the magnification along rotational levers and arms[9]. To investigate the susceptibility of the parallel and gantry structures, the effects of varying levels of backlash are investigated.

Investigating suppliers of servo actuators equipment backlash or repeatability are broken into four categories.

- Low standard precision → 20 arc-min
- High standard precision → 10-15 arc-min
- High precision →2-5 arc-min
- Ultra high precision or direct drive→ < 1 arc-min

The backlash effects are determined by utilising the simulation models to produce the relevant "free" movement of each actuator. The effect of backlash is tested at points

9 1 degree of backlash with a 1m long rod results in a translational end movement of 17mm.

of grasp and the multiple release points. For simplicity's sake only the axes that affect the Xc, Zc of the knuckle are examined, these being axes 1, 2 and 3. This simplification demonstrates the useful differences between the layouts and allows for a simple presentation. The following pick and place locations are tested to simulate packing a real OBJ tray.

- Grasp Locations
  - $[x_i\ y_i]$
- Row Release 1, 2, 3, 4, 5
  - These form the points $[x_{f1}\ y_{f1}]$, $[x_{f1}\ y_{f1}]$, $[x_{f1}\ y_{f1}]$, $[x_{f1}\ y_{f1}]$

The effects of the three movements are generated using the given points as the centre locations for each axis. The system is then moved using the 8 combinations (2^3) of possible +/- maximum backlash across the three axis. The result is an enclosed space given by the 8 resulting XY co-ordinates. This procedure is carried out for each of the four ranges of backlash and across the systems. Figures 3.26 to 3.31 show the possible backlash effect on each of the three different robotic structures. Varying degrees of backlash are tested against the resulting EE displacement. The effect of backlash is demonstrated by the resulting free spaces for each arc-minute (shortened to am) combination. The backlash for each structure is demonstrated with two plots; first at the grasp location and then at the different pack locations. The multiple test locations are necessary due to the rotational movement and it therefore has a non-linear effect in cartesian space. Ideally, the combinations of backlash should produce no movement in the cartesian space. Practically, this requires zero backlash or direct drive equipment that is of considerable expense. The grasp investigation to follow later in this document demonstrates that a 5mm tolerance should be acceptable for the application.

Figures 3.26 and 3.27 demonstrate the backlash exhibited by the proposed robotic arm structure in Section 3.4.1. The backlash is shown to have an inconsistent effect depending upon the desired EE location. The inconsistent backlash is notable in both the extremity of defined size and shape of space. Lower cost 20 arc-minute drive lines may cause an EE error of up to 30mm vertically and 50mm horizontally. To meet the

5mm maximum end effector error requirement, the structure would require ultra high precision equipment.

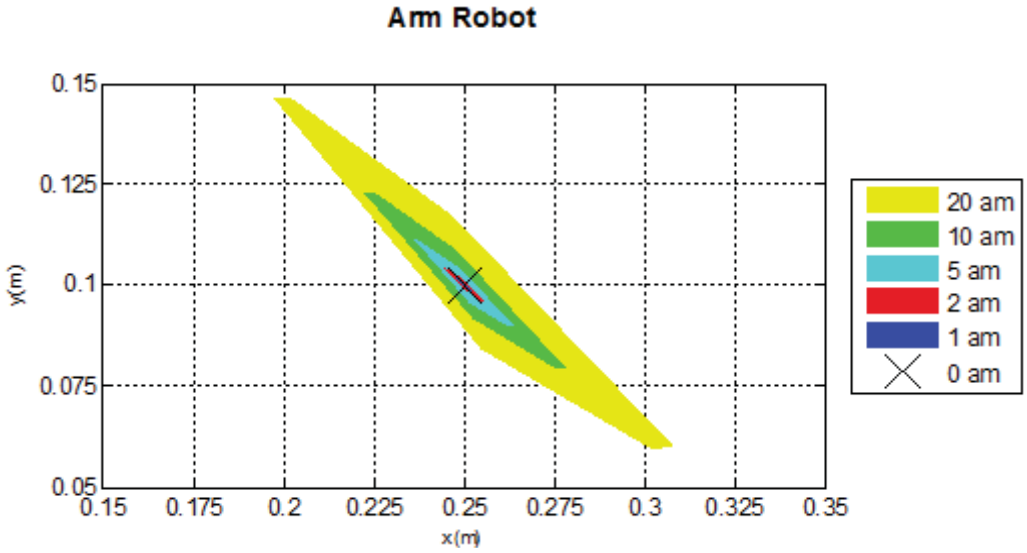

Figure 3.26: Backlash at OBJ pickup location for an arm stucture robot.

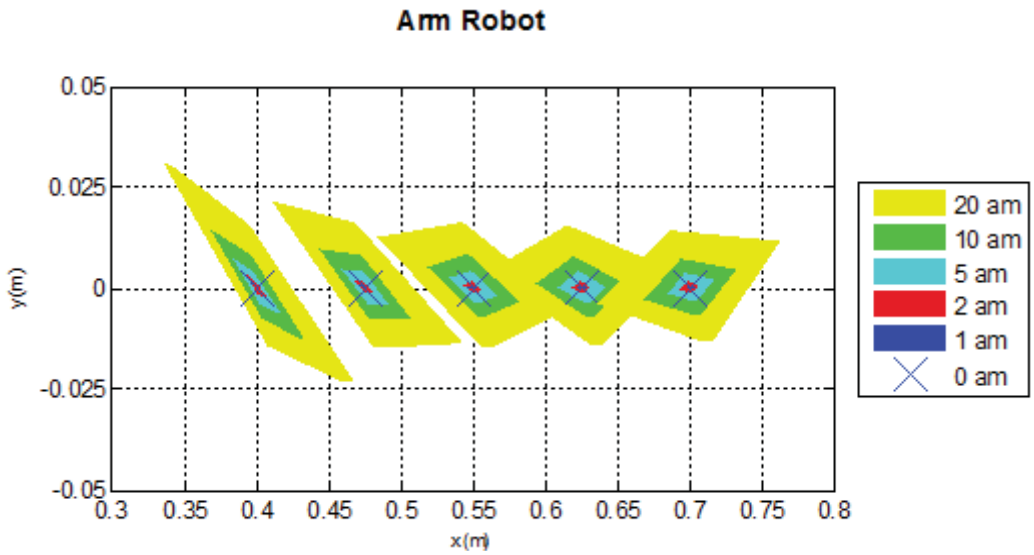

Figure 3.27: Backlash at OBJ placement locations for an articulated arm structure robot.

The backlash effect on the parallel robot is shown in Figures 3.28 and 3.29. Low precision drive-line equipment exhibited almost 50mm of movement vertically and approximately 30mm horizontally. The geometric space constrained by the backlash is relatively consistent compared to the articulated robot already presented.

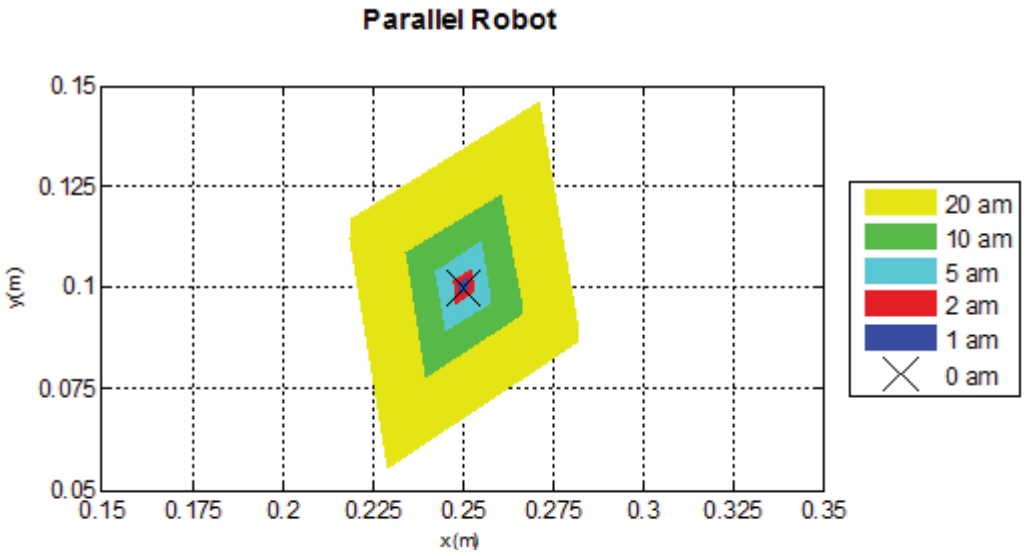

Figure 3.28: Backlash at OBJ pickup location for a parallel structure robot.

From the backlash region, it can be seen that higher uncertainty is in the vertical direction than horizontal. Having the robotic structure vertically inaccurate is potentially problematic since vertical irregularity in motion is more likely to cause damage. The simulated design layout would require high precession drive lines to meet the engineering specifications of 5mm EE tolerance. The shape of the backlash and the extremities however could be fine tuned by physical design to favour vertical precision. Figures 3.30 and 3.31 represent the backlash regions of the gantry robotic structure. The simple actuation of the robotic gantry produced regular shaped backlash regions that are even across all positions.[10] The effect of backlash is slightly less prominent than the two previous systems. The gantry system showed that standard servo type drivelines would provide adequate precision.

10 There is a minor effect from the tilt axes that is to small too see.

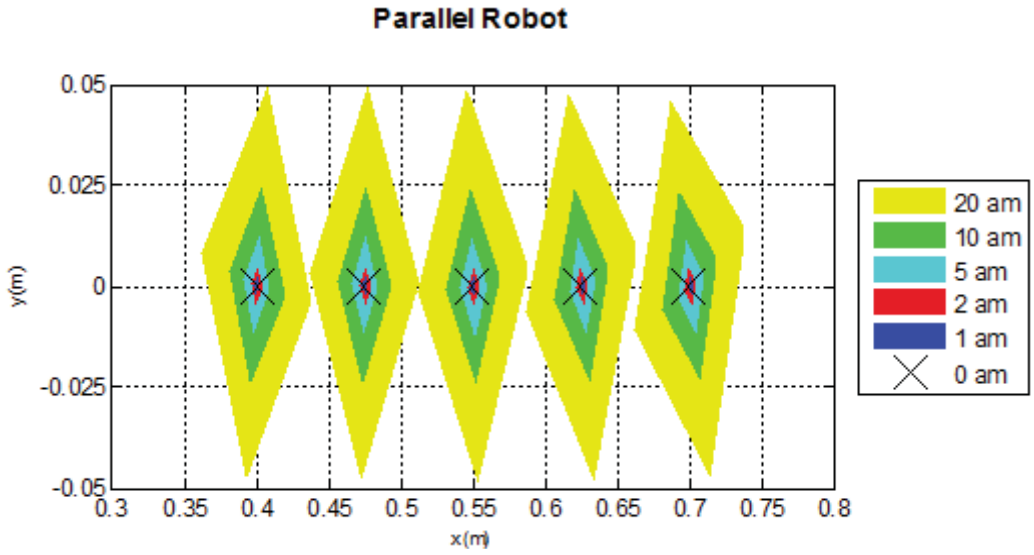

Figure 3.29: Backlash at OBJ placement locations for a parallel structure robot.

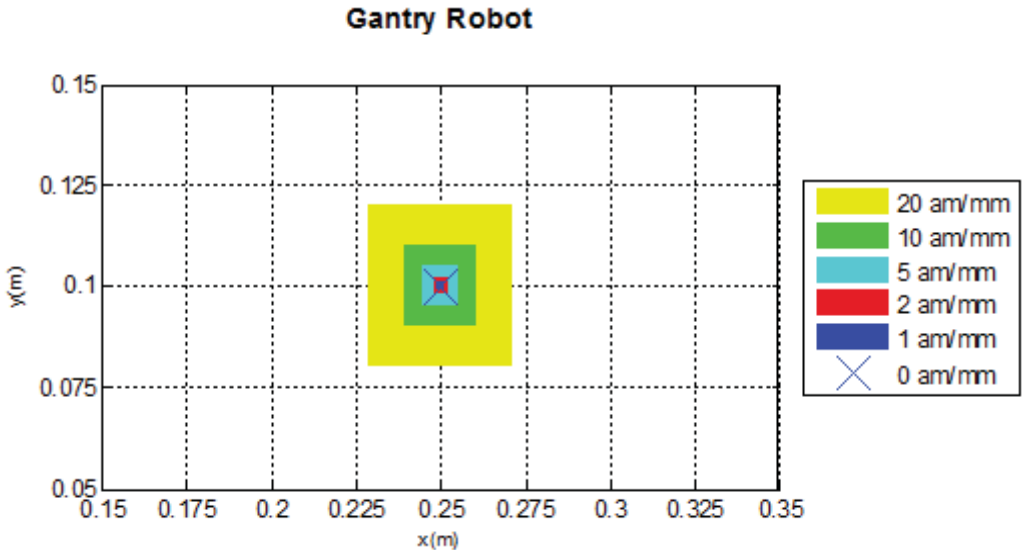

Figure 3.30: Backlash at OBJ pickup location for a gantry structure robot.

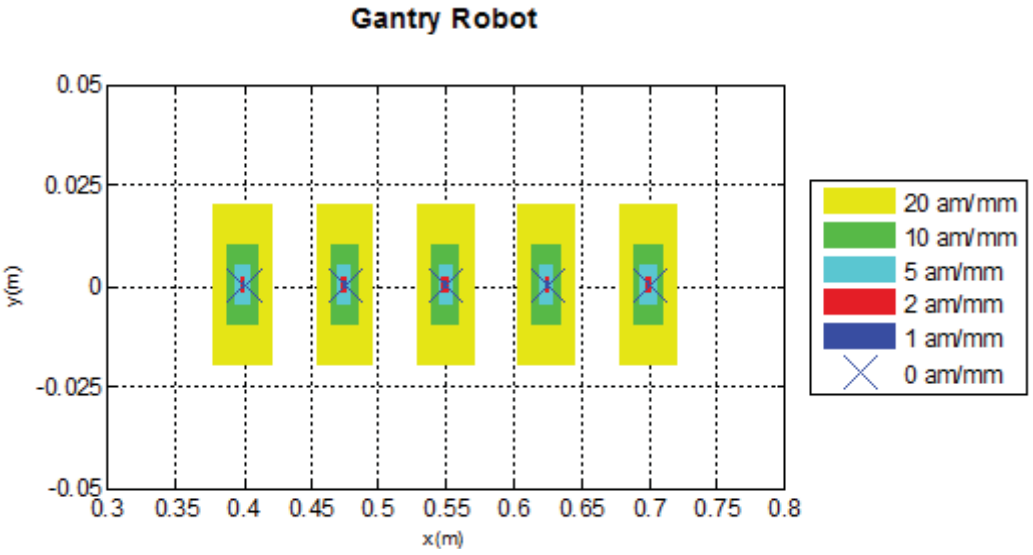

Figure 3.31: Backlash at OBJ placement locations for a gantry structure robot.

3.4.7 Review of Robotic Structure Simulation

The investigation of the packing format and SimMechanics simulations demonstrate that the row packing gantry robot is the best solution for the application. The articulated approach is likely to be technically impossible and certainly is impossible for a low cost application. The problem an articulated structure was that the torque requirements for the estimated mass was simply to great to become a high speed application. The parallel approach simulated for both motion dynamics and the effect of backlash has been shown technically possible with OEM components. The parallel structure from a theoretical point of view would be the most favourable of the three options due to its ability for high speed movement, limited size, and rotational axis. The downside to the parallel approach is the necessity of high performance gearboxes which for the given load are of considerable cost[11]. The robotic gantry system is the most viable system that allows the use of standard duty components and moves the high loading structure to low cost components.

11 The ABB flex-picker utilises 1 arc-minute gearbox

3.5 Gantry Development

The gantry structure shows the best chance of viability. In section 3.4.4 the simulation of the gantry structure was presented with the use of linear actuators. The actuation via linear drives demonstrates a good all around performance in aspects of both torque and repeatability/backlash. The downside to the linear drives is the cost and questionable reliability for the operating environment. Because of these applied reasons other actuation methods are sought. The use of a linear based actuated arrangement could be one of the following options:

- Power screw
- Rack
- Belt drive

Power screws have the greatest accuracy, however, they are limited to velocities under 1 ms^{-1}. Rack and Belt actuators have similar operational applications. They are best suited for high speeds with medium accuracy. Rack drives offer a solution that is more durable whereas belt drives offer a solution more tolerant to malfunctions. Belt drives offer a flexible link, which is both a weakness and advantage. The belt suffers a reduced operational life due to increased fatigue wear and eventually the breakage of the belt. The belt breaking can also be seen as an advantage since in the event of malfunction, it offers some give in system. A malfunction with a rack drive will almost always cause major damage since the fixed components take the impact. In contrast a belt in many cases will either break or loose contact with the driving pulleys thus allowing the impact to be reduced.

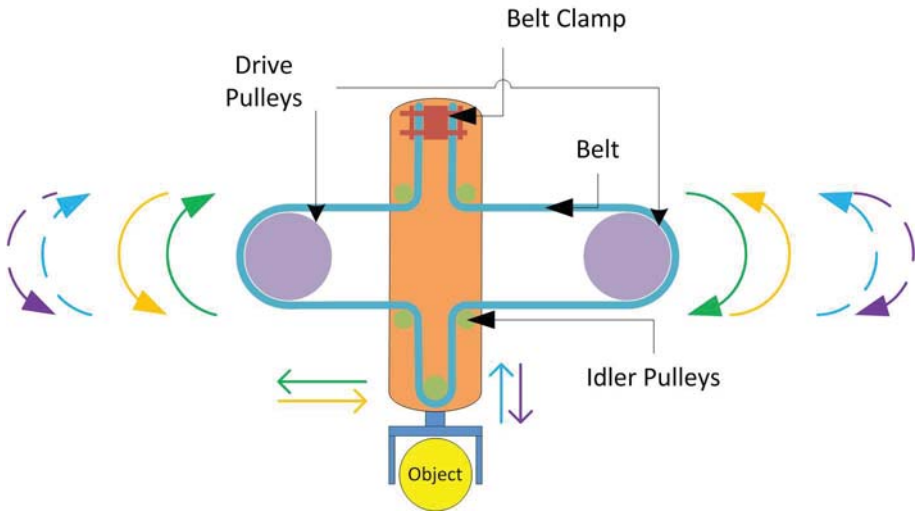

Figure 3.32: Layout of the differential drive.

Actuation inefficiencies are observed in the original gantry simulations. Upon inspection, the peak torque and force are evident for a small proportion of the movement; meaning, the actuation is oversized for most of the motion. The use of a belt allows a differential drive to be utilised. The proposed differential drive actuation system utilises a combination of two motors to drive the robot's knuckle in any direction on the XZ plane.

The combination of rotational actuators and a differential belt connection produces an optimised gantry operation. This layout produces motion actions that maintain smoother impulses. Figures 3.34 to 3.38 are the result of rerunning the original conceptual motion simulations with the developed belt driven gantry structure. Figure 3.33 is the instantaneous power required relating to the torque output. The smoothing effect due to the differential drive is apparent compared to the original gantry simulation. Figure 3.34 shows the torque action from one of the main actuators. What is observed is a greatly reduced level of impulse from the actuator. For 300 OPM the required peak torque is approximately 40 Nm, which is significantly less in magnitude and available with low cost drive-lines.

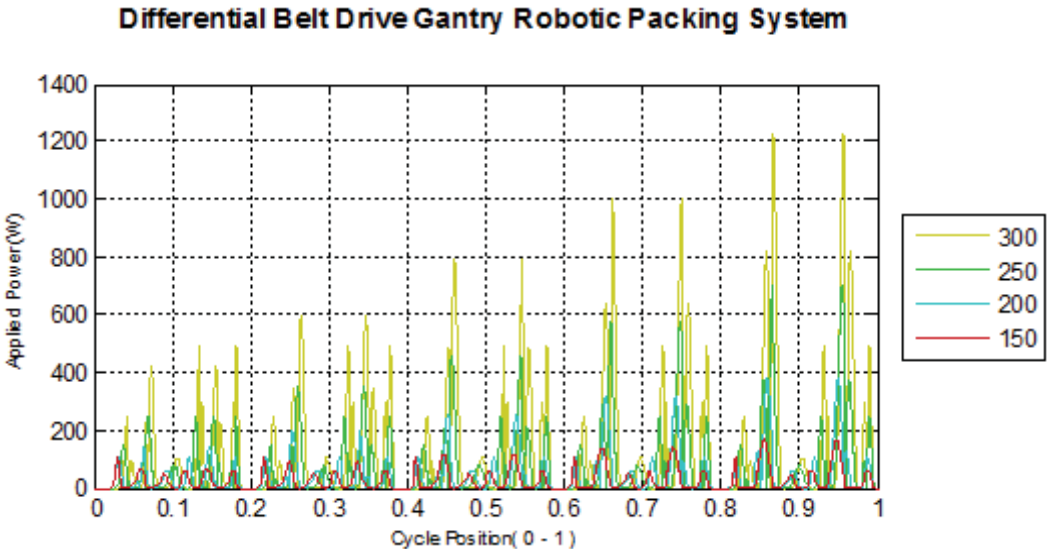

Figure 3.33: Power requirements for the proposed robotic system for axis one.

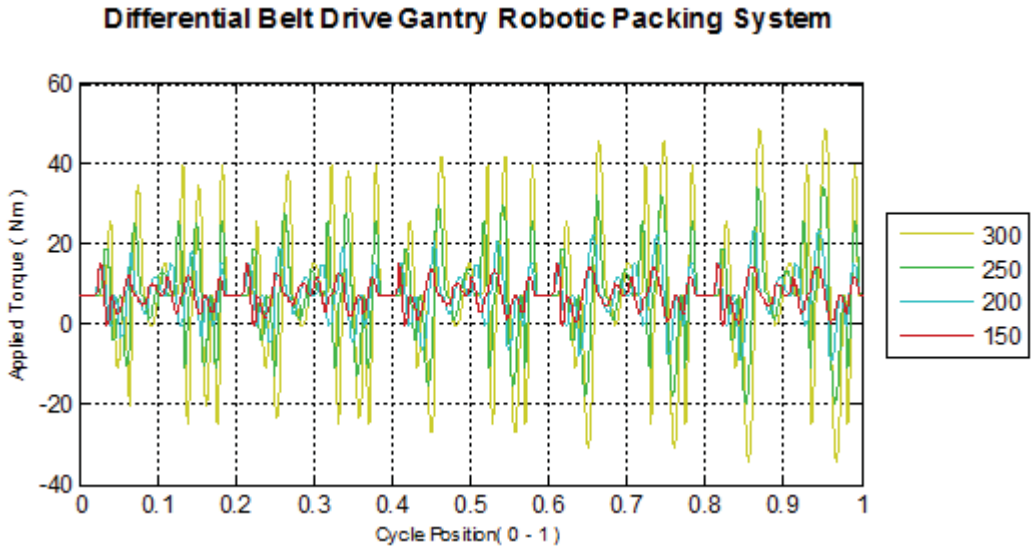

Figure 3.34: Torque requirements for the proposed robotic system for axis one.

Figures 3.35 and 3.36 demonstrate the required servo action applied during the furthest row at 300 OBJs per minute. The numerical evaluation of this designed worst case scenario still only requires low cost servo actuators.

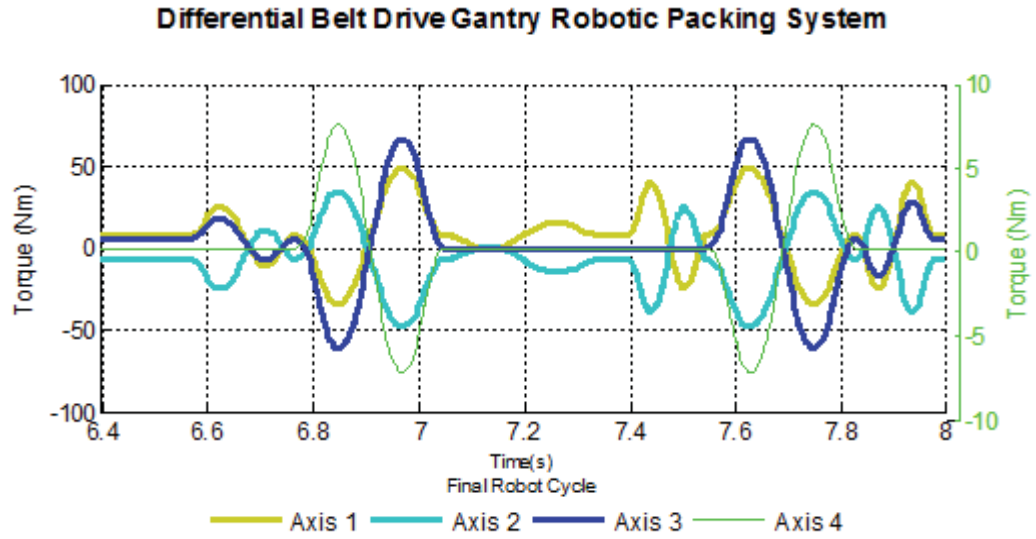

Figure 3.35: Torque requirements for the final packing cycle of the robotic proposed system.

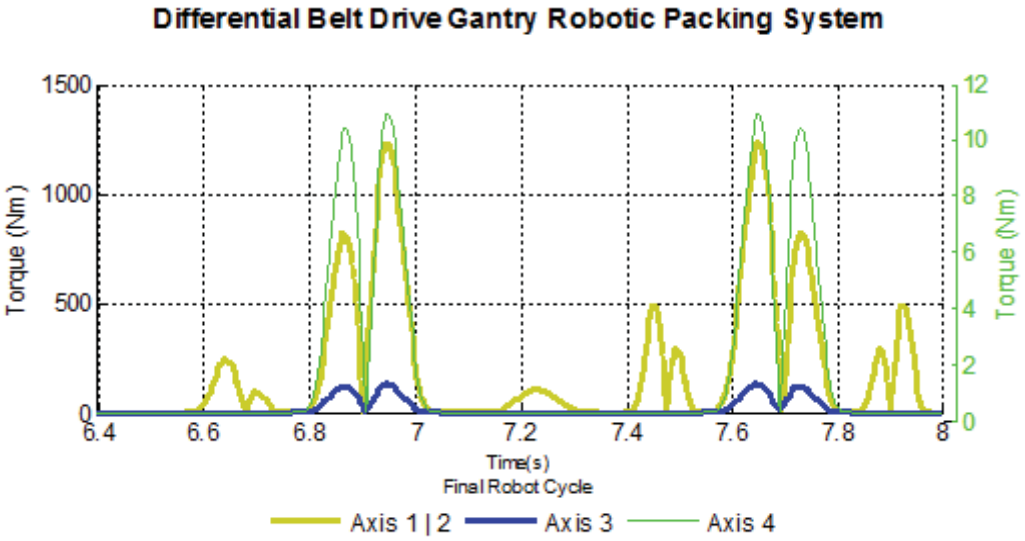

Figure 3.36: Power requirements for the final packing cycle of the proposed robotic system.

Figures 3.37 and 3.38 show the servo system backlash with the belt drive layout. The backlash does not include belt stretch. However, this should relax to zero when stationary. To approximate the repeatability of a real system, the belt driven gantry is simulated with a low cost 12 arc-min back lash drive-line. The result of the backlash is 0.5mm in both the vertical and horizontal directions.

The differential driven belt actuated gantry is chosen for the engineered solution since it offers the following advantages.

- Tolerant of malfunctions
- Belt acts a damper to motion
- Efficient use of servo drives.

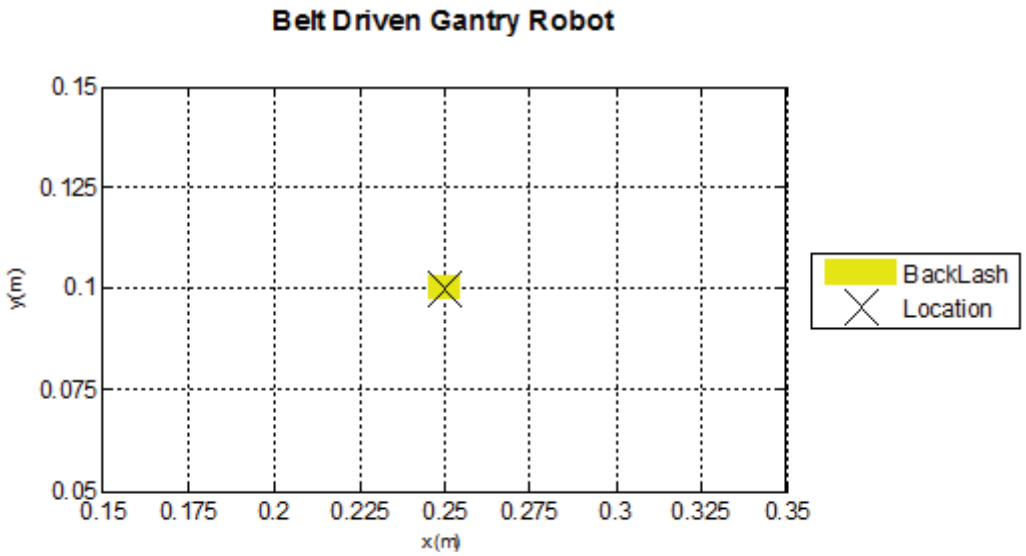

Figure 3.37: Backlash at OBJ pickup location for the proposed robotic structure.

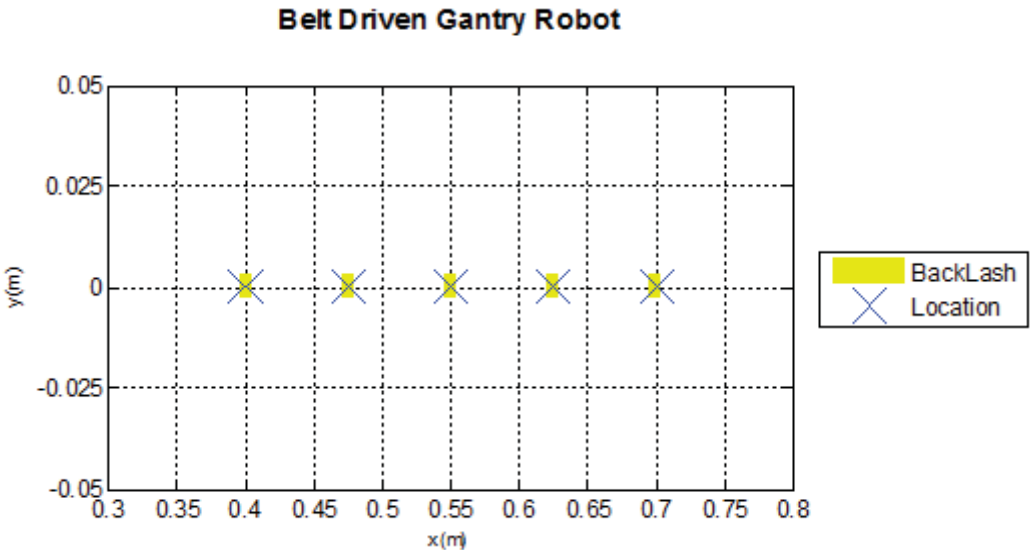

Figure 3.38: Backlash at OBJ placement locations for the proposed robotic structure.

3.6 Proposed Control Overview

The common control solution for OEM robotic systems is an overall controller that sends coordinates with time requirements to a hardware based controller, such as PLCs, microcontrollers and computers. The hardware controller determines the motion for each axis and sends this information to each servo drive. The servo drive internally generates motion profiles for the physical motor.

The control layout for the presented robotic structure is configured using an industrial computer running a real time kernel. The servo drive unit consisting of servo motors, gearboxes and encoders are interfaced with the use of a motion control card, communication hardware and servo drives. Motion planning is generated from within a software solution and transferred to the motion control card.

There are two primary reasons for this configuration. Firstly testing with the NZIC RTP

shows that the EE jerk rather than acceleration is the limiting grasp factor. Investigation has found intelligent servo drives generate only 2nd and 3rd derivative-based motion profiles. To generate higher derivative profiles to suit controlling the jerk, fixed motion curves must be saved to servo drives or motion control cards installed in a computer. Fixed motion curves are not practical since they would limit the production grasp and release coordinates to a few points. Therefore, they would not offer the flexibility to handle varying OBJs.

The second reason is the cumbersome command propagation throughout the system. The common solution means simple pick and place motions are elementary task to program, however more advanced and dynamic state machines are difficult to integrate. A large period of time was spent attempting to integrate the grasp research from chapters 4 & 6 with an existing NZIC RTP with no success[12]. The layout does not allow the easy integration of real time correction to occur. This is because the overall PC controller does not have a synchronous hardware interface and the hardware controller is unable to process complex signals or generate motion curves. Finally the servo drives operate in an open loop configuration.

The conceptual design of the proposed robotic packing system is designed and presented in Figure 3.39. The orientation design is shown in Figure 3.40.

12 The conventional electrical interface proved to awkward to interface real time signals to the robot's controller. To achieve an adequate interface, access to lower level software and electronics would be required. The information and details are intensionally not shared to customers of these products.

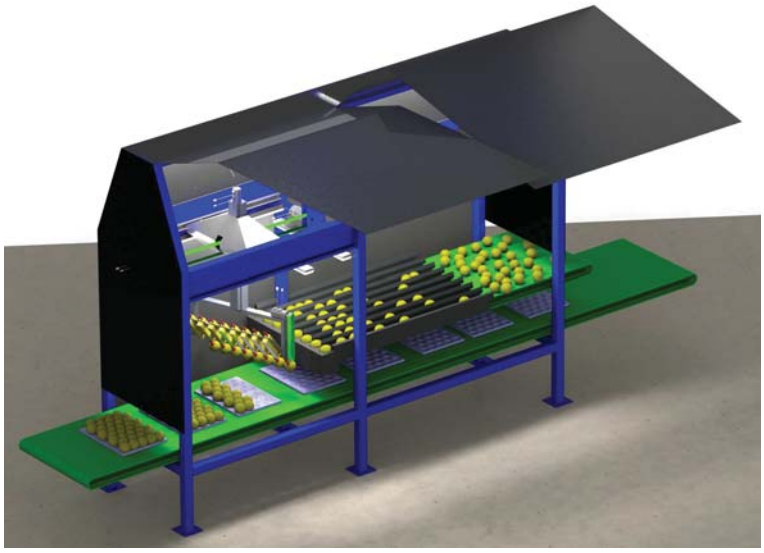

Figure 3.39: Conceptual mock up of the proposed robotic packing system.

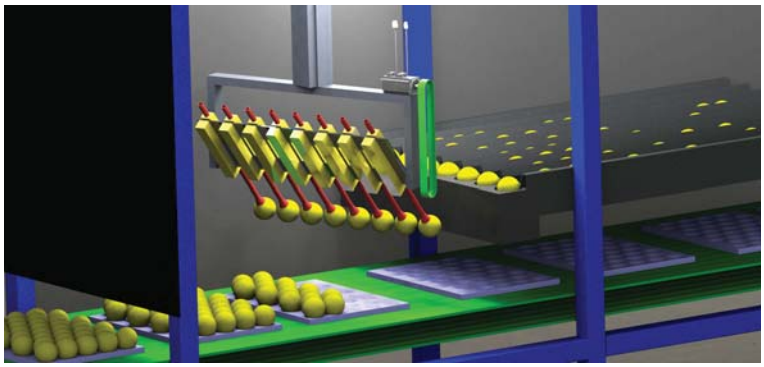

Figure 3.40: Conceptual mock up of EE and orientation units.

3.7 Summary of Robotic System Design

This chapter set out to determine a viable OBJ packing system for NZIC. Through the investigation, the only solution is to break tasks down to a sequence of tasks. The packing system is broken down into three processes: singulation, orientation, and

packing. The singulation was considered a development challenge more suited to follow latter in the commercialisation process. Review of existing OBJ packing systems demonstrated that the two critical technology challenges are the developing a orientation system and a low cost reliable grasping unit. These challenges require further study and in-depth research. The final aspect and the focus of this chapter was an investigation on how to practically meet NZIC's goal. The research started with a abstract view of the physics involved moving the OBJs from an orientation unit to a tray The evaluation demonstrated that any viable system will need to pack multiple OBJs per cycle. The base calculations of the packing dynamics further enforced the critical nature of the OBJ grasping and the exponential impact on the packing rate.

The outcome from the calculations is that for the proposed layouts only a row or pattern format could provide the required packing rate. The row packer is concluded as the favourable initial option when considering a whole range of different business factors. In comparison, the row packer will offer a simplistic design for the management of components, reduced financial risk, and reduced time to market.

The new technologies being the orientation unit and improved grasping can be tested on real machines with no difference in either format. Finally, the calculations show the row packer being capable of packing at the necessary rate of 220-300 OPM. These points do not rule out a pattern format in the future. A pattern packer does offer the best performance in terms of packing rate, and return on investment and should be considered at a latter time.

In determining the best solution, the focus was to develop a practical means of producing such a robot. Three generic robotic structures were considered and their actuation simulated with Mathworks SimMechanics. A generic path generator approximating the required way-points was developed within Matlab. The SimMechanics environment then incorporated the motion profiles into an imported physical model of each system. Simulations demonstrated the necessary actions and power required to actuate each robotic structure. The actions demonstrated that the articulated robotic structure could not become a practical solution since the torques

required were too extreme for standard equipment. Both parallel and gantry structures in a friction-less environment were at least technically possible with existing 3rd party components. The next factor for consideration was production cost. In the section 3.4.6 , the three robotic structures were considered based on their tolerance to the precision grade of 3rd party equipment. Due to the linkage and connection between joints both the articulated and parallel systems were shown to require ultra high precision gearboxes or direct drive actuators. Searching manufacturerss catalogues did not locate suitable gearboxes that came close to providing the required backlash precision with high torque and speed motion. The gantry system, in contrast, largely demonstrated a design tolerant to low cost gearboxes or linear servo drives.

The final part looked at the engineering layout of the system proposal. A significant decrease in cost is made possible by the use of a differential belt drive for actuating the motion in XZ plane. The differential drive provides a large reduction in torque to previous simulations. Excluding the belt stretch factor, the resulting region of repeatability due to backlash is approximately +/- 5mm both vertically and horizontally. This simulation utilised backlash for low cost servo gearboxes and outperforms the initial designs with ultra high precision equipment.

The outcome from the investigation and proposal presented in this chapter is a robotic structure that can technically meet the requirements without any specifically developed electronic components. Financial modelling of the system's market value and production cost ratio (not described here) provide evidence the system is viable if the orientation and grasping technologies can be developed. This cost analysis involved an in-depth consideration of elements with input and review by several NZIC's engineers[13]. Figures 3.41 and 3.42 present the modelled margin of the prototype and production configurations against a OPM based market value[14].

13 This includes manufacturing the EE and orientation devices to be discussed in Chapter 4. The detail is to the level circa of formal quotes for non standard NZIC equipment. Electrical detail to cabling, circuit breakers etc. Labour comparison with similar NZIC assemblies etc.

14 These figures are not manufacturing vs market value. The profitably is measured against NZIC R&D risk vs required margins.

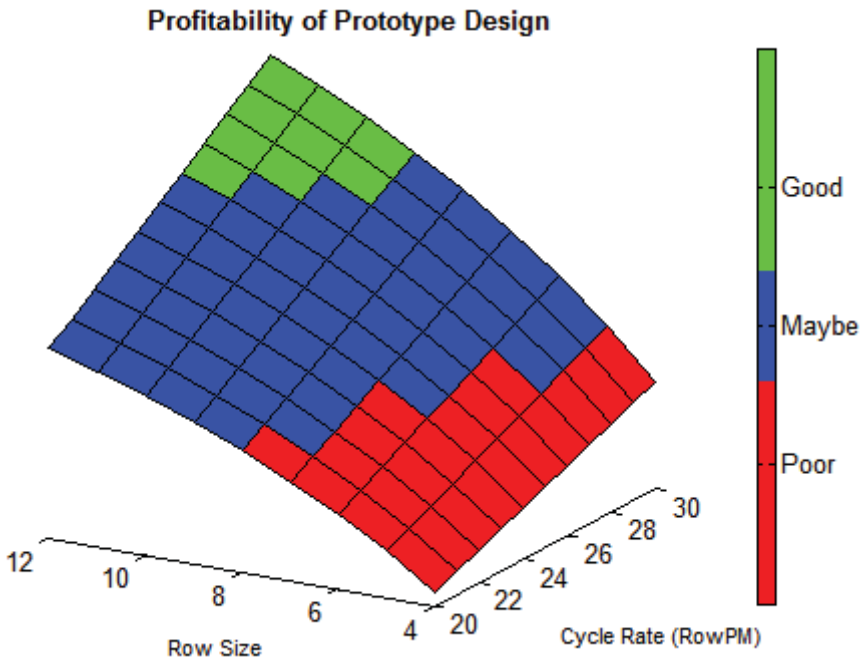

Figure 3.41: Estimated profitability of the prototype design.

The market value of the prototype system does not have a strong return for NZIC and is most likely not worth the development risk involved with such a project. Figure 3.42 demonstrates that the intended production design offers a reasonable level of return for NZIC. The common packing format and estimated cycle rate puts the profitability of the system on the level of reasonable and good returns.

Unfortunately, NZIC's industry was hit by the global financial crisis right at the time the final proposal was presented. The project had already been given the approval to order the components but was then delayed for the foreseeable future.

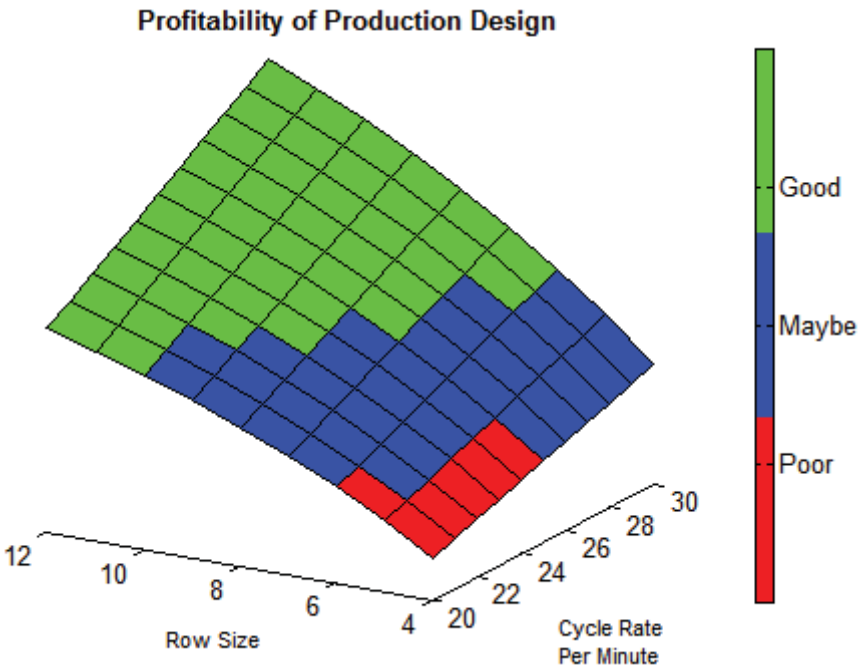

Figure 3.42: Estimated profitability of the production design.

4 Investigation, Design and Engineering of Grasp and Orientation Technology

Previous chapters have presented the investigation for the design of a packing machine as an entire system, discussed the problems, and developed a proposal for an overall viable commercial system for NZIC. Since related robotic technologies have been identified and the system layout has been developed, the focus of this chapter is to identify the most suitable technologies that can solve identified problems and develop a system that is unique to NZIC's applications.

The simulations of packing format identified the critical nature of the dwell time for the grasp and release of OBJs. The need to improve the reliability of OBJ grasping has also been identified while reviewing existing systems. The next important factor separate to the robotics, is the ability of the system to orientate OBJs prior to placement in the tray.

4.1 Investigation on End Effectors

Existing commercial systems discussed in Chapter 2 do not demonstrate a reliability suitable for unsupervised commercial operations. A major issue with existing commercial systems is that these systems do not show any means of fault detection. Consequences from the lack of such feedback is the requirement of heavy human involvement to monitor the system. To remove human involvement, thus saving on labour costs, the ideal solution would implement fault detection and avoidance.

4.1.1 Existing End Effector Technologies

The EE is a core research and development interest relating to industrial robotics. A google scholar search with the phrase "Robotic End Effector" alone returned almost 8000 results[9]. A good starting point of relevant end effector technology is a review of robotic manipulation for the purpose of handling food products[10]. This review has a number of case studies explaining a wide range of methods and constraints for handling items such as fish, eggs, chicken etc.

Taylor's 1995 presentation on flexible material handling splits robotic end effectors into three classifications[11].

1. *Mechanical surface: where the material is clamped or pinched between gripper fingers to give high frictional holding forces;*
2. *Intrusive: where pins are fed into the surface or body of the material and moved to lock it into place;*
3. *Surface attraction: including the use of adhesives/vacuum[11].*

Mechanical interference is the use of a physical device to provide force and therefore surface friction to hold the work object(s). Many of these mechanical interference end effectors have existed for decades, however, they do have draw backs. The challenge with handling OBJs is the sensitivity to damage either by puncture or blunt force. Intrusive end effectors are not an option since the OBJs would be ruined. Additionally, any excessive force to the OBJ's surface will cause damage. Mechanical end effectors in the simplest cases can use a brute force technique to insure the work object is sufficiently contained. The brute force technique is commonly done by applying an action well in excess of that necessary.Returning to an earlier source, "Humankind Emerging" presents the concept of a power and precision grip when discussing the grasping of humans and primates.

- *"Power Grip: A grip involving all fingers of the hand equally, as in grasping a baseball.*
- *Precision Grip: A grip that involves opposing the tip of the thumb to the tips of the other fingers, allowing fine control of small objects."[8]*

The power grip is an ability of all primates and humans in nature and is this grasp type that is common to the brute force interference method. This simple approach is sufficient for grasping rigid objects; however, for the application such an approach is likely to damage the OBJs. In a laboratory such a technique may be possible with fine tuning and careful controlled experiments but factory settings, especially that of NZIC's industry do not constitute controlled environments.

An advantage humans have over other primates is their increased precision grip ability. It is this precision grip ability that allows humans to manage delicate manipulation of fragile objects with sensitive movement. This increased freedom and control of motion is due to the optimal hand structure of more independent moving fingers and longer thumbs plus increased intelligence to sense and control.

The commercialisation of any mechanical grasp detection would need a means of operating similar to a precision grip. This would serve the application by containing each OBJ with minimal interference force and avoid pressure points. To achieve such a capability, the system needs to employ a means of increased intelligence to determining the grasp.

Many works investigated the use of gripper designs with ever improving means of intelligent sensing technologies[12-32]. Array forms of pressure sensors, known as tactile sensors, are beginning to become OEM products from speciality manufactures. Many of these intelligent gripping works operate with a common theme of detecting slip by measuring one or multiple dimensions of tactile sensors. Seen by a control system is the distribution of force and pressure upon the EE structure. The algorithms then attempt to predict slip or other load disturbances by monitoring the change in the distribution shape. This tactile array approach has been expanded further to create materials that utilise pressure ridges similar to skin[13], [15], [33]. The finger prints have the effect of stress concentrations and increase the effect for the sensors. The finger print approach is constrained by an applied problem due to coatings applied to the OBJs. Other research has taken the approach of applying complex control algorithms to determine the optimum grasp actions[14-15],[34-45]. Rather than rigid fingers presented

with tactile sensors, other options consist of using flexible fingers. Flexible fingers would have the advantage of avoiding pressure points and strain gauge wire could be embedded to measure deflection[24]. Additionally, presented in some solutions are fingers that could be expanded by pneumatic pressure. The approach could be quite efficient as it may eliminate the need for more expensive electromechanical drives.

Not mentioned thus far is a second form of end effector described by Taylor as "surface attraction"[11] Surface attraction could include some experimental approaches such as electrostatic, surface freezing or even applying positive air pressure and creating a localised vacuum at the surface. Realistically, industrial surface attraction end effectors constitute electromagnetic or vacuum grasping systems. The OBJ being non magnetic results in surface attraction systems with a pneumatic vacuum cup as the only option.

Pneumatic vacuum cups are the sole means of end effector on all reviewed systems and because of this a good idea about the specific problem is formed. Vacuum cups offer a simple and low cost solution, however pneumatic systems have numerous downsides with the environment and variables of NZIC's industry. The vacuum cup must be able to maintain a negative pressure differential to the surrounding atmosphere. Leaks within the cup due to holes or poor seals will result in high vacuum flows. Leaks at deep vacuum pose a difficult problem for the vacuum generator to remove the remaining air. Therefore, an OBJ with a surface that has a low porosity is necessary. The environment that NZIC's machines operate in is often exposed to the atmosphere, from cold winters to the hot humid summers and often has very high dust levels. This produces many problems with pneumatic systems as it forms blockages within the lines and jams valves. The NZIC RTP system suffers from these environmental problems where dust blocks the pneumatic lines and moisture from condensation damages the valves. The problems still persist even though NZIC has employed standard industrial methods of different filters and water capture devices. Other competing systems that use the pattern format are not known in their susceptibility, however, from images, some differences can be seen. Large tubing indicates some systems are utilising a centrifugal fan based vacuum pump. Such a pump should be more tolerant to foreign debris.

Many works outside the applied objective demonstrate the evolution from basic grippers and pneumatic suction systems right through to high advanced systems that can provide all manners of feedback for a control system. Numerous technologies have been investigated that provide the means of reliably handling the OBJs during pick and place movements. Many of these findings or ideas could be integrated into a final design. The complication is that the final systems is intended for commercial applications. There are constraints that extend to more than the capability to carry out the required tasks. The constraints to the system design further include aspects related to the return on investment and the risk associated with this investment.

After the study and the discussion with NZIC's engineers and managers, the final EE solution for NZIC is required to meet the following requirements:

- A cycle rate of 1.5 – 3s
- Gentle handling of OBJs
- Reliable handling of OBJs
    - Reliably handling over 99.5% OBJs
    - Have fault detection capability
    - Future fault avoidance
- Cost effective
    - Return on investment
- Mature technology
    - Minimise the large commercial risk involved in project.

4.1.2 Conceptual End Effector Designs

Five end effector designs are evaluated using a range of approaches. These approaches consist of the following pneumatic, mechanical and hybrid units.

1. Intelligence vacuum grasping
2. Tactile sensed mechanical fingers

3. Flexible sensed mechanical fingers
4. Expandable enclosure
5. Pneumatic expandable enclosure

4.1.2.1 Intelligent Vacuum Grasping

The simplest proposed solution is to add intelligence functionality to pneumatic vacuum cups as shown in Figure 4.1. The grasp would be sensed by a combination of vertical load on the vacuum cup and the pressure exerted.

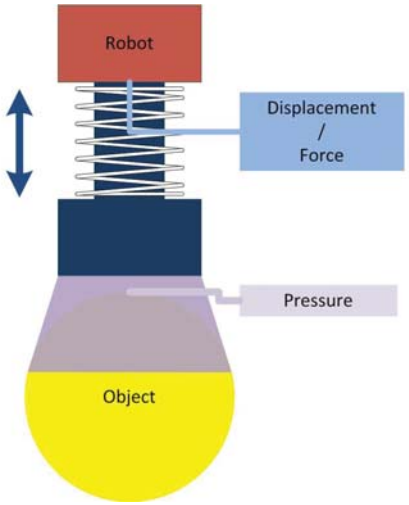

Figure 4.1: Intelligent vacuum cup end effector.

The measure of pressure fluctuation comes from the non-ideal operation of the vacuum generator and time constants of the system. The vacuum depth changes depending upon the flow rate as the system can not provide infinite flow. When an air tight seal is formed the air flow is at its lowest and the vacuum level increases. In the case of a leakage, the air flow increases and therefore the vacuum pressure drops. Additionally, a force measurement of the vacuum cup can detect the load change. Upon grasping and releasing, this load measurement supplies the system with the current grasp effect of the cup.

4.1.2.2 Tactile Sensed Mechanical Fingers

An advanced approach is to develop a three-finger gripping end effector with tactile sensors as shown in Figure 4.2. The sensor on the surface measures against point loading and detects the OBJ slipping. The gripper has each of the fingers actuated individually, allowing the unit to grasp non geometric consistent OBJs. The fingers are actuated by tendons or linkages connected to servo system. Remote servo actuators allow the fingers to be minimal in size and be able to fit within the tight constraints of trays.

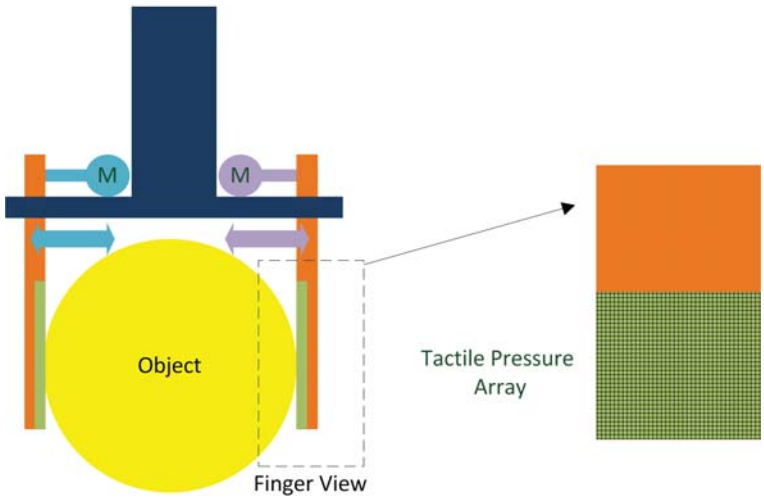

Figure 4.2: Individual actuated fingers with embedded pressure tactile arrays.

4.1.2.3 Flexible sensed mechanical fingers

The tactile sensed mechanical fingers concept is immediately recognised as an expensive and complex device from literature. A lower cost approach utilising flexible sensed fingers intends to reduce the cost of the intelligent end effector illustrated in Figure 4.3. The independently actuated fingers from the previous version are substituted by flexible fingers driven by a single actuator. The single actuator does not allow the same degree of finger control, however, to a limited extent, the flexible nature of the fingers can balance out the grasp pressure. This approach provides a further cost reduction by

avoiding expensive tactile sensor technologies. Strain gauge wire is embedded within the fingers to detect the bending moments. The fingers contain small strain gauge elements vertically stacked. While the low cost sensing technology would not provide the true 2D pressure feedback from tactile sensors, it may be sufficient for the application. The feedback purpose of sensors is to avoid pressure points and detect slippage. Maintaining the calibration of individual strain gauges is difficult, however the system only needs to measure the relative distribution not absolute values. The individual pressure points can then be estimated using a discrete force signal from the finger actuators.

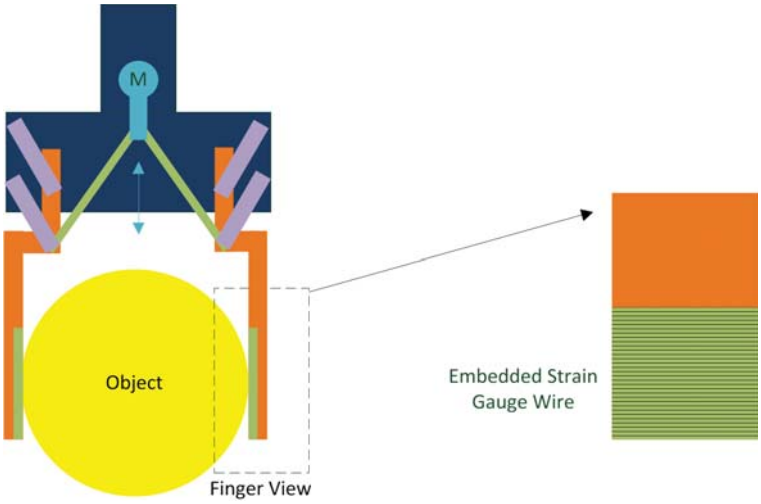

Figure 4.3: Flexible fingers with embedded strain gauge wire.

4.1.2.4 Expandable Enclosure

A novel solution is to utilise a mechanical interference end effector actuated via pneumatic flow control. The OBJ is surrounded with an inflatable skirt structure as illustrated in Figure 4.4. The structure begins the grasp in a deflated state and then lowers around the target OBJ. The structure then inflates a determined thickness to contain the OBJ. This structure contains the OBJ using a large proportion of the surface and therefore greatly reduces contact pressure. With some engineering difficulty, strain gauge wire can be added to the inflatable structure and provide slip feedback. This design could be expanded further to combine the mechanical grasp with supplementary vacuum. The expandable enclosure solution has the benefit of forming a

seal around the surface of the OBJ.

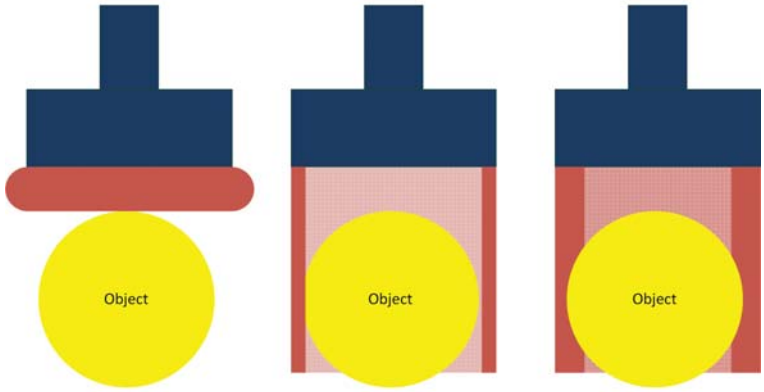

Figure 4.4: Pneumatic expandable enclosure.

4.1.3 Discussion of End Effector Designs

NZIC at the outset had the desire to avoid pneumatics because of the maintenance drawback and the elimination of pneumatics in their other systems was a selling point. In the prior sections, several interference solutions were investigated and many of these have the potential to allow a robot to achieve the tasks with dedicated handling. The downside to these mechanical interference techniques is the manufacturing cost and the complexity of applying new technology. The tactile sensed approach represents the ultimate design. It is flexible and also provides a control system with highly detailed feedback plus gives good corrective actions from the independently actuated fingers. An advantage is that all of the complicated components for such a system are available from manufacturers. The downside of these components is the high cost and they are difficult or impossible to replicate in-house.

The flexible designs with integrated sensing elements give a low cost mechanical grasp technology. The flexible nature of these structures provides a limited means of gentle handling prior to an integrated controller. However, these mechanical systems have a development limitation. The fully developed and in-production manufacturing of the

two flexible systems is unlikely to be of high cost. The costly aspect is likely to be the strain gauge inserts and complicated moulds. The real cost with such systems is the time to go through the process and the numerous moulding developments. These systems come across at first glance as relatively simple processes. In terms of engineering, however, certain aspects such as the hollow geometry, internal gussets, air flow patterns, material fatigue, and inserts become a major hurdle. The flexible designs have not been sufficiently proven within literature and this compounds the risk. They are not only expensive to develop, but they are also unproven.

Pneumatic systems are known to have problems with particles blocking lines and damaging equipment. However these systems are a low cost solution that none of the mechanical solutions could match. The driving factor for considering mechanical solutions is reaching the limit of the vacuum cup end effector before attaining a suitable grasp capacity. The capacity to add grasp intelligence and finding a means of avoiding environmental problems may allow vacuum based designs to operate at a commercial level.

4.1.4 Conclusion and Direction for End Effector Design

Pneumatic vacuum cups are the most viable EE. There is potential for many of the mechanical interference techniques to work, however, to what capability level and production cost is hard to estimate. The reason for considering mechanical methods are due to the problems with existing vacuum based systems. Investigating the pneumatic problems does not show that the approach has an insurmountable fault. The current pneumatic system as utilised by the NZIC rapid tray packer is capable of operating at the required cycle rates for row or pattern packers and within an industrial environment. The challenge is to increase the reliability by utilising grasp feedback in the design, thereby improving the environmental tolerance. Integrating a means of intelligence in the vacuum cup end effectors should increase the reliability and the tasks could be completed without human intervention. Due to the low cost of pneumatic systems, mechanical methodologies should only be considered if there was an inherit flaw with

the vacuum system that could not be easily overcome.

4.2 System Design of OBJ Grasping End Effector

This section gives a detailed design of the proposed system and the methodologies to avoid the related problems. Section 4.1 was focused solely on the aspects of holding the OBJs during motion. This chapter details not only the grasping of the OBJs but the integration of the end effector unit into the proposed robotic system.

Chapter 3 System Design and Investigation developed a packing solution from the overall view of integrating the relevant technologies and the core robotics structure as shown in Figure 4.5.

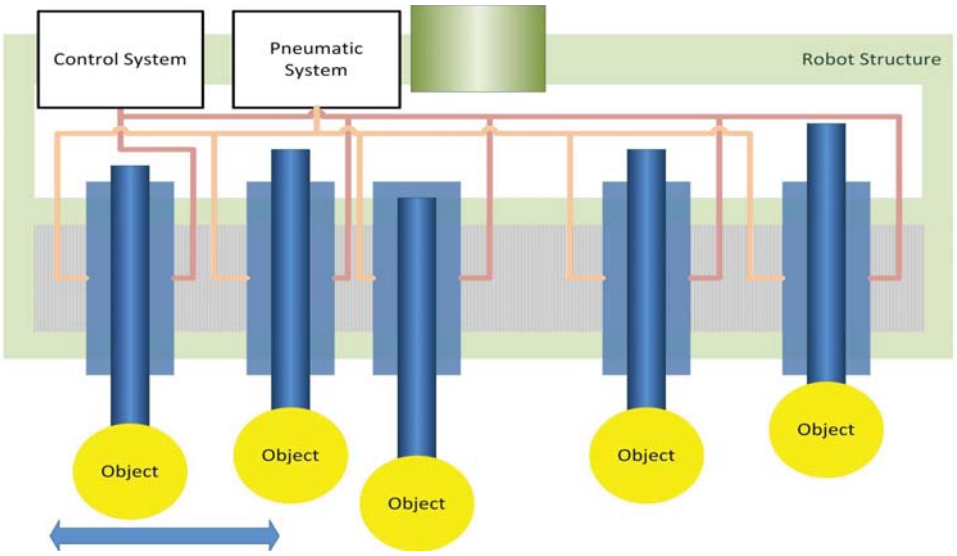

Figure 4.5: System layout of the independent end effectors.

An aspect of the robot structure that has not been discussed so far is the freedom of the EEs to move along the Y axis. The Y axis movement is to be integrated into each of the end effectors design. The robotic core structure is to provide a rigid platform and the end effectors are to translate along this platform to suit each packing operation.

Each EE is to be a self contained unit that controls vacuum grasp, the translational movement along the Y axis, and the optional rotational axis around OBJs Z axis. The end effectors are integrated into the system with connections to pneumatic and control signals. The intention is to have the modules as a "snap on" component that allows the customers to use only the required number of units.

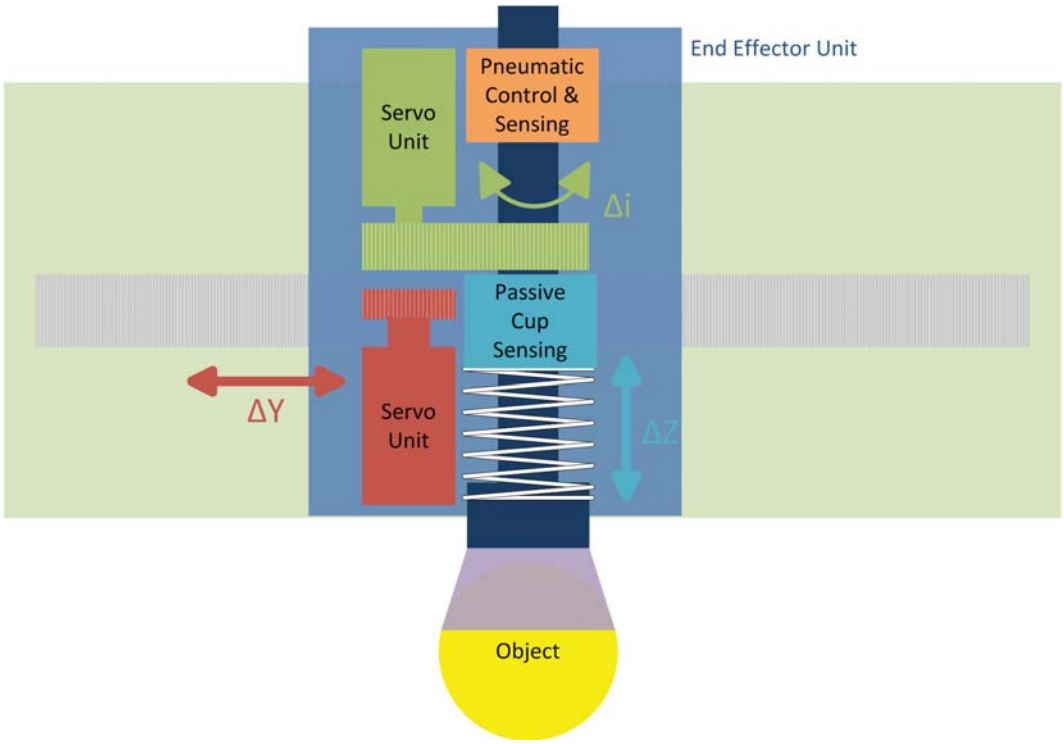

Figure 4.6: End effector layout.

The end effector unit consists of several elements divided into the following purposes: pneumatic actuation, passive vertical motion plus translation, and rotational motion. These three aspects will be discussed individually prior to their integration. The pneumatic system discussed in section 4.2.1 will look at proposed solutions to known problems and the methods of providing a low cost and intelligent control system. In section 4.2.2 the proposed design for providing a means of touch sensing is discussed. Finally in section 4.2.2, the control motion will focus on the flexible low cost servo motion.

4.2.1 Pneumatic System

As shown in Figure 4.6, the pneumatic system contains the elements from the vacuum cup to the vacuum generator and positive pressure source. The investigation of the existing system does not demonstrate a reliable and/or flexible vacuum system for the manipulation of OBJs. None of the systems are known to have a high degree of intelligence or control for individual OBJs. Figures 4.7 and 4.8 outline the vacuum systems employed with NZIC's RTP and the assumed operation of the pattern packers.

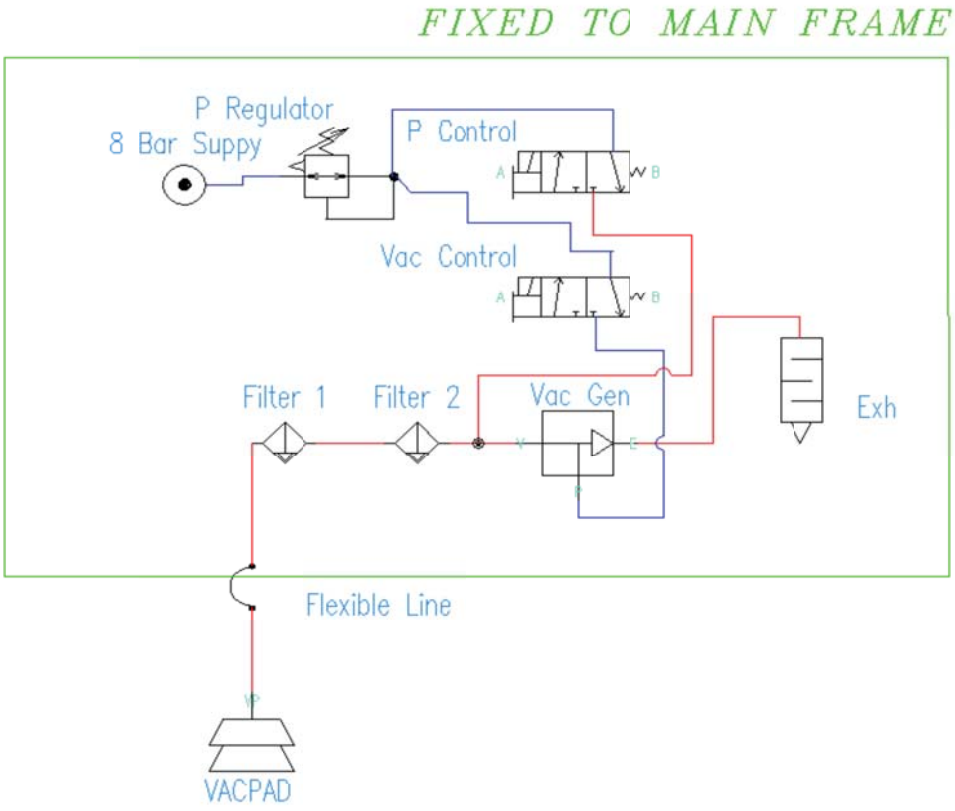

Figure 4.7: Pneumatic diagram representing the vacuum grasping system utilised by NZIC's RTP.

NZIC's RTP is a conventional vacuum grasp unit that uses the internal ABB venturi vacuum generator. The vacuum generator is connected to the eventual vacuum cup via a pneumatic line approximately 1.5m in length with two in-line filters. The pneumatic line is controlled with solenoid valves that operate in four modes: positive supply, closed supply, open supply and vacuum. Vacuum is generated by directing positive air flow to

the venturi vacuum generator. The positive supply is used to eject OBJs from the vacuum cup more rapidly than just opening the line to the atmosphere. The RTP has three problems in operation. The in-line filters begins with a negative effect on the air flow through the vacuum cup air line immediately by impeding the airflow. The venturi vacuum generator is easily blocked or damaged from particles due to the small opening used to create the vacuum. Lastly, the extended air line has a large time constant and the result is such that the period between activating the vacuum generator and achieving peak vacuum depth is approximatively 0.6s, which is too long. Figure 4.7 shows the pneumatic circuit of the vacuum grasping system utilised in NZIC's rapid tray packer.

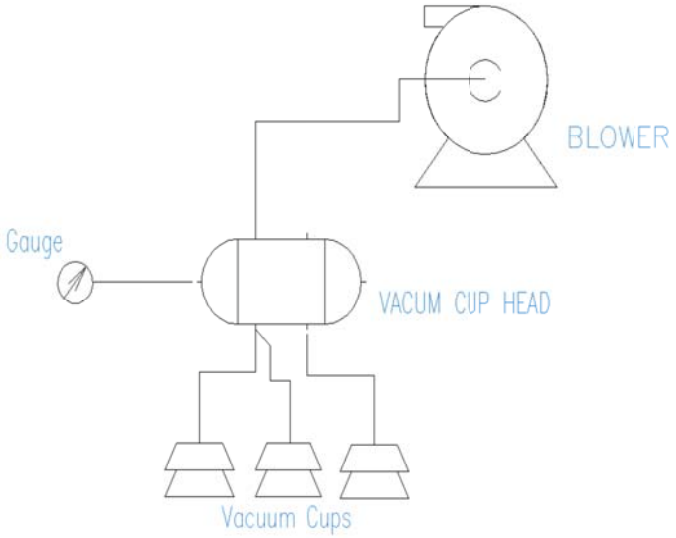

Figure 4.8: The assumed pneumatic system as utilsed by competitors in pattern packer systems.

The pattern packers are assumed to employ an approach similar to that presented in Figure 4.8. These systems probably use a vacuum vain or displacement pump as a source of high flow low pressure vacuum. A single vacuum control valve may exist between the pump and the system. Existing System 4 discussed in section 2.3.4 does include some pressure sensing at this stage. Between the vacuum source and the OBJs, no flow control or sensing is known to exist nor is there evidence to suggest additional positive air supply to increase the ejection rate. This basic approach is evident from the feedback relating to the pattern packer based system. The pattern packers are slow to

grasp and release and in some cases, physically press down on the OBJs to produce a seal. These drawbacks can be attributed to the large volume of exhausted air to attain a sufficient vacuum depth. The challenging ability to exhaust air is the likely reason why some of the systems physically exert force to form a grasp. These systems thereby mechanically form the seal[15] to the OBJ as a means of reducing the OBJ grasping period. Additionally, these systems do not have the ability to apply positive pressure as a means to rapidly eject OBJs. Finally the reliability issues can contribute to the large volume without control of individual vacuum cups. Any leak within the system effects all the vacuum cups and there is no means for fault detection.

To produce a reliable OBJ grasping methodology the proposed vacuum system has four goals. The new system developed is intended to provide a solution for each of the problems in a viable commercial design.

1. Sense the individual pressure at each vacuum Cup.
2. Control the vacuum at each vacuum cup.
3. The ability to eject OBJs from the vacuum cups.
4. Solve the problems caused by the environment.

A proposed solution to the four outlined objectives is presented in Figures 4.9 and 4.10. Each vacuum cup has independent control of the air flow with a connection to positive and vacuum pressure sources. The vacuum cup control has three options: positive air pressure, vacuum pressure, and hold. The physical flow control is located immediately above the vacuum cup buffers to minimise the time delays and reduce the vacuum generator's average flow rate. Positive pressure for OBJ ejection is controlled via a remote and conventional solenoid valve located directly above the vacuum cup feeding into the main cup chamber. To solve the issue of particles blocking the vacuum system, a custom valve unit is utilised as way of switching the vacuum flow.

Typical manufactured vacuum valves have very tight tolerances, small diameter flow paths and a design that is hard to clean. These OEM valves, therefore, require in-line filters which reduces air flow. This makes remote vacuum control difficult and

15 This means an increased risk of OBJ damage.

expensive. The common approach is to have simple individual unfiltered venturi vacuum generators at each cup. Remote vacuum generators are not viable for this application as the orifices can be blocked within minutes. The proposed design methodology is the opposite of common approaches which place a high preference for precision and efficiently. The system will utilise large diameter (> 10mm) butterfly valves. The reason for this customised design is that the large diameter and valve type can robustly handle particles flowing through the pipe. The large diameter valve does not constrict the air flow through a tight point nor redirect the flow, both of which are subject to blockages. A butterfly valve is the preferred option over others such as gate or ball valves. Gate and ball valves offer a superior flow due to the lack of flow restriction within the component. The problem with such types is the sliding motion of valve which will be susceptible to the common particle types and they are difficult to maintain. The butterfly valve has the advantage of axial positioning resulting in a more tolerant design to particles and a simpler device to produce. The actuation of the butterfly valve is with the combination of a PM DC brush motor, spring loaded shaft, and mechanical stops. PM DC motors are more reliable electromechanical devices than solenoids at a lower cost. The spring loaded shaft holds the valve closed when it is not actuated by the motor. The spring is not intended to close the valve but to supply sufficient torque to keep the valve at the closed position, therefore allowing the motor current to be reduced for a period. Mechanical stops and the motor current provide the control system with feed back indicating valve position. In the event of a sticking valve, which will be discussed later, pressure sensors should detect the fault within one packing cycle. Figure 4.9 illustrates the intended vacuum cup control unit with a cut-out to show the valve. The positive pressure air supply enters the vacuum cup buffer after the butterfly valve.

The expectant outcomes of the flow control unit include:

- Control the vacuum at each Cup
- Allow the fast ejection of OBJs
- Solve one aspect of environment conditions

Figure 4.9: Individual vacuum cup control.

4.2.1.1 Pressure Sensing

The surprising aspect off all systems investigated was their common lack of actively sensing the pressure at each vacuum cup. Either the designers of these systems did not realise that feedback was vital or it was considered to be expensive to implement. Conventional industrial PLC pressure switches or sensors are expensive for a multi EE packing system. The proposed solution is to use low cost PCB piezoelectric differential pressure sensors to provide feedback to the system. Piezoelectric sensors are not great sensors and suffer from inaccuracies due to environmental factors and a tendency to vary over their lifetime. However the piezoelectric sensors represent an ultra low cost solution that is able to provide an indication of pressure. The piezoelectric sensors are insufficient as a means of absolute pressure measurement for use as a simple pressure switch or a signal comparison for conventional electric hardware devices such as PLCs. To use these low cost pressure sensors the control system has to monitor the trending signal reading with the derivative as a control input. This behaviour and the control application of such signals is discussed in Chapter 5. The inclusion of low cost

pressure sensing technology provides a solution to the system indicating the vacuum of each individual vacuum cup.

4.2.1.2 Vacuum System

The above section outlined the approach for controlling the vacuum at each individual cup and a robust flow controlling unit. In this section the vacuum system from the end effector to the vacuum generator is detailed. The design goal for the vacuum system is to increase the robustness of the operation and decrease the system delays.

The cup control device previously outlined provides advantages for the system. Figure 4.10 shows the proposed full pneumatic grasp system.

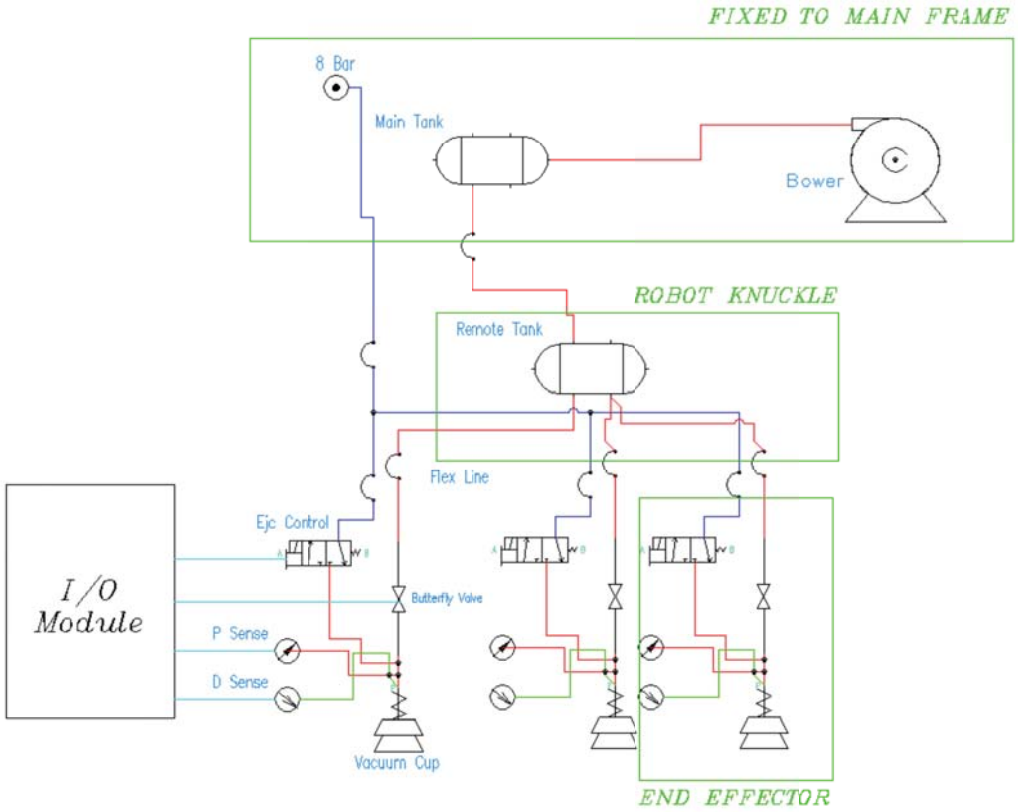

Figure 4.10: Proposed pneumatic grasping system.

The proposed system combines the new cup control unit and intends to solve the remaining pneumatic challenges. Shown in Figure 4.10 is a large common vacuum buffer. Buffer elements in the existing systems have a negative performance effect on the system operation, especially in grasp and release periods. Since the vacuum flow at each cup is now controlled via a remote valve, the buffer improves the system operation by minimising disturbances. The buffer has the effect of improving the vacuum during the grasp period and maintaining the vacuum depth. By having the cups individually controlled, the depth of vacuum buffer can be maintained. Effectively the buffer can be pre-charged to the grasp pressure prior to the actual grasping. Additionally, any vacuum loss can be recovered during the closed valve period. Finally, since the buffer no longer has a negative effect on the system response, the buffer volume can be increased. The larger volume provides the benefit of increasing the overall time constant of the system which is advantageous to reducing vacuum disturbances. There is a downside, however, to the larger vacuum design, if the buffer is overloaded, the system will require an extended recovery period.

To improve the vacuum system's tolerance to particle causing blockages and other faults, a different generation and filtration methodology is applied. The known methodologies use small in-line filters[16] and vacuum is generated by venturi or rotary vane pumps. The vacuum supply source is to use a different approach by applying a single large cyclic filtration and centrifugal generators. The cyclic filter operates by generating a vortex within a chamber due to the position of the source and outfeed. Centripetal forces push particles to the outside of the chamber which then fall to the bottom of the filter structure. The allowance of a buffered vacuum system can be indirectly advantageous in this case whereby no negative effect is placed on the unit with a larger filter catchment. The cleaned air then flows out the top of the filter to the vacuum generator. Benefits of such a system are that the removed particles do not accumulate to block the airflow. The use of a rotary centrifugal generator provides a solution more tolerant to foreign particles compared to venturi or rotary vane pumps. The downside to centrifugal vacuum generators is that the vacuum depth is limited to approximately 0.40 bar. The behaviour investigation in Chapter 5 will demonstrate that a

16 The RTP does use a series of small cyclic filters on the vacuum cup line.

vacuum depth of 0.25 bar is sufficient to hold the OBJs.

4.2.2 Vertical Motion

The vacuum cup arrangement is chosen to provide passive vertical movement. The vertical movement allows for variation of OBJs geometries along each row and a mechanical method of reducing applied force to the OBJs, thereby acting as a passive built in safety measure. The existing system does not noticeably employ such a system, however, multi-bellow vacuum cups do have vertical variation in their construction. An advantage of a separate vertical element is the inherent flexible structure of the vacuum cup be maintained for grasp formation. This separation allows an optimal design for each component. The vertical movement either directly or indirectly allows the use of force or position feedback to the control system. This measurement provides an indication of the grasp event and the applied force for each OBJ.

The solution provides the following benefits:

1. Reduce the damage to OBJs
2. Handle geometric difference of OBJs
3. Provide the control system with the applied force to OBJs
4. Provide the control system with a means of indication grasp formation.

The initial evaluation of the technologies shows that only a linear variable differential transformer approach could meet the requirements and could provide a cost effective solution. During the later stages of research one manufacturer began producing low cost piezoelectric loads cells. Previous load cells had been concluded as a nice approach however deemed far too expensive.

4.2.2.1 Option 1 Linear Variable Differential Transformer (LVDT)

Vertical motion provides a means of achieving several different actions with one component. A linear variable differential transformer is one proposed means of measuring the vertical motion through the force of the vacuum cup. Standard LVDT from manufacturers are of a high cost; however, the design does not require high precision measurement. The proposed structure is to take advantage of the layout of LVDTs to provide a spring loaded motion buffer, pneumatic connection and measurement all within the same device as shown in Figure 4.11. Figure 4.11 shows the cross section of the LVDT based structure.

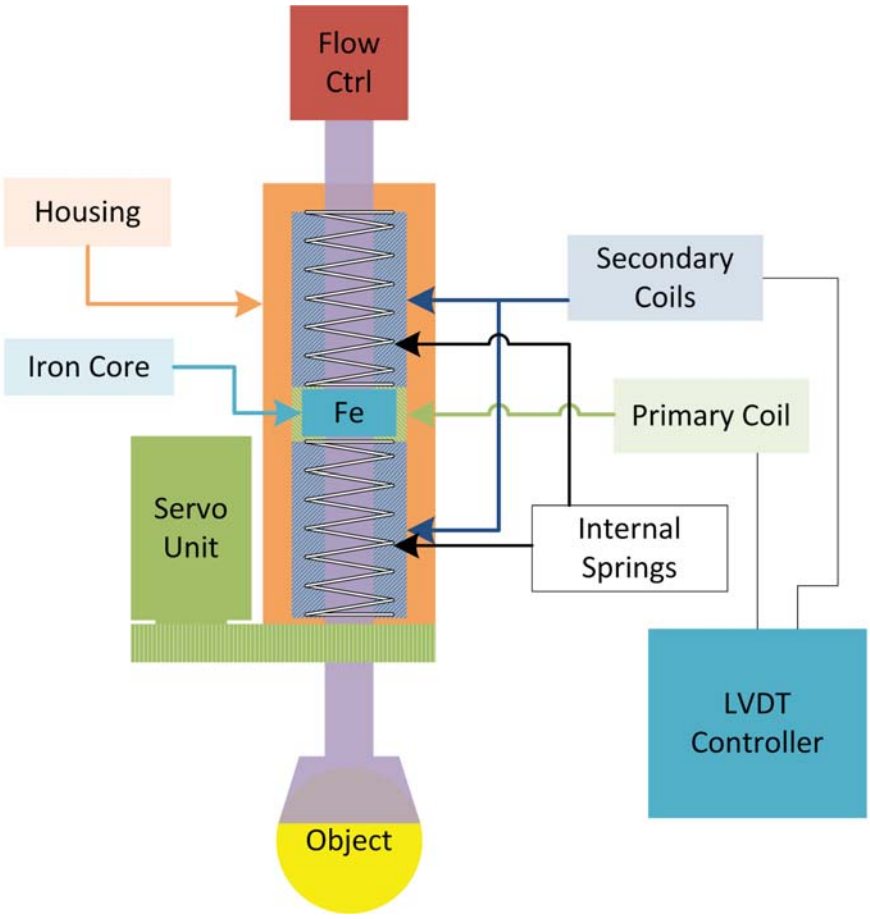

Figure 4.11: LVDT based end effector system.

The buffer is the central component in the design with the iron core fixed around the outside. The iron core provides the means of changing the magnetic field and acts as a stop for the internal springs. The springs are contained at the top and bottom within the LVDT by the end bearings, with the purpose of providing a reactive force to cup load. The LVDT directly measures the motion of the vacuum cup buffer and by using the spring rates, it is able to estimate the applied force. Special ICs such as Analog Device's AD589 offers a simple solution to generating, measuring, and signal processing of wave forms. This design has disadvantages such as the inefficient magnetics due to the spacing of internal components. The introduction of steel springs was identified as a possible issue interfering with the magnetic field. By experimentation with the device, the springs introduce a small 100mV high frequency signal through the sensing electronics[17]. The outcome is a low precision sensor; however, the item cost is significantly reduced. Even with one off the PCBs, customized LVDT machining and winding three versions were manufactured for less than the quoted price for a single unit including the electronic interface. In production, the cost of the designed system could be less than 10% of the prototype system.

4.2.2.2 Option 2 Load Cell

In the later stages of the research project, one manufacturer began producing low cost packaged piezoelectric load cells. The production of low cost load cell type sensors allows the simplification of the structure compared with the LVDT design. Additionally less components within the structure move and this reduces the complexity of the servo driven rotation. The cost of the piezoelectric load cell is similar to that of the LVDT design plus a greatly reduced cost of the electric design[18]. As with pressure sensing this approach avoids expensive precision equipment by using relative transient and time varying signal outputs rather than conventional absolute values. Figure 4.12 shows a load cell based end effector grasp sensing.

17 The springs produce a 10kHz 100mV signal on the base 15V signal with ADC and filter set for 1KHz.

18 The minimum price found for a LVDT IC driver was 20 times the cost of a Wheatstone bridge driver.

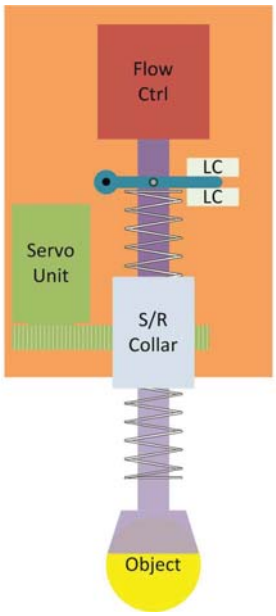

Figure 4.12: Load cell based end effector grasp sensing.

4.2.3 Servo Driven Actuation

The EE has the requirement to translate along the knuckle of the robotic core. Further the design is to allow controlled orientation of the vacuum cup. This may provide a simpler solution for orientation devices to be discussed later. A goal of the proposed system is to have a flexible structure that could arrange the packing format in an automated manner. Of the existing multi-packing systems, only Existing System 4 has the capability to autonomously modify the displacement between EEs. Existing System 4 manipulates the end effector displacement by a patented mechanical structure using a single stepper motor. A similar approach would be possible with another structure. The designs drawback however, is the fixed relation between each of the end effectors. Independence of translation between the end effectors is important for two reasons. Firstly the latest tray layouts are non symmetrical, in an effort to become more space efficient. Therefore, the relationship between the end effectors is not linear. Secondly, the independence of the movement allows for increased precision grasping and releasing of the OBJs. The inspection of media for Existing System 1 to 4 demonstrated the variation between the OBJ and the vacuum cups.

4.2.3.1 Design of Independent Actuation

A variable number of EEs are fitted to the robotic core knuckle structure. The option is to either provide a fixed servo actuator and an entire new actuation structure for each end effector, which is cost and size prohibitive, or move the motors along a fixed structure. The moving motors structure is limited to either non captive power screws or rack and pinion drives. A rack and pinion approach is taken because of the same reasons outlined in Chapter 3. If cost was not a factor, the conventional approach of using special servo motor and drives would be the ideal source of end effector actuation. Instead, simulations of normal DC or BLDC gear motors show these are sufficient. Manufacturers such as Galil Motion Control and Anaheim Automation provide low cost OEM type interfacing electronics and drives for such motors and integrate with PC control systems similar to ”real” servo systems. DC motors are the favourable initial motor selection because of the lower electronic cost and provide a higher low speed torque. However, if needed, switching to a BLDC for reliability purposes is not a major problem due to the standardisation of motor size.

Figure 4.13 presents the mechanical layout of the end effector design. Rotational vacuum cup actuation is lined with a servo driven DC gear-motor which connects with the sensing structure via a sliding collar and cord drive. The physical simplification from the sliding collar is why the low cost load cell structure is now preferred over the built and tested LVDT structure. A cord drive provides large cost savings over other direct approaches, and are commonly utilised by NZIC where relative not absolute motion is required.

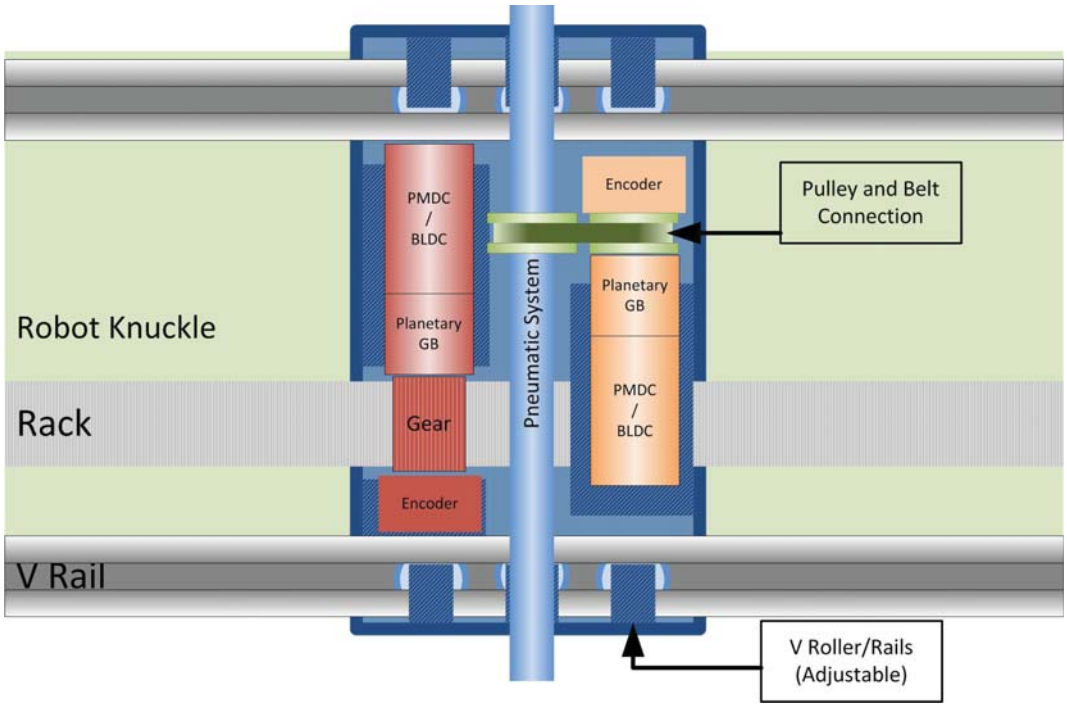

Figure 4.13: Mechanical layout of end effector design.

4.2.4 End Effector System Integration

The EEs are a modular unit as a snap on addition to the robotic knuckle. Each EE is connected to the system, mechanically by the rack and pinion drive plus V rails, pneumatically by standard positive pneumatic lines and special vacuum lines, plus a communication channel for electronics.

Two levels of development are proposed: first a prototype or field trial version followed by a production solution. The prototype system uses possible common OEM IO components in the centre with channels dedicated to each end effector as shown in Figure 4.14. The proposed production model has all the internal processing done on an internal controller with daisy chained EtherCat connection to the system core.

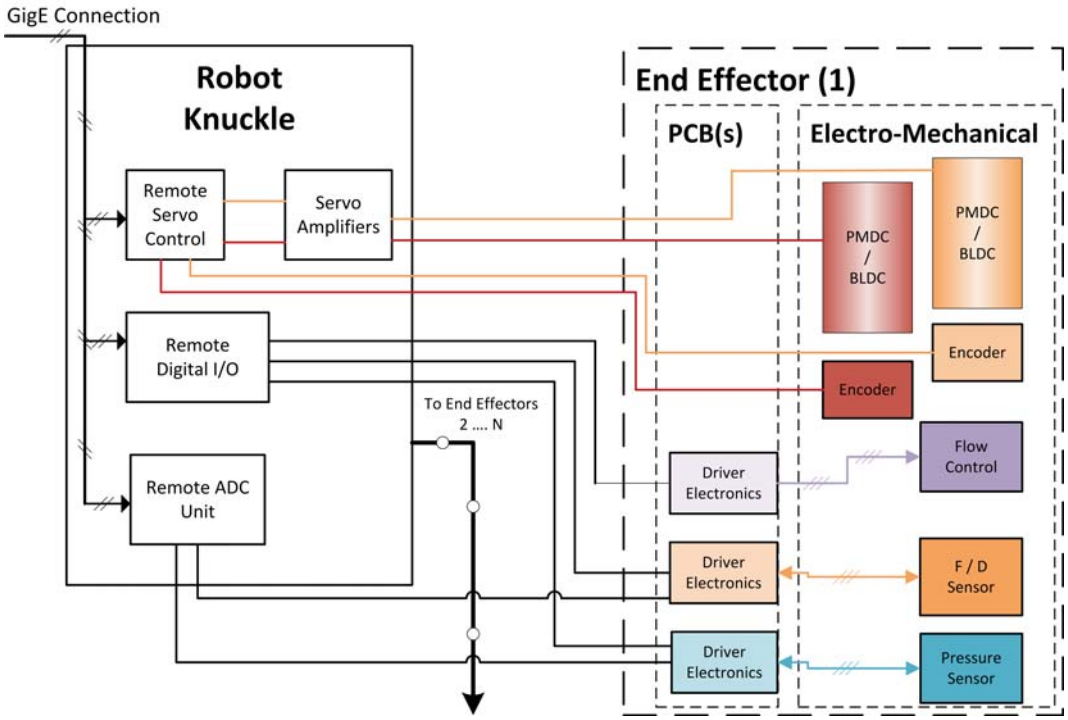

Figure 4.14: Prototype robot end effector control.

The production approach offers a greatly reduced manufacturing cost, however for research objectives, it requires too much development time and the certification process for electronics is of considerable cost. The intention is that at a later stage the research outcome will be integrated into a hardware design.

Each EE is to slide onto the robot knuckle with V guides and mechanical actuation from the rack and pinion drive. OEM remote servo controllers and drives are attached to the knuckle with dedicated channels to each EE. Remote Ethernet IO devices, both digital and analogue, are mounted in the same manner as the servo drives with channels dedicated to the grasp and relative control functions. The overall control of the end effectors is via Ethernet connection to the main control computer. The advantage of the prototype approach is that much of the equipment can be taken off the shelf and immediately put in use with minimal R&D resource. The downside is even low cost OEM marketed devices represent a substantial cost for ten EEs and considerable data transmission is required over the Ethernet communication channels. Figure 4.15

illustrates the proposed electrical/electronic layout of production end effector. E-Stop and PS routing are not shown for clarity.

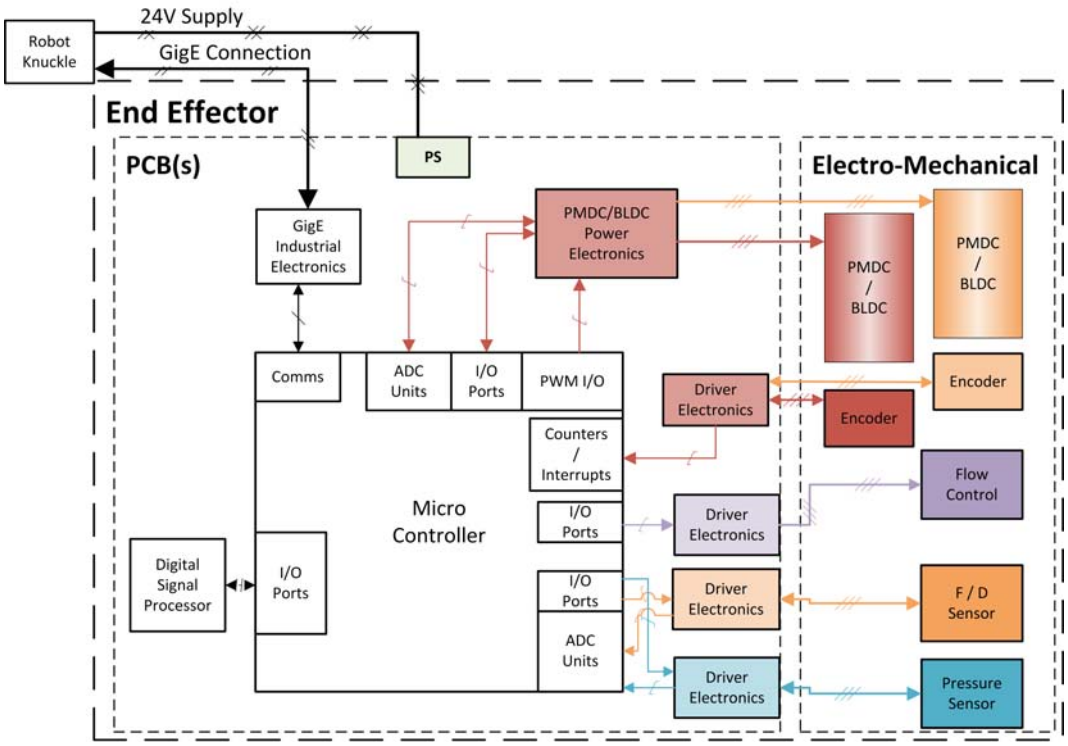

Figure 4.15: Proposed electrical/electronic layout of production EE. E-Stop and PS routing not shown for clarity.

In summary, real time high frequency signals are transmitted over a limited rate communication medium. The improved method is to have control and processing for each EE done on an integrated micro-controller, FPGA[19] and drive control unit. Such a design would remove the need for servo components and allow the heavy signal processing to be done independently. The end result being only small amounts of data transmission and reduced latency. The use of DC or BLDC motors should allow such a device to control the motors without too much difficulty.

19 The FPGA can handle the digital signal processing while leaving the control and communication to micro-controller core.

4.3 Investigation of OBJ Orientation Unit

The investigation of the existing systems demonstrate only two that can orientate near spherical OBJs and only one has full control. Existing System 5 utilises a simple controlled roller approach so that neither the NP or SP of the OBJ is shown. Existing System 6 makes use of a multi-stage roller methodology that attempts to produce a final orientation from a combination of fixed axes manipulations. A review of existing patents demonstrate a range of orientation devices that are typically designed for a particular application[46]–[50]. No strongly relevant or workable designs were found to be directly applicable to the research goal and a range of new concepts are investigated.

4.3.1 Discussion of Presented Orientation Solutions

Four novel conceptual orientation solution have been testest and are explained in Appendix B. Three driven roller approaches are presented, none presented a form that could control rotation of OBJs with any defined motion. None of the four presented layouts gives evidence of providing a robust viable solution.

The solenoid nudge approach does manipulate the OBJs, though with widely varying behaviour responses. Even if this approach did manage to manipulate OBJs, the damage, perceived or real, to the OBJs would be deemed unacceptable.

The problem with perpendicular and cross pattern systems is that the induced torque/ forces from rollers act against each other. Neither system displays any behaviour that supports a conclusion that it could be feasible. OBJs either remain stationary with the rollers spinning resulting in surface damage, or OBJs jump around almost randomly as one roller contact overpowers the others. This behaviour is such that no predictable pattern is observed from the objects.

The behaviour with these two systems is highly dependent on frictional contact and geometric variables. A difficult problem with the given systems is the difference between

static and dynamic friction. The particular problem with such design in the opposing nature of induced torques results in roller OBJ surface slip. Using Coulomb's basic model of friction, a difference exists between static and dynamic coefficients. The effect of this coefficient variation is that once a roller begins to slip, the friction is reduced and a run away condition becomes apparent. The behaviour result is that, if the torque from roller A over powers roller B, roller B's torque is further reduced and the system is hard to mechanically rebalance to an equilibrium.

With perpendicular and cross pattern systems the OBJ is contained solely by the rollers. The drawback of these layouts is that the manipulation behaviour is highly dependent on the geometry of the OBJ. Ignoring the slip considerations, the given systems could only remain constant if the OBJ is in a fixed position and entirely spherical in shape. Experiments with spherical and geometrically consistent tests on OBJs demonstrated that even with a highly controlled set of physical variables, the systems did not produce consistent behaviour. Thus, the perpendicular and cross pattern arrangements are not viable solutions for industrial applications.

The final of the four systems consists of independently driving collinear rollers. An OBJ is contained within a pocket and manipulated via controlling the interdependently driving rollers. The observed behaviour is that the OBJs can be manipulated with a rotational vector of {1,0,0} or {0,0,1}. This is, however, dependent upon containing the OBJs equally above the rollers. Balancing the OBJs on rollers via controls is not a viable control solution and the remaining option would be a variable pocket design to match each OBJ type. The fault with a variable pocket design is the tight tolerance of containing the OBJs. Balancing the OBJs requires the tolerance to be within several millimetres. OBJs contacting the pocket walls unload the rollers and slip behaviour as mentioned previously becomes apparent. The tolerance is furthermore limited to allow for a variation of the OBJ geometries.

The analysis and experiment on the presented options showed that none of these is a solution that gives evidence of a practical system that could robustly handle a range of variables at low cost and high rate. The problem with all the roller options is

maintaining surface friction throughout different behavioural states. Such an outcome makes it hard to implement roller options in the new system.

4.3.2 Belt Drive Development

The roller options presented in sections B.2 to B.4 were all susceptible to the loss of frictional contact from geometric variations. One solution that was found is to replace rollers with a belt drive. Fundamentally, the belt drive approach provides the actuation of a roller with an infinite radius (flat) and offers a means of introducing a flexible point of contact.

Having a "roller" with an infinite diameter and flexible structure assists with solving the problems with the collinear roller system, it provides the following benefits:

- Ensure the object is "balanced"
- Deform for geometric variations
- It's deformation increase surface contact

A new belt drive manipulator was prototyped based on the original collinear roller arrangement. The design replaced the fixed rollers design with two industrial rubber bands that fitted over a pair of driven and idle rollers. The driven rollers utilised a coupling with the original stepper drives and controlled by electronics and software. Figure 4.16 is an image of the original prototype system developed.

The prototyped system is operated in the same manner as previously described using the computer to send commands to a micro-controller which provides the signals for the hardware to operate. No feedback is numerically measured and the behaviour is observed .

The first prototype's manipulation of the OBJs performed towards to the level of the original concepts. Motion of the OBJs, while unstable, clearly demonstrated behaviour that would allow a controlled variable rotation axis. Further, the improved control

demonstrated that the rotational axis was not confined to either {1,0,0} or {0,0,1} but fixed to the plan formed from the XZ axes. This is the behaviour that aligns with the massless model which will be presented in Chapter 5.

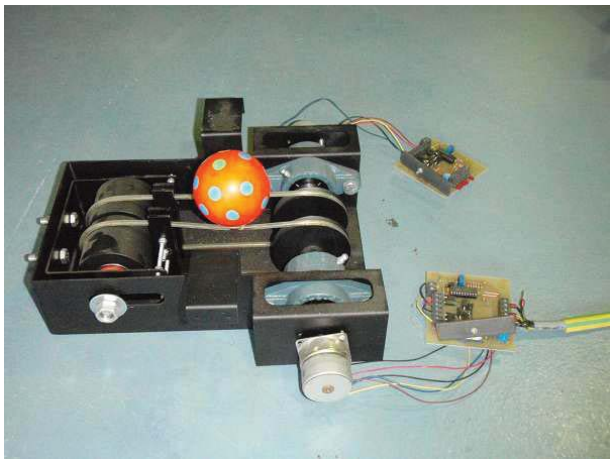

Figure 4.16: Original proof of concept orientation unit.

4.3.3 Conclusions and Recommendation for Orientation Design

The existing systems investigation did not locate an ideal example for an OBJ orientation manipulator. The approach utilised by Existing System 6 provides some evidence that a fall-back option exists if the improved techniques do not exist. Numerous conceptual solutions were prototyped and initially none of these system demonstrated a workable system. The abstract actuation methodology from one of these initial ideas was modified to provide the mechanical interference by the use of industrial rubber bands. This mechanical interference adaptation was able to induce a roughly predictable OBJ rotation. Observing open-loop control has demonstrated a robust interference behaviour across different variables due to OBJs wear and environmental factors. This robust range of behaviour is an important commercial factor as the flexibility would allow reduced human involvement or supervision. The motion behaviour of this new interference structure supports the notion that such a device could be controlled and used within a commercial environment. The proposed orientation manipulator is of a more simplified design than that employed by Existing

System 6. Additionally, the design allows for the utilisation of low cost actuation technologies. The proposed orientation manipulator as a proof of concept requires further development. The system utilised the original stepper motor drives, which did not allow sufficient rotational velocity or torque to test at viable rates.

4.4 Design of OBJ Orientation Unit

The remainder of this chapter will detail the engineering of the orientation unit for the intended commercial prototype. The hardware aspects of the mechanical and electromechanical will be presented in section 4.4.1, The electronic and software interface will be presented within section 4.4.2. The later sections will then detail the open loop control software.

4.4.1 Base Mechanical Models

Section 4.3 Investigation of OBJ Orientation Unit identified a novel orientation manipulator that could provide a viable solution. The presented material within this section takes this initial prototype and redevelops the general operation into a low cost high speed design. Figure 4.17 is the actual electro-mechanical component of the orientation system.

The complete packing system needs to integrate either a row or array of such orientation manipulators in one tight format. The dimensions of each individual orientation manipulator should be compact to reduce the robotic displacement during packing. Minimising XY plane dimensions is the priority since this reduces the inter-OBJ displacement. Minimising the orientation to tray height is advantageous although not critical.

Figure 4.17: Prototype orientation unit.

The system development aims to improve three factors of the prototype design.

1. Increase the rate of manipulation
2. Improve behaviour
3. Minimise unit production cost

Increasing the rate of manipulation is directly affected by selecting the correct motor and drive-train ratio and indirectly with more accurate control methodologies. To improve the behaviour of the manipulation device, a detailed study of the variables is presented in Chapter 6. The design presented within this section is flexible to variables to be tested. Minimising the unit cost is done by reducing the need for expensive components and simplification. The simplification reduces manufacturing cost by minimising the part count and maximising the manufacturing tolerance.

4.4.1.1 Experimentation of Motion Dynamics

The investigation of manipulation concepts identified the critical aspect as consistent frictional contact between the roller/belt and the OBJ. The prototype system explained prior utilises a simple nylon cord of medium surface hardness. Different friction surfaces or layouts are tested using three refinements of the original design.

The experiments investigated the mechanical variables of the design.

1. Cord, belt type and layout
2. Cord displacement
3. Pocket shape

The cord and belt type investigation was completed with three variations from the original proof of concept.

1. Single cord design
2. Staggered cord design
3. Belt design

The single cord design utilises the same proof of concept approach with the lowest surface hardness in an attempt to increase the friction coefficient.

The stagger cord design again utilises the softest belt material but introduces another belt on each pair of rollers. An inner cord is utilised with a reduced roller diameter to contain the OBJS with a V pattern. A possible benefit with such a containment strategy is the increased tolerance of OBJ variation, resulting in increased motion stability. The likely drawback to such a design is the different velocity of the belts due to the change in pulley radius.

The last option is to replace the cords with soft textured flat belts. The belts provide a means of maximising the surface area of OBJ contact with the expectation to stabilise motion behaviour. The second moment of area (SMA) with a belt is reduced along the

vertical axis and increased across the surface plane. The changes in SMA should provide deflection favourable to manipulation. The problem of horizontal cord deflection should be minimised without increasing vertical rigidity. Increasing the belt deflection relative to the vertical axis allows the increase of surface contact and a lower effective spring rate by a lower belt tension as shown in Figure 4.18. The reduced spring rate allows for a more consistent OBJ interference during motion.

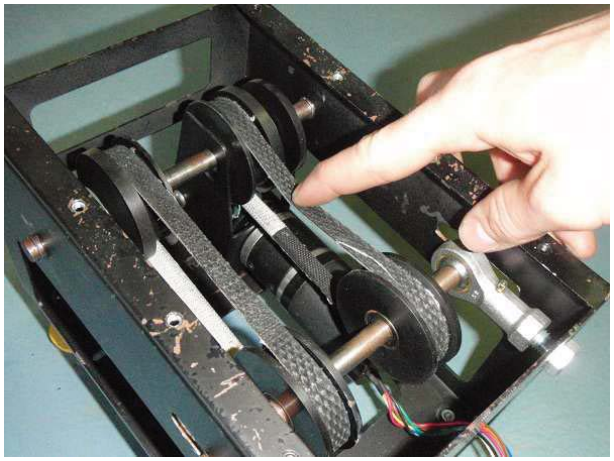

Figure 4.18: Spring rate of the belt tension.

The inter-cord displacement was observed to have behaviour effects on the motion stability and rates as shown in Figure 4.19 and 4.20. The simple relationship between cord separation and steady state rotational behaviour is a straight forward observation with the prototype. Motion stability is another aspect that can be observed and optimised through the control routine.

The final investigated hardware feature is the shape of the OBJ containing pockets. The pockets are observed to have two interaction types with the OBJs, those resulting from stable and unstable motion. Stable motion exhibits frictional contact between the pocket and OBJ's surface. This resulted in differing loading to the drive cords. Unstable OBJ behaviour is exhibited with translational motion and the pocket design induces a behaviour based on the impact dynamics.

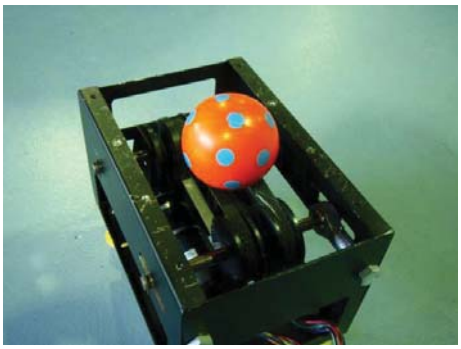

Figure 4.19: Narrow belt arrangement.

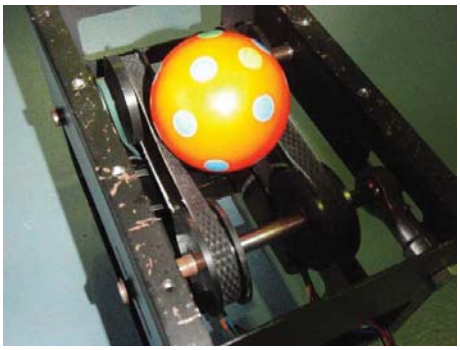

Figure 4.20: Wide belt arrangement.

4.4.1.2 Design Features

The developed system intends to closely resemble a perceived production orientation manipulator. The proposed manipulator is an adjustable design that at a later stage can be fixed to reduce costs.

The design consists of a chassis and several sub assembles

1. Pockets
2. Cords and rollers
3. Drive units 1 & 2

Pockets are produced using plastic vacuum forming over modelled surfaces as shown in Figure 4.21. The drive units are an individual assembly that provides the actuation for each of the cord or belts. A PM BLDC with integrated gearbox connects to the cord's drive rollers with a low cost pulley arrangement. The BLDC motor is utilised as the lowest cost option for the proposed layout. Selecting a sufficiently sized BLDC and gearbox combo allows the system to operate in an open loop configuration. The open loop configuration removes the need for additional feedback devices such as encoders, wiring harness, and electronic hardware resources. BLDC units sourced from high volume OEM manufacturers are only slightly more expensive than PM BDC. The total actuation system is around 60% of cost compared to a BDC approach. An open-loop

actuation is deemed acceptable since an OBJ's motion is controlled via visual servo control methodologies. The first pulley is of simple design with a CNC machined drive surface that couples the the gearbox output. The second pulley has two purposes, first to connect to the driven pulley and the second to drive the manipulator cords. The drive units further include the mechanical components such as bearings, laser cut chassis and fasteners etc. The unit provides a very low production cost design and removes an otherwise complex gear train.

Figure 4.21: Vacuum formed pockets.

4.4.2 Electronic/Software Actuation and Sensing

The remainder of this chapter presents the control elements required to automate the OBJ manipulation. This section covers the physical electrical/electronics and the base software layout. The more advanced and investigated software models are presented in Chapter 5. The layout of the orientation unit control loop is loosely outlined. Many components utilised are software or firmware[20] based and as such many different interface points do exist outside the given actual layout as shown in Figure 4.22.

20 The use of the term firmware is to separate computer and embedded electronics based software

4.4.2.1 General Description

Shown in Figure 4.22 is the control loop path representation of the system consisting of driver control, communication, interfacing electronics, and power electronics.

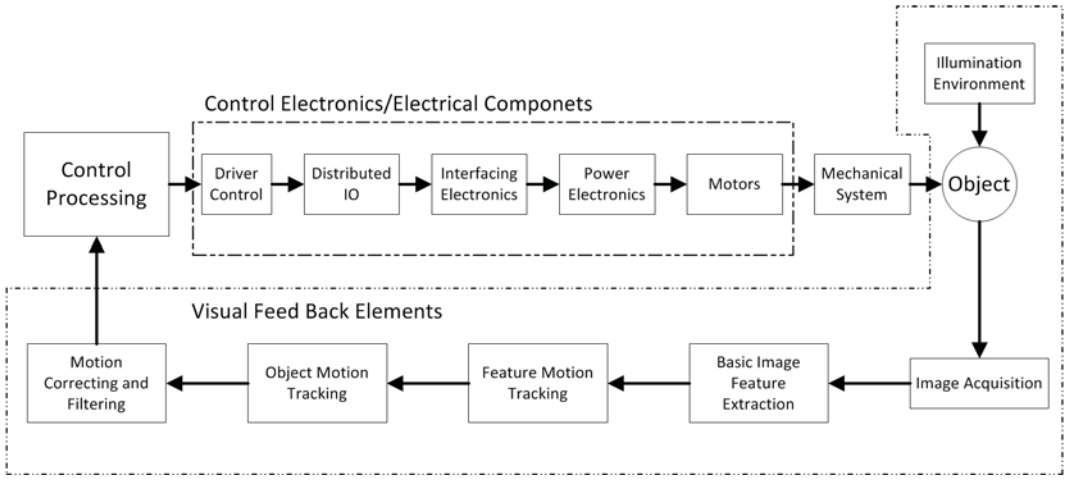

Figure 4.22: Control system loop.

Open Loop Elements

1. Control Processing
    - Not discussed in detail until Chapter 5. For the purposes here, the control loop acts as an abstract controller and provides instantaneous belt drive output.
2. Driver control
    - Specific software components that handle the link between the abstract control motion and the hardware command from software.
3. Distributed IO
    - Channels that communicate with physical electronic signals
4. Interfacing electronics
    - Hardware that interfaces between CMOS 5V signals and industrial commands.

5. Power electronics
    - High voltage or high current electronics for directly driving the motors.

Feed-Back Elements (Discussed in Chapter 5)

1. Lighting Environment
    - Controlled lighting effects for optimised image acquisition.
2. Image Acquisition
    - Camera/lens communication media
3. Base filtering, feature extraction
    - Basic pre-filtering extracting numerical data from images
4. Motion tracing
5. Measuring the motion of the object.
6. Motion correcting/filtering

4.4.2.2 Forward Loop

The low volume solutions remove the need to develop new components. The components existing with third party equipment could operate the system. Production systems that will be later described aim to reduce the cost and should improve the operating performance. These production designs however, require considerable resources to develop standard engineering solutions that would distract from the research intention. It is, however, important to consider later models and direct the research towards important aspects for the long term and avoid non-viable design approaches.

4.4.2.3 Prototype Solution

Low volume production intends to rely on 3rd party components. The preferred option is to utilise low cost PMDC or BLDC gear motors with remote IO and motor drives as the interface between the software and the actuation. This introduces a number of extra

stages for the propagation of control signals to the actuation as shown in Figure 4.23.

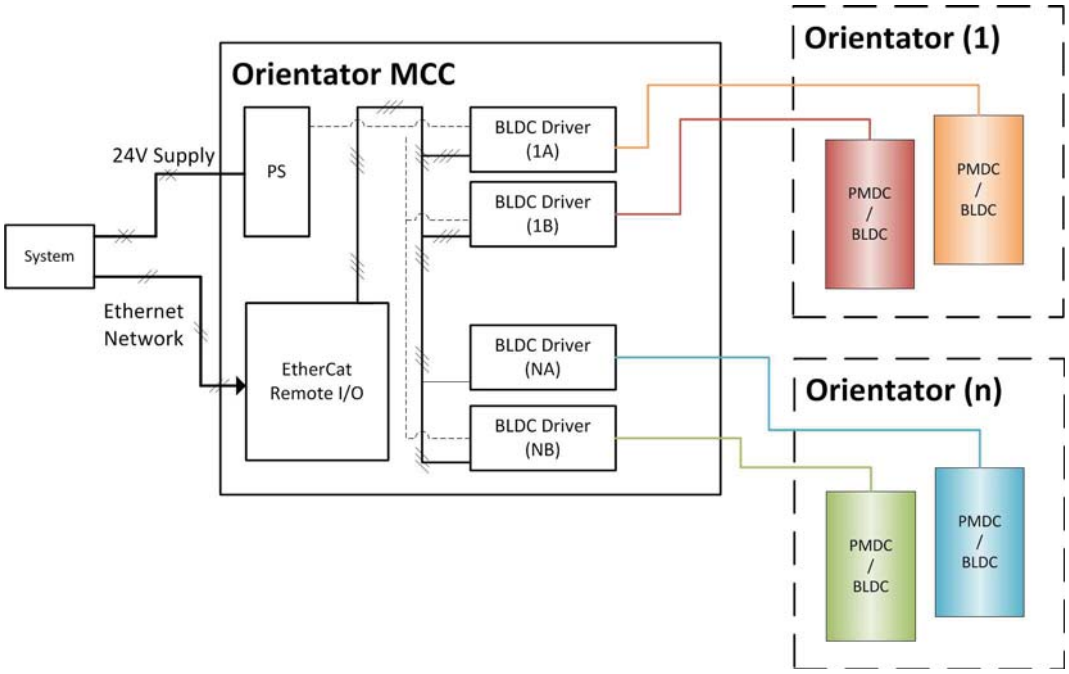

Figure 4.23: Proposed prototype variant of orientation control equipment.

This solution provides a hardware interface from the software to the actuators, with minimal detailed hardware design and the possible later reuse of components.

4.4.2.4 Production Solution

A production version of the system is intended with an increased integrated configuration, similar to the proposed end effector design. The system from topology consists of three components with the majority of functionality achieved within a single control unit as shown in Figure 4.24. Each orientation unit is controlled via an embedded micro-controller unit communicating via EtherCat with the overall system controller. The proposed controller layout would be similar to the EE unit and operate in the same fashion, likely utilising the same core design for both hardware and firmware. Such a design allows the integration of simple servo control since this can be implemented with the new firmware design. Many of the costly components for implementing a prototype servo control system are removed.

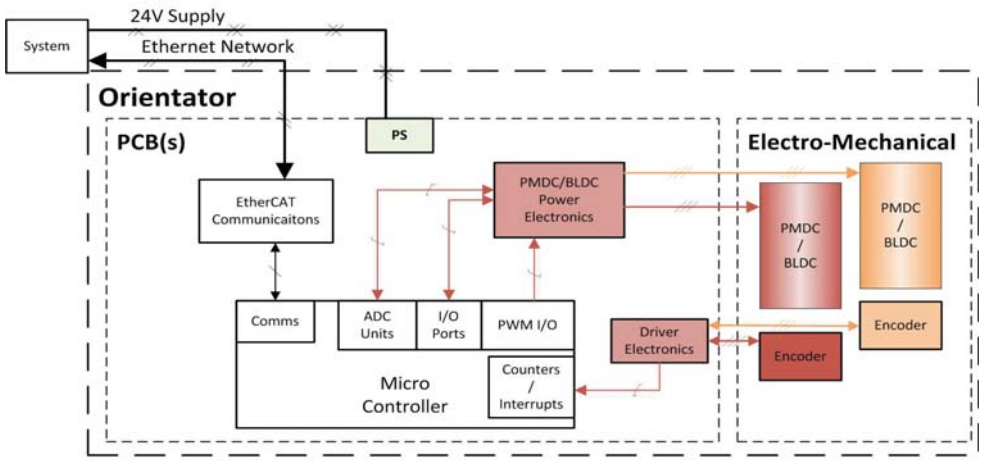

Figure 4.24: Proposed production variant of orientation control hardware.

4.4.2.5 System for the Proof of Concept

The proof of concept implementation was slightly different to the prototype solution outlined. Due to economic considerations, the testing implementation utilised a similar prototype solution but made use of the existing NZIC test equipment. Remote industrial IO was replaced with a USB Labview card, low cost speed control BLDC devices were purchased and a customised interfacing PCB was designed. The concept testing system is shown in Figure 4.25. National Instruments provides an API to control the device from either Matlab or Win32 applications. The given API is then referenced within environment with its own software object attempting to maintain real time control. This is a less than optimal solution due to the asynchronous USB communication and Windows behaviour.

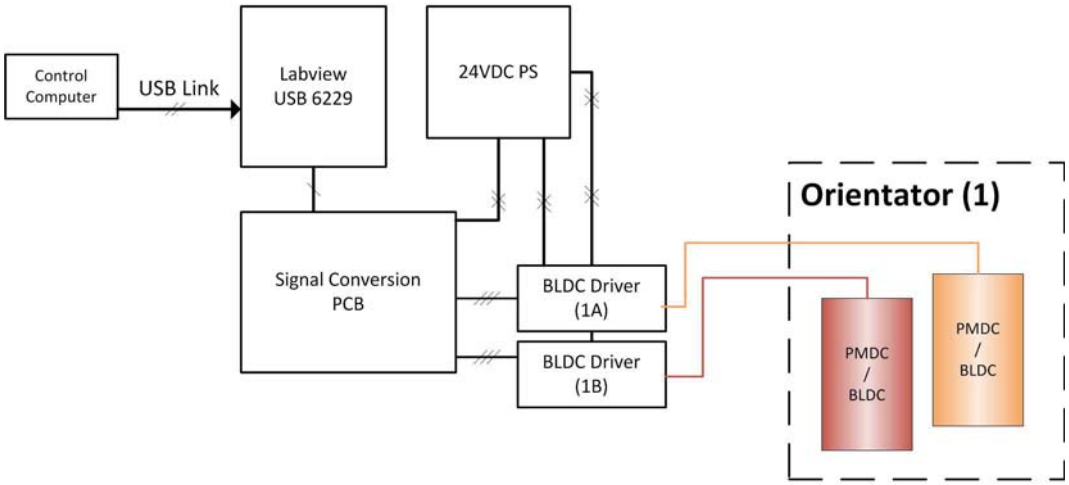

Figure 4.25: Control system for proof of concept testing.

5 Visual Servo Control System

To measure the OBJ's 6-degrees of freedom during manipulation requires the use of a visual feedback system. Integration of a vision feedback system for the purpose of control is known as visual servo control. Shirai and Inoue's work with a robot positioning blocks during the 1970s is the earliest known application visual servo control[51]. Corke and Hutchinson's 2000 review[52-55] and tutorial of the current visual servo works provides a wide range and challenges in this topic. Their works sets out the general configuration and history of the topic and explained the two main approaches of visual servo control. They demonstrated the fields of Image Based Visual Servo(IBVS) and Position Based Visual Servo(PBVS) systems. IBVS can be described as a controller that acts directly on features extracted from the image. PBVS systems on the other-hand, are controllers based on the generated 3D model of the world from the imaging device and additional known information. Many works are available detailing IBVS and PBVS systems for guided robotic manipulators or autonomous vehicle control[56]–[62]. Such works from Davison[63], Wang[64], Cahumetter[65], looked at identifying components and their position within a camera's field of view to guide manipulators.

Limited works on tracking or controlling the rotation of spherical objects have been identified within literature. Many hundreds of other applied works such as those mentioned already exist. The problem is these applications are typically case studies for one application. There seems a large number of works that track the object's centre of gravity or rotational movement. In such cases, however, the orientation of the object is identified by geometric features such as sharp edges or other inconsistent geometric features. The identification and 3D tracking of balls for the purpose of augmented reality has been investigated by Sedaeck and Riege[66]. Tracking of location and orientation of dipole in 3D space has been investigated by Greenspan and Fraser[67]. Again, these works are in a similar field to this topic, however, there are little relevant aspects except for the title. These works determined the object orientation[66], [67] and location by the use of multiple objects or the movement of defined edges. The unique

challenge for the visual servo control based OBJ orientation system is the ability to track surface features around a roughly consistent geometric object. One piece of work that was found to have strong relevance is that of Bradley and Roth[68] Their work determined the orientation of a sphere with the use of colour dots.

5.1 System Overview

The proposed system can be loosely described as a position based visual servo control system. The system utilises a captured image to model the estimated dynamics of the object under physical manipulation. This dynamic modelling is utilised for an open loop behaviour study and the real time control for manipulating the OBJs. In literature , there is little material relevant to such an application. The orientation system to be produced not only realises the expected mechanical and control theories but also a means of measuring system behaviour.

The methodology for motion tracking utilises an approach similar to the strategy that Bradley and Roth[68] reported, using blobs on the surface of a spherical object as the reference for movement. The difference with the presented methodology is mainly the ability to operate with an unknown blob model. These dots on the object are used by the vision algorithm and must act in a similar way to the OBJs in the commercial system. This random positioning of dots also removes the tedious task of placing the dots, which was mentioned as a drawback by Bradly and Roth[68]. Determining the motion of the OBJs is then achieved by tracking the blobs across image frames. Several different mathematical means of determining 6-DOF motion from known reference are presented and tested. Finally, a filtering technique is developed that applies both theoretical averaging techniques and limits with real systems.

Explained within the remainder of this chapter is the vision feedback for the orientation controller. This section outlines the approach from capturing images to producing

motion details used within the control processing. The content covers several stages.

1. Hardware elements
2. Feature extraction
3. Intra-frame alignment
4. Motion capturing
5. Motion filtering

The original development of the machine vision and the filter was achieved within the Matlab environment. Due to the live operation of the code this was later ported to a Win32 based application for real time control. This process while following the same abstract layout and operation has some differences in the implementation.

5.2 Hardware Elements

The hardware elements in this section are:

- OBJ description
- Illumination environment
- Image capturing hardware

5.2.1 Description of OBJs

The real or test OBJs for the purpose of the investigation have reference blobs attached to their surfaces. Figure 5.1 illustrates how the OBJs are presented to the vision system. Two configurations of blobs are applied for the investigation to follow. A simple general motion testing routine is based on tracking a group of coloured blobs around the OBJ. The second configuration attempts to represent a real object in production. This production configuration maintains the coloured blobs with further dedicated colour blobs to represent the NP, SP and SROI. This approach simplifies one portion of the

research by removing the need to integrate NZIC's existing advanced imaging systems into the research. NZIC's real system would track the common manufacturing surface and could conceivably operate with the same approach.

Figure 5.1: Test OBJs showing various tracking blobs.

5.2.2 Illumination Environment

Operation of the system is contained within an enclosed lit cabinet and, where possible, all components are coated with matt black paint. This illumination environment limits undesired light sources, either from the outside environment or internal specular reflections.

The illumination is via six high frequency polarised fluorescent tubes arranged off centre in relation to the manipulation unit. This avoids flicker that would be exhibited since the image capturing frequency is similar to the power grid. The fluorescent tubes are located with two vertical arrangements on each side of the manipulation structure. The lighting provides intensive illumination of vertical edges of the OBJ and reduces intensity of illumination to the top. This change in applied light intensity with the spherical or near spherical shape of the object produces a near uniform planer view for the camera. Figure 5.2 illustrates the conceptual illumination and camera layout.

An additional measure is the cross polarisation to reduce specular reflections directly from the object's surface. The cross polarisation is implemented with polariser film over

the fluorescent tubes and in front the camera lens. Figures 5.3 and 5.4 illustrate the difference between non-polarised and polarised light. The polarised illumination advantage is directly obvious with a visible and clear distinction between surface colours. Non polarised illumination suffers from the direct reflection from the tubes changing the colour perception at the CCD.

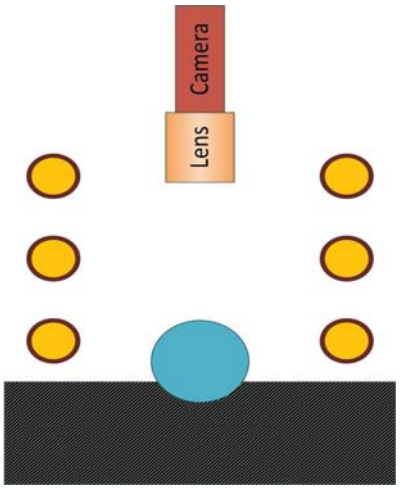

Figure 5.2: Illumination setup.

The disadvantage to cross polarising is the low diffused light transmission of the test OBJ. The reduction of visible light transmission results in shifting the shutter speed from 650us to 3200us between non-polarised and polarised light. The increased shutter period increases the susceptibility of the scene to motion blur, which limits the surface velocity that can be accurately inspected by the vision system. Motion blur with following algorithm begins to present blob tracking problems when the surface displacement exceeds 2mm between image frames. Using the 2mm guide and the shutter periods given above, cross polarising the scene limits the rotational velocity magnitude to approximately 8 $rads^{-1}$. The illumination presented is not a viable arrangement due to the need to keep the tubes at close proximity to the OBJs. This is magnified by the low diffuse light transmission from the test objects. The fluorescence tubes are utilised in the presented test set-up due to the existing systems being similar to NZIC's existing systems. The test OBJs presented are a worst case scenario and have approximately 10-15% of the diffuse transmission compared to the real OBJs.

Figure 5.3: Unpolarised scene.

Figure 5.4: Cross polarised scene.

A practical illumination approach would apply high power narrow beam angle LEDs. The LEDs would provide high intensity source for cross polarisation and the narrow beam would allow the lights to be located at a distance. An indirect illumination environment could avoid the need for cross polarisation though major hurdles are known and only one poorly operating commercial system operates with such a layout.

5.2.3 Image Capture

The final elements in the machine vision hardware is the image capturing process. This includes the camera, optics, communication hardware, and basic software interface. Several configurations are presented in the image capturing system, one for the Matlab environment and another for the real-time win32 environment with variations for un-polarised and polarised illumination. The selected camera for both configurations is an Allied Vision Technologies (AVT) Stingray F-033C[69] as they are included within NZIC's high end equipment. Lens selection is dependent on scene resolution and illumination requirements. Non-polarised illumination uses an Avitar F1.4 ½" lens with focal lengths of 8mm and 16mm for Matlab and Win32 respectively. The Win32 version runs at control cycle 10-20 times higher than the Matlab configuration and includes

more efficient logging capacity. The increased cycle rate of the win32 application allows an increase in scene resolution (pixels vs real mm), achieved with an increased optical zoom and working distance.

The camera configuration for polarised illumination is suited for increased light efficiency. A high speed 17mm F0.95 lens is used to increase light photons reaching the sensor. In theory, F0.95 lens provides double the photons on the sensor compared to "standard" F1.4[21] and was found to be necessity with low diffuse reflectance of the test objects. To complete the cross polarisation, a polariser filter is located in front of the lens with the transmission axis rotated 90º in relation to the source polariser.

The camera is connected with the computer through a copper[22] FirewireB (800mb/s) to a PCI card. Interfacing the camera output to software depends upon the development environment and the manipulator's configuration. The overall processing algorithm was developed within Matlab and later converted to a C++ Win32 application. The detailed implementations between the environments are vastly different.

The Matlab implementation utilises an AVT Matlab plugin to interface with the Matlab image acquisition toolbox. The plugin automatically handles the data formatting to suit the camera configuration within Matlab. An important part of this formatting is time stamping the image frames, setting frame rates, and the full conversion to the intended format[23]. Matlab Camera control is attained within a simple wrapper object handling the communication and callback events.

Implementation within the Win32 c++ (VS 2010 IDE) requires a lower level approach to interfacing with the camera. AVT supplies software drivers (in the form of a dll) and these pieces of third-party software are interfaced with the developed application. Again the camera control is contained within a developed controller object, though it is now responsible for implementation of background tasks, such as:

21 Lenses manufactured for machine vision market are commonly have a F1.4 aperture.

22 The standard allows either copper or fibre optic.

23 Automatically converts "compressed" YUV422 or YUV411 to an even YUV111 format.

- Handle of grabbing and releasing system resources
- Configure communication channels
- Configure buffering within software
- Simple camera control
    - start, stop, capture etc.
- Capture process
    - load into memory, set flag, time stamps, clear resources etc
- Error detection
    - Buffer overflows, communication drop-out etc.

Two forms of image capturing and configuration can be utilised with both implementations. Free running capturing is for open loop behaviour study where the images are stored within the application memory and processed after the motion. Real time capturing is for control within closed loop behaviour where images are processed between individual captures. This variation of processing is forced during development due to the speed of Matlab and the speed of code operation. The Win32 application has no real need for offline processing and this was not implemented. Table 5.1 gives the software configuration for different environments.

The algorithm to follow limits the real time vision processing within Matlab and also limits the capture rate to 4 fps. As a comparison, the same routine was later converted to a Win32 c++ application and increased resolution ran stably at 45fps.

With both configurations, a region of interest is transmitted instead of the entire captured frame. This reduces the usable image resolution and provides the following benefits.

1. Increased frame rate by less data transmission
2. Lower processing requirements due to reduced pixel count
3. Reduced image distortion due to lens effects

Table 5.1: Software configuration of different development environments.

	Matlab	**Win32**
Region of interest size	100 x 100 pixels	250 x 250 pixels
Frame rate (fps)	3.3 (Real time) 60 (Capturing)	40- 50
Colour space	YUV	RGB
Toolboxes/Libraries	Matlab toolboxes	Extensive use of Integration or customisation of 3rd party libraries (*.dlls, or combined code snippets) ○ OpenCV[70] ○ Boost[71] ○ VXL[72]

The first two are advantages that reduce the information to be transmitted and processed. Lens distortion is often mentioned as a major problem with academic works however the machine vision lenses are manufactured to a high tolerance with a quoted non-linearity of less than 0.1% for each of the three lens.

5.3 Feature Extraction

Raw images are transferred to the software portion by being fed into a fixed cyclic buffer contained in the applications memory resources. The first algorithm component's produce a group of numerical vectors that describe an OBJ's properties and visible reference blobs. In this feature extraction, pre-filtering of images has the following objectives.

1. Object mask creation
2. Colour mapping objective

3. Area classifications
4. Sanity checking of areas
5. 3D model generation
6. Reference model

5.3.1 Mask Generation

The OBJs are not rigidly contained with the manipulator structure and therefore need to be tracked within each image. Due to the controlled lighting environment a simple binary mask is sufficient to representing the OBJ's area. An example RGB image is shown in Figure 5.6. The images are transformed into different feature channels. Firstly, the RGB colour-space image is transformed into a YC_rC_b representation, shown in Figures 5.7 to 5.9. The Y channel uses a simple boolean limit. Some minor edge smoothing is utilised to create the binary mask as seen in Figure 5.10. The area and elongation of this binary mask is measured to determine if the shape is valid.

An image object is considered valid if the following two conditions are met.

- Measured OBJ area is greater than 3000 mm^2
- $\frac{L_{Minor\ Axis}}{L_{Major\ Axis}} > 0.9$

If the conditions are met and only one such object is discovered, the vision processing algorithm proceeds. If the conditions are not met, the processing is cancelled due to errors. The processing of an invalid image frame is skipped because capturing useful/reliable information is unlikely and any attempt would increase processing time. A hierarchy controller monitors the processing results and identifies a series of invalid images which trigger other modes of control states to take actions.

5.3.2 Blob Detection

Circular coloured stickers are placed upon the test and real OBJs. The stickers are a

simplification for the process, avoiding the execution of the complicated algorithms for measuring actual features on real OBJs. The coloured blobs attached to the test OBJ are shown in Figure 5.6.

Four types of blobs are utilised for the different objectives. The blobs either represent a real physical feature or a general blob for motion tracking research.

- North Pole
- South Pole
- Region of Interest (ROI)
- Tracking Blob

The tracking blobs are located by searching the region contained by the intensity generated binary mask. The blobs are identified within this region by the remaining CrCb colour channels. Identification of the different blob colours is done by converting the C_rC_b representation to a channel representing each configured blob colour. The activation of the new blob colour spaces represents the fit of each pixel with the defined C_rC_b colour matching. Figure 5.11 demonstrates the colour activation for an image of pixels.

The individual pixel colour classification could be completed with a number of different adaptive techniques. However, the use of polarised light simplified the image processing problem and a simple fixed binary threshold was found adequate. The result of filtering is a simple binary image channel for each colour classification.

As with producing the OBJ mask, a rough object recognition algorithm searches the image to identify possible items. A first pass of the algorithm removes small noise blobs from the image. The remaining image is dilated and eroded in a simple attempt to join pixel groups of the same common real blob.

The remaining binary image is again searched with the object tracing algorithm and processed in detail to determine which of the remaining blobs are valid. The blobs, as seen in the image, are round coloured stickers placed on the object's surface.

Identification of valid blobs is more involved than a simple procedure with the spherical object mask. The planar projection seen by the camera is dependent upon the polar location of the sticker.

The problem faced with different polar locations has two root causes:

- Reduction in surface resolution
- Change in projected geometry

Figure 5.5 demonstrates the problem with the theoretical projection of the blobs with two different view points. These problems are due to the spherical geometry of the OBJ and therefore a change surface normal relative to the CCD sensor. For the effect of varying surface projection, an adaptive blob filtering technique is applied. Both the measured blob area and shape must match a minimum area and shape model. Additionally, the orientation of the blobs major axis must match the vector normal to the COG.

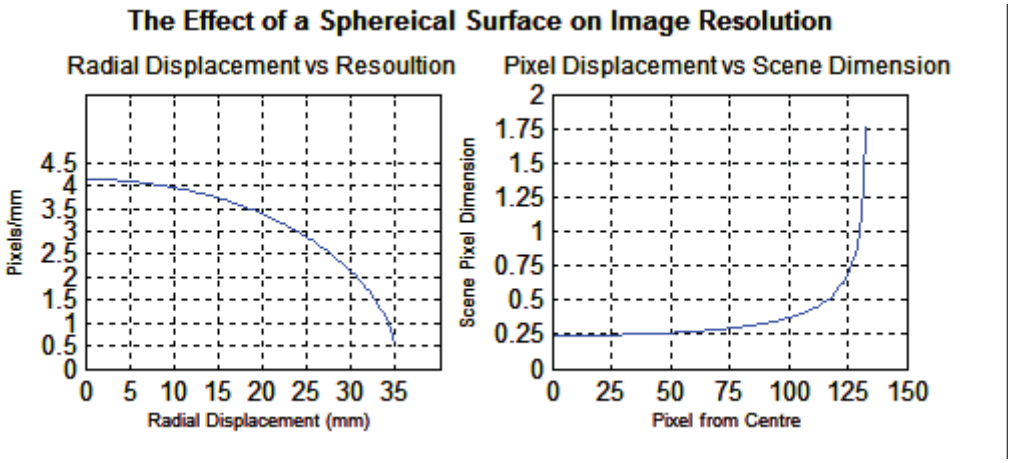

Figure 5.5: Effects of imaging a spherical object.

The planer image location of the blobs are transferred to 3D Cartesian location relative to the OBJ's centre. The 3D location is calculated with the assumption of a perfectly spherical object. This assumption presents a problem with real OBJs, however, experimentation discussed in Chapter 6 demonstrates the approach works as intended.

To improve on the assumption, the method will need to reconstruct the OBJ geometries from a series of images which is a complicated process with unconstrained motion. Figure 5.6 to 5.14 show the steps of this process.

Figure 5.6: Raw image captured with cross polarisation.

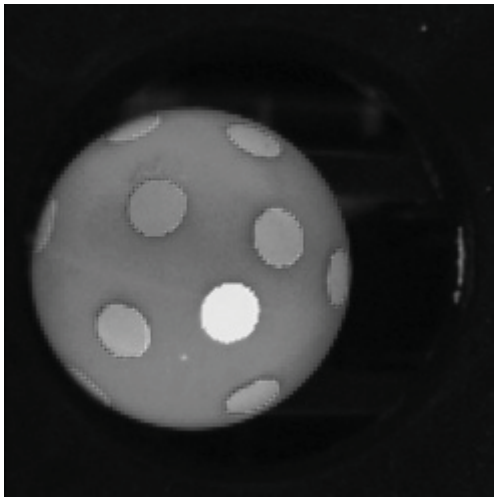

Figure 5.7: Intensity image produced from the raw image.

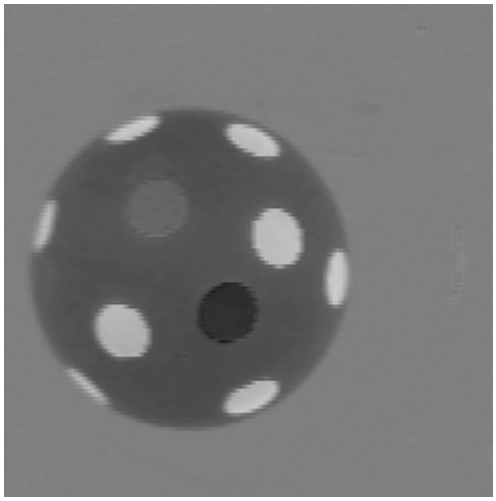

Figure 5.8: Red component of the image.

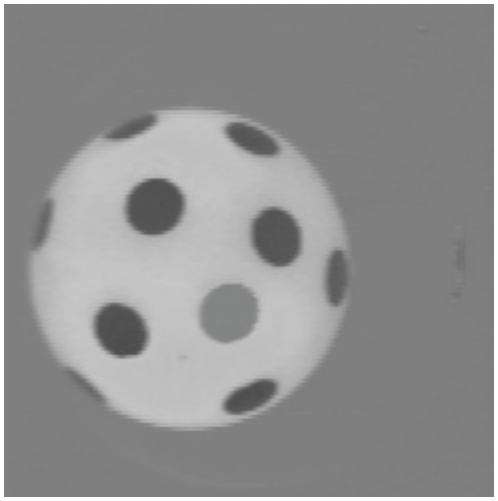

Figure 5.9: Blue component of the image.

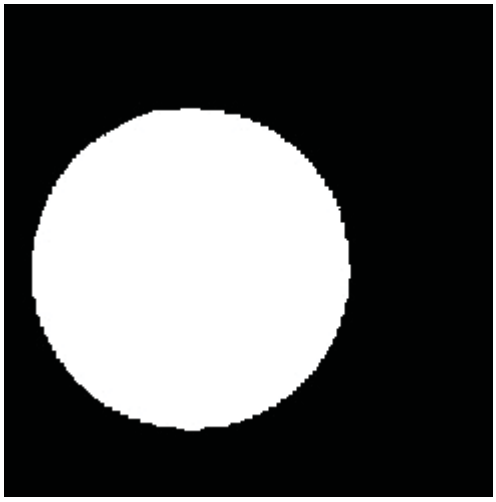

Figure 5.10: Mask produced using intensity image.

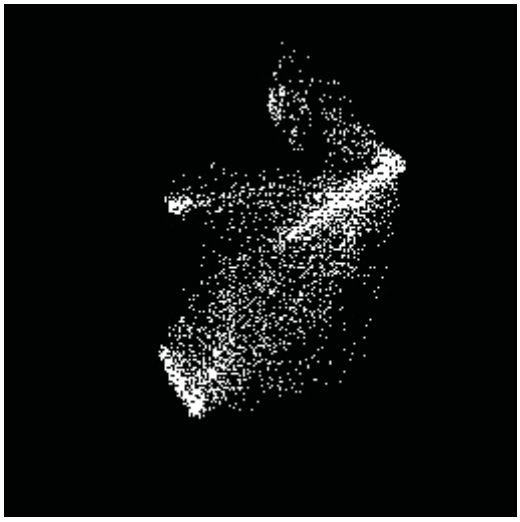

Figure 5.11: Colour space of image.

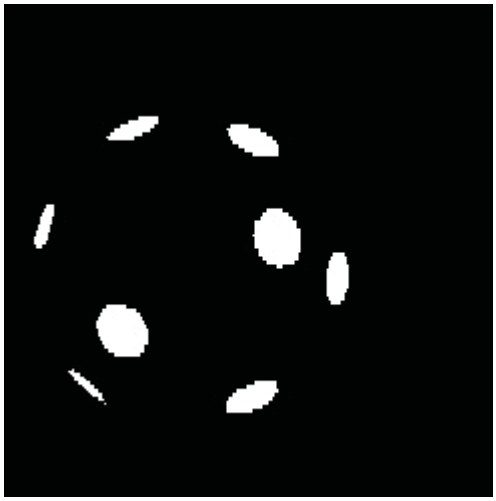

Figure 5.12: Blue dots after filtering.

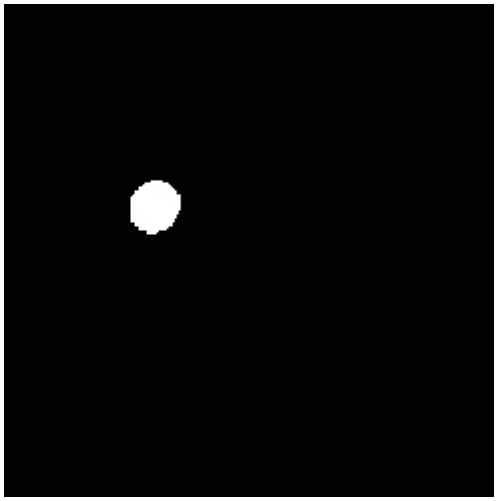

Figure 5.13: Green dot after filtering.

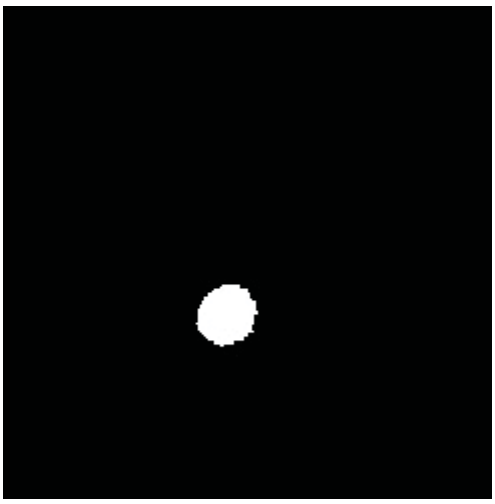

Figure 5.14: Yellow dot after filtering.

The real 3D location of each blob is determined by using planer image's locations and assuming the OBJ is a perfect sphere. Equations 5.1 to 5.3 outline the process to calculate the relative 3D blob location. Equations 5.1 and 5.2 describe the blobs in polar terms based on the OBJ's centre of area. Figure 5.15 demonstrates this problem using a real lens where the image scene is actually a cone and not a planar representation. Equation 5.3 estimates the latitude positions of the blob based on the assumption that object is sphere as shown in Fig. 4.43. Finally, Equation 5.4 combines the previous four to produce a blob location in the relative Cartesian space.

$$\theta_{long} = \begin{cases} \arctan\left(\frac{y}{x}\right), x \geq 0 \\ \pi - \arctan\left(\frac{y}{x}\right), x < 0 \wedge y \geq 0 \\ \arctan\left(\frac{y}{x}\right) - \pi, x < 0 \wedge y < 0 \end{cases} \tag{5.1}$$

$$ArcLength = \sqrt{x^2 + y^2} \tag{5.2}$$

$$\theta_{lat} = \arccos\left(\frac{ArcLength}{Radius}\right) \tag{5.3}$$

$$\begin{bmatrix} x \\ y \\ z \end{bmatrix} = \begin{bmatrix} Radius \times \cos(\theta_{lat}) \times \cos(\theta_{long}) \\ Radius \times \cos(\theta_{lat}) \times \sin(\theta_{long}) \\ Radius \times \sin(\theta_{lat}) \end{bmatrix} \tag{5.4}$$

Upon completing the processing of the incoming image frame, the calculated OBJ's properties, listed below, are extracted for later intra-frame motion processing.

- Object major and minor dimensions
- Object XY position
- Blobs information
    - Blob XYZ
    - Blob Type

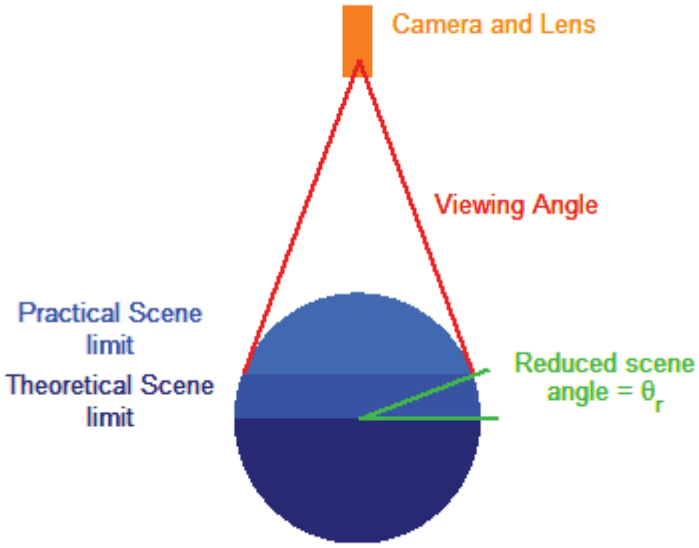

Figure 5.15: Diagram of non-infinite length lens and their scene limiting effect on inspecting spherical objects.

5.3.3 Intra-Frame Blob Tracking

Tracking a well defined and unique feature between image frames is a relatively straight forward process. The OBJ's position is determined and a translation to the physical coordinates gives the measure of motion during the sample period. OBJs with predefined or geometric discontinuities allow the determination of the object's orientation.

The blobs placed representing the OBJ's points of interest are a predefined pattern that can be tracked between image frames. These three reference points, however, do not provide enough information to determine the fully flexible OBJ. The NP and SP are π radians apart and therefore are not visible simultaneously. To measure the rotation, additional points or a robust method of matching against a predefined model are required.

A direct approach would be to increase the number of unique dots visible upon the OBJ. The drawback of such an approach is the need for a high number of unique features. Six different reference points could be theoretically utilised and were applied in a trail to directly measure the axis.

An immediate problem is the need to have 6 unique reference points plus the addition of an OBJ unmarked surface. An abstract viewpoint should make this implementation a simple task by simply varying the colour and/or the shape of the blobs. In practical terms, however, applying this methodology runs into several problems that are difficult to overcome. The three main problems are:

1. 6 reference points is the minimum with infinite camera working distance.
    - A real system will need more than 6 points because the camera field of view does not cover the full π radian view.
2. 7 Different colours are difficult to differentiate in a real system.
    - The real images do not utilise the full activation of the different colour spaces. Figure 5.11 is a demonstration of this problem and the result is that the colour dimensions between blobs are not distinct regions. Refinements with cross polarising the scene illumination provided a system that could detect four different colours without sensitive calibration.
3. The change in pixel resolution and distortion makes shape matching difficult.
    - Shape matching works when the blobs are located on the top area of the OBJ. In this location the surface is near planar to the camera and the resolution is sufficient. Towards the OBJ edge, the distortion and reduction in resolution increases. Individually, these problem could be overcome by a further correcting algorithm, however the information is insufficient. Figure 5.5 displays the surface resolution against the planar radial position as seen by the camera.

A different solution was sought with a methodology similar to Bradley and Roth. Their approach utilised numerous non-unique blobs and matched the intra-blob pattern to a stored model. The algorithm searches the different possible intra-blob patterns and

finds the best fitting orientation for the image. This approach was shown to work in their research. However, for this research and applications drawbacks exist.

At the centre of the processing algorithm is a fixed model representing the location of the blobs. The location of the blobs are predetermined by a pseudo random generator and then fixed to the object's surface. Bradley and Roth outlined the disadvantage to this approach, which is the need to manually fix the blobs in a determined position. The task of accurately positioning the sphere with three degrees of rotational freedom is difficult and is intensely time consuming.

Directly applying Bradley and Roth's approach to the desired visual servo system would magnify the outlined drawbacks. Their methodology is highly dependent upon the correct placement of dots. Many different OBJ's are to be tested by the system and this time consuming task, along with the corresponding human error, would become an even greater problem. Additionally, experiments to be presented in Chapter 6, operate the manipulator for extended periods of 24 hours a day, 7 days a week. The 24/7 automated systems need to handle time varying changes such as blobs wearing and image artefacts from surface damage.

The direct application of the methodology is not a practical approach, however, the problems are from the predetermined model. To avoid the model based drawback a intra-frame adaptation is applied.

A blob reference is generated for each image frame. Determining matching blobs between frames is computed by matching the prior blob reference with the different combination of blobs in the existing image. A number of the best matching frame references are then utilised to estimate the rotational displacement vector. The rotational vectors are then searched with a basic sanity check to estimate the rotation displacement.

The use of intra-frame references removes the need for a fixed blob model. This removes the root cause of the problems encountered by Bradley and Roth. The

consequence is that additional sources of errors are inherent.

1. The approach measures the intra-frame rotational displacement rather than the fixed position. The effect of such is the total position change during a period includes the sum of errors.
2. A limit exists for the measurable rate of rotation based on the frame capture rate and the number of blobs.

Comparing the fixed model with intra-frame model, the fixed model approach is probably the most accurate of the two methods; however it is not practical. Due to the drawbacks, the rotational vector as found by the proposed algorithm, is not directly applied.

5.4 Inter-Frame Feature Tracking

In the prior section, the relative Cartesian locations of the blobs were calculated from the pixel locations and known system constants or assumptions. These describe each blob with a 3D Cartesian position relative to the OBJ's centre. To link the blobs across numerous frames, an intra-frame blob reference procedure is presented. This frame reference intends to produce a unique combination of vectors that describe the intra-blob displacements. Since the blobs are fixed to the OBJ's surface, the relative positions of these blobs remain constant between image frames.

The group of blobs are arranged from highest to lowest latitude (Z axis value). Bradley and Roth mentioned this serves the purpose of utilising the centre most point as the starting location. Assuming an independent motion between image frames, then such a point is most likely present in both images.

To create a reference, refer to Fig. 4.44 to 4.46. The points P_n are rotated to a set alignments which is used for comparisons. The alignment places P_1 on the ball's Z axis

and P_2 at some location on the positive of the X axis. This produces a fixed alignment procedure for any two given points.

Stage 1: Alignment of P1 to the Z axis

First the rotation matrix to transform P_1 to the Z axis {0,0,1} is determined by Equations 5.5 and 5.6. Equation 5.5 determines the direct axis of rotation between P_1 to the Z axis. Equation 5.6 determines the magnitude of the rotation for alignment using the axis found from equation 5.5.

$$R_{Axis} = \frac{P_1 \cdot Z_{Axis}}{\left| P_1 \cdot Z_{Axis} \right|} \tag{5.5}$$

$$R_{\Theta} = \arccos\left(\frac{P_1 \cdot Z_{Axis}}{\left| P_1 \cdot Z_{Axis} \right|} \right) \tag{5.6}$$

This gives the rotation axis and the angle needed to form the rotation matrix that transforms P_1 to {0,0,1}.

$$R_{Mat} = \begin{bmatrix} R_x^2(1-\cos(\Theta))+\cos(\Theta) & R_x R_y(1-\cos(\Theta))-R_z\sin(\Theta) & R_x R_z(1-\cos(\Theta))+R_y\sin(\Theta) \\ R_x R_y(1-\cos(\Theta))+R_z\sin(\Theta) & R_y^2(1-\cos(\Theta))+\cos(\Theta) & R_y R_z(1-\cos(\Theta))-R_y\sin(\Theta) \\ R_x R_z(1-\cos(\Theta))-R_y\sin(\Theta) & R_y R_z(1-\cos(\Theta))+R_x\sin(\Theta) & R_z^2(1-\cos(\Theta))+\cos(\Theta) \end{bmatrix} \tag{5.7}$$

Next,

$$P_{Aligned\ Stage1} = P_{Raw} . R_{Mat} \tag{5.8}$$

Equation 5.7 is applied to each blob therefore rotating all the blobs around a common rotation vector as if they were fixed to the OBJ's surface. Figure 5.17 demonstrates the transformation thus far.

Stage 2: Alignment of P_2 around the Z axis

The dot locations are rotated around $P_1(0,0,1)$ to align P_2 so that $P_{2y} = 0$ and $P_{2x} > 0$

The axis is known as [0,0,1] and the rotation required is the result of an arctan2 function to provide a rotational displacement from $-\pi$ to π radians. A new rotation matrix

is calculated similar to Equation 5.7 with the new axis and displacements. The result of this transform is that P_1 is still located at the OBJ top, dead centre of the camera and P_2 is situated on the X axis with positive location. As with the rotation in stage 1, all the remaining blobs are also transformed. Since P_1 and P_2 are in the defined positions the same intra-blob layout can be later attained.

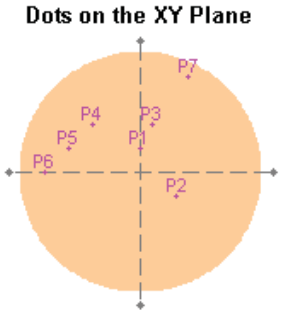

Figure 5.16: The location of dots P_n prior to alignment procedures.[81]

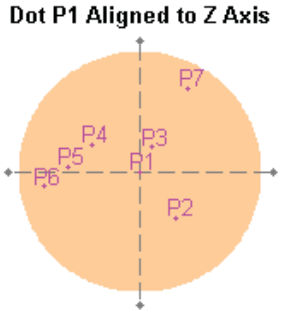

Figure 5.17: The location of dots P_n when P_1 is aligned to the Z axis.[81]

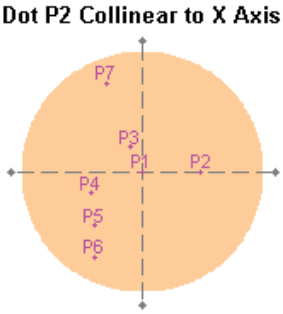

Figure 5.18: The location of dots P_n when P_2 is aligned to the X axis.[81]

To provide values to match with the current image, a dot layout reference is achieved by taking the intra-dot vectors of $P_{aligned}$ that describe the different dot combinations. The number of different combinations is determined by the software configuration and visible points. This decision governing the number of visible points is based on several factors, including motion feedback. In a perfect system and with no occlusions, the greater the number of dot combinations, the tighter the match to the conditions. The downside is the exponential increase in combinations to search as shown in Figure 5.19.

The software configuration determines the number of references to be searched for matching blobs. A maximum and minimum set of blob references are configured depending upon the runtime environment and capturing mode. The intention is to have as many blobs represented within the constraints of processing rate. Figure 5.20 demonstrates the blob reference computations to be calculated, based on the variables of total blobs and blobs to match between image captures.

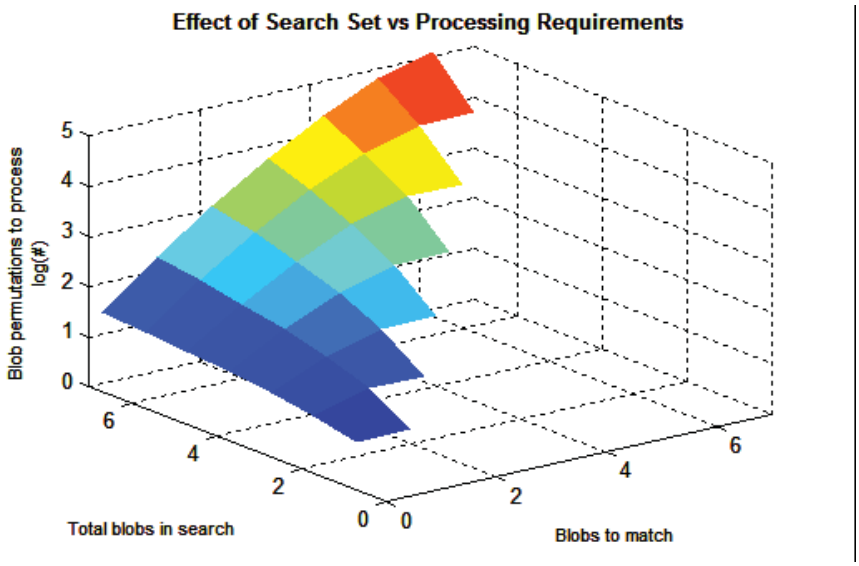

Figure 5.19: The effect of increasing search sets and the resulting exponential increase in processing loops required. Note that the processing loops are displayed as Log_{10}.

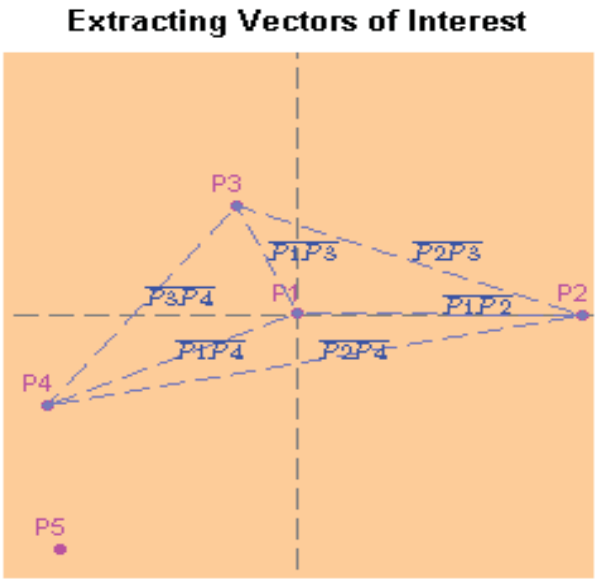

Figure 5.20: Extraction of the 6 vectors to define the location of the four closest points.[81]

5.5 Matching Intra-Frame Dot References

The intra-frame dot references are matched by a two-pass algorithm. The first pass searches all possible combinations for a defined number of possible fits, utilising a sum of squares error technique. If the result of the first pass does not produce a clear reference match then a more intelligent matching algorithm utilises an algorithm that considers occlusions. Depending upon the software configuration, a blob reference is created for each permutation that is utilised in the comparison. The procedure is similar to that already explained in the preceding section. The configuration sets out the maximum number of blobs to investigate N_i with permutations of length N_p.

1. The blobs are arranged from the highest to the lowest latitude. These are named $C_1 \ldots C_{ni}$
2. The permutations are determined with N_i and N_p
   - $N_i = 5$, $N_p = 3$, the permutations would be $|C_1\ C_2\ C_3|$, $|C_1\ C_2\ C_4|$,$|\ C_1\ C_2\ C_5|$, … $|C_5\ C_4\ C_3|$
3. A reference is created for each permutation arrangement
4. Each reference is matched to the prior fixed utilising a biased sum of squares of the error measuring algorithm.
5. The N best matching permutations are evaluated to determine if the current match is sufficient or if the second pass is required.

To determine the correct dot matching between frames, a sum of squares technique is used to compare the difference between the referenced values. This comparison is done with magnitudes and the direction, furthermore two different weightings are bias towards the centre dot. Vectors that contain the P_1 dot are scaled by 2:1 over the remaining vectors. Direction errors are wrapped within the range $\{-\pi, \pi\}$.

5.5.1 Intelligent Pass

The second pass searches the possible matching references by modelling the movement with an internal feedback loop. Estimating this movement, the rotation vector is simplified in the version of the preceding section 5.6 . The routine seeks for a rough sanity check and concludes which blobs are likely to be present in both images.

A rough rotation vector is produced with the first two reference points in each matching permutation.

The rotation velocity vector is subjected to a simple sanity check. Theoretically the object could be rotating at any rate and have infinite rotational angular acceleration. Practically, however, it is known that the object should not be rotating at a rate greater than 10π $rads^{-1}$ nor should it be subjected to a high angular acceleration as the input torque is insufficient.

Those combinations that pass the sanity check are searched for blob occlusions. Occlusions are searched via the application of the rotation vector (or inverse) to the prior and current permutation.

Applying the rotation vector to produce the rotational matrix for comparison can be investigated. The 3D model of the OBJ, as seen by the prior and current images, can be produced. This provides two sources of blob checking.

1. The 3D model of blob locations can be identified as the blobs should be present in both or only one image.
2. The 3D model allows the blob location error to be measured with rotational displacement.

5.6 Determining the Unit Axis of Orientation

The previous section detailed the two-pass methodology for matching tracking blobs across image frames. Accurately traced blobs are passed to an algorithm that determines the motion of the OBJ. Motion of the OBJ is described in the x,y,z,i,j,k degrees of freedom, these being the three Cartesian and three rotational degrees of movement. The Cartesian coordinates are a simple procedure to determine using the mask COG. The challenging aspect to this motion tracking is determining the rotational vector (i,j,k). Three methods of finding the rotation vector are described and implemented. The first two are the generalised form of common methodologies produced by Horn[73], [74] in which variations and similar forms are used extensively by others[75]–[78], and the common twist/screw matrix that describes screw threads. The last algorithm is a proposed intersection of planes methodology that finds a best fit axis without the over head of mapping the translational motion.

5.6.1 Finding an Axis with the Intersection of Planes Methodology

Since the blob locations are measured relative to the OBJ's COG, the motion tracking operation only needs to find the motion's rotation vector. The translational motion of the OBJ is already known and therefore a simple approach is taken to find the rotational aspect. The blob locations rotate around a common axis that must intersect with the relative position {0,0,0}. The rotation direction is found by combining a series of planes that each describe a space of possible rotation axis vectors. Each matched pair of blobs (P_m and C_m) gives an initial and final point in 3D space. Utilising these points, a plan can be found that contains all the theoretical rotation vectors that could achieve this movement. This is different to the direct cross product approach that finds only one vector describing the most direct rotation vector. The result is such that blob pairs P_m, and C_m produce m number of planes.

The true direction of the rotation vector can be found with the inter-plane intersects since the following two conditions are met. These two conditions are utilised both directly and indirectly to determine the rotation vector.

1. A line of intersection is always defined for two planes that are non-parallel.
2. Since all the dots on the surface of the ball are rigidly connected to all the blobs they are therefore rotating around a common axis.
3. The rotation axis should intersect at point {0,0,0}

It is assumed that no planes are parallel with this application since the points are rotating around a reasonably close origin. Theoretically, all the calculated planes from the individual dots should intersect along a common line, this being the axis of rotation. In a real system, however, measurement errors will result in the intra-plane intercepts showing an approximation. A biased sum of squares methodology first finds the best fit axis then the best fit rotation displacement.

The process is split into several stages.

1. Computing the planes for each individual blob pairs
2. Computing the line of intersection for each plane combination
3. Determining the error of each intersection
4. Determining the best axis
5. Determining the best rotation displacement

5.6.1.1 Computing Planes

For each pair of dots, P_m and C_m, the axis of rotation must fall along the plane perpendicular to the linear displacement and intersect the centre of this displacement. To find this plane, the special relationship between the orthogonal matrix (perpendicular) is used to solve the equation for a plane.

$$M \cdot N = 0 \tag{5.9}$$

Where N is the vector determining the displacement and M is the vector representing

the mid point between P_m and C_m. P represents the prior points, C represents the current points.

$$N_m = \left[C_{mx} - P_{mx}, C_{my} - P_{my}, C_{mz} - P_{mz} \right] \tag{5.10}$$

$$M_m = \frac{\left[C_{mx} + P_{mx}, C_{my} + P_{my}, C_{mz} + P_{mz} \right]}{2} \tag{5.11}$$

Substituting Equations 5.10 and5.11 into Equation 5.9 obtains Equation 5.12 that expands to equation 5.13, which describes the plane from each dot's movement. Equation 5.13 groups all the constant values to the right for clarity.

$$N_x(x - M_x) + N_y(y - M_y) + N_z(z - M_z) = 0 \tag{5.12}$$

$$N_x x + N_y y + N_z y - (N_x M_x + N_y M_y + N_z M_z) = 0 \tag{5.13}$$

The operation gives *i* number of planes, with *i* being the number of matched dots between the image frames. Figure 5.21 to 5.22 demonstrate the approach to find the possible axis of rotation. Figure 5.21 shows how the plane of possible axis is generated with the prior and current position of a tracked blob. Figure 5.22 illustrates the different combinations of the resulted planes from different possible rotational axes. In this figure the three different planes intersect along one common line, this being the true rotational axis.

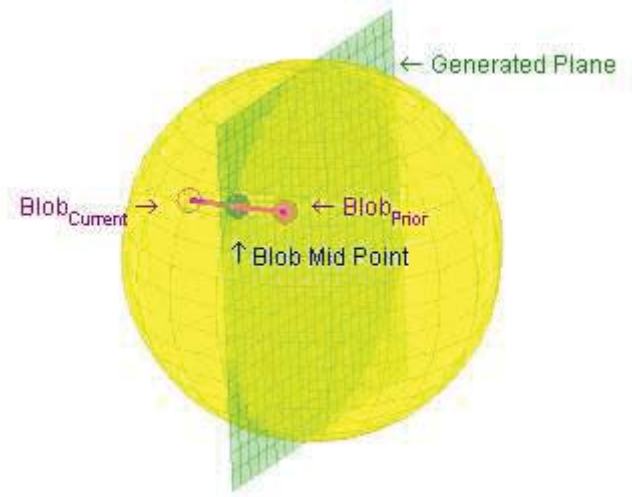

Figure 5.21: Generating a plane of possible rotational axis from a pair of blobs.

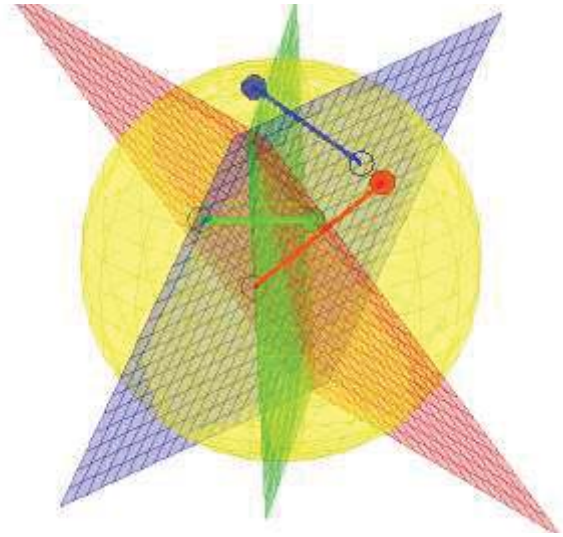

Figure 5.22: Example of a created axis of rotation from the intersection of different blob planes.

5.6.1.2 Computing Plane Intersections.

Theoretically, the resultant planes calculated from the individual dots should intersect along a common axis of rotation. The number of intersections is determined by the total possible combinations of planes, numerically calculated by $N_{int} = {}^2C_i$. Each inter-plane intersection forms a 3D line that can be described by a simple linear equation. The direction of this line is given by the cross product of normal vectors of the planes. Computing this process forms N_{int} of general forms of an axis direction or 3D gradient.

$$I_{ab_{Direction}} = N_a \times N_b = Dir_{ab} \tag{5.14}$$

The two planes intersect when Equation 5.12 is satisfied for each plane. This relationship gives two equations with three variables. A line is an infinite 3D feature, therefore, it must intersect with each of the X, Y, and Z axes. By solving either $I_x = 0$, $I_y = 0$ or $I_z = 0$, the two equations can then be solved. $Z = 0$ is chosen for this application as it will provide a simple error measurement for the next process.

$$I_{ab_{offset}} = \begin{bmatrix} -\dfrac{N_{b_x}N_{a_z} - N_{b_z}N_{a_y}}{-N_{b_x}N_{a_y} + N_{a_x}N_{b_y}} & -\dfrac{N_{b_y}N_{a_z} + N_{a_x}N_{b_z}}{-N_{b_x}N_{a_y} + N_{a_x}N_{b_y}} & 0 \end{bmatrix} = Off_{ab} \tag{5.15}$$

The vector that describes the plane intersection can be found by substituting the results of Equations 5.14 and 5.15 into the generic equation for a line in 3D space. This vector can be described by equation 5.16 and is the estimated axis of rotation using the combination of two dots. Figure 5.14 graphically illustrates this equation.

$$Dir_X(x - Off_X) + Dir_Y(y - Off_Y) + Dir_Z(z - Off_Z) = 0 \tag{5.16}$$

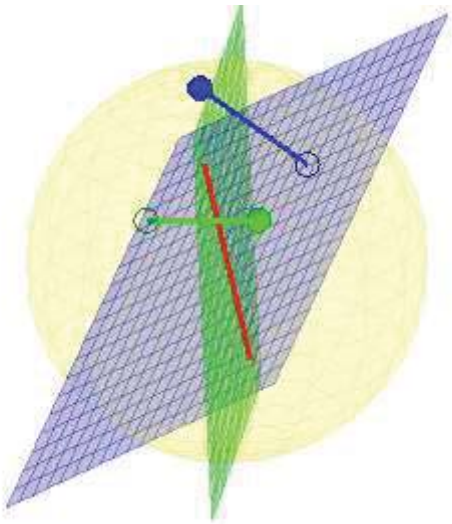

Figure 5.23: Axis found by intersection of two different blob planes.

5.6.1.3 Determining the Best Fit Rotation Direction

Thus far the full 3D theoretical axis of rotation has been computed for each combination of blobs. Applying the third constraint *"The Rotation Axis should intersect point {0,0,0}",* with the result of Equation 5.15 (Off_{ab}) for each plane combination produces a vector describing the known intersection error with the XZ plane. The magnitude of Off_{ab} is applied to find of the best fit of the axis. The larger the magnitude, the less trustworthy the intersection line. Figure 5.13 is an example of a typical real measurement where one combination gives a result that is clearly incorrect. Figure 5.12 is a zoomed in inspection of each rotation vector around the datum point. The dotted lines represent the Off_{ab} vector that describes the Z axis intersection for each rotational axis found. To determine the best fit axis, the outlying combinations according to Off_{ab} are excluded from the calculation. The weighting of the remaining combinations are calculated via the inverse of the magnitude squared. The direction of the best fit axis is determined by the weighted averaging of the plane intersection combinations.

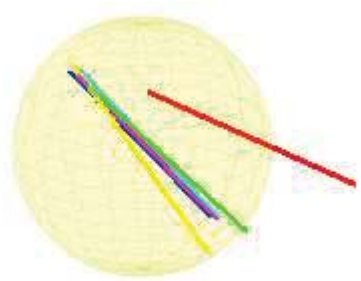

Figure 5.24: Measurement of rotation axis found by the intersection of planes.

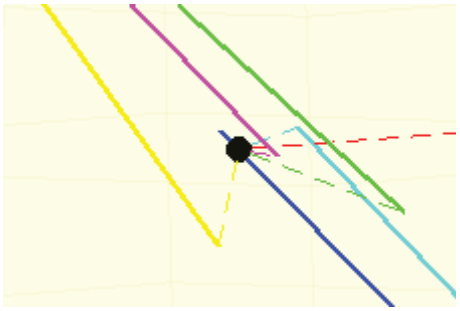

Figure 5.25: Up-close view demonstrating the offset from {0,0,0} as utilised for means of error measurement.

The simplified equation for finding the best fit direction of rotation iis shown in Equation 5.17 below.

$$\%I_{Mean} = \frac{\sum_{j=1}^{j=n} \frac{1}{|Offset_j|^2} I_j}{\sum_{j=1}^{j=n} \frac{1}{|Offset_j|^2}} \tag{5.17}$$

The true implementation utilises a two-pass routine with weighting to exclude outliers and avoid dividing by zero.

5.6.1.4 Determining the Best Fit Rotation Displacement

The rotation magnitude that best fits the found axis is calculated with a two-pass algorithm, both of which utilise the sum of square errors. The first pass measures the accuracy of the blob pairs normal vectors to the best fit axis(radius of rotation). The second pass determines the blob pair accuracy for the rotation displacement.

As a point rotates around an arbitrary axis, a vector can describe the normal intersection. A pure rotation around this axis results in the blob's normal intersecting with the same point along the axis. Introducing error or translation movement has the

effect of introducing a relative movement along the axis of rotation. This movement can be in the form of translation along the axis line and/or a change in the normal length. The blobs are given as relative positions to the OBJ's COG, therefore any change in this intersecting vector is a measurement of machine vision error. The first best fit operation measures these errors in terms of magnitude and finds a weighted error for each blob. This first weighting serves two purposes: measuring a weighting based on a "known" reference and to immediately exclude outlying blob pairs.

$$T_{Translation} = (P_{Current} - P_{Prior}) \cdot I_{Axis} \tag{5.18}$$

$$R_{Current} = |P_{Current} \times I_{Axis}| \tag{5.19}$$

$$R_{Prior_{Raw}} = |P_{Prior} \times I_{Axis}| \tag{5.20}$$

$$P_{Prior_{Correct}} = P_{current} - T_{Translation} I_{Axis} \tag{5.21}$$

$$\theta_{CurrentPrior} = \cos^{-1}\left(\frac{P_{Current} \cdot P_{Prior_{Corrected}}}{|P_{Current}||P_{Prior_{Corrected}}|}\right) \tag{5.22}$$

The adaptive weighting methodology provides the means to measure the error proportionally without error overflow as the normal magnitude tends to zero[24]. Equation 5.23 produces a limited error factor based on the theoretical translation along the rotational axis. Equation 5.24 produces another error factor based on the relative variation radius between the prior and current blob locations. Lastly, Equation 5.25 produces a weighting based on the average blob radius to the OBJ's total radius to bias towards less noise susceptible measurements. The three weightings are then combined into one factor in Equation 5.26.

$$\%Error_{Translation} = 1 - min\left(\frac{2T_{Translation}}{R_{Current} + R_{Prior_{Raw}}}, 1\right) \tag{5.23}$$

$$\%Error_{Radius} = 1 - min\left(2\frac{|R_{Current} - R_{Prior}|}{R_{Current} + R_{Prior_{Raw}}}, 1\right) \tag{5.24}$$

$$\%RadiusWeight_{Blob} = \sin\left(\left(\frac{R_{Current} + R_{Prior}}{2R_{Object}}\right)\left(\frac{\pi}{2}\right)\right) \tag{5.25}$$

$$\%BlobWeight_{Raw} = RadiusWeight_{Blob}\, Error_{Radius}\, Error_{Translation} \tag{5.26}$$

24 The problem with dividing by 0 or close to 0.

The first pass rotation magnitude measurement is then calculated by computing the blob's individual error against the total weighted mean of the remaining blob pairs. The weighted mean and the standard deviation are shown in Equations 5.27 and 5.28.

$$\theta_{Mean} = \frac{\sum_{i=1}^{i=n} BlobWeight_i \, RotationMagnitude_i}{\sum_{i=1}^{i=n} BlobWeight_i} \tag{5.27}$$

$$\sigma_{Mean} = \frac{\sum_{i=1}^{i=n} BlobWeight_i \left(RotationMagnitude_i - \theta_{Mean} \right)^2}{\left(n_{non\,zero} - 1 \right) \frac{\sum_{i=1}^{i=n} BlobWeight_{n_{non\,zero}}}{n}} \tag{5.28}$$

The second pass refines the displacement calculation by applying a weighted window process as represented in figure 5.26. The window has three portions: full weighting of 1 applied to the measurements within a software configured factor of standard deviation of the computed mean, a sum of squares error applied to the roll off stage and 0 to the final excluded results.

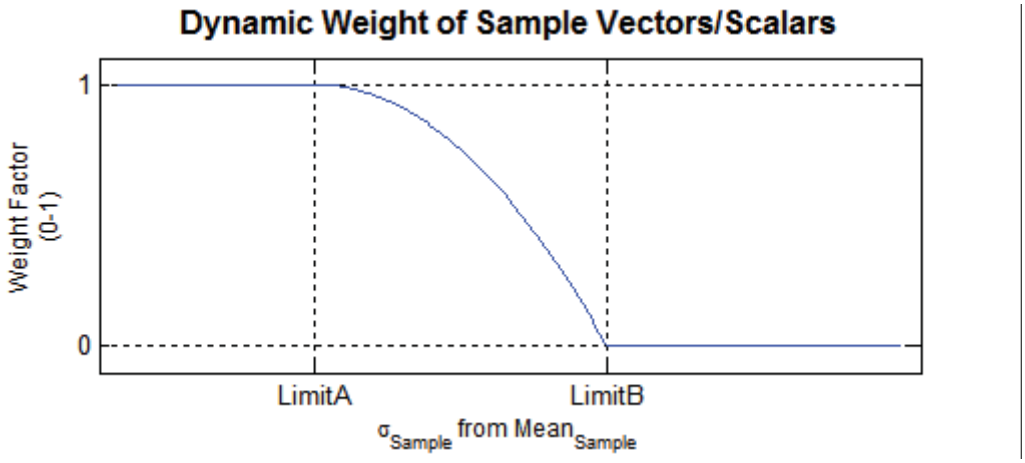

Figure 5.26: Dynamic weighting function.

Equations 5.29 to 5.31 produce the final calculated rotational magnitude prior to producing the rotational vector. Equation 5.29 determines the difference between an individual sample of the mean rotational rough magnitude from Equation 5.28. Equation 5.30 produces the new weighting for each specific sample point. Finally, Equation 5.31 gives the corrected rotational magnitude utilising the new weighting.

$$\%Diff_i = \frac{\left|RotationMagnitude_{mean} - RotationMagnitude_i\right|}{\sigma_{Mean}} \tag{5.29}$$

$$\%Weight_{Final_i} = \begin{cases} 1 & Diff_i \le Limit_A \\ \dfrac{(Diff_i - Limit_A)^2}{(Limit_B - Limit_A)^2} & Limit_A \le Diff_i < Limit_B \\ 0 & Diff_i > Limit_B \end{cases} \tag{5.30}$$

$$\theta_{Mean} = \frac{\sum_{i=1}^{i=n} BlobWeight_i \, RotationMagnitude_i}{\sum_{i=1}^{i=n} BlobWeight_i} \tag{5.31}$$

The final output of the intersection of planes and visual servo system is calculated using Equation 5.32 by combining the calculated axis direction (Equation 5.17) and magnitude (Equation 5.31). This vector is then stored as time stamped intra frame rotation displacement vector.

$$\%R_{t_n - t_{n-1}} = I_{direction}\theta_{Mean} \tag{5.32}$$

6 Behaviour Investigation

The successful application of a fully automated self organising packing system has identified two technical areas of challenge. Presented so far has been the background into the topic and the proposed technologies developed to solve the problem for commercial applications. This chapter will investigate the behaviour of the new systems presented in Chapters 4 and 5. The behaviour study is in two parts, the pneumatic grasping of the OBJs and the study of the orientation system.

Literature study found very little relevant information above elementary levels, reviews of the existing systems showed the utilisation of pneumatics with little detailed thought. This study made on pneumatic grasping of the given OBJs has two stages. The first stage investigates the base properties of the grasp formation to determine if such pneumatic approaches are viable. The second stage applies the proposed grasping design to test and verify the model behaviour.

The second part of the chapter focuses on the the motion behaviour of the OBJs while under manipulation. Observed so far are the general trends of predictable behaviour. This motion is not a clean output as the study needs to verify if the motion is such that OBJ can be orientated correctly. The algorithms for the proposed visual servo control feed back are tested for accuracy. A detailed testing routine then inspects the motion stability of the proposed Orientation device.

6.1 Base Study of Pneumatic Grasping of OBJs

Proving a reliable OBJ handling manipulator is an important piece of this research Through the literature study, evidence shows that pneumatic vacuum cup EEs are common for OBJ packing systems. These pneumatic EEs were used in every packing system investigated and offer a low cost solution. There are however known reliability

issues of pneumatically grasping OBJs. The difficultly forming or maintaining the OBJs to vacuum cup seal could be attributed to a range of sources; these being

1. Geometry of the OBJ surface
    - Specifically the NP and SP regions
2. Geometry with surface/COG moments
3. Surface contaminants
4. Mechanical deflection of vacuum cup

Secondary to determining the means of maintaining the vacuum seal, is the influence of the pneumatic variables on the systems other measurements. The following aspects are studied to gain an understanding of grasp influence:

- Vacuum pressure.
- Vacuum cup design.
- Pick and place tolerances.
- Porosity of OBJs

6.1.1 Equipment, Variables and Procedure

The base study of pneumatic OBJ grasping was done at a suppliers headquarters with a vacuum test rig (VTR) and a series of vacuum cups. To limit the testing dimensionality the cups were reduced to recommended "practical" designs. Table 6.1 lists the vacuum cups that were recommend. The XP-B40 was recommended as the best option for lifting OBJ of type A. The two other options were the XP-BL30 and XP-BL40. OBJs of type B were lifted by the XP-B30, XP-B20 and XP-BL30.

Table 6.1: Vacuum cup at supplier.

Vacuum Cup	Type	Width	Durameter[25]
XP-B20	Single Bellows	20	50
XP-B30	Single Bellows	30	50
XP-B40	Single Bellow	40	50
XP-BL30	4 Bellows	30	50
XP-BL40	4 Bellows	40	50

6.1.1.1 OBJ Porosity Testing

Verifying OBJ porosity is aimed at determining the level of extent vacuum cups can be utilised to manipulate the OBJs. Grasping OBJ_B is known to cause problems with surface contaminants and forming a reliable seal generation on NZIC's RTP. OBJ_A is assumed to have a low porosity, however, this is verified and provides a comparison with $OBJs_B$ results. Figure 6.1 shows the porosity measurements during the base study. Twenty OBJs of each type have been tested for porosity across the different portions of their surface. The porosity of two variations of OBJ_A demonstrate an unmeasurable porosity on the VTR[26]. As expected, OBJ_B demonstrates a large porosity and provides a strong explanation of why NZIC RTP has such difficulty with OBJ_B. The OBJ porosity figure has an element named "Object B -1 97%" that is governed by producing a mean with 97% confidence interval based on the mean and standard deviation of the measurements. The confidence intervals for $OBJs_A$ are not shown since the values are negligible.

25 Durameter is an application unit that describes the hardness of the material.

26 The measurements of Object A-1 and A-2 have been offset to show their porosity readings in the figure.

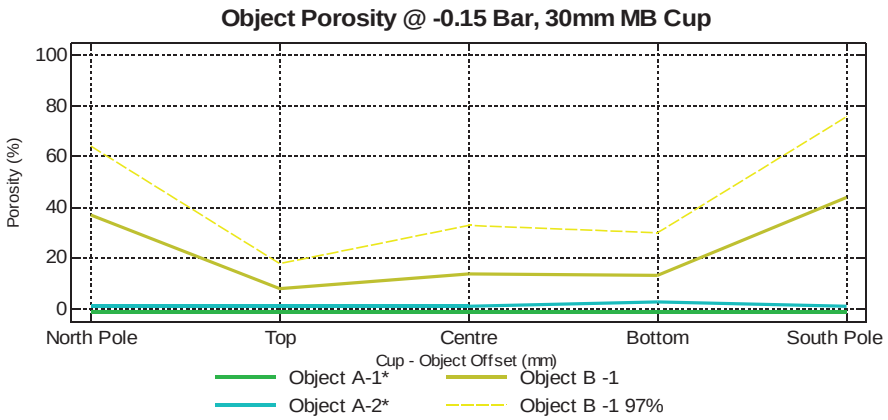

Figure 6.1: Porosity testing of real OBJS with test equipment.

6.1.1.2 OBJ Grasp Tolerance

A further testing procedure investigates the machine's tolerance of grasping and holding OBJs. The procedure is a multi-variable experiment to gain an understanding of each variables effect on the grasping. The variables are as follows:

- Offset from the OBJ's COG
- Vacuum pressure
- Vacuum cup design
- Robotic interaction

OBJs are grasped at different displacements from the OBJ's COG and it is determined if such a grasp is sufficient. Table 6.2 outlines the variable used for the grasp testing.

Table 6.2: Physical variable range for grasp tolerance testing.

Variable	**Range**			
Vacuum depth (bar)	0.1	0.15	0.2	
Grasp displacement(mm)	0	10	20	30

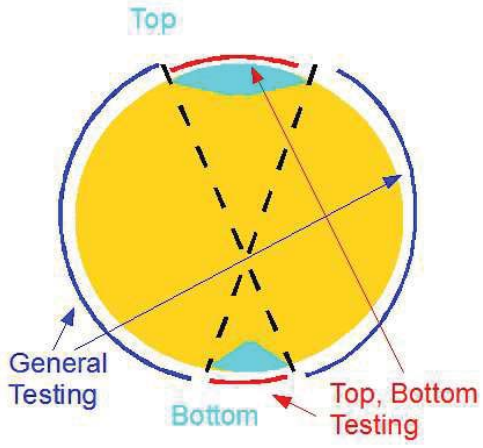

Figure 6.2: Grasp testing regions on the OBJ's surface.

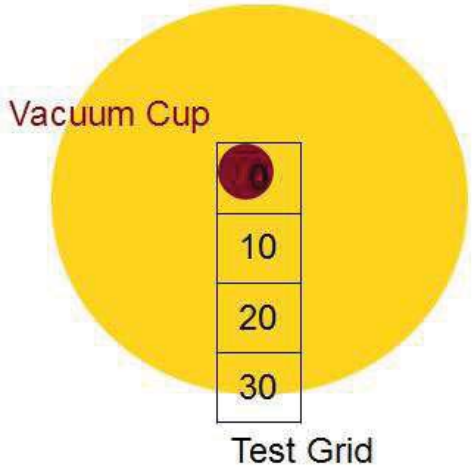

Figure 6.3: Grid for testing the position tolerance of OBJ grasping.

Developing a robotic solution to provide an improved grasp flexibility exhibits an increase in production cost. The study aims to understanding if such a functionality would produce a significant performance advantage. Firstly, to investigate the possible advantage, two forms of surface interaction were evaluated. Vertical interaction is maintaining the vacuum cup and buffer in a vertical position, this would be the low cost option. second, a normal interaction is when the vacuum cup and buffer is held at an angle perpendicular to the OBJs surface.

Each test point is measured subjectively ten times using a the Boolean result "Sufficiently held." This measurement "Sufficiently held," is an judgement if the force and seal produced from the vacuum cup is sufficiently reliable to transfer the OBJs. The estimate is based on a small shake motion in the horizontal and vertical planes, the shake is assumed sufficient for a pattern packing format and possibly slow row packing.

Figures 6.4 to 6.7 show the sufficiently held outcome across the variables. Each plot is the sufficiently held outcome for one OBJ and interaction type. Multiple lines are present representing a cup design with the corresponding vacuum pressure. The vacuum cup and vacuum description for the figures is in the form of XXYY-Z.ZZ.

- XX is the cup design
  - MB → multiple bellow cup
  - SB → single bellow cup
- YY is the cup width at the sealing surface
  - 40 → 40mm diameter
  - 30 → 30mm diameter
- ZZ is the vacuum depth in Bar

Figure 6.4 is the outcome of lifting OBJ type A with a fixed vertical cup arrangement. The multiple bellow cups have a wide range of OBJ grasp tolerance. The 30mm diameter cup demonstrates a wider range of grasp tolerance compared to the 40mm version. This supports the judgement that OBJ grasp is not primarily governed by the total exhibited vacuum cup force. Rather the important cup property is the flexibility to deform and match the OBJ's surface contours. The single bellow cups do not provide evidence of generating a reliable grasp. The single bellow cup only shows a high degree of grasp containment with the cup centred upon the OBJ's COG and the highest tested vacuum depth. The failure of the single bellow design further supports the evaluation that flexibility of the seal area is a critical element.

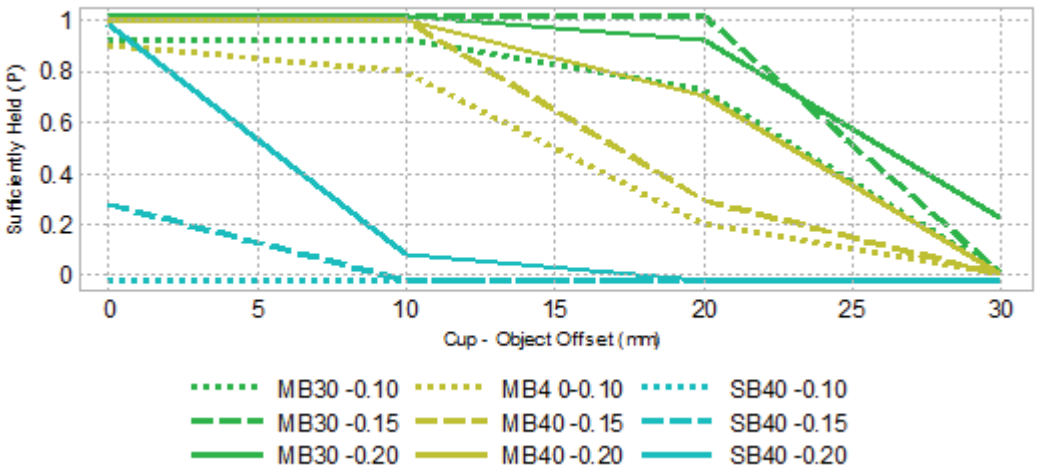

Figure 6.4: OBJ Type A vertical lift.

Figure 6.5 shows the outcome of lifting OBJ type A with a vacuum cup at the normal to the OBJ's surface. The nine configurations all demonstrated an improved OBJ grasp response compared to the vertical lift. Multiple bellow cups of 30 and 40mm diameter when applied with a higher vacuum depth, sufficiently grasp the OBJ across the full range of COG displacement The grasp behaviour of the single bellow design also improves and expands the vertical lift performance for increased COG displacement.

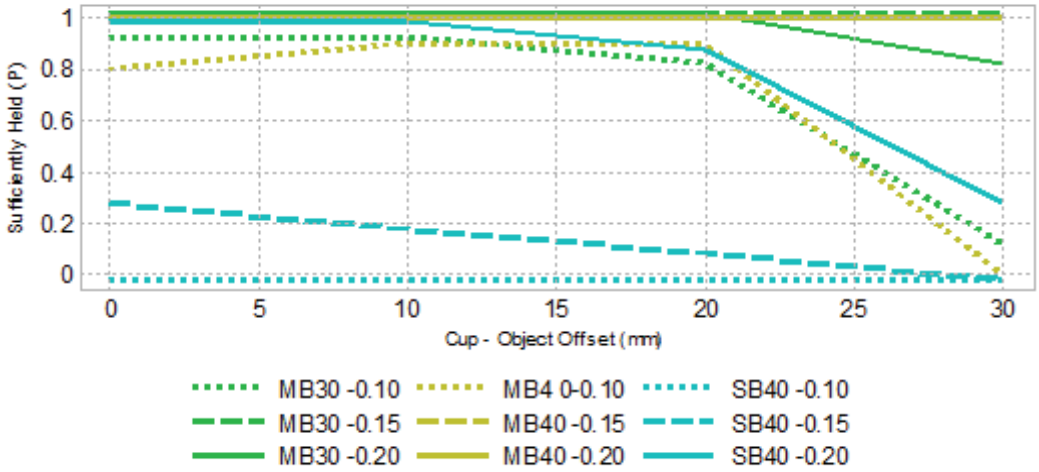

Figure 6.5: OBJ type A normal lift.

Figures 6.6 and 6.7 demonstrate the pneumatic grasping of OBJ_B. OBJ_B is more challenging to successfully grasp than type A.

The 30mm multiple bellow vacuum cup demonstrates a reasonable grasp outcome when used with a high vacuum pressure to overcome the higher porosity. OBJ grasping with the 20mm diameter multiple bellow cups are not displayed since grasp was insufficient in all cases. Comparing the plots of vertical and normal grasp demonstrates only a small increase in reliability is present. The lack of difference between the two grasp types suggests that the limiting element of grasping OBJ_B is the applied vacuum pressure due to OBJ porosity and not the rigidity of the cup design. The rigidity of the cup design is still a factor as can be seen from the difference between 30 and 40mm cup diameters.

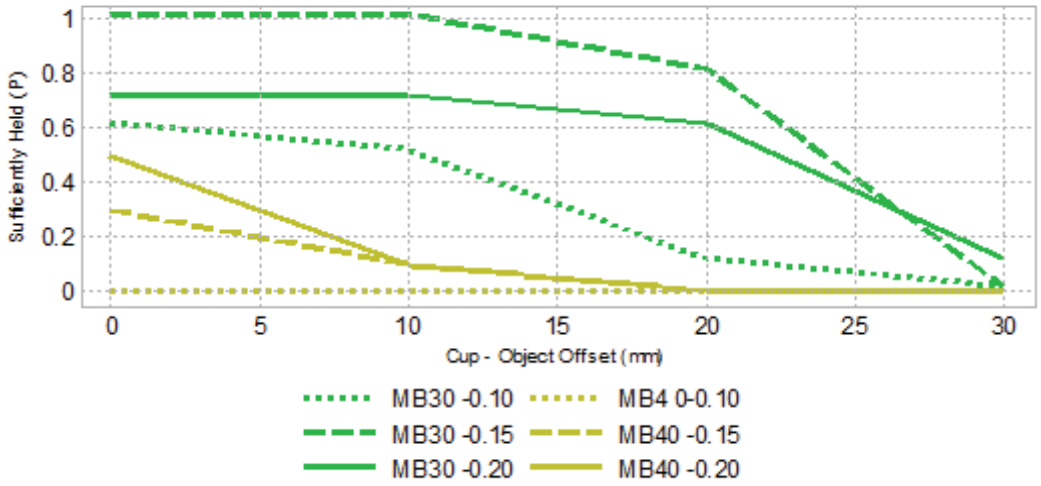

Figure 6.6: OBJ Type B vertical lift.

.

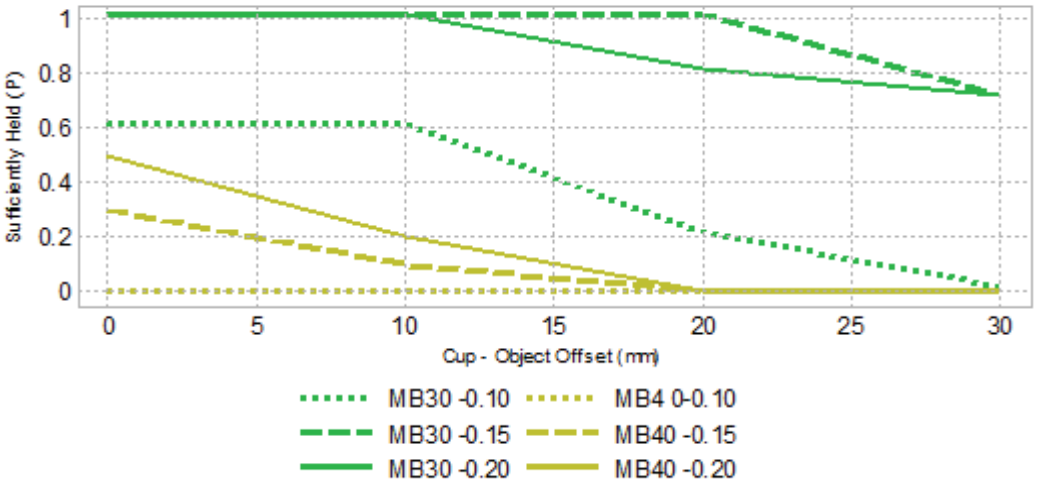

Figure 6.7: Object Type B normal lift.

6.1.2 Conclusion

This section investigates the applied use of pneumatic vacuum grasping of OBJs. The objective is to evaluate if the proposed robotic packing solution should continue to utilise such a pneumatic solution and if so, what variables should be considered in the final design. The outcomes of porosity and sufficiently held test support pneumatic

vacuum lifting as the preferred option for moving OBJ_A. Investigation of cup designs shows the packing system should utilise multiple bellow designs and vacuum cups with the lowest possible rigidity. Once the vacuum pressure reaches a critical level, the width of the vacuum cup does not seem to offer improved reliability. In such cases, a wider cup dimension reduces the flexibility of the seal formation and reduces the grasp performance. The vacuum cups tested are all made with food grade silicon having a medium shore durameter value of 50. Custom cups with a durameter value of 10 can be ordered, and this may allow the wider units to seal with the OBJs.

The grasping of OBJ_B demonstrates a lower level of performance. The extent of reliable lifting of OBJ_B was lower than OBJ_A. A pneumatic solution is it not a good approach for OBJ_B, however, due to industry changes, the market for such system is insignificant compared to OBJ_A. A hybrid solution that utilises a vacuum cup and a mechanical interference approach could be a good approach. However, the current solution, that relies solely on the vacuum cup, will require a high flow rate vacuum generator to overcome the porosity.

6.2 Intelligent Grasp Sensing

The prior section detailed an initial human investigation to decide if pneumatic vacuum cups are viable a handling solution. From initial results, it can be concluded that a pneumatic approach should be exhausted until proven non-viable. The investigation presented within this section applies the proposed vacuum grasping system as presented in Chapter 4. The review of literature and basic experiments have shown the need to utilise grasp sensing with the handling of OBJs.

The study intended to utilise the developed robotic solution from Chapter 3 with the intelligent EE design from Chapter 4. Unfortunately, with the project on hold, no robotic system was built to complete these experiments in detail. To provide some

confirmation of expected EE behaviour and detailed engineering, a grasp simulator will be presented. Where applicable limited testing using the NZIC RTP is demonstrated.

The section is split into three components

1. Modelling of grasp system basics
    - Create the model and Matlab Simulation environment for proposed end effector design.
2. Effects of modelled variables
    - Investigate the effect of variables for the optimal design solution at later stage. These effects demonstrate the directly measured feedback signals and induced motion of the system.
3. Applied signals collection
    - Where possible the models are compared with real measurements attained with limited NZIC RTP testing.

6.2.1 Simulation of Pneumatic Grasp

The simulation of the vacuum grasping seeks to define the expected behaviour of sensor feedback and the actions induced upon the OBJs The first aim seeks to provide a means of optimising a detailed engineering solution. The second is to investigate correlations between the grasp and sensor feedback of vacuum depth and induced vertical motion.

These two aims are related by the physical structure that features interactions between the flow and mechanical dynamic responses. The primary control input is the activation of a vacuum generator which in turn begins the sequence of grasping the OBJs. An ideal infinite flow rate vacuum generator would supply an instantaneous pressure change from open atmosphere to the seal grasp region. Figures 6.8 and 6.9 demonstrate the response of a real vacuum generator with limited flow rates and an applied pressure effect on a closed system similar to the NZIC RTP. The flow characteristics in Figure 6.8 are generated from a SMC pneumatic data-sheet[79] for a 0.7mm nozzle high flow

vacuum generator. The five lines represent the flow vs pressure characteristics of the vacuum generator when powered with a positive air supply ranging from 100kPa – 500kPa. Figure 6.9 demonstrates the pressure of the closed RTP vacuum system while air is exhausted with the modelled SMC ZH07BL generator.

The pressure curves in Figure 6.9 broadly resemble the NZIC RTP applied testing in the last part of this section. The difference between the simple curve and the actual sensor readout is due to a number of other transient features. This means that other physical factors are present to an observable degree and the modelling presented here intends to investigate these.

Further, the preceding section concluded that a low vacuum depth of 20-25kPa seemed sufficient to contain the OBJs. To apply feedback to the controller using a simple vacuum switch, the response would require a grasp period in excess of 300ms. Modelling the grasp response should allow the prediction of the eventual grasp state and a decreased reaction to disturbance.

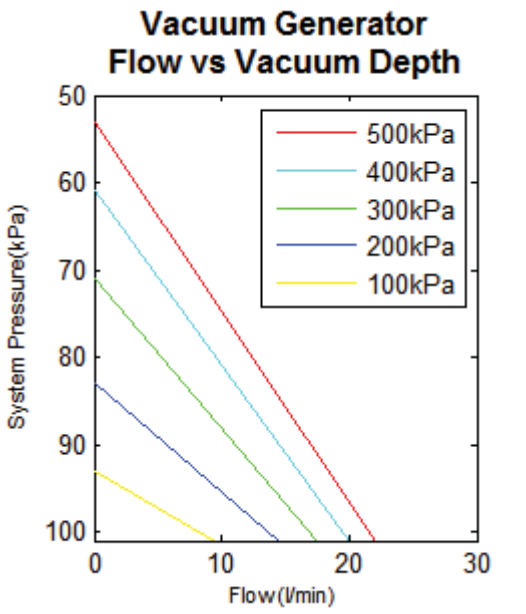

Figure 6.8: Real behaviour of vacuum generator.

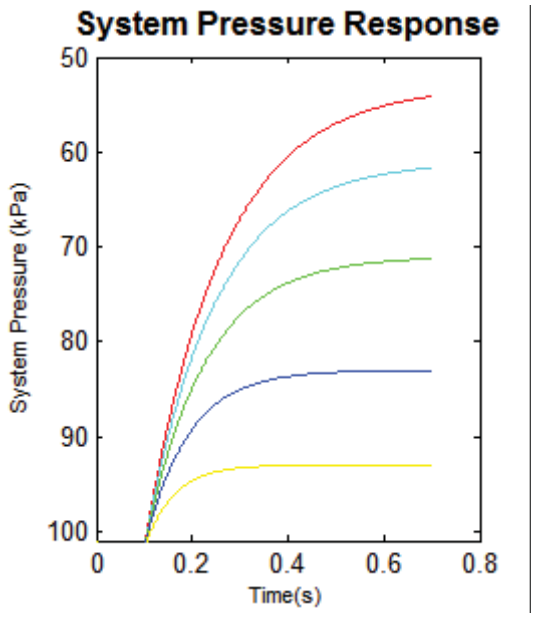

Figure 6.9: Vacuum system response of the RTP with closed vacuum lines.

To investigate the behaviour response of the system, a more variable model is required.

The models investigates the following grasp actions.

- Vacuum generators
- Vacuum supply lines
- Dynamic cup volume
- Mechanical cup response
- Mechanical load response
- Leak effects

To achieve this investigation, the grasp simulation factors the following aspects in grasp behaviour.

- Vacuum generation
- Pneumatic geometry
- Vacuum cup
    - Diameter/volume
    - Piecewise spring rate and damping ratio
- Buffer
    - Mass
    - Piecewise spring rate and damping ratio
- Seal formation
- System leaks

The interaction of the different variables is modelled within a series of simultaneous equations. The two important features to model for grasp sensing are the complex effects from the vacuum cup and induced motion. During the initial OBJs grasp investigation, these two effects were noted to have a relationship with grasp success. The behaviour of the vacuum cup is complicated since it is a flexible structure that includes both mechanical and pneumatic actions. The vacuum cup structure acts as a mechanical spring and damper unit, and a variable volume chamber. The variable volume chamber has an effect on the flow dynamics, therefore resulting in a pressure

response and increases complexity of grasp sensing. At steady state, a load acting on the vacuum buffer is a response that can be expected, and is measured by several existing systems. However, as with the vacuum pressure, the vacuum buffer motion is a complex transient observable during the grasp period. Figures 6.10 and 6.11 are examples of simulating the OBJ grasp. The parameters are presented in the appendix. Figure 6.10 demonstrates the feedback signals sensed by the EE electronics. These transient signals are then processed by the DSP/FPGA within the micro-controller package to predict grasp action.

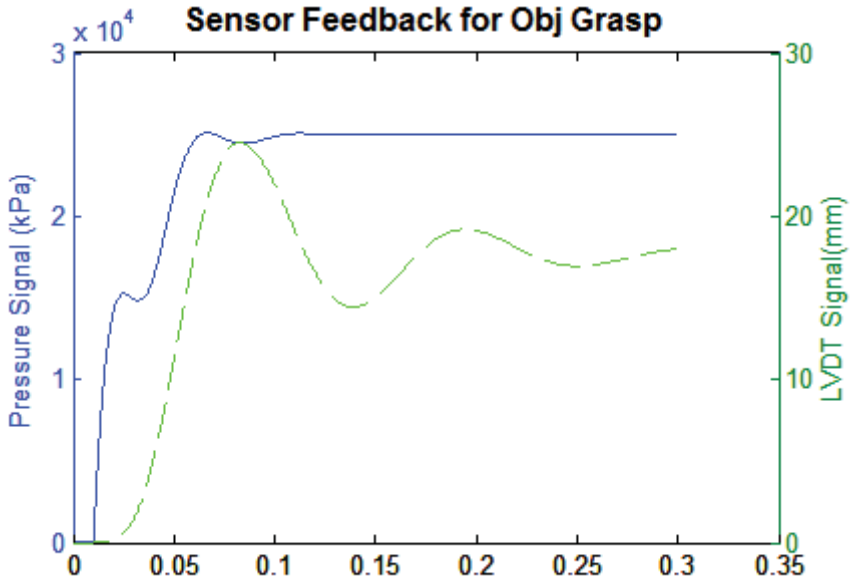

Figure 6.10: The modelled sensor feedback from proposed grasp unit.

Figure 6.11 demonstrates the resulting action of other responses during the OBJ grasp. These behaviours can not be directly sensed by the eventual control system, however, are utilised as means to investigate the induced behaviour. Figures with the same layout as Figure 6.11 are presented in the appendix to demonstrate the effect of the main grasp variables that will be shown in the next section. The top left and right plots in figure 6.11 are sensor feedback measurements of the vacuum depth and LVDT displacement. OBJ displacement is the compressed measurement of the vacuum cup. The OBJ velocity and OBJ acceleration are the time derivatives of this measurement. The LVDT velocity and acceleration are the derivatives of the LVDT signal. Grasp seal is a Boolean

value that is true when the instantaneous force exerted by the vacuum cup is sufficient enough to support the OBJ's mass. Table 6.3 lists the correlation between variable index and line colour within the figures.

Table 6.3: Variable layout within Appendix.

Variable Number	**1**	**2**	**3**	**4**	**5**
Line Colour	Red	Green	Blue	Cyan	Yellow

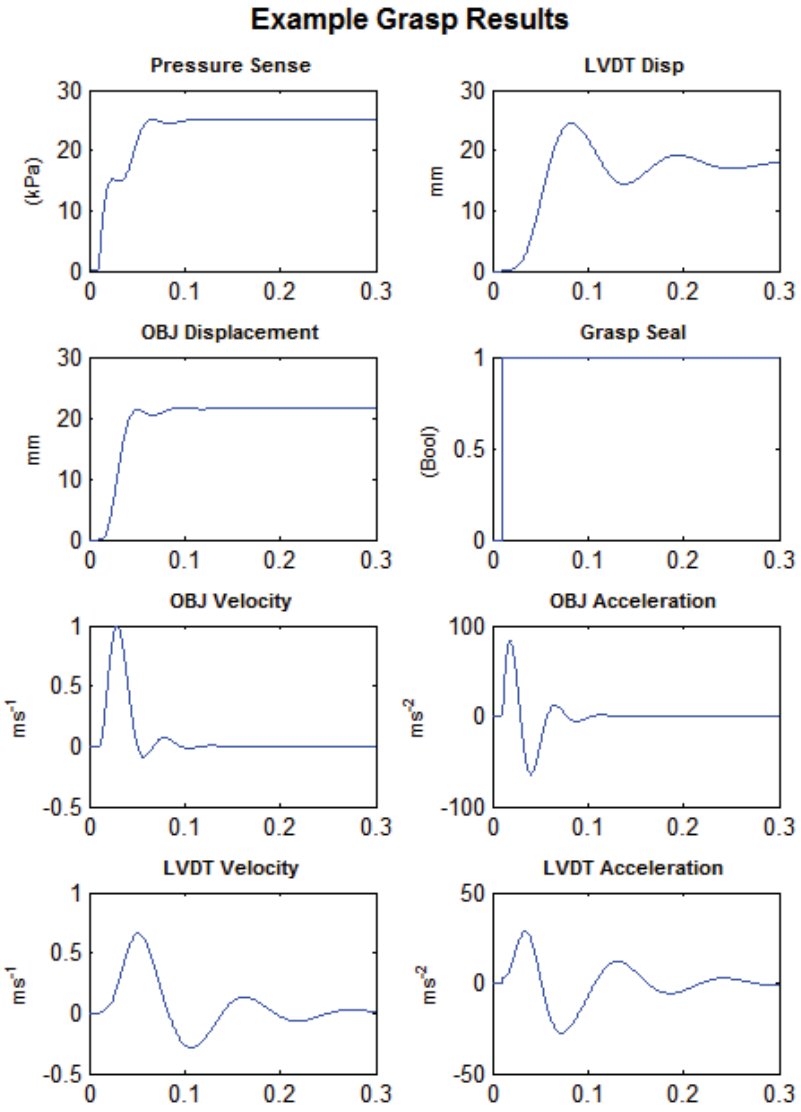

Figure 6.11: Example simulation outputs of grasp behaviour .

6.2.2 Grasp Variable Study

The grasp simulator is utilised as a means to demonstrate the effect of each variable on the response. The modelled system has a high degree of variables with time varying response. The following transient gasp responses are located in Appendix C for clarity.

- OBJ mass
- Vacuum pressure and flow rate
- Vacuum cup properties
    - Cup spring rate
    - Cup diameter
- Buffer properties
    - Spring rates

Figure C.1 illustrates the effect of OBJ mass on the grasp behaviour. The mass change from 40 to 120 grams demonstrates a small overall difference in pressure response. The noticeable difference is the change in transient response around the knee of the curve as the pressure becomes steady. The effect of this response is clearly visible within the induced velocity and motion of the OBJ. The larger overall effect is on the LVDT motion due to the load change. The displacement has a linear response as could be expected from a first order system, and the motion demonstrate the change in spring frequency.

The change in grasp response due to vacuum depth and flow rate is presented in Figure C.2 and C.3. These responses demonstrate the flow rate of the vacuum generator has a larger effect on the variation of transient response variation than the actual vacuum depth. The change in vacuum depth produces an overall scaling of all measurements as expected, however, the actual shape of the responses remain similar. Changes in the vacuum flow rate do produce an overall scaling of the OBJ and LVDT motion profiles. However, the pressure and displacement outputs also differ in shape. As the flow rate changes, a difference can be seen by the overshoot and surrounding region of the

pressure and OBJ displacement. LVDT displacement is demonstrated with variation to the time constant and overshoot of the device.

The variation of the vacuum cup design is illustrated in Figure C.4 and C.5. Figure C.4 demonstrates the different vacuum cup spring rates; this being the function of the mechanical design of the structure. Figure C.5 shows the grasp response against a change of vacuum cup width at the surface of OBJ seal. Both cup variables demonstrated a transient change around the knee of the pressure response. The variables change the ratio, period and shape of the pressure response curves. At low cup spring rates or a wider cup design, the transient shape is less pronounced. This is because as the induced pneumatic force becomes sufficiently large compared to the mechanical cup effects. Each variable has a similar linear effect upon the total displacement of the LVDT, however, the motion responses show variation. Changing the spring rate scales the induced motion of the LVDT. Whereas a change in vacuum cup width changes the LVDT frequency response.

The effect of LVDT spring rate is the final variable investigated and demonstrated in Figure C.6. The values of the OBJ motion are consistent with this figure since the variables that effect the pneumatic response are identical. The change in LVDT spring rate has the effect of changing the displacement and frequency response, which is expected in a spring and damper system.

6.2.3 Grasp Pressure Response of the NZIC RTP

Since the proposed robotic system was not able to be produced, limited grasp sensing research was carried out using the existing RTP. Using the RTP has some limitations due to load limits, the control system, and the significant repair cost.

A piezoelectric pressure sensor was fitted to the existing RTP and externally logged with a computer. The LVDT buffer arrangement was added for some proof of concept experiments; however, doing so was outside design limits of the RTP. The ABB340

does not allow a simple attachment of the developed EE because of the load moment, limited vertical working envelope, pneumatic supply, and the lack of suitable fastening points. This means that testing with the LVDT component is limited to slow movements with an element of inaccuracy. Figure 6.12 is the image of the LVDT EE and electronics.

Figure 6.12: Prototype LVDT end effector including the PCB.

Interacting with the RTP control system is limited to remote Ethernet control and some very basic sequential embedded programming utilising ABB's rapid language. The rapid language is an abstract layer of programmer commands and does not allow real time control during motion. The real time control is completed within lower level equipment inaccessible to the developer. General purpose IO are not accessed in real time and crude interrupt routines are not invoked until the current abstract command is completed. The one way to change the motion during a command execution is to activate the E-Stop routines from hardware or software. This is not good for the robot due to the mechanical stresses imposed. The inability for real-time motion correction is the reason why the utilisation of motion control cards was suggested in Chapter 3 and why these experiments operate solely as open loop data collection. Figure 6.13 shows a test OBJ being grasped during capturing pressure responses.

Figure 6.13: Testing grasp pressure response.

The last limitation is that the ABB 340 robot is a high end system with ultra light equipment intended for high speed motion. The servo drivelines are high end devices from ABB and the mechanical linkages are predominantly carbon fibre. Replacing any of these components is of significant cost and combined with an unforgiving structure[27] plus troublesome control system makes any high speed testing too dangerous. Figure 6.14 is an example of the grasp pressure response when configured to operate with a low vacuum pressure. The figure demonstrates the oscillation of the pressure feed back as simulated above.

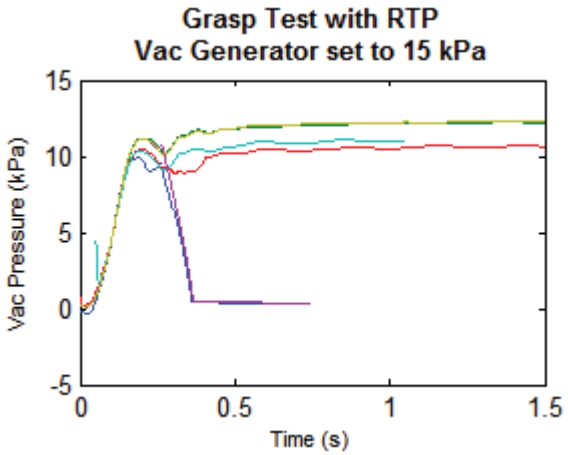

Figure 6.14: Grasp testing using NZIC's RTP.

27 Spherical rose joints are one point of release.

6.3 Verification of Visual Servo Feedback Processing

In Chapter 5 a new visual feedback system has been proposed for the mechatronic orientation unit. The intra-frame blob tracking and measurement of the rotational displacement vector are critical elements to the algorithms function. Simulators are utilised to test both elements against different operational variables and the rotational vector is further compared to implementations of horn's method and the twist matrix.

Each simulator creates a random blob layout and then applies random rotational movements. The variable configuration or algorithm set-up is then compared against the known result. The difference between the real and modelled values are then compared across the different variables.

The simulation routines have three aspects used to represent the real capture systems

1. Produce a pseudo random OBJ blob representation
2. Produce a pseudo random motion of OBJ blob representation
3. Map blob representation to the 2D image format.

To create blob layouts, a simulation routine generates a group of pseudo random blob locations mapped to an equivalent spherical surface. The blob generator attempts to map random locations to the OBJ model with the following criteria:

1. Max number of blobs = 30
2. Min inter-blob distance = 15mm
3. Max unsuccessful pseudo search iterations = 50

The blob generator is finished when either the number of valid blobs is 30 or 50 successive iterations have failed to produce a valid blob location. A blob is considered valid and added to the layout when its COG displacement is greater than 15mm to any existing blob. The outcome from the blob generator is a group of vectors that represent n number of blobs.

The random motion generator works in a two stage process. First, a randomised rotation vector is produced for each simulation iteration. A unit rotation vector is created by generating a random number for each axis and then normalised with the Z dimension in positive range. The magnitude is generated by creating a random value between $-\pi/2$ to $\pi/2$. The generated blob layout is rotated with the combined rotation vector to produce prior and current blob locations.

To enter the simulated blob motion into different test cases, the 3D blob locations are converted to a planar image view. The generated 3D blob formats are converted into the equivalent XY planar representation with occluded blobs removed. The outcome from the simulation environment is two groups of blob references represented in the XY plane similar as capture images.

6.3.1 Intra-Frame Blob Matching

The performance of the intra-frame blob matching is found by investigating seven different search configurations against varying degrees of location error and the total number of visible blobs. The number of visible blobs provides a challenge since there is no guarantee the prior referenced blobs are visible in the current set. One aspect of this challenge is therefore to investigate the configuration's behaviour when not all the blobs can be successfully matched. The blob matching algorithm presented in Section 5.4 has been simulated with seven search configurations. Table 6.4 outlines each of the software configurations simulated, with details specifying blobs to match, blobs to search and gives a total number of search items. A naming convention for each search configuration is supplied in the leftmost column.

Table 6.4: Blob matching simulation.

Configuration Name	Blobs to Match	Blobs to Search	Search Permutations
C33	3	3	6
C34	3	4	24
C35	3	5	60
C36	3	6	120
C44	4	4	24
C45	4	5	120
C46	4	6	360

The dot matching consistency of configurations C36, C45 and C46 are shown in Figures 6.7 to 6.9. The surface shows the probability of the correct intra-frame dot matching with respect to measurement error and the number of visible dots. The three configurations shown provide the most reasonable performance when weighted against processing requirements. C46 provides the best matching of approximately 90% success rate within the bounds of expected variable location: however, it is of considerable computational cost. The configuration C46 requires considerable processing resources with a computational period in the range of 4-6ms per image on the test machine. Utilising the existing control computer and the higher resolution image configuration, the camera frame rate, is limited to 35 fps for the real time motion study. To allow higher frame rates the C36 and C45 configurations require a lesser computing resources with C45 providing the greater accuracy.

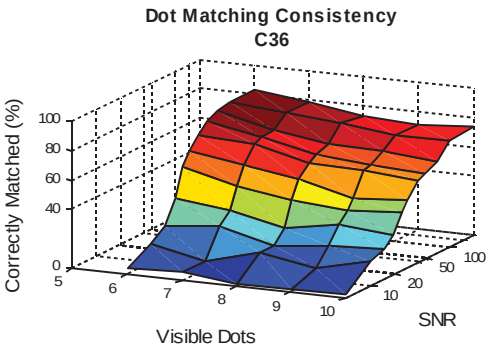

Figure 6.15: Dot matching consistency of C36 blob matching.[81]

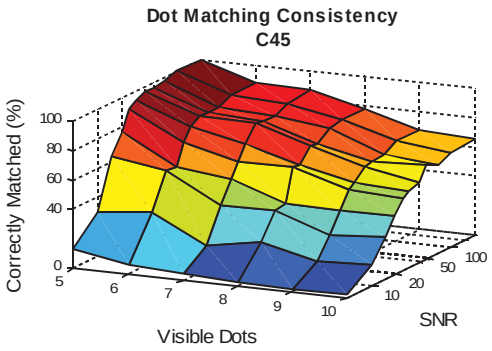

Figure 6.16: Dot matching consistency of C45 blob matching.[81]

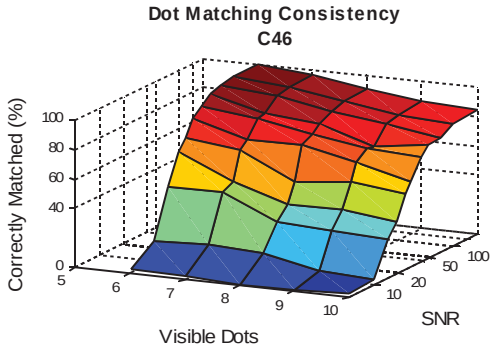

Figure 6.17: Dot matching consistency of C46 blob matching.[81]

6.3.2 Determination of Rotation Axis

The accuracy of the IOP algorithm is verified with a simulation principle similar to blob matching. The blob location for prior and current locations, with defined measure error, were simulated and passed to the developed algorithms. The testing routine applied these blobs against the full set of algorithms and blob/noise configurations.

Figures 6.18 to 6.20 demonstrate the horn's, twist and the IOP methodologies subjected to varying amounts of noise and visible reference blobs. The surface vector represents the mean angle of error between the calculated and known true axis. The twist method is shown as highly susceptible to even a small degree of measurement error and is the

least reliable of the three investigated algorithms. Horn's and the proposed IOP algorithms demonstrate a trade off between peak accuracy and stability. Figure 6.21 is the direct comparison between the IOP and Horn's algorithm and demonstrates their relative accuracy. The IOP provides a higher level of accuracy when blob locations contain small measurement errors. The drawback of the IOP is that axes errors can be seen to rise as measurement errors increase. Horn's approach provides the most stable result across the entire range of dot errors, however, it provides less accuracy when the measurement error is low.

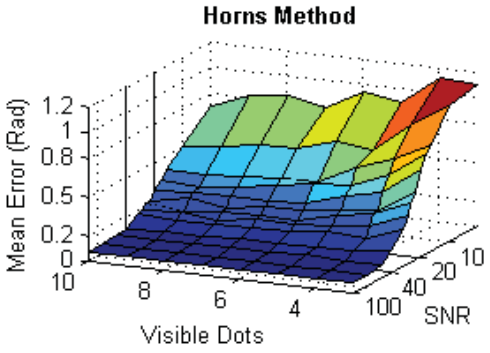

Figure 6.18: Horn's method.[81]

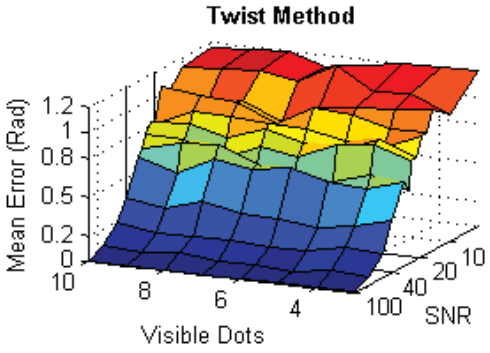

Figure 6.19: Twist method.[81]

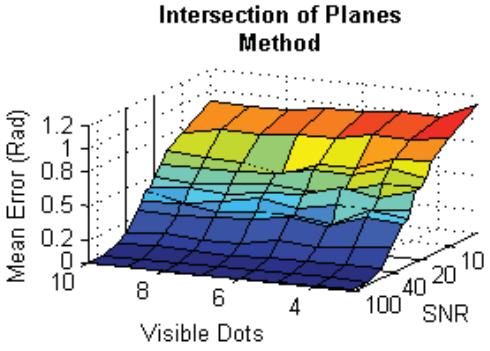

Figure 6.20: IOP Method.[81]

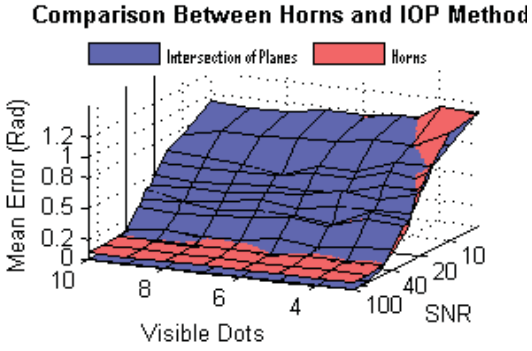

Figure 6.21: Comparison between IOP and Horns' methods.[81]

6.3.3 Applied Testing

An applied utilisation of tracking the OBJs with the developed feedback loop is displayed in Figures 6.22 and 6.23. Three induced steady state OBJ motions are produced with the orientation unit and then monitored by the developed vision

algorithm. Figure 6.22 demonstrates the directional tracking of the rotation with the angle representing the XZ plane of the orientation unit. Figure 6.23 demonstrates the magnitude of the rotation of the matching direction. Both figures demonstrate noisein the measurement of their respective signals. This noise is not necessarily from the errors associated with the inspection system, the mechanical motion shows variation during human inspection.

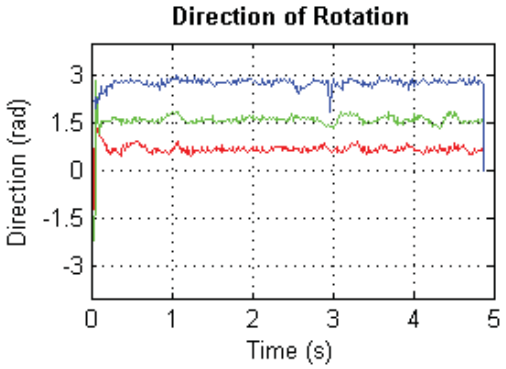

Figure 6.22: Direction of rotation.[81]

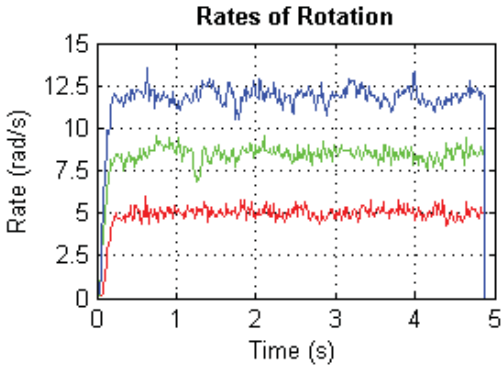

Figure 6.23: Rates of rotation.[81]

6.4 Principle Behaviour of Rotation System With Spherical OBJs

During the prototype investigation, the belt system demonstrated a general trend of behaviour. The orientation unit was originally intended as a system that should generate a stable rotation on either the X or Z axis. Further study noticed that the device could generate a variable rotation with an axis anywhere on the XZ plane The observed behaviour demonstrated a motion that was subjected to a large variation. To the human eye, the behaviour follows a reliable trend within certain operating conditions. The system if refined, could be a possible solution for solving one of the main obstacles of this research.

The following motion model produces the rotation vector based on the mechanical configuration and measured or induced motion. Table 6.5 lists the known variables during motion, these are either known as control outputs or visual feedback inputs.

Table 6.5: Variables for orientator motion model.

Variable Name	**Variable Description**	**Variable Name**	**Variable Description**
ABeltP	Absolute belt position vector	AObjP	Absolute OBJ position vector
RBeltP	Relative belt OBJ position vector	AObjV	Absolute OBJ velocity vector
ABeltV	Absolute belt velocity vector	Obj_r	Radius of the OBJ
RBeltV	Relative belt OBJ velocity vector	Obj_m	OBJ mass
$Belt_{SR}$	Spring rate of belt due to tension	RAxis	Rotation axis vector
RL	Remaining load divided by the belts.		

Equation 6.13 gives the relative displacement vector between each belt and the OBJ. Equation 6.14 shows the height offset between the OBJ COG and the belt surface based on an infinite spring rate. Equation 6.15 determines which belt is displaced the greatest. Equations 6.16 and 6.17 determine the uneven loading on the furthest displaced belt. The remaining belt load is calculated in Equation 6.18. Equations 6.19 and 6.20 give the true relative OBJ COG to belt surface displacement. The direction of the rotation vector is found in Equation 6.21. This equation is a piecewise function for periods when only one belt supports the OBJ.

$$RBeltP_a = ABeltP_a - AObjP_a \tag{6.1}$$

$$ObjZ_{Belt_a} = Obj_r - \sqrt{Obj_r^2 - RObjP_{a_x}} \tag{6.2}$$

$$BeltSelect = ObjZ_{Belt_a} > ObjZ_{Belt_b} \tag{6.3}$$

$$ObjZ_{Diff} = \left| ObjZ_{Belt_a} - ObjZ_{Belt_b} \right| \tag{6.4}$$

$$Load_{Single\ Belt} = ObjZ_{Diff} \cdot Belt_{SR} \tag{6.5}$$

$$RL = 9.8\text{x}\, Obj_{Mass} - Load_{Single\ Belt} \tag{6.6}$$

$$ABeltP_{a_z} = \frac{\frac{Load_{Remaining}}{2} + (BeltSelect)\, Load_{Single\ Belt}}{Belt_{SR}} \tag{6.7}$$

$$ABeltP_{b_z} = \frac{\frac{Load_{Remaining}}{2} + (!\, BeltSelect)\, Load_{Single\ Belt}}{Belt_{SR}} \tag{6.8}$$

$$RAxis_{Stage1} = \begin{cases} ((RBeltP_a + RBeltV_a) \times (RBeltP_a + RBeltV_a)) \times [0\,1\,0], RL > 0 \\ [0\,1\,0], RL = 0 \end{cases} \tag{6.9}$$

$$RAxis_{Stage1} = \frac{RAxis_{Stage1}}{|RAxis_{Stage1}|} \frac{|RBeltV_a|}{\frac{RAxis_{Stage1} \times RBeltP}{|RBeltP|}} \tag{6.10}$$

Two factors are to be answered for the novel orientation unit:

1. Does the device operate as intended
2. What effect do the mechanical variables have on the device's operation.

The motion study of the orientation unit investigates the physical variables that effect this behaviour. Four physical variables were identified as having an effect on the device and each of these is presented.

Physical system variables

1. Drive contact
2. Contact diameter
3. Belt tension
4. Pocket shape

6.4.1 Motion Behaviour Study Procedure

The OBJ behaviour in terms of the measured motion and its stability is gathered across the range intended rotational vectors. This process provides a mapping between the

estimated model and the actual response. This initial investigation should provide an indication if control is possible and to what degree of stability.

The two control variables for the steady state behaviour study are:

1. Direction of rotation vector
2. Magnitude of rotation vector

These control variables form the true rotational vector and with systems from Chapter 4 were converted to the hardware signal governing the belt velocities.

The motion study operates an automated procedure that collects the raw rotation measurement. The steady state behaviour is captured in the form a M x N x C matrix of tests. Where;

- M is the number of rotation directional steps
  - Applied test $-\pi/2$ to $-\pi/2$ with resolution of $-\pi/8$
- N is the number magnitudes
  - 0 - 4π $rads^{-1}$ resolution of $\pi/2$
- C is the number of testing loops.

The automated test controller works as a SCARA controller and for each test element loads a predefined motion path of the rotational velocity vector into the orientation control software. The motion of the OBJ is tracked producing a tracking file for each test element which is later processed. This process provides a mapping between the estimated model and the real behaviour for each hardware configuration. This process is then repeated for all hardware configurations.

Figure 6.24 and 6.25 demonstrate the motion behaviour for a configuration example of the following:

- Single cord design
- 40mm cord separation
- Medium cord tension

- Shallow pocket

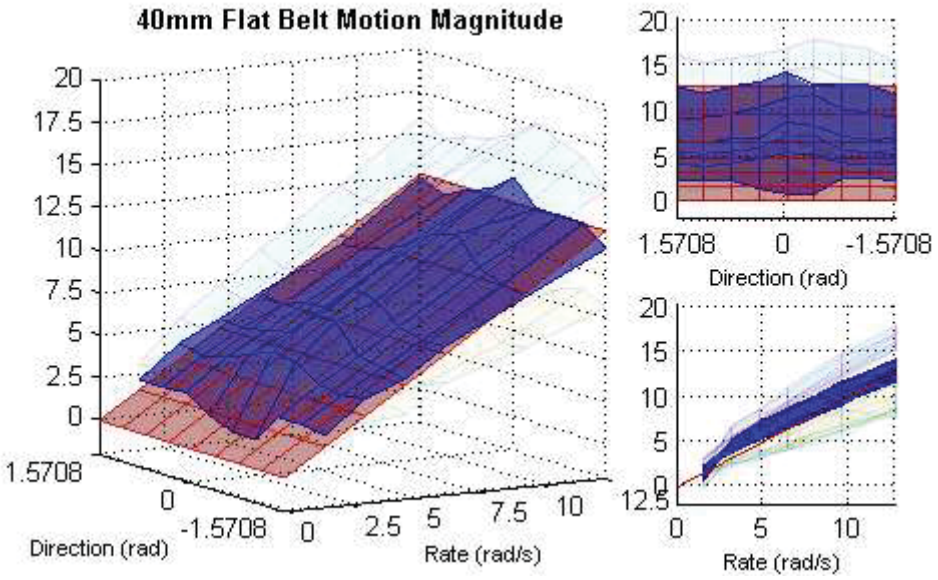

Figure 6.24: Mapped rotational velocity magnitude against modelled and real behaviour.

Each figure displayed for both the magnitude and direction has three view points of the motion behaviour. The left plot displays the general 3D mapping of the output against the test array of direction and magnitude. The top right plots this 3D mapping inline with the direction input to demonstrate the directional fit. The bottom right illustrates the mapping with the magnitude input. Four surfaces are mapped to each plot that demonstrate the model fit in mean behaviour and stability. The calculated model response from Chapter 4 is displayed as the red surface. The dark blue surface represents the mean real behaviour. Finally, the mean real behaviour plus or minus one standard deviation is shown by the light blue and yellow transparent surfaces.

Each hardware configuration tested is shown in Appendix D *Orientation Motion Models*.

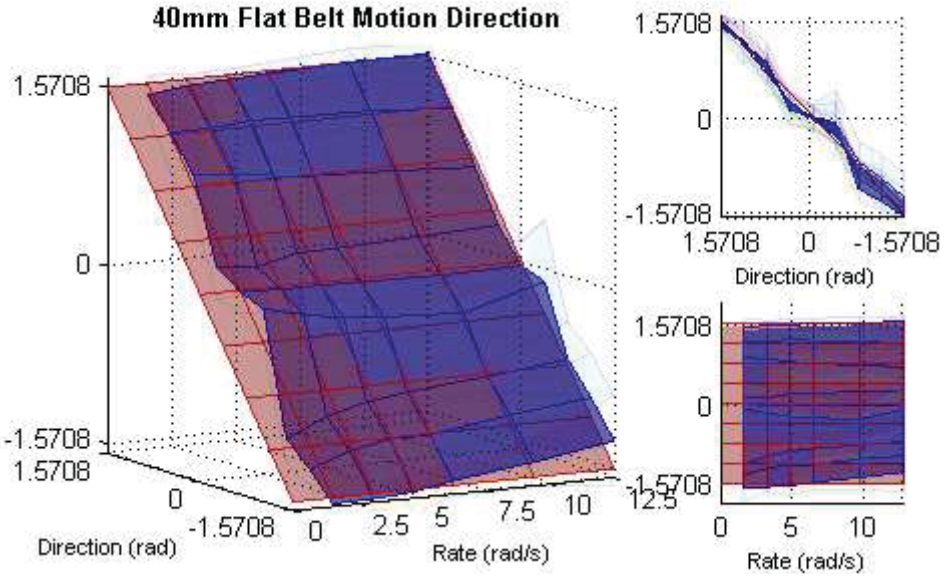

Figure 6.25: Mapped rotational velocity direction against models and real behaviour.

6.4.2 Belt Design and Rotation Behaviour

A test matrix of configurations has been conducted to investigate the effect of belt design upon the OBJ behaviour. Table 6.6 lists the variables for each matrix element.

Table 6.6: Test matrix of belt design

Variable	Point 1	Point 2	Point 3
Belt Design	Single Cord	Double Cord	Flat Belt
Belt Separation	30mm	40mm	50mm
Belt Tension	Medium		
Pocket Design	Shallow		

Appendix D.1 to D.3 demonstrate the motion behaviour of the three belt designs against the belt separation. Figure D.1 to Figure D.6 demonstrate the rotation behaviour of each hardware configuration as the examples above.

Table 6.7: Index of single cord designs

Figure D.1	Motion magnitude of 30mm cord separation
Figure D.2	Motion direction of 30mm cord separation
Figure D.3	Motion magnitude of 40mm cord separation
Figure D.4	Motion direction of 40mm cord separation
Figure D.5	Motion magnitude of 50mm cord separation
Figure D.6	Motion direction of 50mm cord separation

All the single cord belt separations demonstrate behaviour similar to the predicted motion model from Chapter 4. The 40mm belt separation demonstrates the best motion stability since both magnitude and direction of the rotation form the closest fit across all control actions. The 40mm belt separation corresponds to closely matching the radius of the 75mm test OBJ. The 50mm belt separation demonstrates the best mean fit to the direction; however, it demonstrates a wildly varying motion magnitude.

The behaviour difference of cord separation is directly shown in the Figure D.7 to D.10. These figures are warped using the model to real behaviour error squared. This is to heighten the variation of each configuration compared to the ideal behaviour. Table 6.8 lists the figures that compare the belt separation effects on the single cord design.

Table 6.8: Comparison between single cord belt separations.

Figure D.7	The mean magnitude error squared
Figure D.8	The magnitude standard deviation squared
Figure D.9	The mean direction error squared
Figure D.10	The direction standard deviation squared

The 30mm belt separation is visibly the least performing of the three belt separations with a poor model fit and poor stability in both magnitude and direction. The 40mm and 50mm show a close approximation in real behaviour with slightly better magnitude stability.

The behaviour of the dual cord approach is demonstrated in Appendix D.2 with the

individual belt configuration behaviours shown in Figure D.11 to D.16 and the comparisons from Figure D.17 to D.20. The dual cord design is shown not to provide a full range of variable direction upon the OBJs XZ axis. This matches the initial concerns since the dual belts will interact with the OBJ surface at different velocities causing slip behaviour. An interesting action is that the dual cord design produces roughly two controlled rotation directions along the X and Z axis. This could be useful in a case whereby the controller intends to produce only these co-linear manipulations. However, it should be noted that there is a high variation in direction in the Z axis based rotation.

The final layout investigates the use of flat belts for the motion manipulation. Appendix D.3 shows the result of the configuration's behaviours'. The flat belt design produces widely varying motion behaviour depending upon the belt separation. A belt separation of 30mm provides a reasonable direction behaviour across the full range of control inputs. However, the magnitude does not provide good stability and becomes severely unstable at high rates. A flat belt separation of 50mm produces a motion behaviour similar to the dual cord approach. The 50mm belt separation is unable to provide a variable motion direction. This matches the belt slip prior seen in the dual cord design and is likely caused by the belt being twisted due to the angle of interaction with the OBJ.

Appendix D.4 contains plots that compare the three belt approaches. These figures use the same error warping as above to heighten the variation of each configuration. Table 6.9 is the list of figures that compare the belt separation effects to the theoretical motion model. Due to the unacceptable failure rate of the single cord design, the preferred option utilises is the flat belt arrangement.

Table 6.9: List of figures fro the direct comparison of belt designs.

Figure D.31	Comparison of belt drives using mean magnitude error squared
Figure D.32	Comparison of belt drives using magnitude standard deviation squared
Figure D.33	Comparison of belt drives using mean direction error squared
Figure D.34	Comparison of belt drives using direction standard deviation squared

The dual cord arrangement has shown to provide a poor manipulation behaviour and this is evident in the direct comparison to the single cord and flat belt arrangements in all figures. The single cord and flat belt systems demonstrate a close match to the ideal model behaviour. Both approaches demonstrate an even fit between the mean motion magnitude and the ideal model. When D.32 is inspected the flat belt shows an increased magnitude consistency. Measuring the rotation direction, the flat belt provides the slightly more consistent mapping to the model. The single cord design, however, offers a slightly more consistent behaviour.

Overall the single cord and flat belt units provide a motion behaviour that follows the general modelled behaviour. The single cord has shown a improved tolerance to belt separation. In a practical sense, this is useful as it would also mean the single cord is more tolerant to changes in the OBJ geometry. The drawback of this single cord design is the tendency of the OBJ to become stuck against the pocket walls or fall between cords. This fault of the single cord design required constant supervision[28] during the process of gathering the motion behaviour. The OBJ, during the human supervised tests, faulted requiring human intervention 83 times out of the total test point size of 1680 resulting in failure rate of 4.9%. The failure spread across its three belt separations listed is below in Table 6.10.

28 The dual cord and flat belt designs could be left unattended for the entire test lasting over 24 hours.

Table 6.10: Failure rate of single cord designs.

Belt Separation	Failures	Test Cycles	Failure Percentage
30mm	24	560	4.3%
40mm	12	560	2.1%
50mm	47	560	8.4%
Totals	83	1680	4.9%

Table 6.10 shows the single cord design failure rate has been skewed by the wider cord displacement of 50mm. The medium being the preferred belt separation, showed a significantly reduced failure rate of 2.1%. This value however is still excessive for a production machine. In Chapter 3, it has been discussed that the eventual OBJ packing system intends to operate at 300 OPM. The failure rate of 2.1% operating at 300 OPM would average 6 faults per minute during production and is therefore not suitable for the commercial application.

6.4.3 Belt Tension and Rotation Behaviour

The flat belt arrangement with 40mm of belt separation has been identified as the preferred drive layout. In Chapter 4, it was identified that the belt tension could effectively produce a spring rate adjustment between the OBJ and belt surface. The section investigates if the belt tension has an effect on motion behaviour.

Table 6.11: Test matrix of belt tension.

Variable	Point 1	Point 2	Point 3
Belt Design	Flat Belt		
Belt Separation	40mm		
Belt Tension	Low	Medium	High
Pocket Design	Shallow		

Belt tension is split into three values based on the mechanical limits of the system. Low tension is the minimum limit that allows the drive pulleys to maintain contact with the belts. This results in the 100g OBJ displaced 6mm lower compared to a solid surface.

High tension is the upper limit that allows the BLDC and gear train to provide consistent motion; this results in OBJ displacement of 2mm. The medium level is the belt tension that displaces the OBJ by 4mm. Appendix D.5 contains the four figures displaying the warped correlation between the model and real behaviour. A medium belt tension can been seen as the best performing option across all four measurements. A high belt tension reduces the damping effect upon the motion and results in the OBJ moving around inside the pocket.

6.4.4 Pocket Design and Rotation Behaviour

The final hardware variable is pocket shape of that contains the OBJ during manipulation. Due to a reduction in budget, the moulding process is limited to two general pocket shapes. The two pocket types are described as a shallow and deep design. The shallow pocket design is a simple round hole with vertical edges of 15mm depth. The deep pocket is an inverse spherical design that intends to contain OBJ with a similar surface shape. Table 6.12 Sets out the configuration for the study of the pocket design.

Table 6.12: Test matrix of pocket design.

Variable	**Point 1**	**Point 2**	**Point 3**
Belt Design	Flat Belt		
Belt Separation	40mm		
Belt Tension	Medium		
Pocket Design	Shallow	Deep	

Appendix D.6 contains the captured motion behaviour of the deep pocket design and compares the behaviour with the equivalent of shallow pocket design. Figure D.41 and D.42 demonstrate the raw motion behaviour of the pocket design in the same manner as the previous section. The deep pocket behaviour is compared with the motion behaviour of Figures D.23 and D.24, these being the same hardware configuration except for the pocket design. Figure D.43 to D.46 compare the two pocket types utilising the same technique. The two pocket designs have a similar overall motion behaviour. The shallow pocket offers a mean magnitude closer matching the ideal model behaviour

The deep pocket design however provides a direction matching the ideal model with improved accuracy. The downside to the deep pocket design is OBJs are subjected to surface damage due to the constant contact between the pocket and the OBJs.

6.4.5 Conclusions On OBJ Orientator Physical Design

The physical motion behaviour of the proposed OBJ orientation unit has been thoroughly tested with four physical variables of design. The OBJ interaction was found to produce the predicted motion behaviour with two of proposed cord/belt interactions. A flat belt is the preferred interaction type since it demonstrates flexible motion controlled with a degree of stability and provides reliable unsupervised operation. A belt separation of 40mm which is approximately equal to the OBJs radius was found as the preferred displacement. A medium belt tension and shallow cup design are concluded as the best detailed design requirements.

7 Conclusions and Recommendations

The intention of this research was to investigate and then develop an automated packing solution for the NZIC. The initial work briefly reviewed automation and robotics technologies in a general sense. An in-depth review of automated packing machines within NZIC's industry was presented in Chapter 2. The findings from the review gave two directions of development for the automated packing solution. Chapter 3 utilised findings from the review of the technologies and analysed the required performance of the abstract systems. A proposed system design was presented and developed utilising existing technologies for a viable cost. Chapter 4 was a large body of material that investigated new applied technologies to suit the specific requirements for the proposed system. This section looked at the specific units to manipulate the objects with the unique requirements of the application. Presented within each unit was not simply the hardware layout but the sub-system integration and possible variations or directions across their commercial production life cycle. Chapter 5 developed an visual servo feedback algorithm used for studying the OBJ behaviour during orientation manipulation. Chapter 6 studied the real behaviour of the proposed OBJ handling subsystems and applied some basic control functions.

7.1 Conclusion

This project set out to design an entirely new packing system for NZIC. A detailed investigation was done and a proposed overall design has been completed. However it was not prototyped because of the economic conditions at the time. The simulation, analysis, testing , and detailed costing against potential customer gains have demonstrated that the system could be commercially feasible.

An intelligent OBJ grasp EE has been developed and tested. The base testing of OBJ

grasping with pneumatic vacuum cups provided evidence that the technology is appropriate for the application. The low cost pressure sensing utilising transient changes provides feedback about grasp quality. The LVDT load measuring layout was briefly tested as it was not safe to fully test with existing equipment. The device did measure the OBJ load as expected, however the load cell design is probably the better solution in the future. Before a final verdict can be attained on the EE, the full robot system has to be field trailed against for a much greater range of possible events.

Manipulating of OBJ's rotational degrees of freedom has been achieved with a novel low cost device. The entire subsystem from mechanical action to abstract vision processing algorithms have been developed and then a prototype solution applied. The device was intended to have variable rotation vector to minimise the movements to attain a final position. The device has shown promise of providing a relatively consistent variable rotation vector. A reasonable transient behaviour has been observed for magnitude changes and special cases of rotational vector control. Where the device fails is the lack of precision motion between rotational vectors not colinear to the standard cartesian axes. The effects of a unconstrained inertia tensor produces unsteady motion until the OBJ reaches another steady state. The motion does become steady, however, the unstable transient period makes later position control near impossible. The conclusion for the orientation system is precision position control will require a combination of fixed axes manipulations. This limitation then reduces the efficiency of the device, therefore, an expensive but easier to control direct acting device should be considered. The underlying fault with the orientation unit is the allowed unit cost was simply too low for the function.

7.2 Future Directions

The future direction for the system can be split into two sections; the application of grasp and orientation capacities, and the development of the robotic solutions for

NZIC.

The EE solution, specifically the OBJ grasping has been developed and where possible simulated or verified for behaviour. Prior to any further substantial development of the packing system, the proposed grasp control unit should be field trialled, however this requires a suitable robotic system. One possible means to test the vacuum control unit is to produce rapid prototype construction and attach this device to an existing in use NZIC's RTP. The prototype construction could then operate as an open loop data gathering system similar to the orientation study in Chapter 5. The constraint with this approach is that only a small number of RTP exist and handle the significantly smaller market of OBJ_B. It is known that the grasp behaviour of OBJ_a is significantly different to OBJ_B and therefore a conclusive result would be difficult to attain. To fully test the OBJ grasp unit, the best solution is to produce the proposed prototype design and operate as data a collection device.

The proposed orientation control unit produced a general trend of motion as hoped. However it was unable to offer precision position control. Evaluating the robotic packing simulation and OBJ grasp modelling, it appears such a orientation unit, if ever fine tuned, is still likely to be the limiting factor in the performance of the system. The option of utilisation the direct servo actuation of the OBJ should be reconsidered. The direct servo actuation would increase the build cost of the system by a moderate level. However it should provide a OPM rate that could recover the extra cost.

This research has been particularly challenging due to NZIC having no internal technologies suitable for the application and OEM components either not suitable or of excessive cost. This has required the development of almost all background technologies to test certain concepts. A further problem was the need to deal with open ended design requirements that constantly change. The proposed robotic solution that automates the packing of OBJs with a defined tray format is perhaps the toughest task to complete in NZIC's industry. To take the proposed solution to commercially realisable system would still be of considerable R&D investment and risk. Many of the background technologies required for the robotic packing solution could be applied to

other tasks in NZIC's industry that are currently conducted by human labour. Robotic or mechatronic systems could be produced to carry out simpler tasks such tray handling, lidding and box packing. Automating these tasks would not provide such high initial returns on R&D investment. It would however provide a platform to develop the robotic technologies. In these cases, the motion control and feedback processing technologies could be developed to suit simpler processes, offering reducing commercial risk and time to market.

8 References

[1] International Standard Organisation, 'ISO 8373:2012', International Standards Organisation, Standard 2, 2012.

[2] Oxford Dictionaries, '"automatic". Oxford Dictionaries.' [Online]. Available: definition/english/.

[3] Merriam-Webster.com, 'Automation'. Merriam-Webster.

[4] Encyclopædia Britannica, 'Automation'. 2013.

[5] Institution of Mechanical Engineers, 'What is Mechatronics? | Institution of Mechanical Engineers'. [Online]. Available: http://www.imeche.org/knowledge/industries/mechatronics-informatics-and-control/about-the-group/mechatronics-forum/what-is-mechatronics. [Accessed: 14-Apr-2013].

[6] International Federation of Robotics, 'History of Industrial Robots'. 2012.

[7] ABB, 'IRB 360 FlexPicker Industrial Robot', Switzerland, DataSheet, Feb. 2009.

[8] Bernard Campbell, James D Loy, and Kathryn Cruz-Uribe, *Humankind Emerging*, 9th ed. Boston, USA: Person Education inc, 2006.

[9] '"robot end effector" - Google Scholar'. [Online]. Available: http://scholar.google.co.nz/scholar?q=%22robot+end+effector%22&btnG=&hl=en&as_sdt=1%2C5. [Accessed: 10-Jul-2013].

[10] P. Y. Chua, T. Ilschner, and D.G. Caldwell, 'Robotic manipulation of food products – a review', *Industrial Robot: An International Journal*, vol. 30, no. 4, pp. 345–354, 2003.

[11] Paul M Taylor, 'Presentation and gripping of flexible materials', *Assembly Automation*, vol. 15, no. 3, pp. 33–35, 1995.

[12] Tongpadungrod P.[1], Rhys T.D.L., and Brett P.N., 'An approach to optimise the critical sensor locations in one-dimensional novel distributive tactile surface to maximise performance', *Sensors and Actuators A: Physical*, vol. 105, no. 1, pp. 47–54, Jun. 2003.

[13] D. Yamada, T. Maeno, and Y. Yamada, 'Artificial finger skin having ridges and distributed tactile sensors used for grasp force control', in *Intelligent Robots and Systems, 2001. Proceedings. 2001 IEEE/RSJ International Conference on*, 2001, vol. 2, pp. 686–691 vol.2.

[14] M. Teichmann and B. Mishra, 'Reactive Robotics I: Reactive Grasping with a Modified Gripper and Multifingered Hands', *The International Journal of Robotics Research*, vol. 19, no. 7, pp. 697–708, 007 2000.

[15] G. Canepa, R. Petrigliano, M. Campanella, and D. De Rossi, 'Detection of incipient object slippage by skin-like sensing and neural network processing', *Systems, Man, and Cybernetics, Part B: Cybernetics, IEEE Transactions on*, vol. 28, no. 3, pp. 348–356, 1998.

[16] P. K. Allen, A. T. Miller, P. Y. Oh, and B. S. Leibowitz, 'Using tactile and visual sensing with a robotic hand', in *Robotics and Automation, 1997. Proceedings., 1997 IEEE International Conference on*, 1997, vol. 1, pp. 676–681 vol.1.

[17] E. G. M. Holweg, H. Hoeve, W. Jongkind, L. Marconi, C. Melchiorri, and C. Bonivento, 'Slip detection by tactile sensors: algorithms and experimental results', in *Robotics and Automation, 1996. Proceedings., 1996 IEEE International Conference on*, 1996, vol. 4, pp. 3234–3239 vol.4.

[18] Leon D. Harmon, 'Automated Tactile Sensing', *The International Journal of Robotics Research*, vol. 1, no. 6 ?, pp. 822–827, Jun. 1982.

[19] S.-T. Wu, S.-C. Mo, and B.-S. Wu, 'An LVDT-based self-actuating displacement transducer', *Sensors and Actuators A: Physical*, vol. 141, no. 2, pp. 558–564, Feb. 2008.

[20] Z. Doulgeri and J. Fasoulas, 'Grasping control of rolling manipulations with deformable fingertips', *Mechatronics, IEEE/ASME Transactions on*, vol. 8, no. 2, pp. 283–286, Jun. 2003.

[21] N. Wettels, A. R. Parnandi, Ji-Hyun Moon, G. E. Loeb, and G. Sukhatme, 'Grip Control

Using Biomimetic Tactile Sensing Systems', *Mechatronics, IEEE/ASME Transactions on*, vol. 14, no. 6, pp. 718–723, Dec. 2009.

[22] T. Yoshikawa, 'Multifingered robot hands: Control for grasping and manipulation', *Annual Reviews in Control*, vol. 34, no. 2, pp. 199–208, Dec. 2010.

[23] B. D. Argall and A. G. Billard, 'A survey of Tactile Human–Robot Interactions', *Robotics and Autonomous Systems*, vol. 58, no. 10, pp. 1159–1176, Oct. 2010.

[24] L. Beccai, S. Roccella, L. Ascari, P. Valdastri, A. Sieber, M. C. Carrozza, and P. Dario, 'Development and Experimental Analysis of a Soft Compliant Tactile Microsensor for Anthropomorphic Artificial Hand', *Mechatronics, IEEE/ASME Transactions on*, vol. 13, no. 2, pp. 158–168, Apr. 2008.

[25] M. . Lee and H. . Nicholls, 'Review Article Tactile sensing for mechatronics—a state of the art survey', *Mechatronics*, vol. 9, no. 1, pp. 1–31, Feb. 1999.

[26] J. M. Romano, K. Hsiao, G. Niemeyer, S. Chitta, and K. J. Kuchenbecker, 'Human-Inspired Robotic Grasp Control With Tactile Sensing', *Robotics, IEEE Transactions on*, vol. 27, no. 6, pp. 1067–1079, Dec. 2011.

[27] A. Schmitz, M. Maggiali, L. Natale, and G. Metta, 'Touch sensors for humanoid hands', *RO-MAN, 2010 IEEE*, pp. 691–697, 13.

[28] R. S. Dahiya, D. Cattin, A. Adami, C. Collini, L. Barboni, M. Valle, L. Lorenzelli, R. Oboe, G. Metta, and F. Brunetti, 'Towards Tactile Sensing System on Chip for Robotic Applications', *Sensors Journal, IEEE*, vol. 11, no. 12, pp. 3216–3226, Dec. 2011.

[29] S. Chitta, J. Sturm, M. Piccoli, and W. Burgard, 'Tactile Sensing for Mobile Manipulation', *Robotics, IEEE Transactions on*, vol. 27, no. 3, pp. 558–568, Jun. 2011.

[30] L. Seminara, M. Capurro, P. Cirillo, G. Cannata, and M. Valle, 'Electromechanical characterization of piezoelectric PVDF polymer films for tactile sensors in robotics applications', *Sensors and Actuators A: Physical*, vol. 169, no. 1, pp. 49–58, Sep. 2011.

[31] H. Yousef, M. Boukallel, and K. Althoefer, 'Tactile sensing for dexterous in-hand manipulation in robotics—A review', *Sensors and Actuators A: Physical*, vol. 167, no. 2, pp. 171–187, Jun. 2011.

[32] R. S. Dahiya, G. Metta, M. Valle, and G. Sandini, 'Tactile Sensing—From Humans to Humanoids', *Robotics, IEEE Transactions on*, vol. 26, no. 1, pp. 1–20, Feb. 2010.

[33] D. D. Damian, H. Martinez, K. Dermitzakis, A. Hernandez-Arieta, and R. Pfeifer, 'Artificial ridged skin for slippage speed detection in prosthetic hand applications', *Intelligent Robots and Systems (IROS), 2010 IEEE/RSJ International Conference on*, pp. 904–909, 18.

[34] H. Lin, P. M. Taylor, and S J Bull, 'A mathematical model for grasping analysis of flexible materials', *Modelling and Simulation in Materials Science and Engineering*, vol. 13, no. 2, pp. 185–201, Mar. 2005.

[35] S. H. Jazi, M. Keshmiri, and F. Sheikholeslam, 'A new approach on dynamic analysis and control synthesis of object grasping by manipulators', in *Proceedings of the 18th conference on Proceedings of the 18th IASTED International Conference: modelling and simulation*, Montreal, Canada, 2007, pp. 149–154.

[36] J. A. Domínguez-López, R. I. Damper, R. M. Crowder, and C. J. Harris, 'Adaptive neurofuzzy control of a robotic gripper with on-line machine learning', *Robotics and Autonomous Systems*, vol. 48, no. 2–3, pp. 93–110, Sep. 2004.

[37] C. Goldfeder, P. K. Allen, C. Lackner, and R. Pelossof, 'Grasp Planning via Decomposition Trees', in *Robotics and Automation, 2007 IEEE International Conference on*, Rome, Italy, 2007, pp. 4679–4684.

[38] S. Ekvall and D. Kragic, 'Learning and Evaluation of the Approach Vector for Automatic Grasp Generation and Planning', in *Robotics and Automation, 2007 IEEE International Conference on*, Rome, Italy, 2007, pp. 4715–4720.

[39] M. Shibata and S. Hirai, 'Soft object manipulation by simultaneous control of motion and

deformation', in *Robotics and Automation, 2006. ICRA 2006. Proceedings 2006 IEEE International Conference on*, Orlando, Flordia, USA, 2006, pp. 2460–2465.

[40] J. A. Domínguez-López, R. I. Damper, R. M. Crowder, and C. J. Harris, 'Adaptive neurofuzzy control of a robotic gripper with on-line machine learning', *Robotics and Autonomous Systems*, vol. 48, no. 2–3, pp. 93–110, Sep. 2004.

[41] N. . Glossas and N. . Aspragathos, 'Fuzzy logic grasp control using tactile sensors', *Mechatronics*, vol. 11, no. 7, pp. 899–920, Oct. 2001.

[42] R. Platt, A. H. Fagg, and R. A. Grupen, 'Null-Space Grasp Control: Theory and Experiments', *Robotics, IEEE Transactions on*, vol. 26, no. 2, pp. 282–295, Apr. 2010.

[43] O. Kroemer, C. H. Lampert, and J. Peters, 'Learning Dynamic Tactile Sensing With Robust Vision-Based Training', *Robotics, IEEE Transactions on*, vol. 27, no. 3, pp. 545–557, Jun. 2011.

[44] E. D. Engeberg and S. G. Meek, 'Adaptive Sliding Mode Control for Prosthetic Hands to Simultaneously Prevent Slip and Minimize Deformation of Grasped Objects', *Mechatronics, IEEE/ASME Transactions on*, vol. 18, no. 1, pp. 376–385, Feb. 2013.

[45] S. Ivaldi, M. Fumagalli, M. Randazzo, F. Nori, G. Metta, and G. Sandini, 'Computing robot internal/external wrenches by means of inertial, tactile and F/T sensors: Theory and implementation on the iCub', *Humanoid Robots (Humanoids), 2011 11th IEEE-RAS International Conference on*, pp. 521–528, 10 2011.

[46] C. M. Gosselin and others, 'Two degree-of-freedom spherical orienting device', U.S. Patent 5966991Oct-1999.

[47] J.-J. Lucas, 'Device to handle and to orient flat workpieces arranged in batches', U.S. Patent 5293984Mar-1994.

[48] P. Bhattacharjee, A. Chatterjee, R. W. Lanjewar, U. S. Patkar, and N. P. Mukherjee, 'ORIENTATION UNIT FOR A FRUIT SORTING AND GRADING MACHINE', U.S. Patent 1874631Apr-2010.

[49] P. Maillard, 'Spherical Orienting Device and Method for manufacturing the same', U.S. Patent 2256397Jul-2012.

[50] M. Grange and A. Casagrande, 'Device for positioning an object in all directions', U.S. Patent 8047518Nov-2011.

[51] Y. Shirai and H. Inoue, 'Guiding a robot by visual feedback in assembling tasks', *Pattern Recognition*, vol. 5, no. 2, pp. 99–106, IN3, 107–108, Jun. 1973.

[52] P. I. Corke and S. A. Hutchinson, 'Real-time vision, tracking and control', in *Robotics and Automation, 2000. Proceedings. ICRA '00. IEEE International Conference on*, 2000, vol. 1, pp. 622–629 vol.1.

[53] P. I. Corke and S. A. Hutchinson, 'A new partitioned approach to image-based visual servo control', *Robotics and Automation, IEEE Transactions on DOI - 10.1109/70.954764*, vol. 17, no. 4, pp. 507–515, 2001.

[54] P. I. Corke, 'Spherical image-based visual servo and structure estimation', in *Robotics and Automation (ICRA), 2010 IEEE International Conference on*, 2010, pp. 5550–5555.

[55] S. Hutchinson, G. D. Hager, and P. I. Corke, 'A tutorial on visual servo control', *Robotics and Automation, IEEE Transactions on DOI - 10.1109/70.538972*, vol. 12, no. 5, pp. 651–670, 1996.

[56] P. Azad, T. Asfour, and R. Dillmann, 'Accurate shape-based 6-DoF pose estimation of single-colored objects', *Intelligent Robots and Systems, 2009. IROS 2009. IEEE/RSJ International Conference on*, pp. 2690–2695, 10.

[57] N. Vahrenkamp, S. Wieland, P. Azad, D. Gonzalez, T. Asfour, and R. Dillmann, 'Visual servoing for humanoid grasping and manipulation tasks', *Humanoid Robots, 2008. Humanoids 2008. 8th IEEE-RAS International Conference on*, pp. 406–412, 1.

[58] J. H. Kim, Shih-Kang Kuo, and C.-H. Menq, 'An ultraprecision six-axis visual servo-control system', *Robotics, IEEE Transactions on*, vol. 21, no. 5, pp. 985–993, Oct. 2005.

[59] N. Guenard, T. Hamel, and R. Mahony, 'A Practical Visual Servo Control for an Unmanned Aerial Vehicle', *Robotics, IEEE Transactions on*, vol. 24, no. 2, pp. 331–340, Apr. 2008.

[60] Ying Wang, Haoxiang Lang, and C. W. de Silva, 'Visual servo control and parameter calibration for mobile multi-robot cooperative assembly tasks', *Automation and Logistics, 2008. ICAL 2008. IEEE International Conference on*, pp. 635–639, 1.

[61] Xiangjin Zeng, X. Huang, and M. Wang, 'Visual servoing based on fuzzy adaptive PID with Modified Smith Predictor for micromanipulation', *Advanced Intelligent Mechatronics, 2008. AIM 2008. IEEE/ASME International Conference on*, pp. 290–295, 2.

[62] V. Niola, C. Rossi, and S. Savino, 'An application of vision systems to the path planning of industrial robots', in *Proceedings of the 2nd international conference on Advances in brain, vision and artificial intelligence*, Naples, Italy, 2007, pp. 586–594.

[63] A. J. Davison, 'Real-time simultaneous localisation and mapping with a single camera', in *Computer Vision, 2003. Proceedings. Ninth IEEE International Conference on*, 2003, pp. 1403–1410 vol.2.

[64] K. Hashimoto, T. Kimoto, T. Ebine, and H. Kimura, 'Manipulator control with image-based visual servo', in *Robotics and Automation, 1991. Proceedings., 1991 IEEE International Conference on*, 1991, pp. 2267–2271 vol.3.

[65] F. Chaumette and S. Hutchinson, 'Visual servo control. I. Basic approaches', *Robotics & Automation Magazine, IEEE DOI - 10.1109/MRA.2006.250573*, vol. 13, no. 4, pp. 82–90, 2006.

[66] D. Sykora, D. Sedlaeck, and K. Riege, 'Real-time Color Ball Tracking for Augmented Reality', in *Eurographics Symposium on Virtual Environments*, Eindhoeven, The Netherlands, 2008, vol. 14, pp. 9–16.

[67] Michael Greenspan and Ian Fraser, 'Tracking a sphere dipole', presented at the International Conference on Vision Interface, 2003.

[68] D. Bradley and G. Roth, 'Tracking a Sphere with Six Degrees of Freedom', NRC Institute for Information Technology; National Research Council Canada, 47397, 2004.

[69] 'Stingray F-033 - High-quality industrial FireWire camera, VGA - Sony ICX414 - Allied Vision Technologies'. [Online]. Available: http://www.alliedvisiontec.com/apac/products/cameras/firewire/stingray/f-033bc.html. [Accessed: 26-Feb-2012].

[70] World Wide Collabrations, *OpenCV*. .

[71] World Wide Collabrations, *Boost C++ Libraries*. .

[72] *VXL Computer Vision Research Libraries*. .

[73] B. K. P. Horn, 'Closed-form solution of absolute orientation using unit quaternions', *J. Opt. Soc. Am. A*, vol. 4, no. 4, pp. 629–642, Apr. 1987.

[74] B. K. P. Horn and E. J. Weldon, 'Direct methods for recovering motion', *International Journal of Computer Vision*, vol. 2, no. 1, pp. 51–76, Jun. 1988.

[75] D. Martinec and T. Pajdla, 'Robust Rotation and Translation Estimation in Multiview Reconstruction', *Computer Vision and Pattern Recognition, 2007. CVPR '07. IEEE Conference on*, pp. 1–8, 17.

[76] S. Umeyama, 'Least-squares estimation of transformation parameters between two point patterns', *Pattern Analysis and Machine Intelligence, IEEE Transactions on*, vol. 13, no. 4, pp. 376–380, Apr. 1991.

[77] J. M. Fitzpatrick, J. B. West, and C. R. Maurer, 'Predicting error in rigid-body point-based registration', *Medical Imaging, IEEE Transactions on*, vol. 17, no. 5, pp. 694–702, Oct. 1998.

[78] N. W. Oumer and G. Panin, '3D point tracking and pose estimation of a space object using stereo images', *Pattern Recognition (ICPR), 2012 21st International Conference on*, pp. 796–800, 11.

[79] SMC Pneumatics, 'Vacuum Ejector Datasheet Series ZH'. SMC Pneumatics, 2009.

[80] KUKA Roboter GmbH, *Food Palletizing Robot*. 2005.

9 List of Relevant Publications by Author

[81] M. C. Edmondson and L. Tang, 'Vision Processing for Position Based Visual Servo Control of Spherical Objects', *Image Processing, Computer Vision and Pattern Recognition(IPCV)*, *Worldcomp 2011 International Conference on*, Las Vegas, 2011, pp. 713–719, vol 2.

A Calculation Details for Robotic Motion Analysis

A.1 Matlab Code for Generating Jounce Controlled Motion Curves.

```
function [MotionCurves] = MotionGenerator(InitPos, FinalPos,
InitTime,FinalTime,SampleRate)
%Generates the motion curves of Acc, Vel and Dis for one movement.
%
TotalTime = FinalTime -InitTime;
T = TotalTime/7;
Displacement = FinalPos - InitPos;
jd = Displacement/(6*T^4);
Samples = floor(TotalTime*SampleRate);
DataOut= zeros(3,Samples);
    for i=1:Samples
        time = i/SampleRate - 1/SampleRate;
        Region = ceil (time/T);
        ts = mod(time,T);
        switch(Region)
            case {0,1}
               DataOut(3,i) =  (jd*ts^2)/2;
               DataOut(2,i) =  (jd*ts^3)/6;
               DataOut(1,i) =  (jd*ts^4)/24+InitPos;
            case 2
               DataOut(3,i) =  (T^2*jd)/2 + (jd*ts*(2*T - ts))/2;
               DataOut(2,i) =  (T^3*jd)/6 + (jd*ts*(3*T^2 + 3*T*ts -
                  ts^2))/6;
               DataOut(1,i) =  (jd*T^4)/24 + (jd*T^3*ts)/6 +
                  (jd*T^2*ts^2)/4 + (jd*T*ts^3)/6 -
                  (jd*ts^4)/24+InitPos;
            case 3
               DataOut(3,i) =  T^2*jd - (jd*ts^2)/2;
               DataOut(2,i) =  T^3*jd + (jd*ts*(6*T^2 - ts^2))/6;
               DataOut(1,i) =  (7*T^4*jd)/12 + (jd*ts*(24*T^3 +
12*T^2*ts - ts^3))/24+InitPos;
```

```
            case 4
               DataOut(3,i) =  (T^2*jd)/2 - T*jd*ts;
               DataOut(2,i) =  (11*T^3*jd)/6 + (T*jd*ts*(T - ts))/2;
               DataOut(1,i) =  (49*T^4*jd)/24 + (T*jd*ts*(22*T^2 +
3*T*ts - 2*ts^2))/12+InitPos;
            case 5
               DataOut(3,i) =  -(T^2*jd)/2 - (jd*ts*(2*T - ts))/2;
               DataOut(2,i) =  (11*T^3*jd)/6 - (jd*ts*(3*T^2 +
3*T*ts - ts^2))/6;
               DataOut(1,i) =  (95*jd*T^4)/24 + (11*jd*T^3*ts)/6 -
(jd*T^2*ts^2)/4 - (jd*T*ts^3)/6 + (jd*ts^4)/24+InitPos;
            case 6
               DataOut(3,i) =  (jd*ts^2)/2 - T^2*jd;
               DataOut(2,i) =  T^3*jd - (jd*ts*(6*T^2 - ts^2))/6;
               DataOut(1,i) =  (65*T^4*jd)/12 + (jd*ts*(24*T^3 -
12*T^2*ts + ts^3))/24+InitPos;
            case 7
               DataOut(3,i) = (jd*ts*(2*T - ts))/2 - (T^2*jd)/2;
               DataOut(2,i) = (T^3*jd)/6 - (jd*ts*(3*T^2 - 3*T*ts +
ts^2))/6;
               DataOut(1,i) = (143*jd*T^4)/24 + (jd*T^3*ts)/6 -
(jd*T^2*ts^2)/4 + (jd*T*ts^3)/6 - (jd*ts^4)/24+InitPos;
        end
    end
MotionCurves = DataOut;
end
```

A.2 Variables Setup for the Comparison between Pack Layouts

Single Unit	Variable
Rate	120, 200, 225, 250, 275, 300
Pick and Place Time (s)	0.05,0.10,0.15,0.
Travel Δxyz (m)	[0.15, 0.15, -0.05] [0.40, 0.35, -0.05] [0.65, 0.55, -0.05]

Twin Unit	Variable
Rate	120, 200, 225, 250, 275, 300
Pick and Place Time (s)	0.05,0.10,0.15,0.
Travel Δxyz (m)	[0.15, 0.15, -0.05] [0.28, 0.35, -0.05] [0.40, 0.55, -0.05]

Optimised Single Unit	Variable
Rate	120, 200, 225, 250, 275, 300
Pick and Place Time (s)	0.05,0.10,0.15,0.
Travel Δxyz (m)	[0.15, 0.075, -0.15]

Row Packer	Variable
Rate	120, 200, 225, 250, 275, 300
Pick and Place Time (s)	0.05,0.10,0.15,0.
Weibull Shape factor	1.25, 1.50, 1.75, 2.00
Displacement Δxyz (m)	0.15,0.00,-0.15
Tray Layouts	6.5 x 6 , 6 x 6, 6 x 5, 5.5 x 4

Pattern Packer	Variable
Rate	120, 200, 225, 250, 275, 300
Pick and Place Time (s)	0.05,0.10,0.15,0.20
Weibull Shape factor	1.25, 1.50, 1.75, 2.00
Displacement Δxyz (m)	0.50,0.00,-0.15
Tray Layouts	6.5 x 6 , 6 x 6, 6 x 5, 5.5 x 4

A.3 Robot Simulation Grasp and Release Coordinates

	X Axis (Longitudinal m)	Z Axis(Vertical m)	Robotic Knuckle Tilt (Degrees)	Robotic Knuckle Rotate(Degrees)
Grasp Location	0.25	0.1	-20	0
Pack Location 1	0.1	0	0	15
Pack Location 2	0.025	0	0	15
Pack Location 3	-0.05	0	0	15
Pack Location 4	-0.125	0	0	15
Pack Location 5	-.02	0	0	15

B Conceptual Orientation Solutions

Several radical design solutions were considered as a new orientation approach.

1. Solenoid nudging
2. Perpendicular driving rollers
3. Quad driven rollers
4. Asymmetrical driver rollers

B.1 Solenoid Nudging

A novel approach is to nudge the OBJ to the correct orientation with the use of solenoids as shown in Figure B.1. Four solenoids would be positioned under a pocket containing the OBJ. The OBJ is manipulated with a single or structured push from the solenoids below. The purpose of OBJ orientation is to position the OBJ's to improve human perception[29] of quality and not a critical measurement, therefore it could be possible to gently nudge the OBJ into a correct orientation.

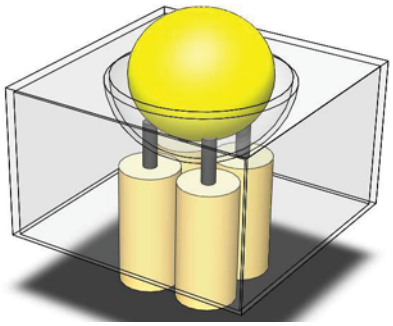

Figure B.1: Solenoid oreintation concept.

B.2 Perpendicular Driven Rollers

The perpendicular driven roller has two driven rollers with perpendicular axes as shown in Figure B.2. These two axes intend to produce a variable rotational axis for the OBJ.

29 Consumers will pay a higher price based on presentation.

This roller layout intends to separate inducing either Z or X axes rotations.

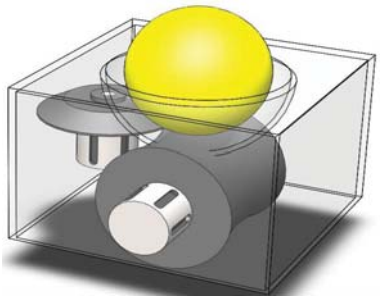

Figure B.2: Perpendicular orientation concept.

B.3 Cross Pattern Driven Rollers

Figure B.3 illustrates the cross pattern driven rollers. Four independently driven rollers are located at the four corners surrounding the OBJ on a horizontal plane. The variation of the roller velocities is intended to induce different OBJ rotations.

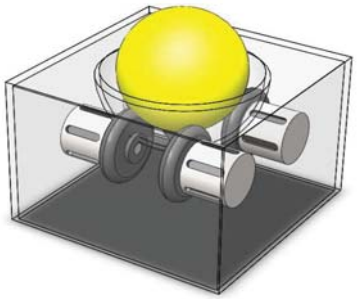

Figure B.3: Perpendicular concept.

B.4 Independently Collinear Driven Rollers

The OBJ is located above two independently driven collinear rollers as shown in Figure B.4. The OBJ is constrained above the rollers with a concave cup design. The inter-roller rotation velocity determines the rotation axis of the OBJ.

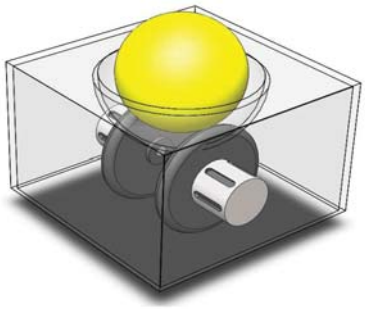

Figure B.4: Co-linear rollers orientation concept.

C Grasp Effects

C.1 Effect of Mass

Mass(g) 40 60 80 100 120

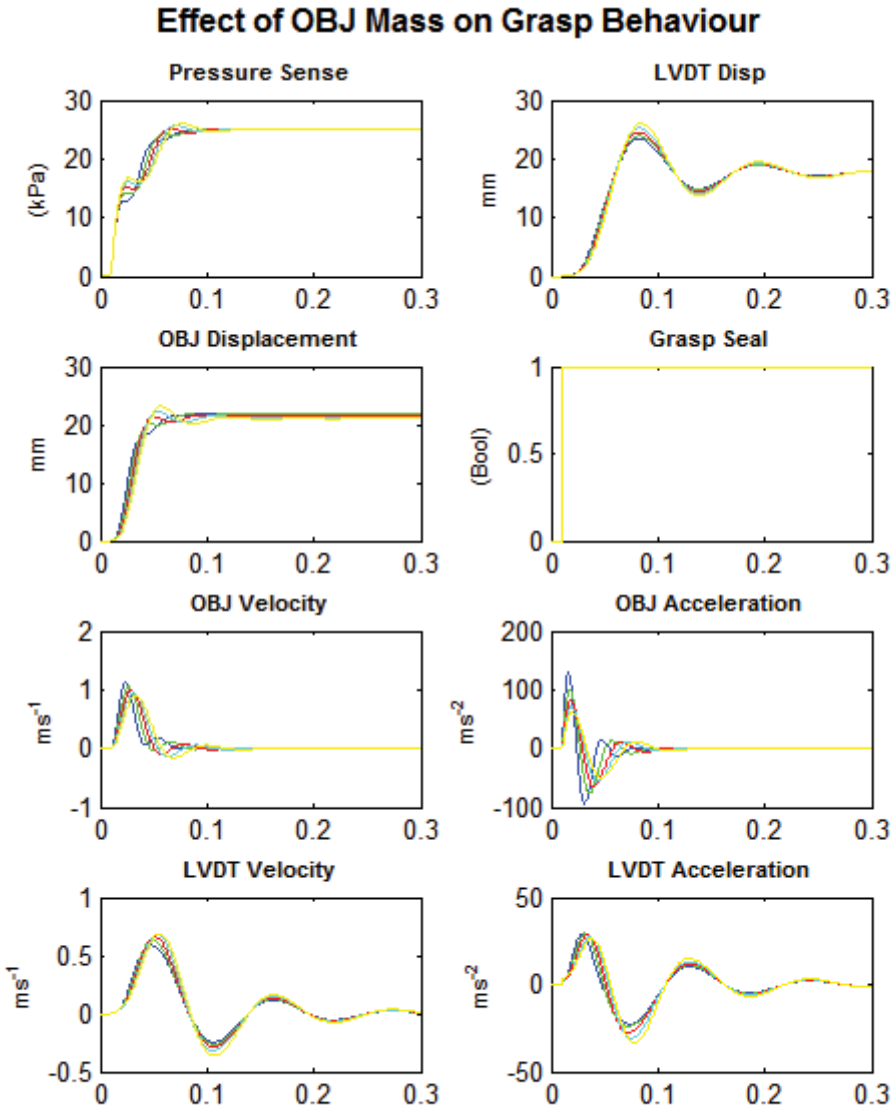

Figure C.1: Effect of Mass

C.2 Effect of Vacuum Depth

Vacuum Depth(kPa)	-15	-20	-25	-30	-35

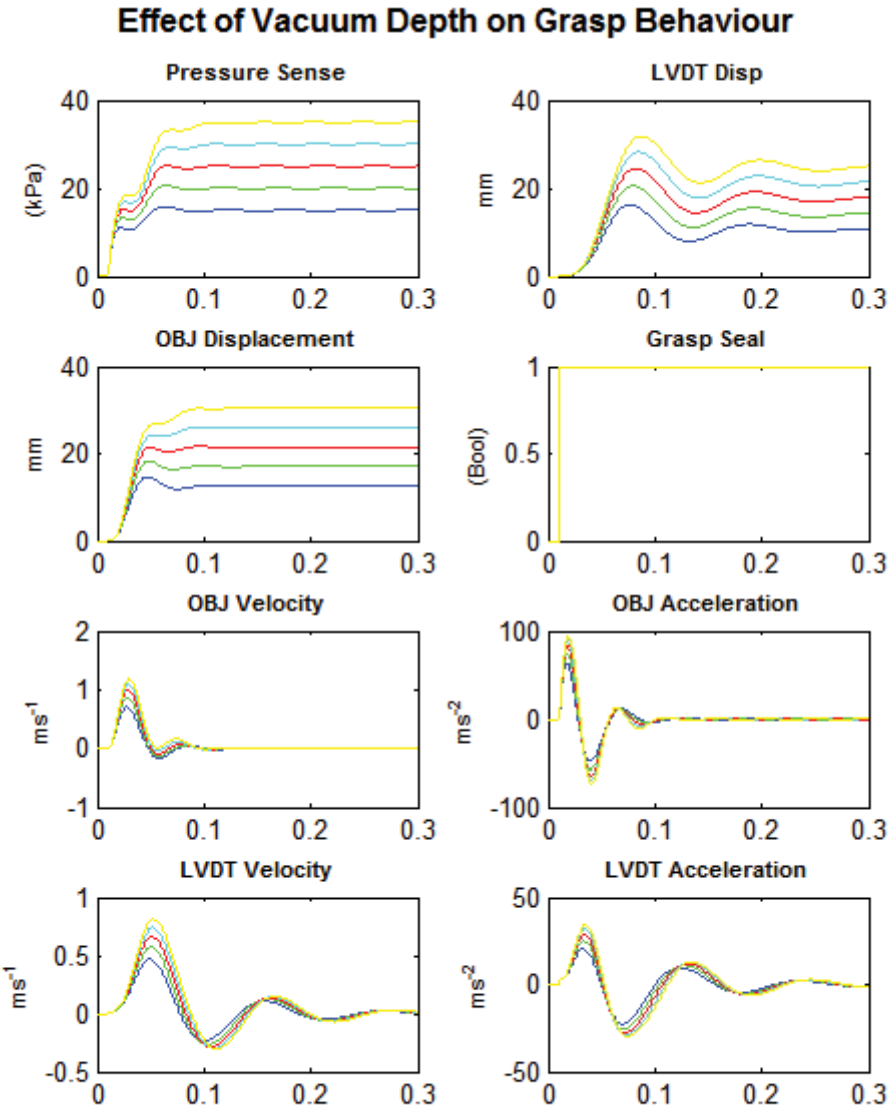

Figure C.2: Effect of Vacuum Depth on Grasp

C.3 Effect of Flow Rate

FlowRate (l/min @ 101kPa	44	64	84	104	124

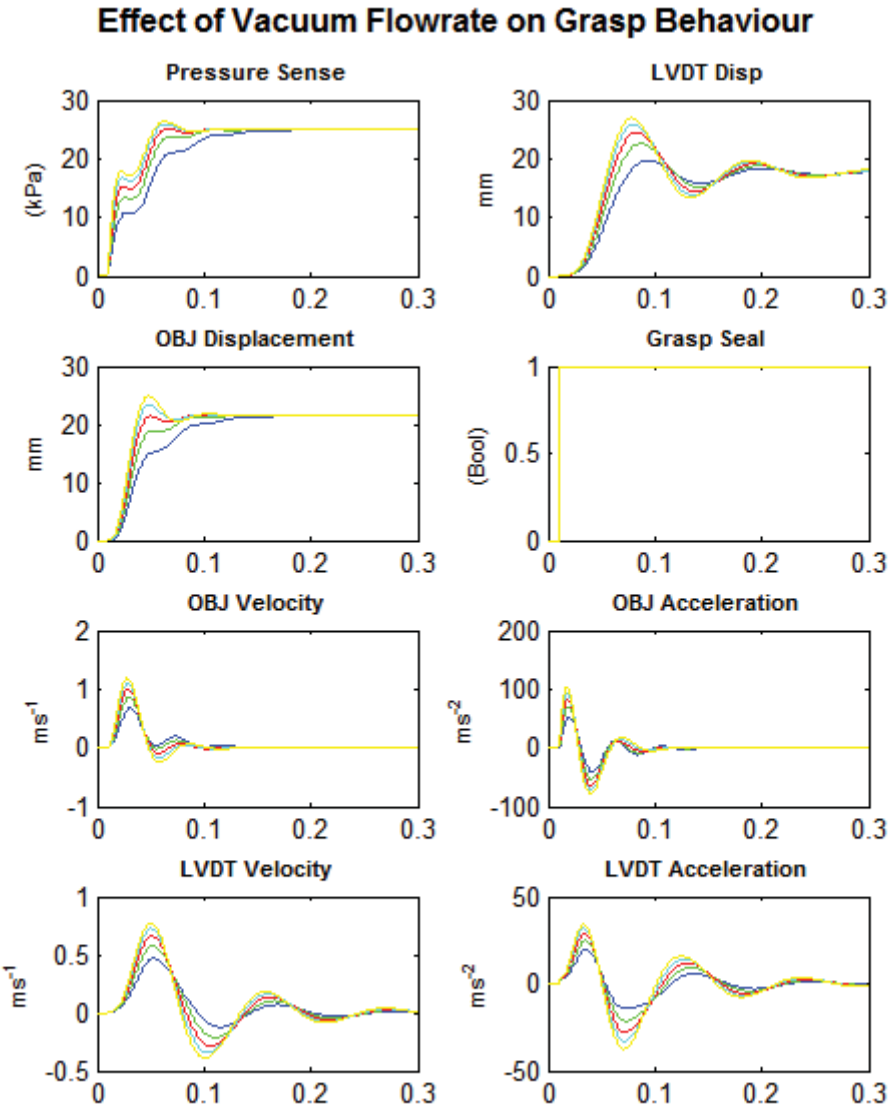

Figure C.3: Effect of FlowRate on Grasp

C.4 Effect of Vacuum Cup Spring Rate

Spring Rate (N/m)	384	584	784	984	1184

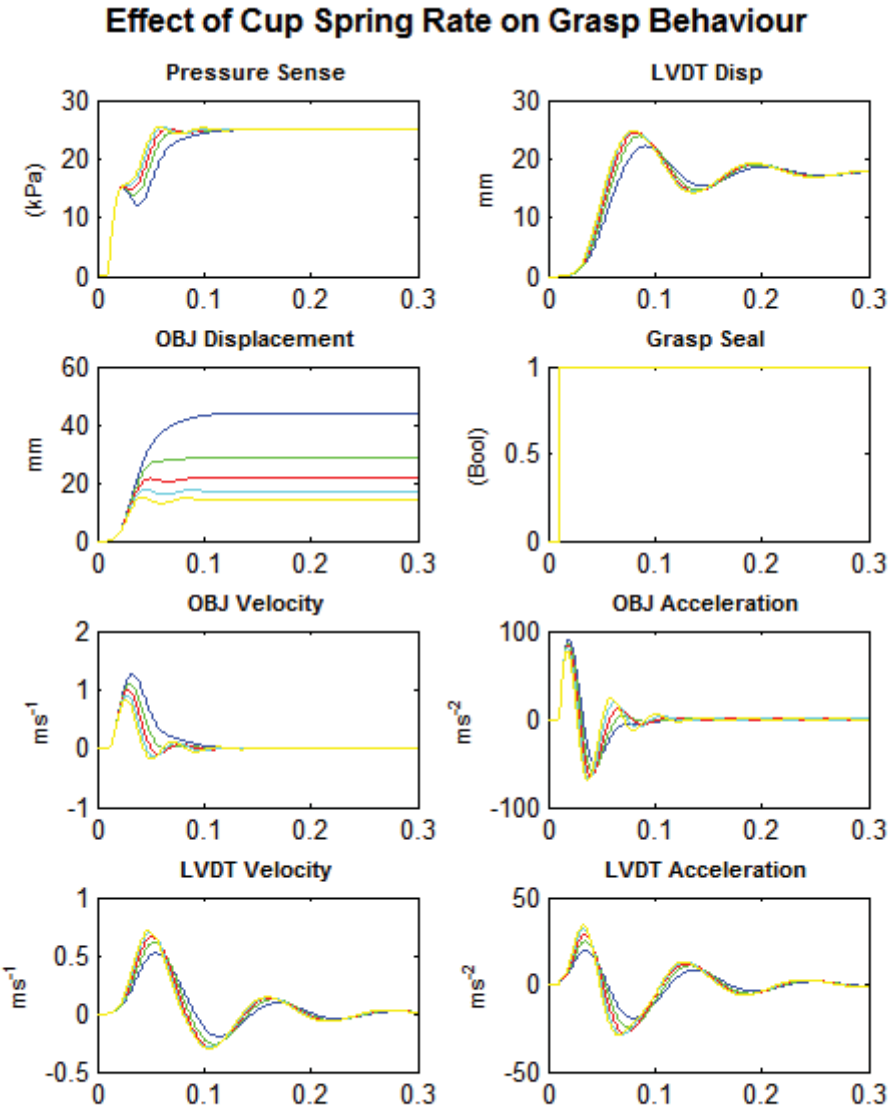

Figure C.4: Effect of Vacuum Cup Rate

C.5 Effect of Vacuum Cup Diameter

Diameters (mm)	20	25	30	35	40

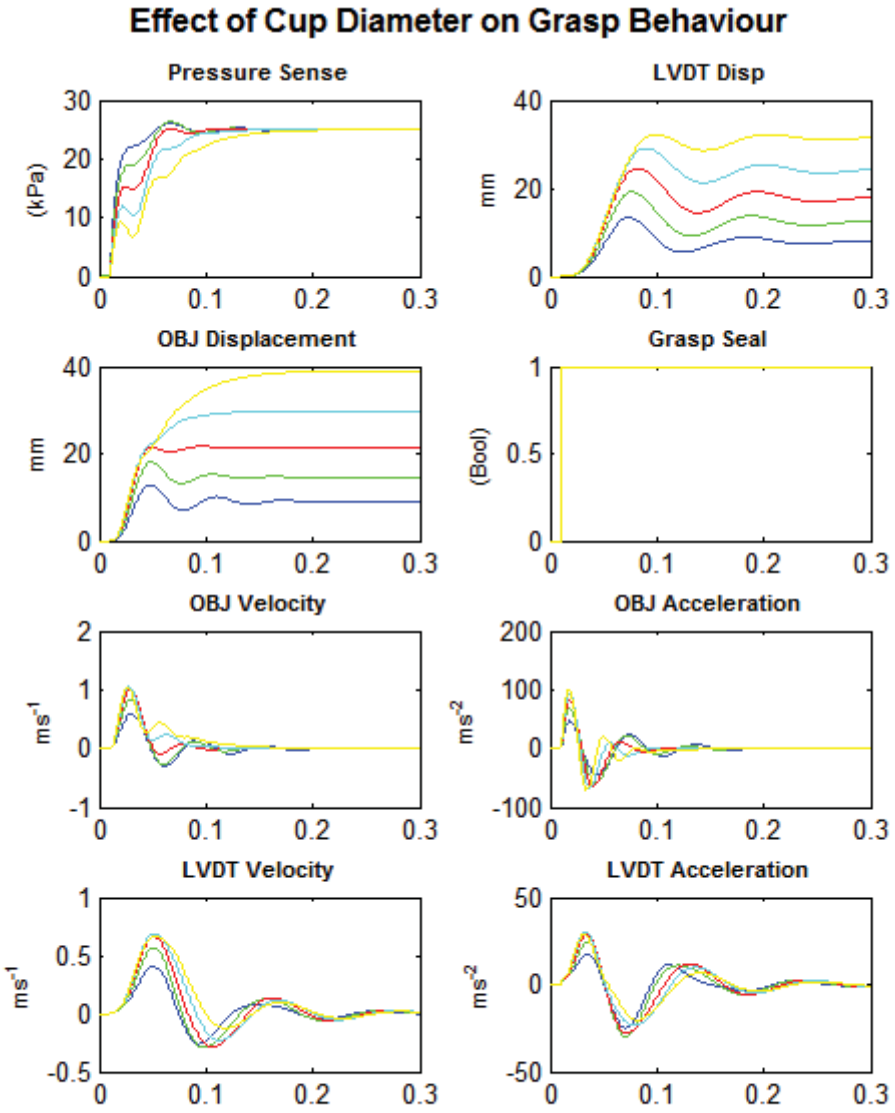

Figure C.5: Vacuum Cup Diameter Effects

C.6 Effect of LVDT Spring Rate

Spring Rates (N/m) 600 800 1000 1200 1400

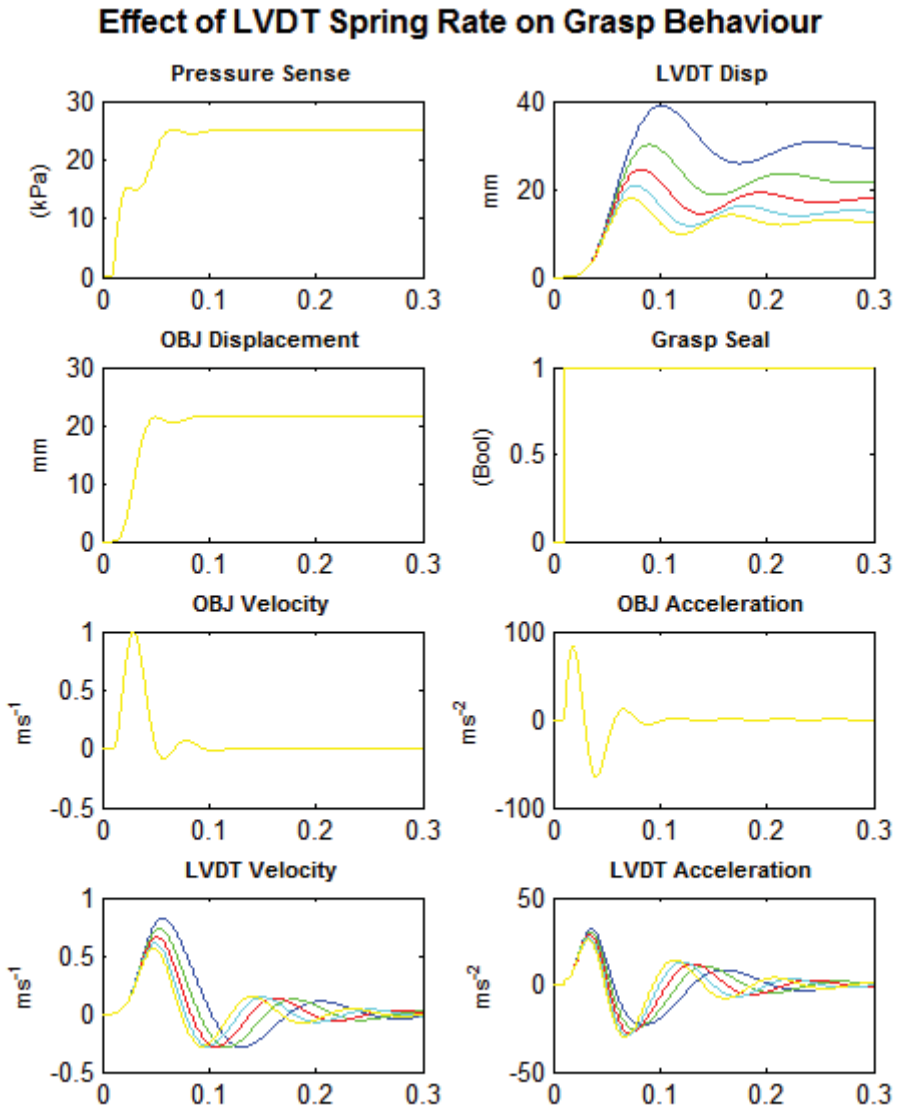

Figure C.6: Effect of LVDT Spring Rates

D Orientation Motion Models

This append contains the detailed motion modelling results for the discussion in section 6.4 .

D.1 Behaviour of the Single Cord Design

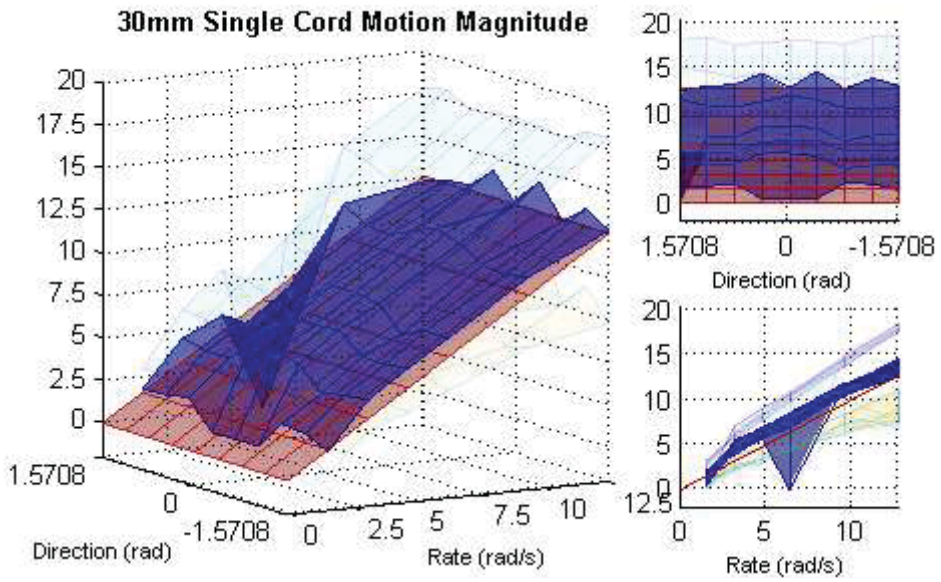

Figure D.1: Motion magnitude behaviour of single cord belts of 30mm separation.

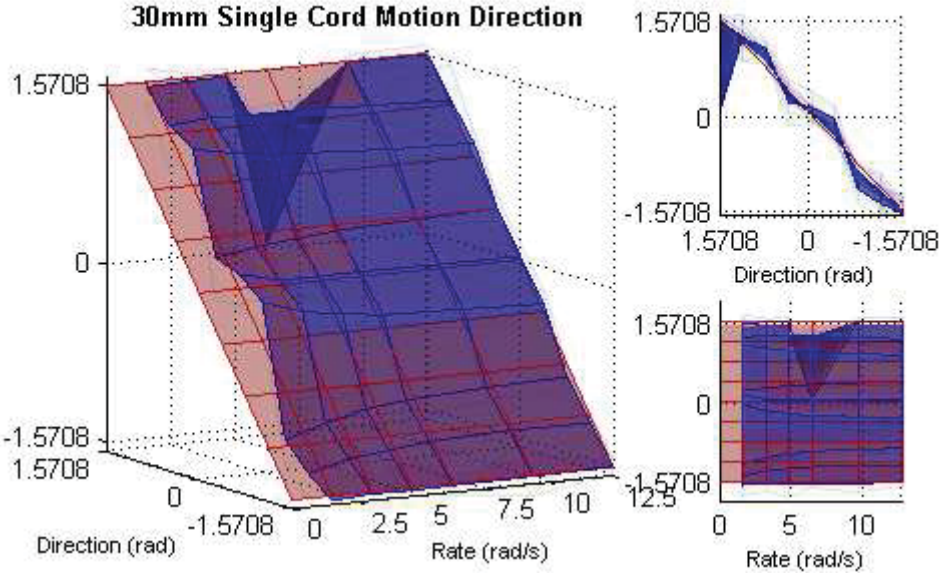

Figure D.2: Motion direction behaviour of single cord belts of 30mm separation.

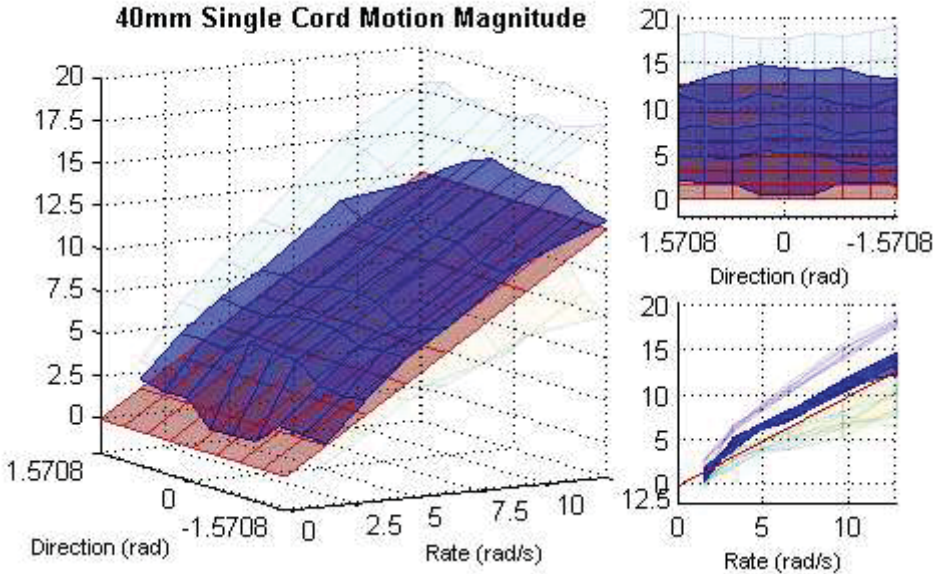

Figure D.3: Motion magnitude behaviour of single cord belts of 40mm separation.

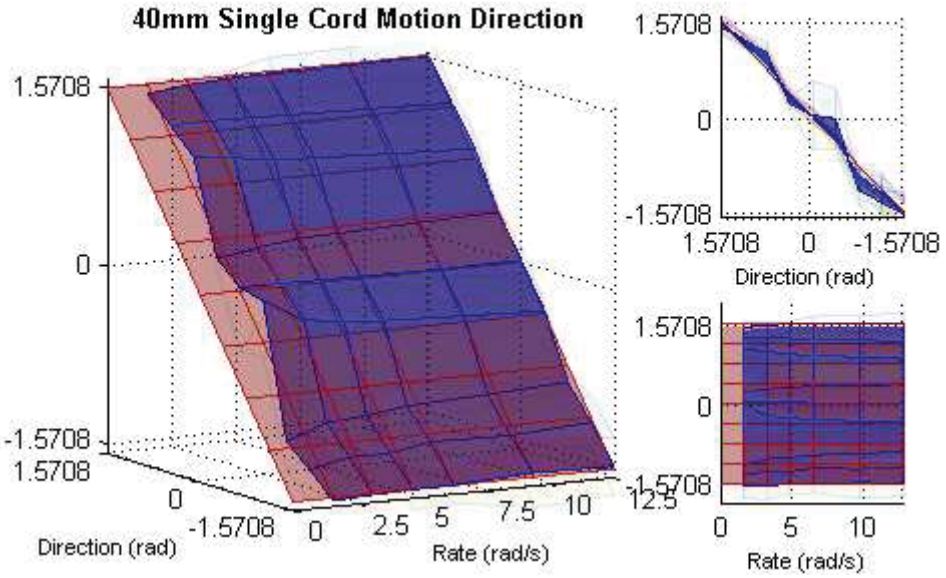

Figure D.4: Motion direction behaviour of single cord belts of 40mm separation.

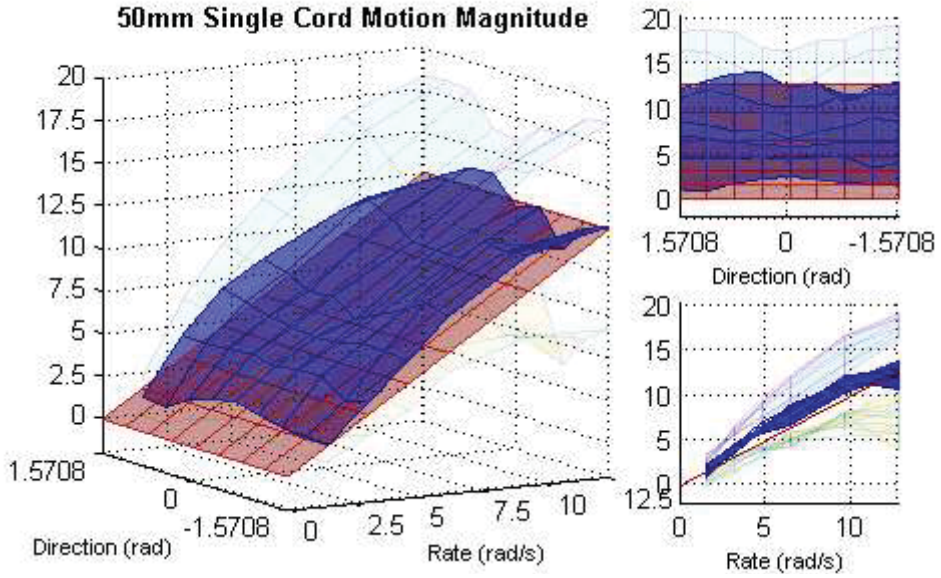

Figure D.5: Motion magnitude behaviour of single cord belts of 50mm separation.

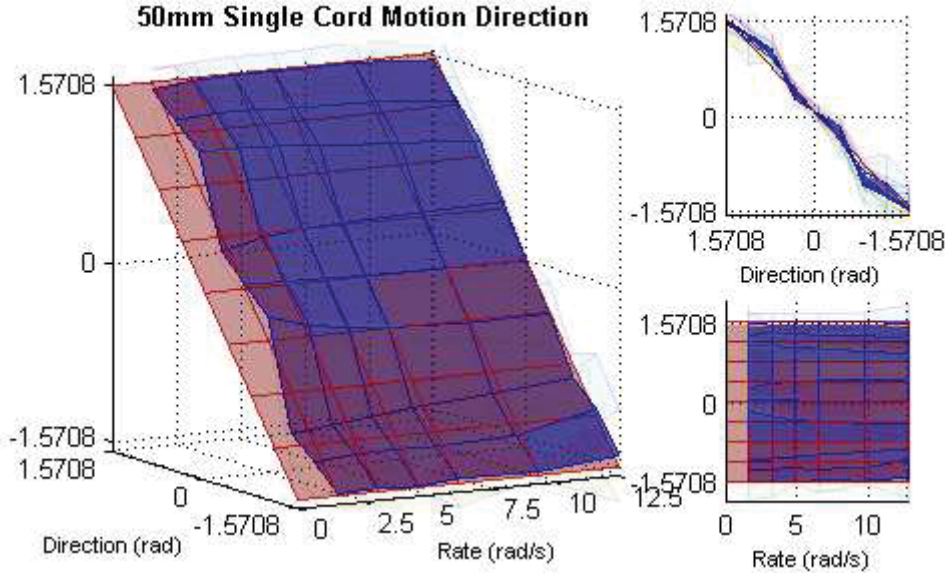

Figure D.6: Motion direction behaviour of single cord belts of 50mm separation.

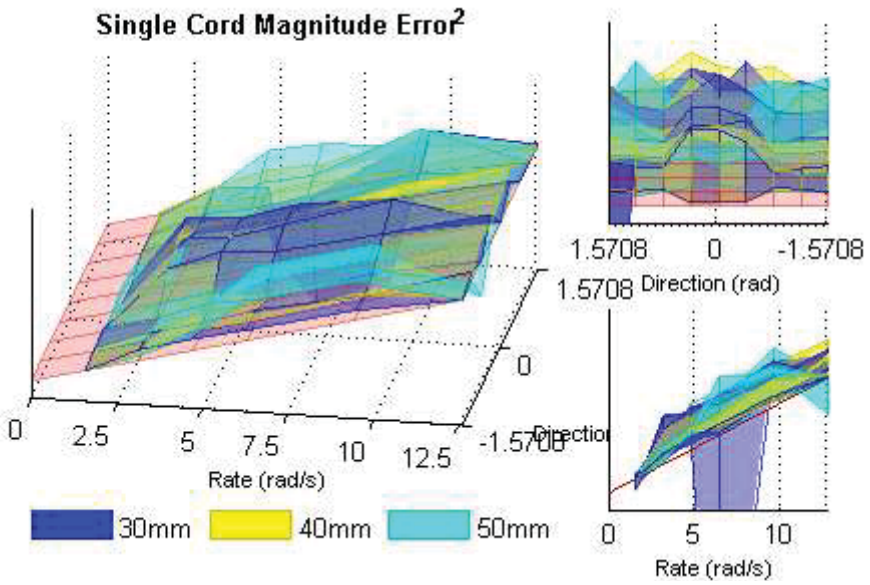

Figure D.7: Warped illustration of the magnitude error of Single Cord of varying belt separation.

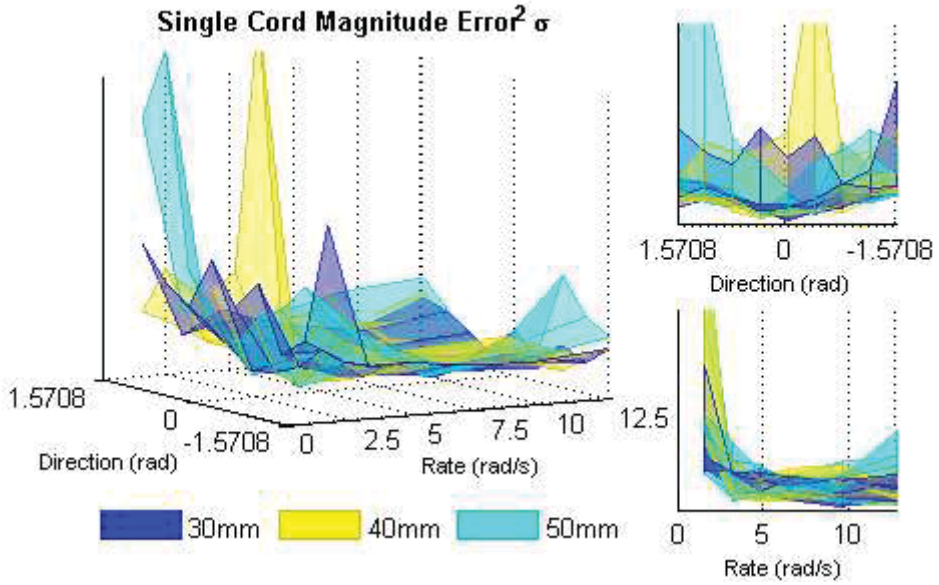

Figure D.8: Warped illustration showing the mean magnitude for single cord belt design of varying separation.

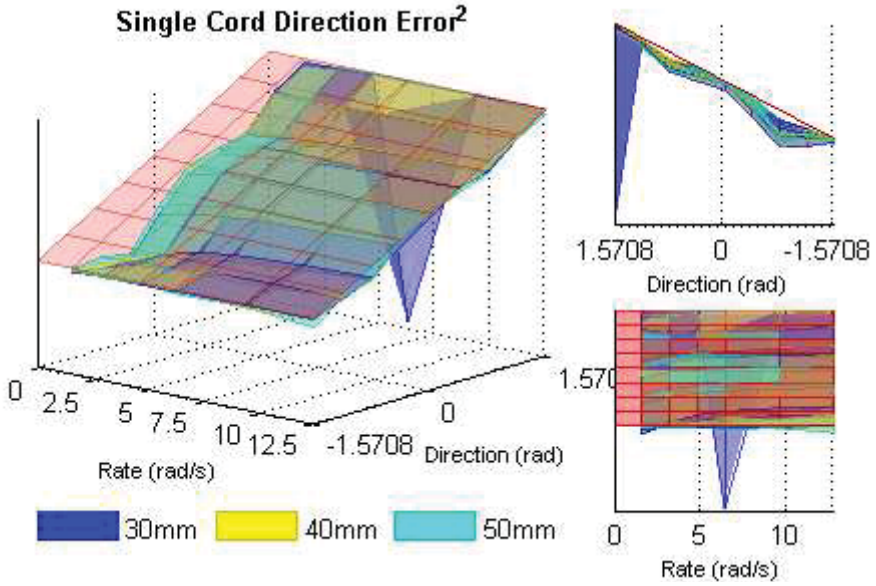

Figure D.9: Warped illustration showing the mean direction for single cord belt design of varying separation.

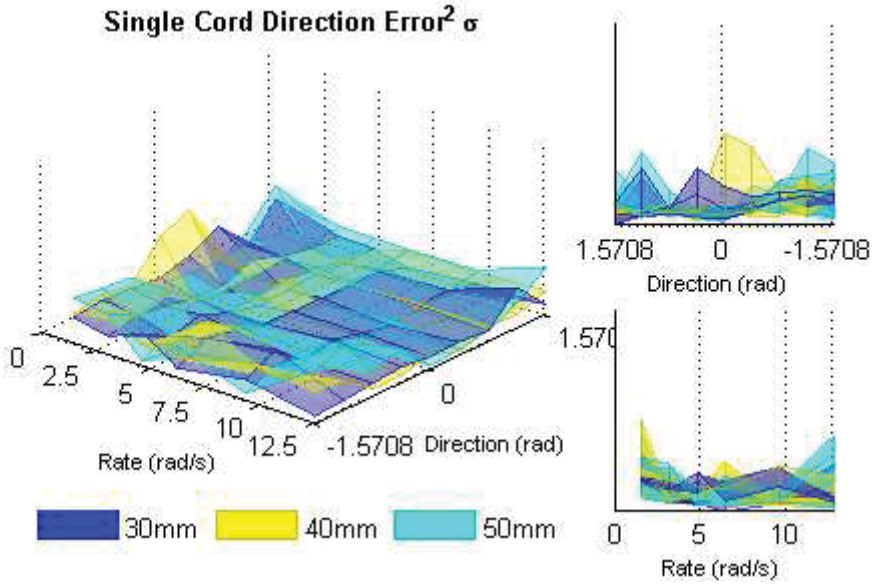

Figure D.10: Warped illustration showing the direction standard deviation for single cord belt design of varying separation.

D.2 Behaviour of the Dual Cord Design

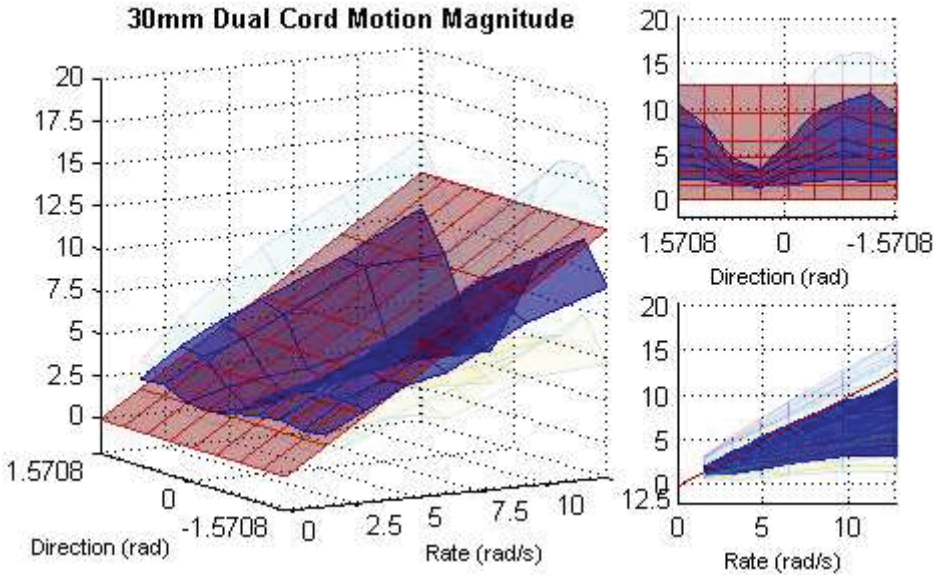

Figure D.11: Motion magnitude behaviour of dual cord belts of 30mm separation.

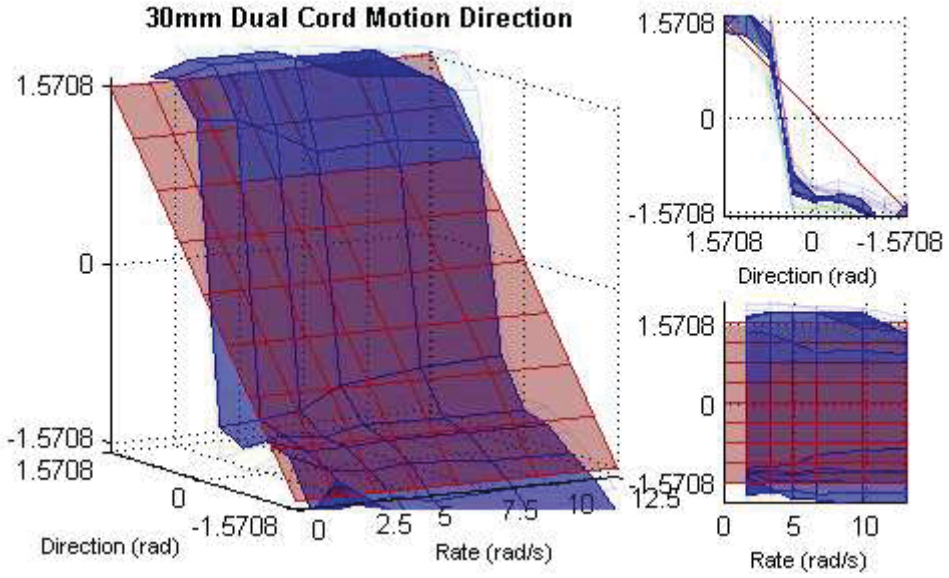

Figure D.12: Motion direction behaviour of dual cord belts of 30mm separation.

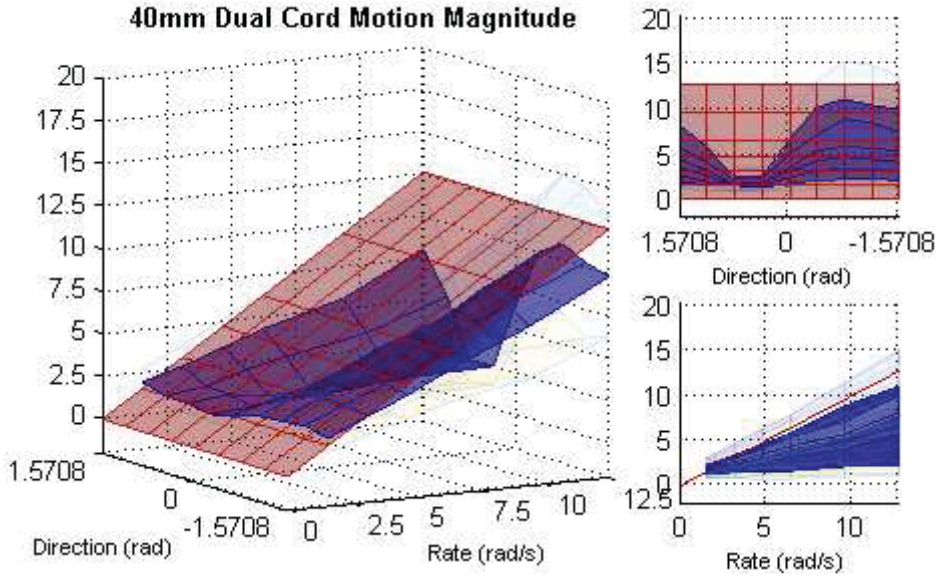

Figure D.13: Motion magnitude behaviour of dual cord belts of 40mm separation.

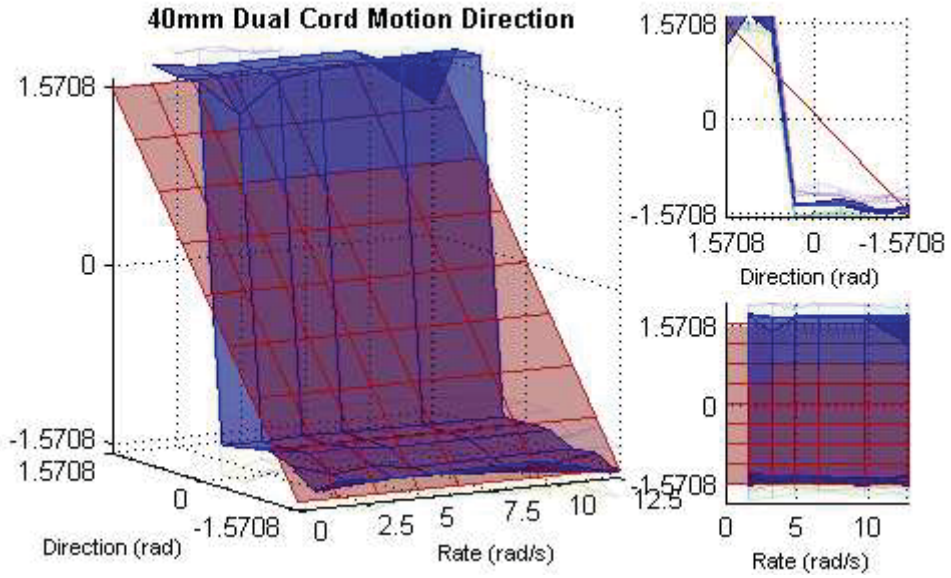

Figure D.14: Motion direction behaviour of dual cord belts of 40mm separation.

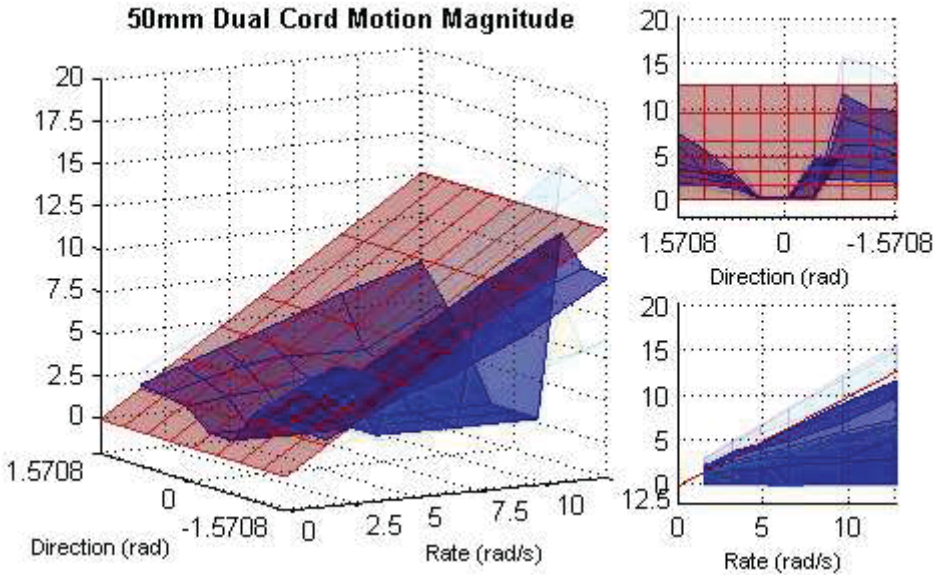

Figure D.15: Motion magnitude behaviour of dual cord belts of 50mm separation.

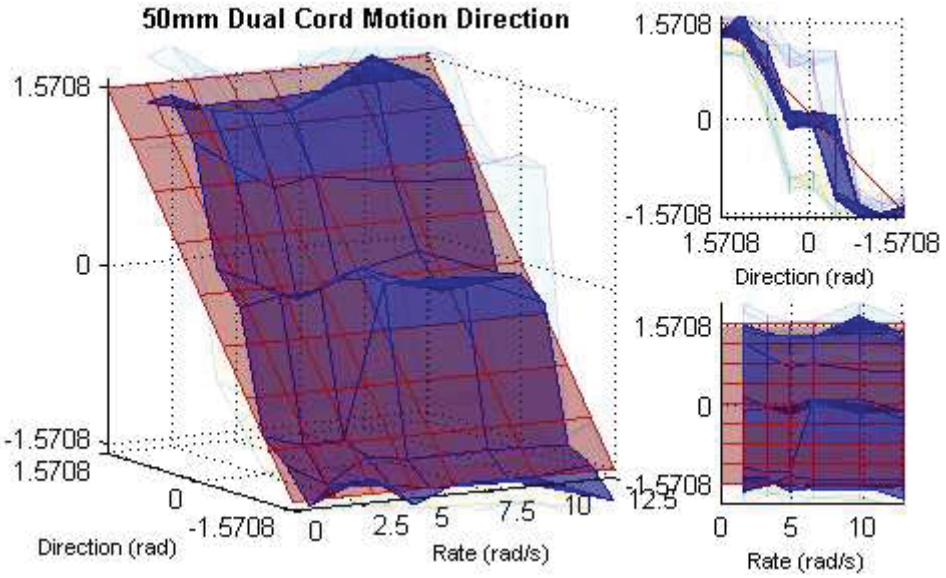

Figure D.16: Motion direction behaviour of dual cord belts of 50mm separation.

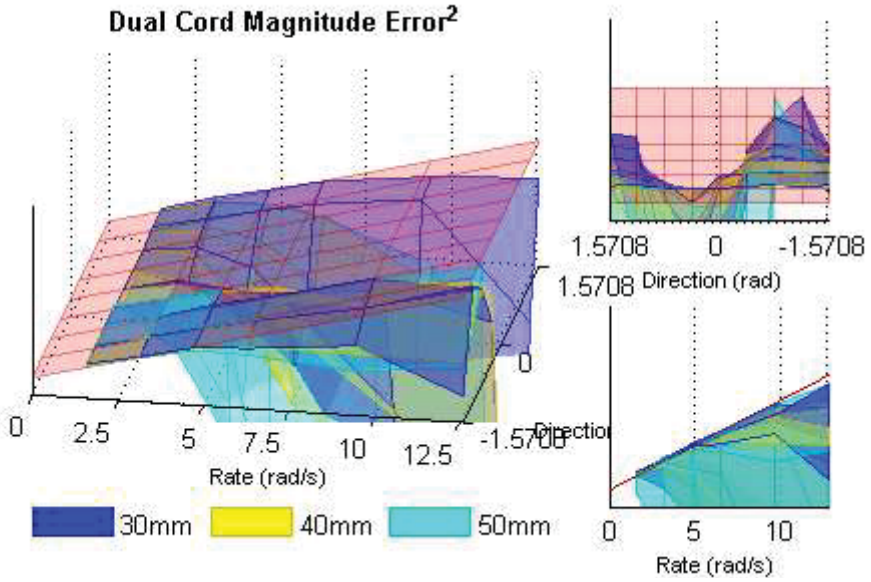

Figure D.17: Warped illustration of the magnitude error of dual cord of varying belt separation..

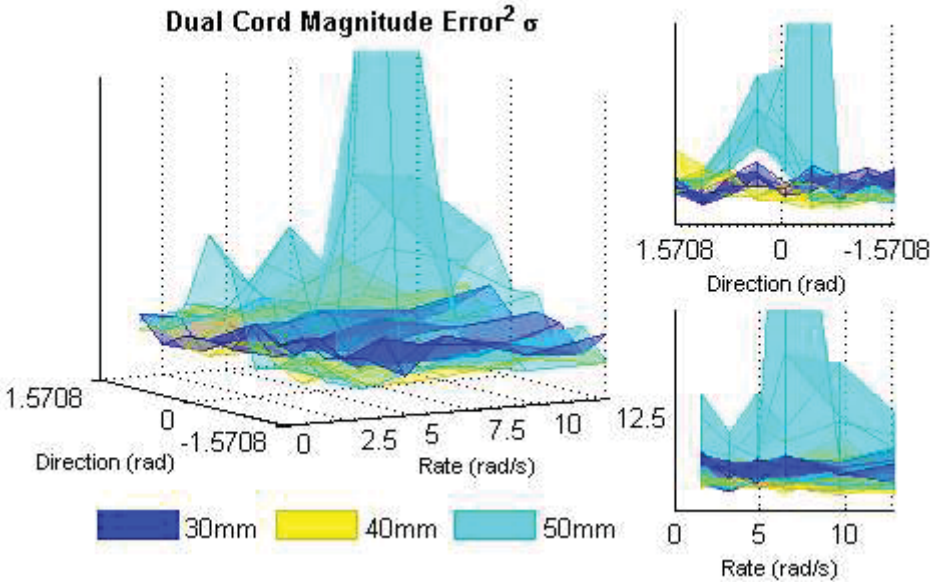

Figure D.18: Warped illustration of the magnitude error standard deviation of dual cord of varying belt separation.

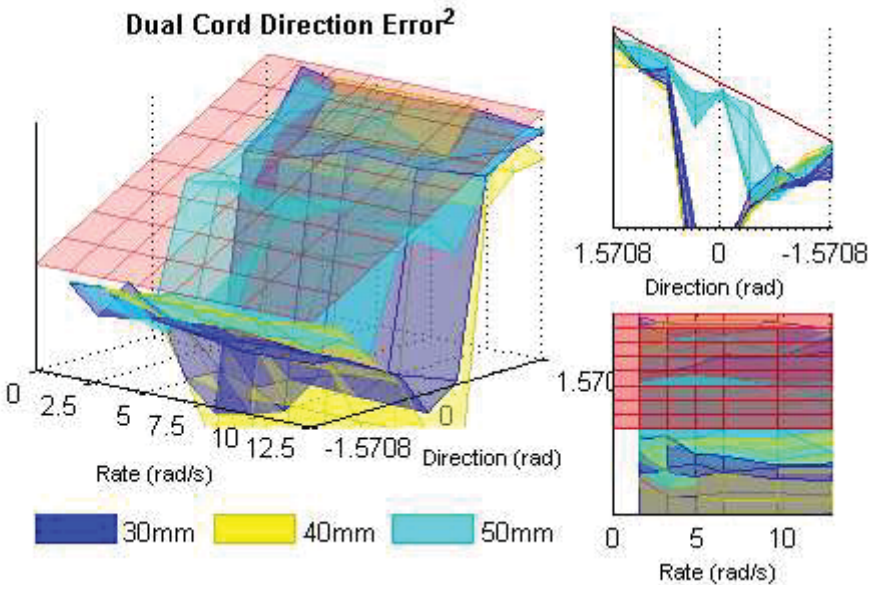

Figure D.19: Warped illustration of the direction error of dual cord of varying belt separation..

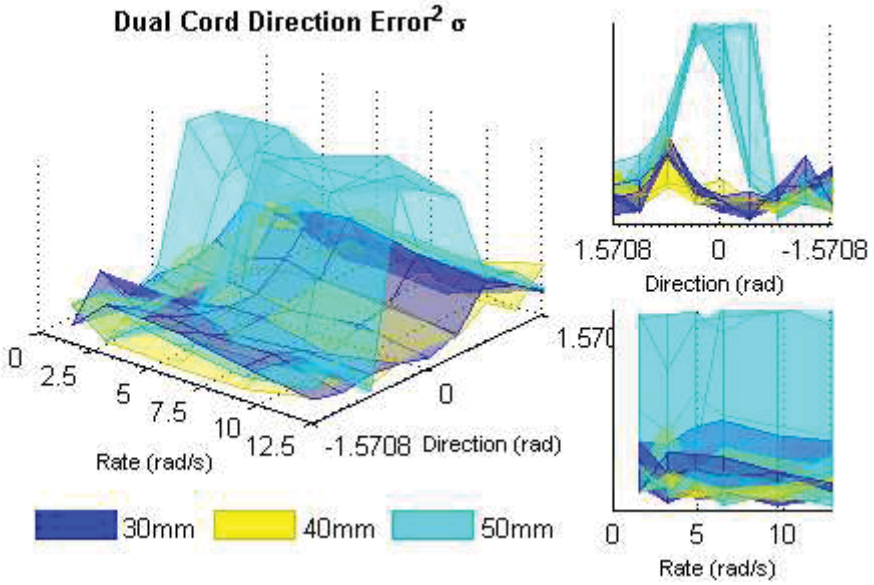

Figure D.20: Warped illustration of the direction error standard deviation of dual cord of varying belt separation.

D.3 Behaviour of the Flat Belt Design

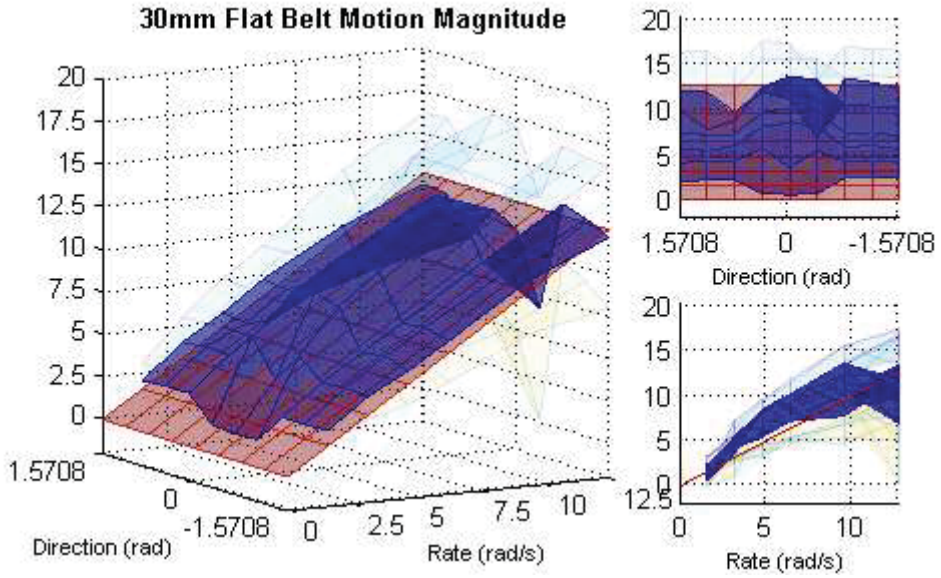

Figure D.21: Motion magnitude behaviour of flat belt of 30mm separation.

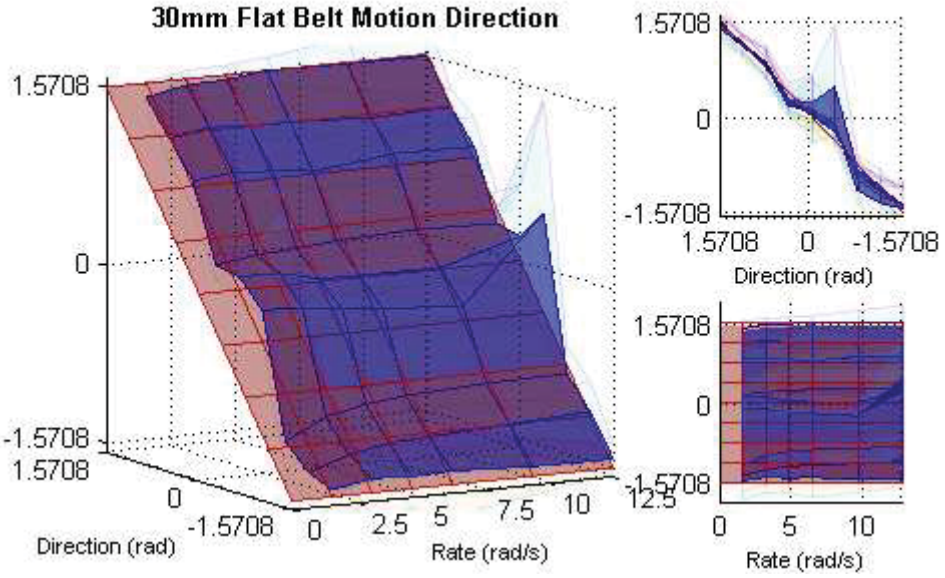

Figure D.22: Motion direction behaviour of flat belt of 30mm separation.

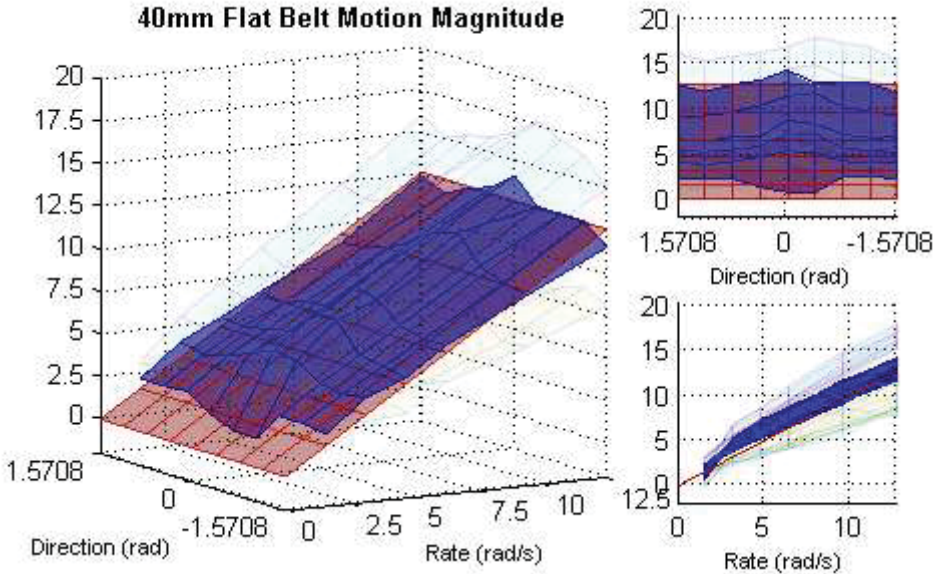

Figure D.23: Motion magnitude behaviour of flat belt of 40mm separation.

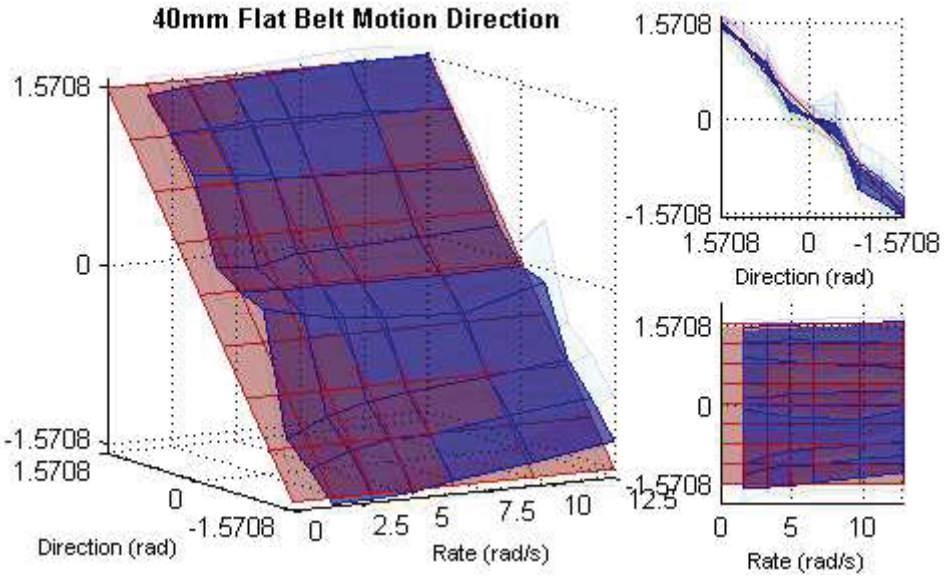

Figure D.24: Motion direction behaviour of flat belt of 40mm separation.

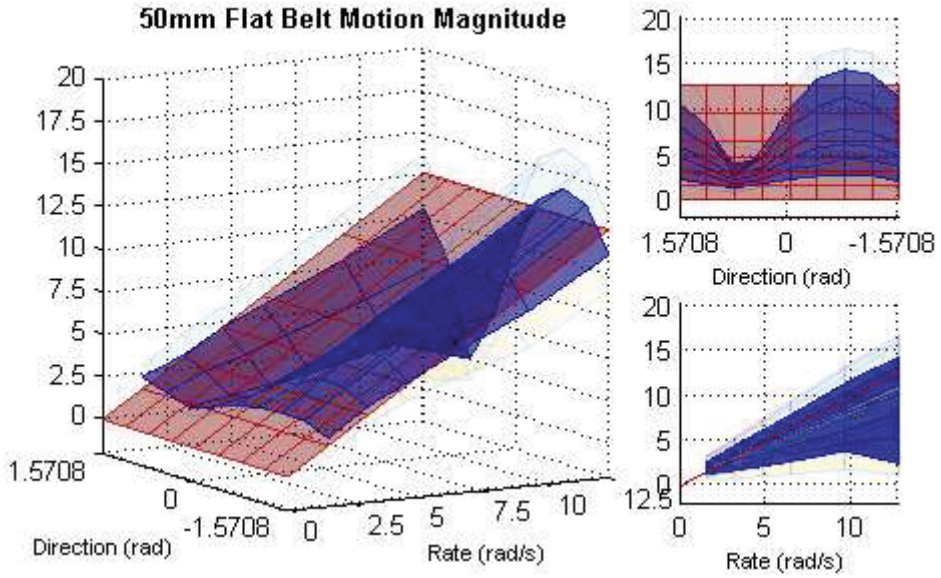

Figure D.25: Motion magnitude behaviour of flat belt of 50mm separation.

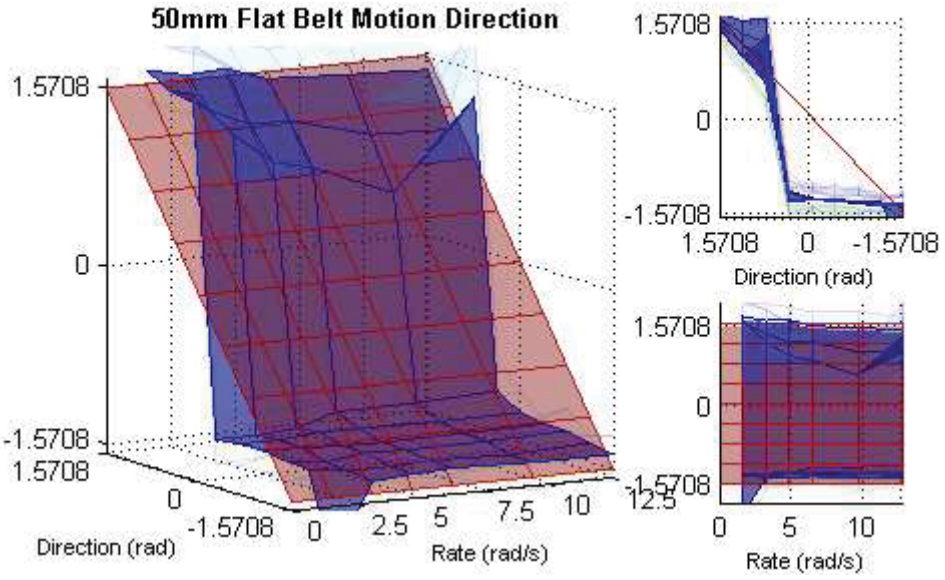

Figure D.26: Motion direction behaviour of flat belt of 50mm separation.

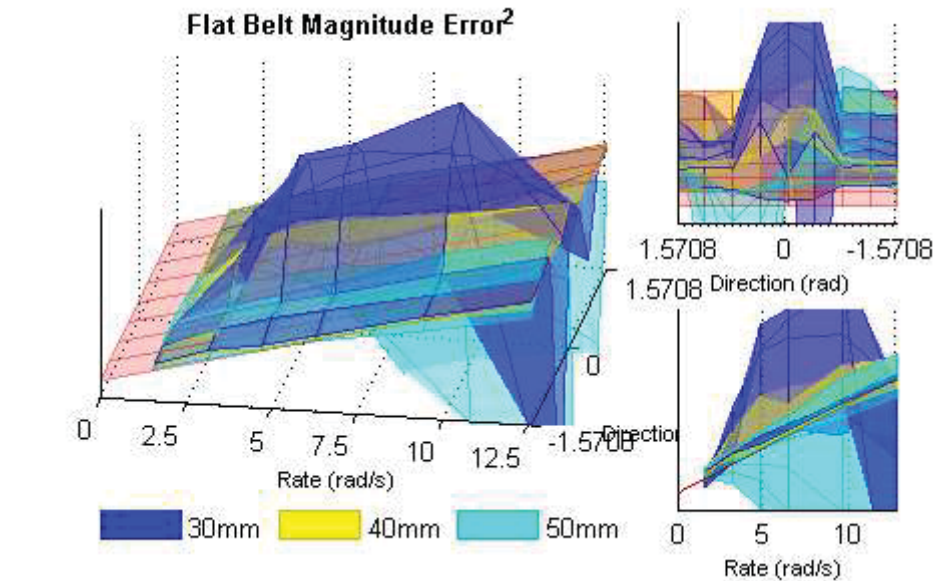

Figure D.27: Warped illustration of the direction error of flat belt of varying belt separation.

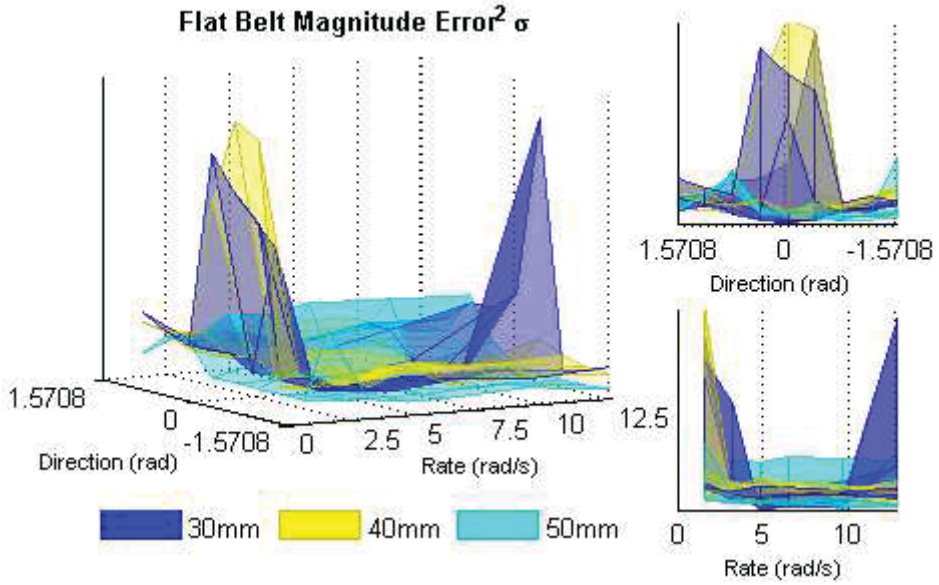

Figure D.28: Warped illustration of the magnirude error standard deviation of flat belt of varying belt separation.

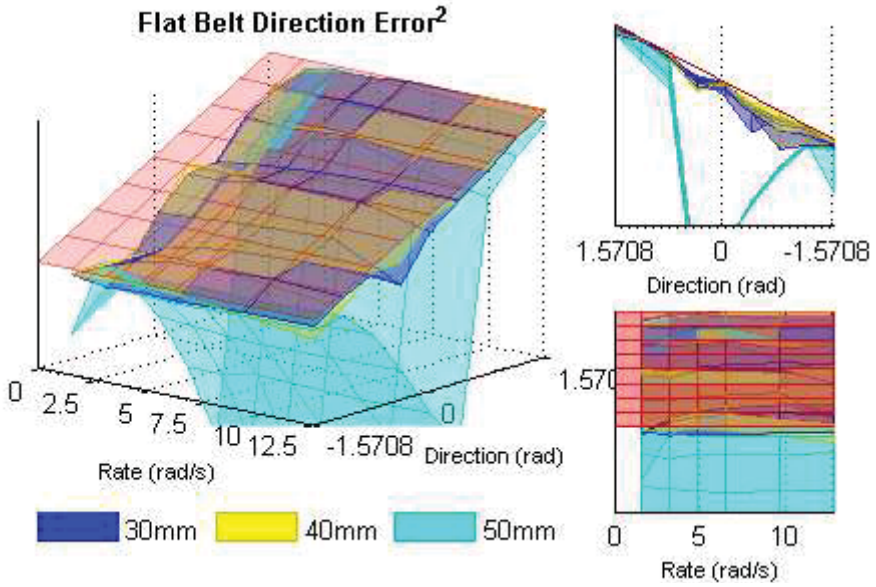

Figure D.29: Warped illustration of the direction error of flat belt of varying belt separation.

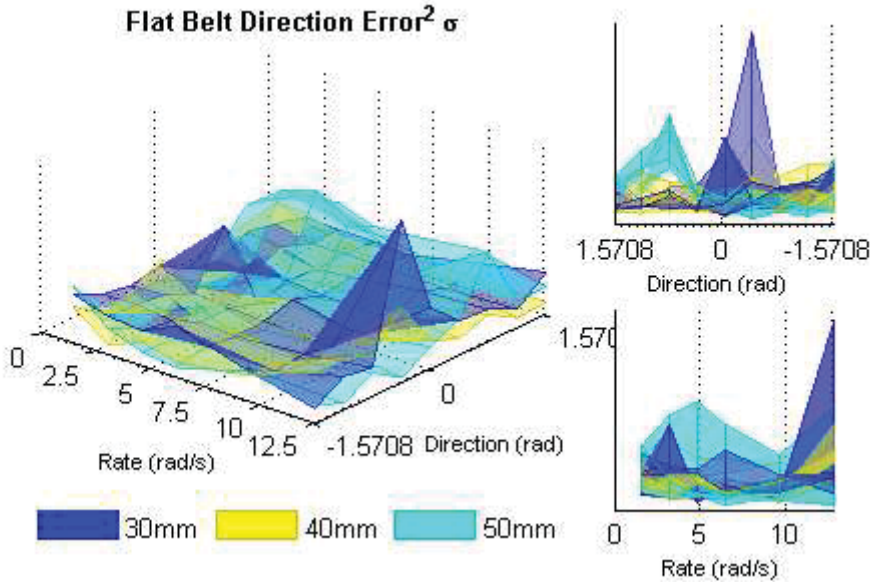

Figure D.30: Warped illustration of the direction error standard deviation of flat belt of varying belt separation.

D.4 Effect of Drive Types

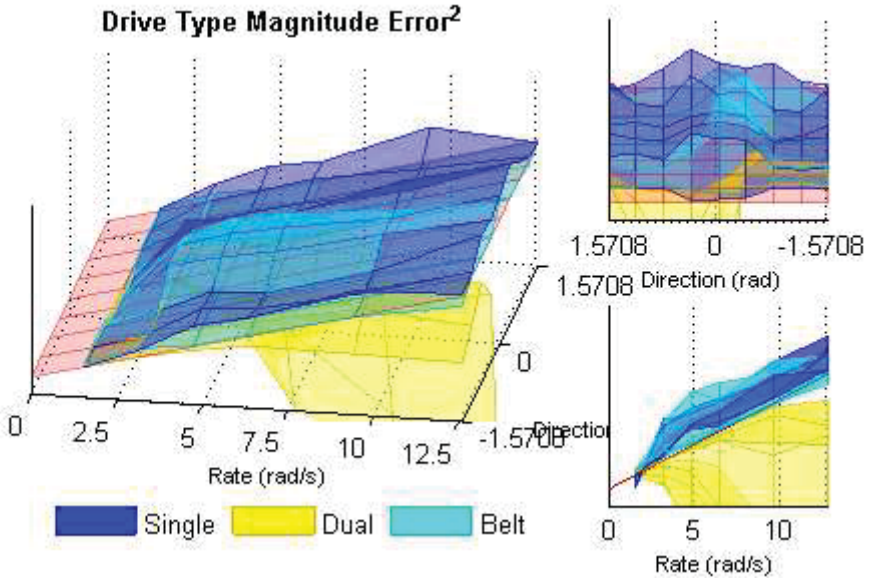

Figure D.31: Warped illustration of the magnitude error of drive types.

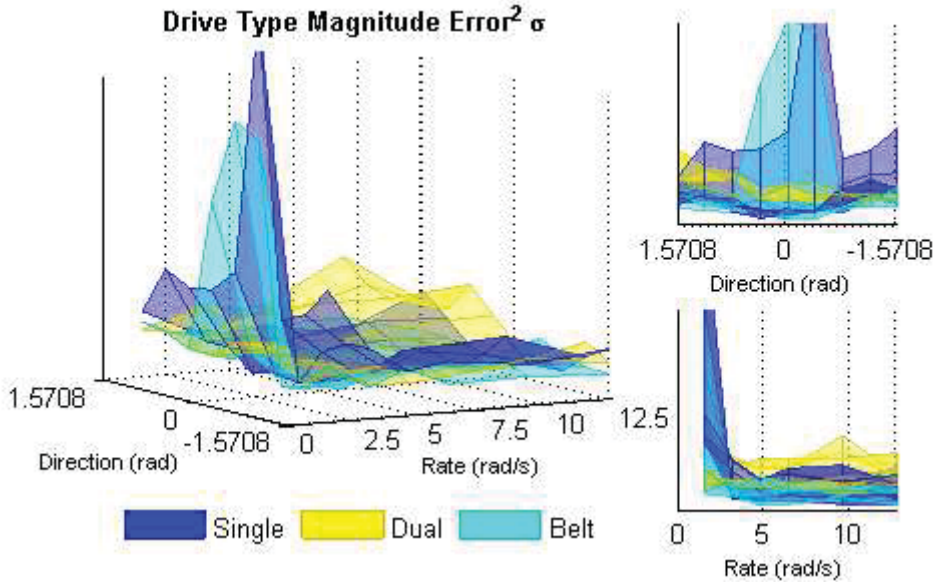

Figure D.32: Warped illustration of the magnitude error standard deviation of drive types.

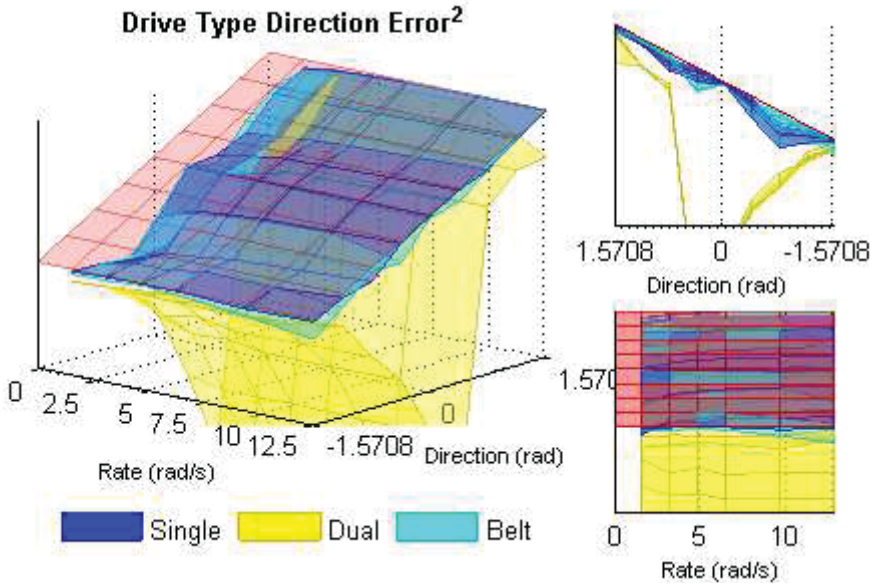

Figure D.33: Warped illustration of the direction error of drive types.

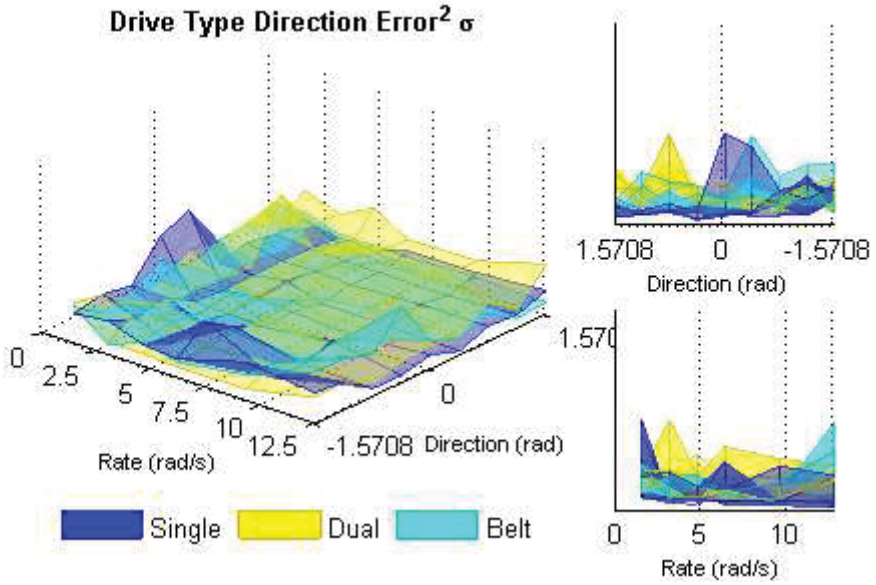

Figure D.34: Warped illustration of the direction error standard deviation of drive types.

D.5 Effect of Belt Tension

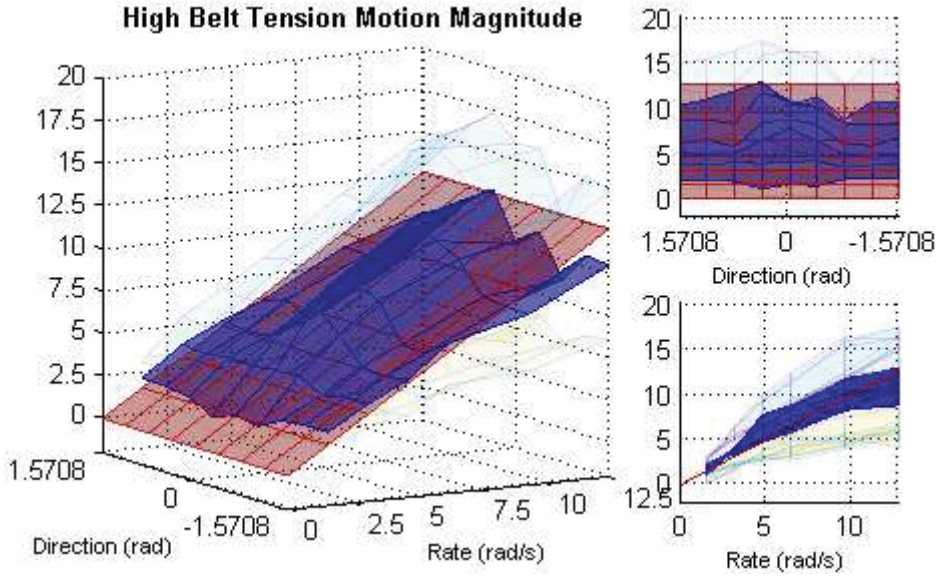

Figure D.35: Motion direction behaviour of high belt tension

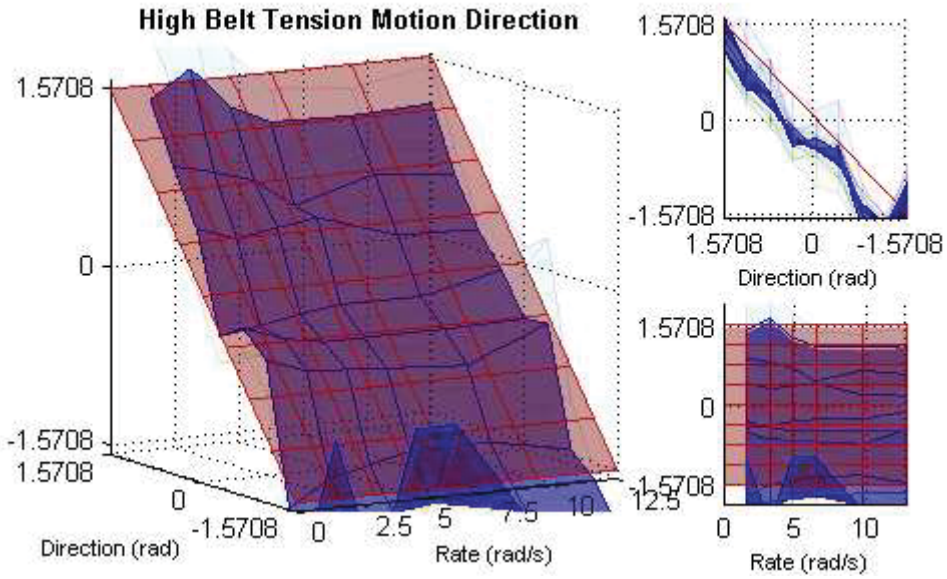

Figure D.36: Motion direction behaviour of high belt tension

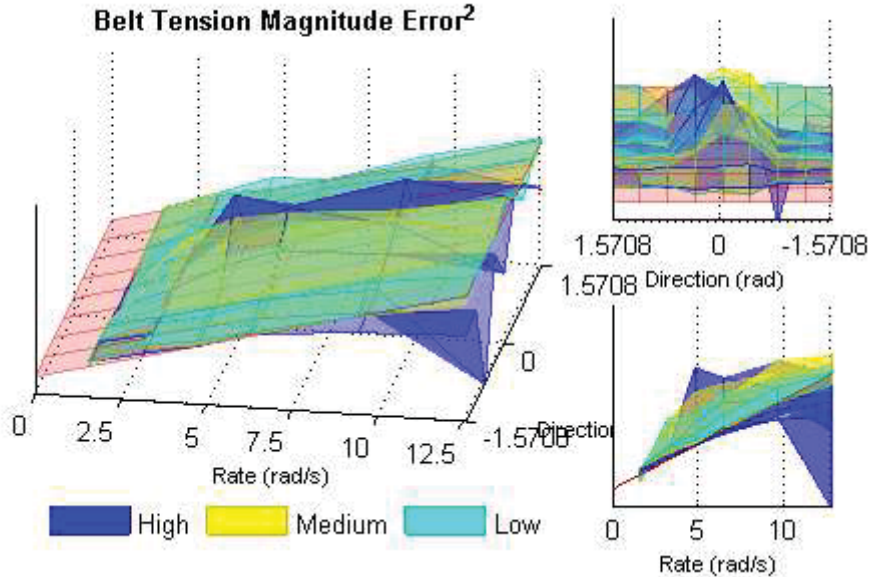

Figure D.37: Warped illustration of the magnitude error of belt tensions.

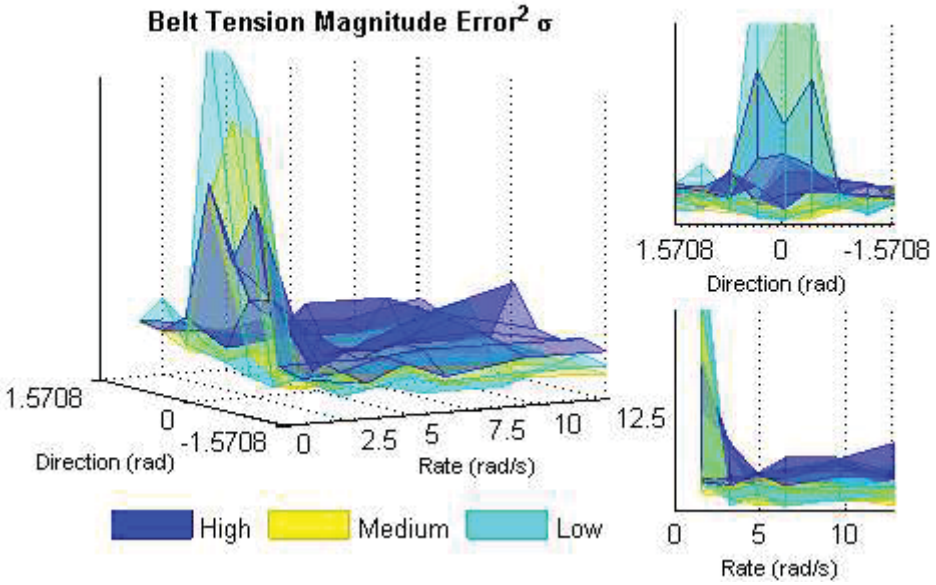

Figure D.38: Warped illustration of the magnitude error standard deviation of belt tensions.

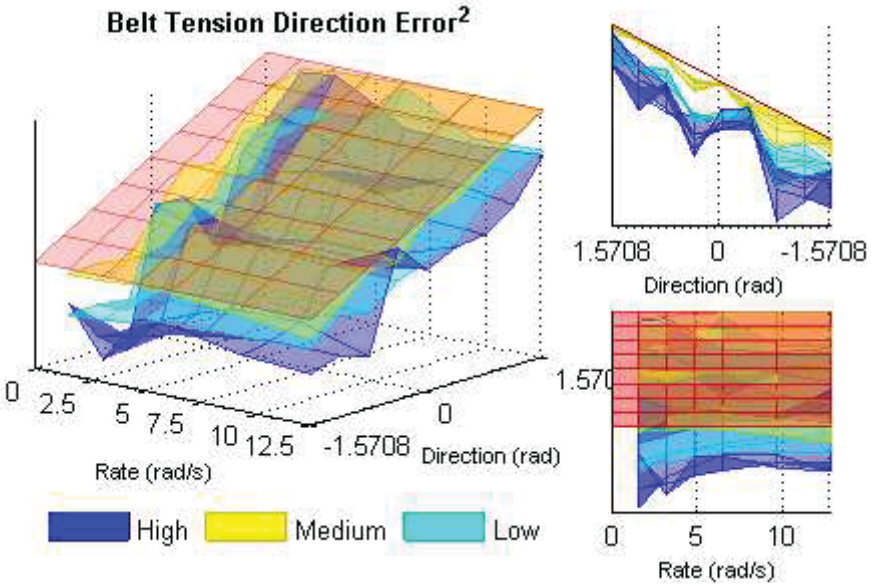

Figure D.39: Warped illustration of the direction error of belt tensions

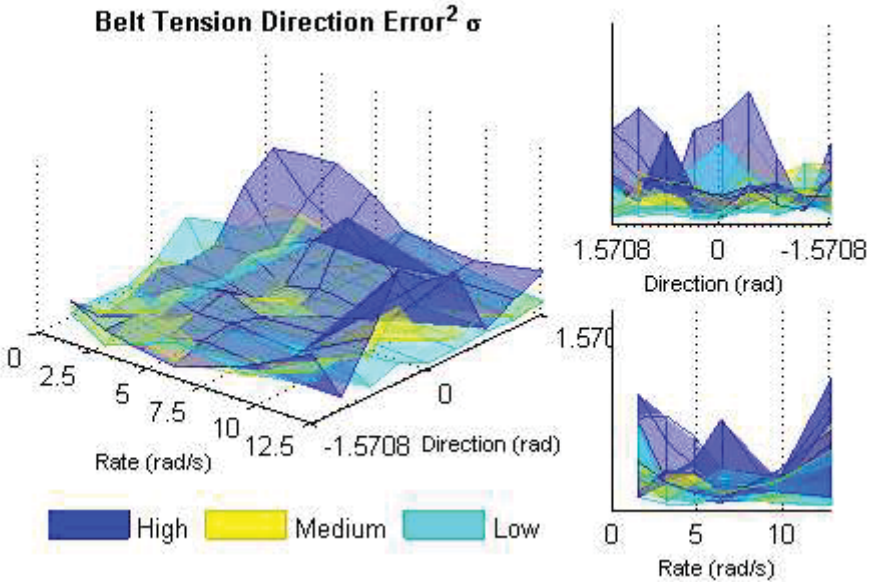

Figure D.40: Warped illustration of the direction error standard deviation of belt tension

D.6 Effect of Pocket Design

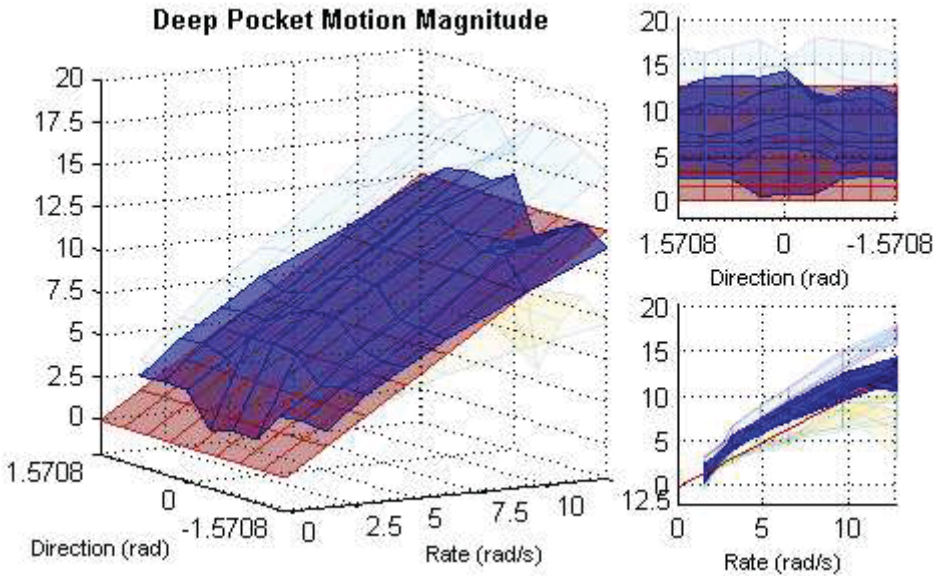

Figure D.41: Motion Magnitude behaviour of Deep Pocket Design

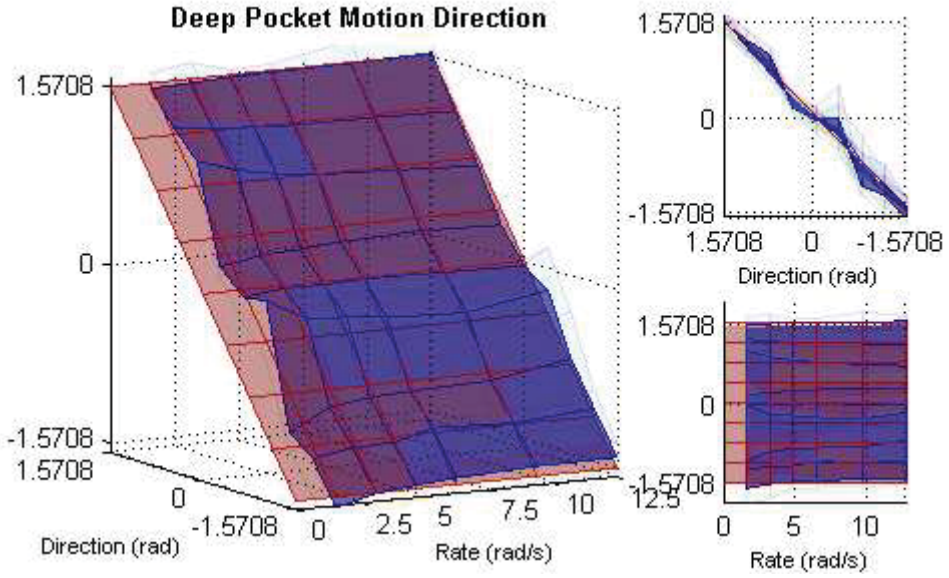

Figure D.42: Motion Direction behaviour of Deep Pocket Design

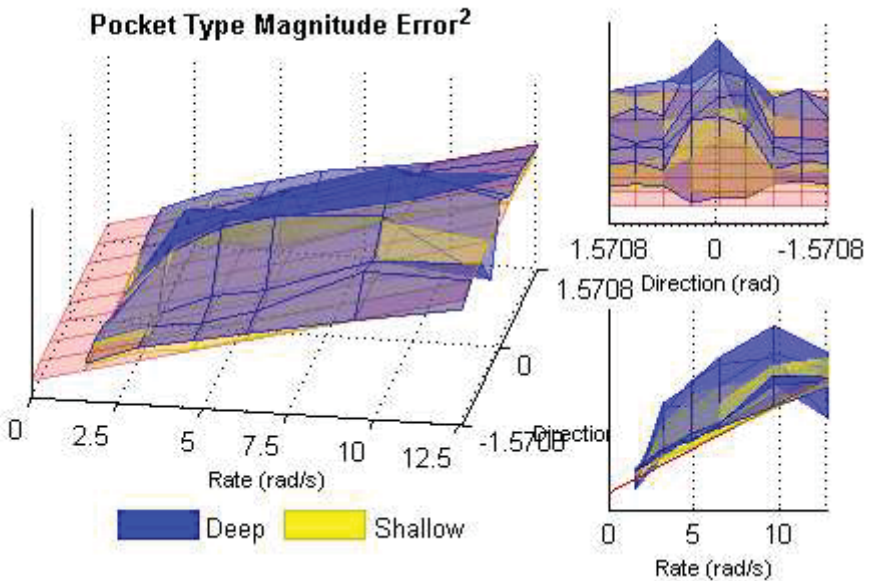

Figure D.43: Warped illustration of the magnitude error of pocket designs.

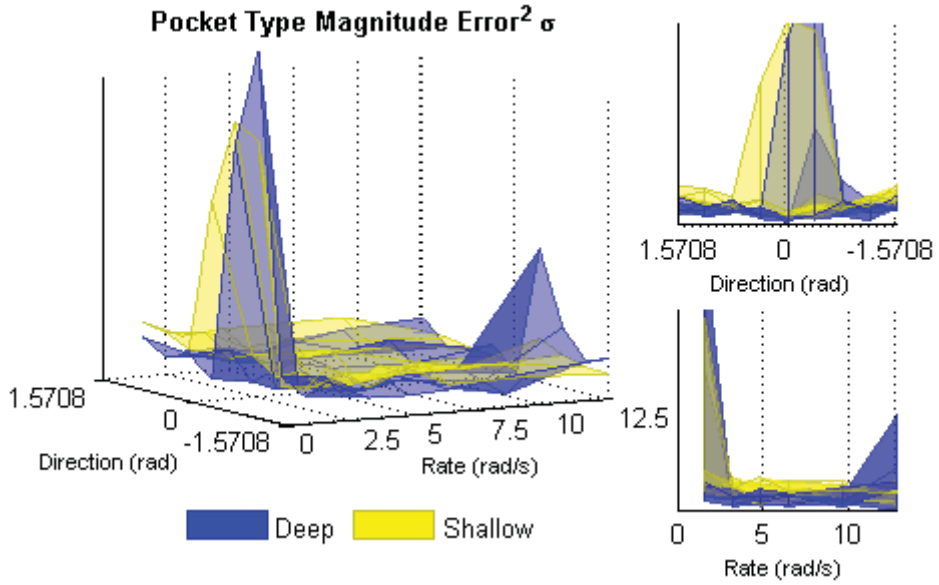

Figure D.44: Warped illustration of the magnitude error standard deviation of pocket designs

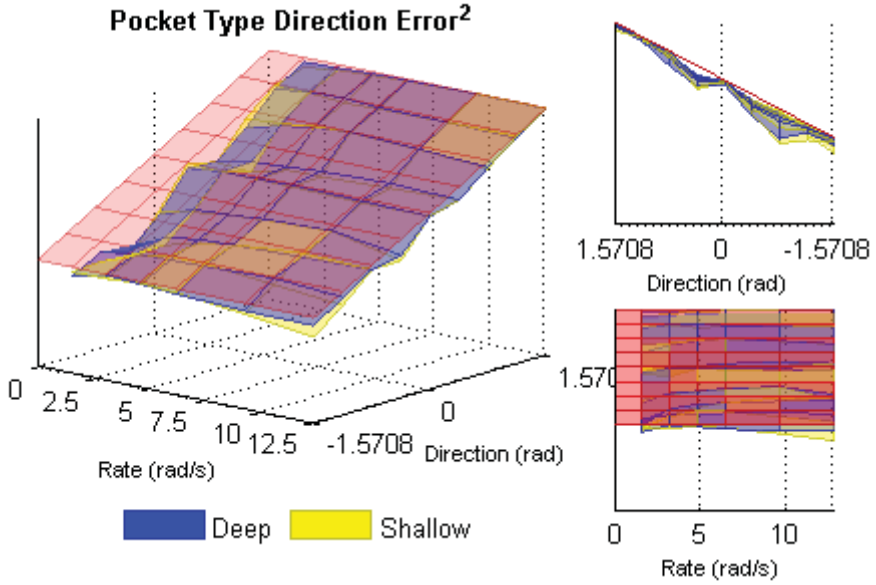

Figure D.45: Warped illustration of the direction error of pocket designs

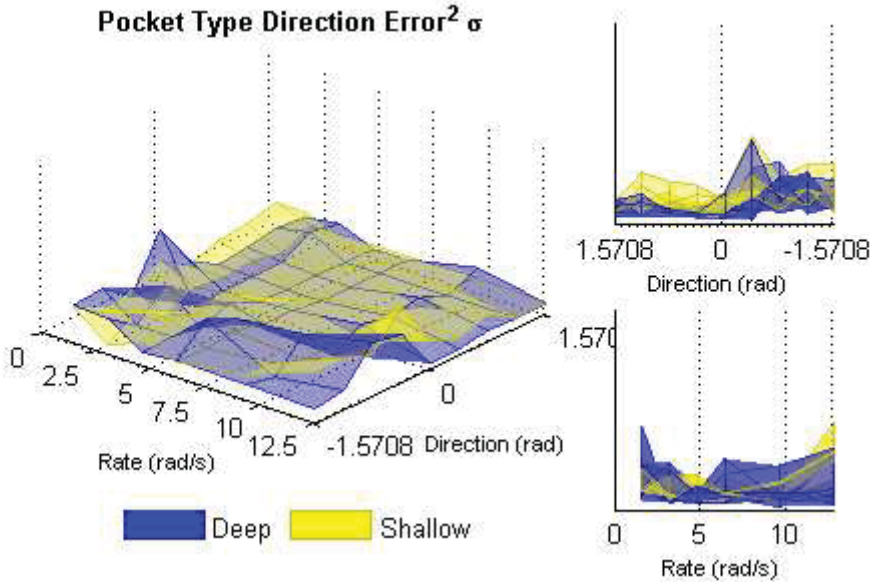

Figure D.46: Warped illustration of the direction error standard deviation of pocket designs